

Bioactive Compounds from Marine Sources

Dem Fachbereich Maschinenbau und Verfahrenstechnik
der Technischen Universität Kaiserslautern
zur Erlangung des akademischen Grades

Doktor-Ingenieur (Dr.-Ing.)

vorgelegte

Dissertation

von

Herrn

M. Sc. Ahmed Elsayed Ahmed Farag Zayed
aus Tanta, Ägypten

Kaiserslautern, 2018

Vorsitzender: Prof. Dr. Eberhard Kerscher

1. Referent: Prof. Dr. Roland Ulber

2. Referent: Prof. Dr. Nicole Frankenberg-Dinkel

mündliche Prüfung (Disputation) am: 26.06.2018

[D386]

Printed with the support of the German Academic Exchange Service

Declaration

I hereby confirm that the dissertation was performed by myself and all used aids are specified in the work. In addition, either the dissertation or parts of it have not been submitted yet as examination papers for a state or other scientific institutes. Dissertation results have not been submitted also yet to another department or university.

Date

Signature

.....

.....

Erklärung

Hiermit bestätige ich, dass die Dissertation von mir selbst durchgeführt wurde und alle verwendeten Hilfsmittel in der Arbeit angegeben sind. Darüber hinaus sind die Dissertation oder Teile davon noch nicht als Prüfungsunterlagen für einen Staat oder andere wissenschaftliche Institute eingereicht worden. Dissertationsergebnisse wurden auch noch nicht an eine andere Abteilung oder Universität übermittelt.

Datum

Unterschrift

.....

.....

Acknowledgment

It is my pleasure to thank all people whose thoughts, ideas, suggestions, reassurance, and support shaped this piece of research. First, I would like to thank **ALMIGHTY ALLAH (MY GOD)** for continuously blessing me with persistence, health, and faith to complete my Ph. D. Degree.

All gratitude must be extended to my supervisor **Prof. Dr. rer. nat. Roland Ulber** for giving me the opportunity to perform my thesis work independently at the Institute of Bioprocess Engineering, TU Kaiserslautern. It was always possible to ask questions and to get encouragement and precious advice to go on with my work. Especially in hard times his support was of great value.

Special thanks and appreciation must be for **Prof. Dr. Kai Muffler**, who was my previous group leader. Useful discussions and information exchange were very helpful even after he left our institute.

I would like to express my appreciation and gratitude to **Prof. Dr. Nicole Frankenberg-Dinkel** and **co-workers** for co-operation in molecular biology work.

In addition, I would like to extend my appreciation to **Prof. Dr. Steffen Rupp**, **Dr. Thomas Hahn**, **Mrs. Doris Finkelmeier**, and **Dr. Anke Burger-Kentischer** from Fraunhofer Institute for Interfacial Engineering and Biotechnology (IGB) for performing anti-viral, anti-fungal, anti-bacterial and cytotoxic studies.

Prof. Dr. Roland Krämer from Heidelberg University is also grateful for his donation of perylene diimide derivative compound who synthesized it personally in his lab.

I would also like to acknowledge the cooperation and creativity of **Dr. med. Michael Püttmann** and **Mrs. Gabi Bruckmann** for their help in anticoagulant measurements, **Dr. Broder Rühmann** and **Dr. Jochen Schmid** for compositional analysis and **Prof. Dr. Lothar Elling** for performing the MP-CE analysis.

Thanks are due to my colleagues at the institute for interesting discussions making them more than colleagues but friends. They have challenged me to "grow into" an interesting and challenging research culture.

The Project was funded by the Egyptian Ministry of Higher Education and DAAD (Funding program number 57076387), so both are gratefully acknowledgment and the fruitful co.operation between Egypt and Germany.

Finally, I extend my deepest gratitude to all the **members of my family** for their continuing prayers, encouragement, understanding, and support. They have guided and encouraged me with great energy and endless faith in my abilities. They never doubted I would really finish my dissertation one day. My children, **Mariam and Mooaz**, suffered my anxieties, bad moods and absences (both physical and mental). I am truly grateful for **my wife Aya Abdella** for her constant assistance, encouragement, and understanding and highly appreciated backup.

Ahmed Zayed

Kaiserslautern, 29.06.2018

List of Abbreviations

- $^1\text{H-NMR}$	Proton-Nuclear Magnetic Resonance spectroscopy
- 2,4-D	2,4-Dichlorophenoxyacetic acid
- AHT	Anhdrotetracyclin
- APPT	Activated Partial Thromboplastin Time
- ASP-12 NTA	Artificial Sea water Provasoli-12-Nitrilotriacetic acid
- BAP	6-Benzylaminopurine
- BSA	Bovine Serum Albumin
- CHNS	Carbon-Hydrogen-Nitrogen-Sulphur
- CMV	Cyto Megalo Virus
- CPPU	1-(2-chloro-4-pyridyl)-3-phenylurea
- DEAE-C	Diethylaminoethyl-cellulose
- DMF	Dimethyl Formamide
- DMSO	Dimethyl Sulfoxide
- DPPH	2,2-Diphenyl-1-picrylhydrazyl radical
- E	Einstein
- EAE	Enzyme-aided Extraction
- FAO	Food and Agriculture Organization
- FDA	Food and Drug Administration
- FPLC	Fast Protein Liquid Chromatography
- FT-IR	Fourier Transform Infrared spectroscopy
- FucTs	Fucosyltransferase
- GlucNAc	<i>N</i> -Acetyl Glucosamine
- GMP	Good Manufacturing Practice
- GPC/SEC	Gel Permeation Chromatography/ Size Exclusion Chromatography
- GRAS	Generally Recognized As Safe
- GT	Glycosyltransferase
- h	hour
- HEPES	4-(2-hydroxyethyl)-1-piperazineethanesulfonic acid
- HMWF	High Molecular Weight Fucoidan
- HPLC	High Performance/Pressure Liquid Chromatography
- HSV	Herpes Simplex Virus
- i.d.	Internal diameter

- IAA	Indole-3-acetic acid
- IC ₅₀	Half maximal Inhibitory Concentration
- IEX	Ion Exchange Chromatography
- ISI	Institute for Scientific Information
- K	6-Furfurylaminopurine (Kinetin)
- kDa	Kilo Dalton
- L:D	Light: Dark light regime
- LMWF	Low Molecular Weight Fucoidan
- m	Meter
- MAB	Maleic Acid Buffer
- MAE	Microwave aided or assisted extraction
- MES	2-(<i>N</i> -morpholino)ethanesulfonic acid
- min	Minute
- Mn	Number-Average Molecular Weight
- Mp	Peak Molecular Weight
- Mw	Average-Weight Molecular Weight
- MWCO	Molecular Weight Cut-Off
- OD	Optical Density or Absorbance
- PABA	<i>para</i> -amino benzoic acid
- PAP	3'-phosphoadenosine 5'-phosphate
- PAPA	<i>para</i> -amino phthalic acid
- PAPS	3'-phosphoadenosine 5'-phospho-sulphate
- PBS	Phosphate-buffered Saline
- PCR	Polymerase Chain Reaction
- PDD	Perylene Diimide Derivative
- PDI	Polydispersity Index
- PES	Provasoli Enriched Sea water
- PESA	Provasoli Enriched Sea water Alternative (without vitamins)
- PMP	1-phenyl-3-methyl-5-pyrazolone
- psi	Pounds per Square Inch
- PT	Prothrombin Time
- PTC	Plant Tissue Culture
- RFU	Relative Fluorescence Unit

- RI	Refractive Index
- rpm	Rate per Minute
- S	Siemens
- s	second
- SAR	Structure Activity Relationship
- SDS	Sodium dodecyl Sulphate
- SDS-PAGE	Sodium Dodecyl Sulphate-PolyAcrylamide Gel Electrophoresis
- Sepabeads® EC-EA	Sepabeads® Enzyme carrier-Ethyl amino derivatized beads
- STC	Seaweed Tissue Culture
- STs	Carbohydrate Sulphotransferase
- TA	Thionin Acetate
- TB	Toluidine Blue
- TPF	1,3,5-Triphenylformazan
- Tris	tris(hydroxymethyl) aminomethane
- TT	Thrombin Time
- TTC	2,3,5-Triphenyltetrazolium chloride
- UAE	Ultrasound aided or assisted extraction
- UV/Vis	Ultraviolet–visible spectroscopy
- WHO	World Health Organization

Latin Symbols

- λ	- Wave length
- Σ	- Sum
- δ	- Chemical shift

Abstract

Fucoidan is a class of biopolymers mainly found in brown seaweeds. Due to its diverse medical importance, homogenous supply as well as a GMP-compliant product is of a special interest. Therefore, in addition to optimization of its extraction and purification from classical resources, other techniques were tried (e.g., marine tissue culture and heterologous expression of enzymes involved in its biosynthesis). Results showed that 17.5% (w/w) crude fucoidan after pre-treatment and extraction was obtained from the brown macroalgae *F. vesiculosus*. Purification by affinity chromatography improved purity relative to the commercial purified product. Furthermore, biological investigations revealed improved anti-coagulant and anti-viral activities compared with crude fucoidan. Furthermore, callus-like and protoplast cultures as well as bioreactor cultivation were developed from *F. vesiculosus* representing a new horizon to produce fucoidan biotechnologically. Moreover, heterologous expression of several enzymes involved in its biosynthesis by *E. coli* (e.g., FucTs and STs) demonstrated the possibility to obtain active enzymes that could be utilized in enzymatic *in vitro* synthesis of fucoidan. All these competitive techniques could provide the global demands from fucoidan.

Zusammenfassung

Fuciodane sind Biopolymere mit sulfatiertem Homo- oder Heteropolysaccharidrückgrat. Sie kommen hauptsächlich in Braunalgen (Phaeophyta) vor. Durch ihre medizinische Bedeutung ist eine einheitliche Versorgung und GMP-konforme Produktion von besonderem Interesse. Aus diesem Grund wurden in dieser Arbeit verschiedene Techniken zur Fucoidan-Produktion angewendet (z.B. Optimierung von Extraktion und Aufreinigung aus klassischen Quellen, marine Gewebekultur und heterologe Expression von Enzymen, die in die Biosynthese von Fucoidan involviert sind). Die Ergebnisse zeigen, dass nach Vorbehandlung und Extraktion 17,5 % w/w Fucoidan aus der Braunalge *F. vesiculosus* gewonnen werden konnte. Durch Aufreinigung mittels Affinitätschromatographie konnte eine höhere Reinheit im Vergleich zu einem kommerziellen Produkt erreicht werden. Biologische Analysen ergaben verbesserte antikoagulante und antivirale Eigenschaften. Kallus- und Protoplastkulturen von *F. vesiculosus*, sowie Kulturen im Bioreaktor repräsentieren neue Wege, Fucoidan biotechnologisch herzustellen. Außerdem demonstrierte die heterologe Expression von mehreren Enzymen der Fucoidan-Biosynthese in *E. coli* (z.B. FucTs und STs) die Möglichkeit, aktive Enzyme zu erhalten, die in enzymatischer de-novo-Synthese von Fucoidan eingesetzt werden können. All diese Entwicklungen könnten dabei helfen, die globale Nachfrage an Fucoidan zu befriedigen.

Table of contents

1. State of the Art and Objectives	1
1.1. Marine-derived products	1
1.2. Seaweeds	4
1.3. Fucoidan and its bioactivities	6
1.4. Goals of the work	9
2. Optimization of Fucoidan Extraction and Purification from Brown Macroalgae	11
2.1. Introduction	11
2.1.1. Definition and functions	11
2.1.2. Fucoidan chemistry	12
2.1.3. Methods of extraction	14
2.1.4. Purification	15
2.1.5. Fucoidan from <i>F. vesiculosus</i> or bladder wrack	17
2.2. Material and Methods	20
2.2.1. Algae harvesting and pre-treatment	20
2.2.2. Optimization of fucoidan extraction	21
2.2.3. Quantitative assay for crude fucoidan fractions' contents	23
2.2.4. Perylene diimide derivative synthesis (PDD)	24
2.2.5. Immobilization of thiazine dyes and perylene diimide derivative	24
2.2.6. Adsorption kinetics in crude fucoidan	24
2.2.7. Fucoidan purification and optimization	25
2.2.7.1. Batch process.....	25
2.2.7.2. FPLC process.....	26
2.2.8. Purified fucoidan fractions characterization	27
2.2.9. Process scaling-up and application of optimized conditions	31
2.3. Results and Discussion	33
2.3.1. Pre-treatment, extraction and preparation of crude extract	33
2.3.2. Characterization of crude fucoidan fractions	34
2.3.3. Application and optimization of fucoidan purification	36
2.3.4. Application of PDD for fucoidan purification	44
2.3.4.1. Adsorption kinetic in crude fucoidan.....	45
2.3.4.2. Multiple use of immobilized PDD.....	46
2.3.4.3. FPLC automated purification process.....	47
2.3.5. Physico-chemical characterization of purified fucoidan fractions	48
2.3.5.1. Elemental Analysis (CHNS Analysis).....	48

2.3.5.2.	Molecular weight parameters.....	50
2.3.5.3.	Melting point.....	51
2.3.5.4.	Specific optical rotation	52
2.3.5.5.	Monomeric composition	52
2.3.6.	Spectroscopical identification of purified fucoidan fractions	53
2.3.7.	Pharmacological activities	55
2.3.8.	Process scaling-up and application of optimized conditions	62
2.4.	Conclusion and Prospectives.....	65
3.	Development of Axenic Protoplast and Callus-like Cultures from <i>F. vesiculosus</i>	66
3.1.	Introduction.....	66
3.1.1.	Marine biotechnology challenges	66
3.1.2.	Marine microbes and macroalgae tissue culture	67
3.1.3.	Development of marine macroalgal cultures	68
3.1.4.	Growth requirements and previously-performed trials	69
3.2.	Materials and Methods.....	72
3.2.1.	Harvest and pre-treatment of algae	72
3.2.2.	Surface sterilization.....	72
3.2.3.	Sterility investigation	74
3.2.4.	Genotyping of microbial contaminants.....	74
3.2.5.	Vitality investigation (2,3,5-Triphenyltetrazolium chloride (TTC) assay)	75
3.2.6.	Protoplast isolation and culture development	76
3.2.7.	Development of protoplast and callus-like cultures	76
3.3.	Results and Discussion.....	79
3.3.1.	Sterility investigations.....	79
3.3.2.	Vitality investigation.....	80
3.3.3.	Protoplasts isolation and culture development.....	81
3.3.4.	Callus-like development from <i>F. vesiculosus</i> explant	82
3.4.	Conclusion and Prospectives.....	85
4.	Heterologous Expression of Enzymes Involved in Fucoidan Biosynthesis	88
4.1.	Introduction.....	88
4.2.	Heterologous expression of algal fucosyltransferases (FucTs).....	93
4.2.1.	Material and Methods	95
4.2.2.	Results and Discussion.....	100
4.3.	Carbohydrate sulphotransferases (STs)	111
4.3.1.	Material and Methods	113

4.3.2. Results and Discussion	116
4.4. Conclusion and Prospectives	124
5. Conclusion	126
6. Future Outlook	127
References	128
Appendix	143
Appendix A	143
Chemical structures of some marine-derived bioactive compounds.....	143
Appendix B	147
Reagents and buffers.....	147
Appendix C	155
Medium composition and preparations.....	155
Appendix D	160
Protocols.....	160
Appendix E	164
Calibration curves, instruments' charts and analysis reports.....	164
Appendix F	180
Lists of Figures, Tables, Schemes and devices.....	180

1. State of the Art and Objectives

Since the early life of the humankind on the Earth, nature represents the most powerful source for his major needs from food, energy and therapeutics. Oceans cover more than 70% of the Earth's surface, and therefore, they continue to offer exceptional scaffolds improving the quality of the human life. For example, marine microbes, which represent 98% of ocean biomass [1], perform vital functions in global food chain cycle, CO₂ fixation as well as assimilation of nutrients to maintain oxygen, nitrogen and phosphorous in their normal environmental levels [2].

In addition, the interest in marine-related fields has grown in the last period (e.g., taxonomy, ecology, chemistry,...etc.) to explore such source for bio- and chemical diversity and other valuables, such as the marine-derived bioactive compounds. The obtained results were promising and have encouraged the performance of further studies to discover new medicaments from natural sources and provide the global market with its required demands.

1.1. Marine-derived products

Marine organisms represent around 50% of the worldwide biodiversity [3] in addition to their chemical and genetic diversities, and therefore represent a potential source of broad spectrums of commercially-valuable and diverse products, such as polysaccharides, enzymes, peptides, lipids, steroids and terpenoids [4,5]. From more than 300,000 described organisms, 12,000 novel compounds have been discovered attracting a great interest in the last decades [6]. Most of these compounds are produced as secondary metabolites as a defense mechanism to protect themselves against invaders. Marine-derived products have a wide range of applications in pharmaceuticals as anti-tumor and anti-viral among others, nutraceuticals as dietary supplements and food additives, agrochemicals with insecticidal, herbicidal, and fungicidal activities and cosmetics as photo-protective and anti-aging compounds. These compounds are believed to be superior to that derived from terrestrial nature in terms of their chemical novelty and their ability to induce potential activities [7]. They are mainly obtained from different marine taxonomic groups including antarctic fungi, bacteria, epiphytic bacteria and fungi, macroalgae or seaweeds, microalgae and mediterranean sponges [8].

In addition, advances in marine pharmacology have helped in the discovery of a lot of marine-derived bioactive compounds. The real marine drug development has started with the discovery of Cephalosporin C in the 1940s from the mediterranean fungus *Acremonium chrysogenum*. It was the

first compound in the antibiotic class of cephalosporin. Moreover, isolation of spongouridine and spongothymidine in the 1950s from the Caribbean sponge *Tethya crypta* led to the synthesis and approval of the more active nucleoside analogues cytarabine and vidarabine as potent anti-cancer and anti-viral drugs, respectively [9,10]. Some examples of these marine-derived products were summarized in **Table 1**.

Table 1: Selected categories and examples of marine-derived products

Product category	Compound name	Biological source	Importance	Ref.	
• Pharmaceuticals	Mycosporine-Gly	<i>Palythoa tubereulosa</i>	Anti-oxidant	[11]	
	C-Phycocyanin	<i>Spirulina platensis</i>		[12,13]	
	Fucoidan	Brown macroalgae (e.g., <i>Fucus vesiculosus</i>)	Anti-coagulant	[14]	
	Eunicellane diterpenoid	- <i>Klyxum molle</i> - <i>Cladiella krempfi</i>	Anti-inflammatory	[15]	
	Carotenoid	<i>Padina boergesenii</i>	Hepatoprotective	[16,17]	
	Axisonirile-3	<i>Acanthella klethra</i>	Anti-malarial	[18]	
	α -Kainic acid	- <i>Digenia</i> sp. - <i>Sargassum</i> sp.	Anti-parasitic	[19]	
	Vidarabine (Ara-A)	<i>Tethya crypta</i>	Anti-viral	[10]	
	Avarol	<i>Disidea avara</i>			
	Cytarabine (Ara-C)	<i>Cryptotheca crypta</i>	Anti-tumor	[20]	
	Fucoxanthin	Microalgae (e.g., bacillariophytes) and brown macroalgae (<i>Laminaria japonica</i>)		[21]	
	Borophycin	Cyanobacteria (e.g., <i>Nostoc linckia</i> and <i>N. spongiaeforme var. tenue</i>)		[22]	
	Chalcomycin	<i>Streptomyces</i> sp. HK-2006-1		Anti-microbial	[23]
	Sesterterpene sulphate	<i>Dysidea</i> sp.			[24,25]
	- Cristatumins A - Cristatumins D	<i>Eurotium cristatum</i> EN-220	[26]		

Cont., Table 1: Selected categories and examples of marine-derived products

Product category	Compound name	Biological source	Importance	Ref.
• Cosmetics	Scytonemin	<i>Cyanobacteria</i> sp.	Topical photo-protective	[21]
	Astaxanthin	<i>Haematococcus pluvialis</i>	Anti-aging	
• Nutraceuticals, food additives and dietary supplements	Arachidonic acid	<i>Porphyridium</i> sp.	Polyunsaturated fatty acids (PUFAs)	[8]
	γ -Linolenic acid	<i>Arthrospira</i> sp.		
	Alginate	Brown algae (e.g., <i>Laminaria</i> sp.)	Gelling, emulsifying agents and stabilizers	[27,28]
	Agar	Red algae (e.g., <i>Gelidium amansii</i>)		[29]
	Carrageenan	Red algae (e.g., <i>Kappaphycus alvarezii</i>)		[30,31]
• Others - Enzyme inhibitors	Speradine A	<i>Aspergillus tamari</i>	Inhibitory activity against Ca ²⁺ -ATPase and histone deacetylase	[32]
- Source of enzymes	Polyketide synthase	<i>Pseudoceratina clavata</i>	Polyketide synthesis	[33]
	Alginate lyase	<i>Microbulbifer</i> sp.	Alginate degradation	[34]
	Fucoidanase	<i>Dendryphiella arenaria</i>	Degradation to low molecular weight fucoidan (LMWF)	[35]

As **Table 1** showed, a lot of marine-derived products have been commercialized such as agar-agar, alginate, carrageenan...etc. However, few drugs succeeded to be approved by FDA and marketed such as ziconotide (Prialt[®]) as a potent analgesic, trabectedin (Yondelis[®]), and cytarabine or ara-C (Cytosar-U[®]) as anti-tumour agents, vidarabine or ara-A (Vira-A[®]) and *iota*-carrageenan (Carragelose[®]) as an anti-viral, and omega-3-acid ethylesters (Lovaza[®]) which is a combination of ethyl esters of eicosapentaenoic acid (EPA) and docosahexaenoic acid (DHA) for treating hypertriglyceridemia [17]. Other compounds are still investigated in different pre-clinical and clinical phases and marketed shortly [36].

License of investigational pharmaceutical products for human use should obey the GMP guidelines in most of the world countries. The application of these principles assure production of a high-quality

product, consistency between the investigational product and the future commercial product and thus reliability and the relevance of clinical trials to the product's efficacy and safety [37]. This low number of approved drugs reflected the presence of different challenges and problems to produce GMP-compliant bioproducts which include a sustainable supply without harmful ecological consequences, identification of a practical formulation, structural complexity and low therapeutic index of marine-derived compounds [36].

1.2. Seaweeds

Seaweeds or macroalgae have a long history of multiple applications as a human food (e.g., *Laminaria japonica*, *Undaria pinnatifida*, *Pyropia* sp. (formerly *Porphyra*) and *Sargassum fusiforme*) especially in the South-east countries, biofuels, source of various valuable products, in water purification from organic and inorganic wastes or a commercial source of hydrocolloids including agar, carrageenan and alginate. Interestingly, hydrocolloids' global annual production has recently reached 100,000 tons with a market value above US \$ 1.1 billion [38]. Moreover, according to FAO statistics (FAO, 2014, 2016), of the top seven most cultivated seaweed taxa, three were used mainly for hydrocolloid content: *Eucheuma* sp. and *Kappaphycus alvarezii* for carrageenans, and *Gracilaria* sp. for agar [39]. These benefits have urged the commercial market to find out competitive techniques to increase the global yield from seaweeds, such as sea farming or aquaculture and biotechnology. In 2014, the annual production of cultivated seaweeds reached 27.3 million tons, representing 27% of the total marine aquaculture production [40]. **Fig. 1** shows the global production of seaweeds in tons aquaculture, according to the FAO, 2016 report [39]. In addition, a 2015 report from the market analyst Smithers Rapra expected that the global market for marine biotechnology or blue biotechnology for industrial applications has the potential to reach US \$4.8 billion by 2020, rising to US \$6.4 billion by 2025 [41].

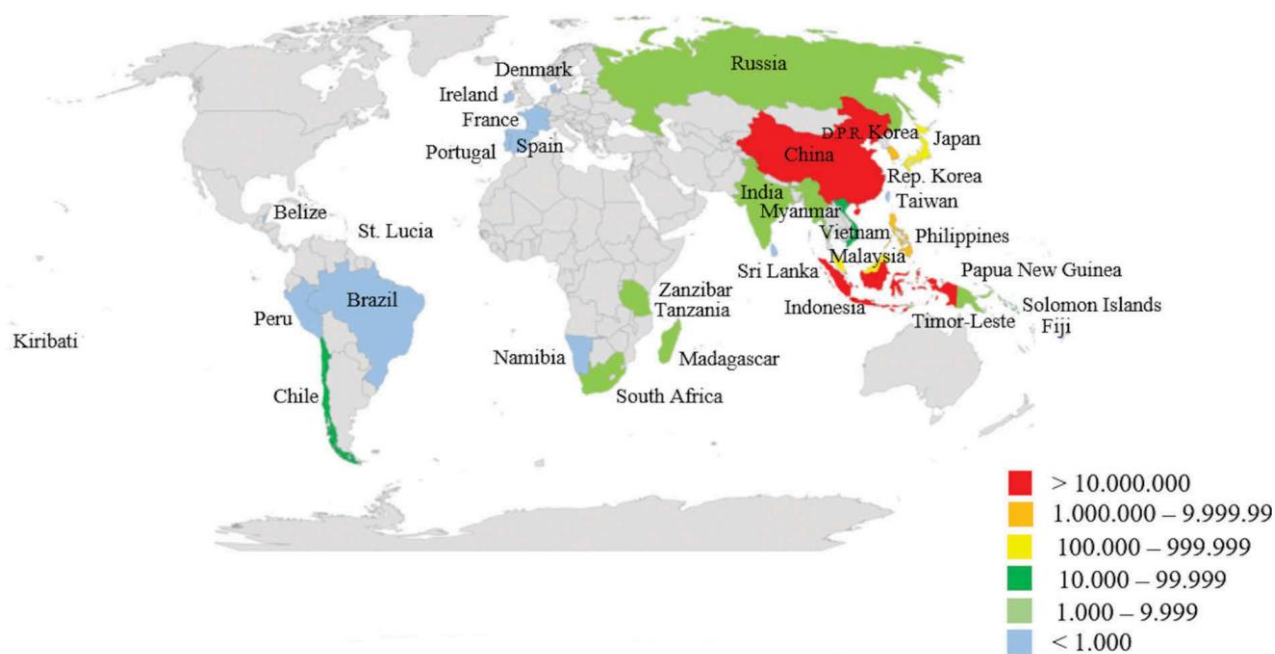


Fig. 1: Seaweed production in the year 2014 by Aquaculture [39]

Colour scale in wet metric tons (FAO, 2016).

Sulphated and non-sulphated polysaccharides from marine macroalgae have a wide-ranging of interesting medical applications, such as anti-coagulant and/or anti-thrombotic, immunomodulatory ability, anti-tumor, hypoglycemic, antibiotics, anti-inflammatory and anti-oxidant making them promising pharmaceutical products [42] including Phaeophytes or brown algae (e.g., fucoidan, laminarin and alginate), Rhodophytes or red algae (e.g., porphyrin and carrageenan) and Chlorophytes or green algae (e.g., rhamnans and ulvan). Unfortunately, structural and content heterogeneity of non-sulphated polysaccharides within the same genus resulted in poor investigation regarding chemical structure, biological activities and their structural-activity relationship (SAR) in comparison with sulphated analogues. Sulphated polysaccharides showed diverse molecular weights, monosaccharide compositions, sulphate contents and positions, which interact with various biological systems at different levels leading to diverse and interesting pharmacological activities [42,43,44,45].

Particularly, brown macroalgae or Phaeophyceae consists of *ca.* 285 genera and 1181 species [46] distributed not only on Fucales and Laminariales, which are the main commercial resources of the algal sulphated polysaccharides, but also contains Chordariales, Dictyotales, Dictyosiphonales, Ectocarpales, and Scytosiphonales. Fucales are one of the largest and most diversified orders within

the class Phaeophyceae. They are composed of 8 families (41 genera and 485 species); namely the Ascoseiraceae, Cystoseiraceae, Durvillaeaceae, Fucaceae, Hormosiraceae, Himanthaliaceae, Sargassaceae, and Seirococcaceae [47]. As **Fig. 2** shows, the major species of brown macroalgae are often dominant components of tropical to temperate marine forests and intertidal communities.

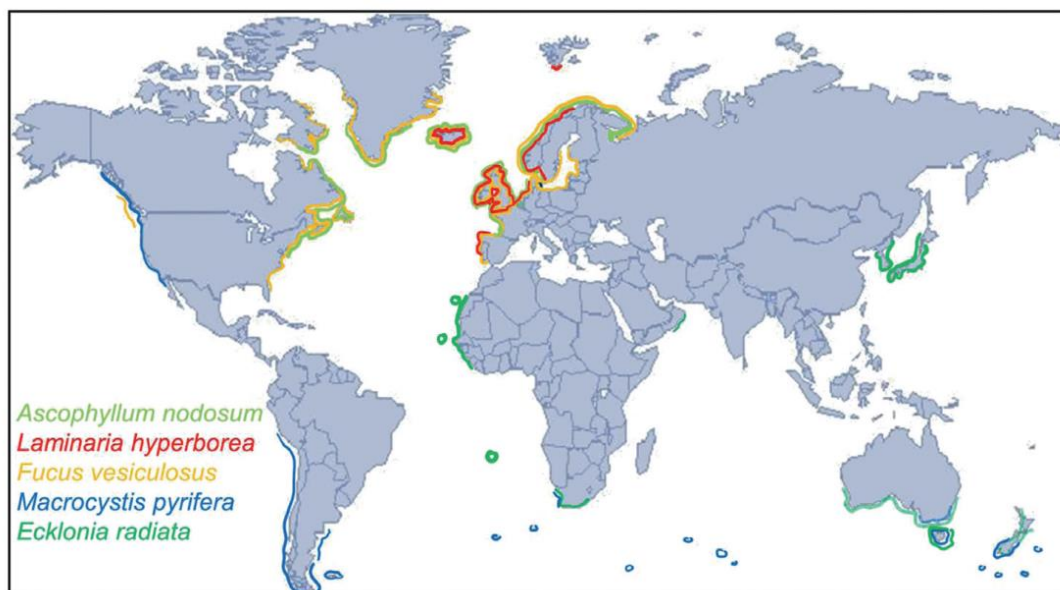


Fig. 2: Global distribution of the major brown macroalgae species [48]

1.3. Fucoidan and its bioactivities

Fucoidan is a marine polysaccharide isolated mainly from brown macroalgae with interesting and promising pharmacological activities [14]. Several articles discussed and proved potential, versatile and promising pharmacological activities of fucoidan, such as anti-coagulant and anti-thrombotic activity owing to structural similarity with heparin [49,50], anti-inflammatory [51], anti-oxidant [52], anti-viral against number of viruses like HSV [53], CMV [54] and HIV [55] ...etc., resulting in great interest in fucoidan in the last few decades as a candidate for drug discovery from nature with less side effects. Several features are involved and affect these activities, such as monosaccharide composition, molecular weight, sulphate esters content and sulphation pattern [56].

In more details, the following sections describe some of these activities.

1.3.1. Anti-coagulant activity

Physiologically, blood coagulation system or hemostasis functions through two cascades; namely extrinsic and intrinsic pathways, which are stimulated differently either by tissue injury or abnormal pathological conditions. However, they converged in a common pathway at the step of conversion of prothrombin to thrombin which catalyze the formation of the non-soluble fibrin blood clot. Extrinsic cascade is initiated as a response to a tissue or vascular injury that stimulates secretion of tissue factor or tissue thromboplastin from traumatized tissue. However, contact with exposed vessel wall or negatively charged surfaces, such as lipoprotein particles, release of phospholipids from activated platelets or even bacteria resulted in activation of contact or intrinsic coagulation pathway. Coagulation cascades are monitored through a number of clinical laboratory tests, such as APTT for the intrinsic pathway, PT for extrinsic pathway, and TT for common pathway.

Despite heparin has a long history to treat patients with thrombosis since 1940, it has suffered from a number of side effects including bleeding, thrombocytopenia in addition to possible pathogenic contamination from animal during production phases [57]. Several publications discussed the potential anti-coagulant activity of fucoidan [49,50,58]. They demonstrated that fucoidan acts in a heparin-like manner and interfered mainly with intrinsic pathway of coagulation system. It showed prolonged APTT and TT without a significant effect on PT. Moreover, not only negative charge distribution of fucoidan structure contributed to inhibition of thrombin, but also its enough long polysaccharide chain, high molecular weight, and structure comfortability were required for thrombin deactivation and discontinue of the fibrinogen conversion to fibrin [43].

1.3.2. Anti-viral activity

Fucoidan has a potential anti-viral activity against a number of enveloped viruses like HSV [53], CMV [54] and HIV [55] comparable to chemical drugs analogues such as ribavirin and acyclovir. Moreover, it has antiviral activity irrespective of whether these are DNA or RNA viruses [59]. Furthermore, Elizondo-Gonzalez, *et al.* proved the anti-viral activity of *Cladosiphon okamuranus* fucoidan against the enveloped virus Newcastle Disease Virus (NDV) in poultry field [60]. They found that fucoidan interferes with virus replication to inhibit viral-induced syncytia formation and cell-to-cell contact, possibly by blocking the fusion (F) protein. It mediates fusion of the virus and

cell membrane, an essential step for entry of the viral genome in the cell cytoplasm and initiation of a new infectious cycle [61]. Recently, fucoidan showed inhibitory activity against Hepatitis B Virus (HBV) replication by activation of the extracellular signal-regulated kinase (ERK) pathway, which leads to production of type I interferon (INF) [62]. Chemically, sulphate ester groups at C-4 of α -(1-3)-linked fucopyranosyl units appeared to be involved in the anti-herpetic activity of fucoidan (HSV-1 and HSV-2). This structure activity relationship was investigated in the brown seaweed *Cystoseira indica* fucoidan [63].

1.3.3. Cytotoxic and anti-tumor activity

Interestingly, a lot of researches discussed the potential anti-cancers activity of fucoidan [64]. Several fucoidans from *Sargassum fulvellum*, *S. kjellmanianum*, *L. angustata*, *L. angustata* var. *longissima*, *L. japonica*, *Ecklonia cava*, and *Eisenia bicyclis* have been found to have remarkable growth inhibitory activities against various types of tumors. Fucoidan induces cell apoptosis of several cancerous cell lines, such as melanoma, HT-29 colon cancer, MCF-7 human breast cancer, HS-Sultan human lymphoma through activation of different caspases-dependent pathways [65]. Other theories suggested activation of macrophages which resulted in production of cytokines such as IL-1, IL-2 and IFN- γ with subsequent stimulation of T-cell [65].

1.3.4. Anti-oxidant and radicle scavenging activity

Antioxidants are medically beneficial compounds that fight against harmful reactive oxygen and free radicle species. Anti-oxidants are also important in food industry, where they prevent food deterioration. Despite potential fucoidan anti-oxidant activity against different free radicles (e.g., DPPH, superoxide, hydroxyl and lipid peroxides) [66] was discussed in many publications *in vitro*, most of these assays were investigated in crude fucoidan extracts [67,68,69], or/and its purified fractions [70]. It was observed that crude fucoidan had higher activity than its purified fractions and these findings indicated that co-extracted contaminants such as polyphenols interfere with this activity.

Nevertheless, its biogenic resources function potential ecosystem services and due to oppressive harvest from wild marine forests in the last decades, their populations in many regions around the world have declined and/or spatially shifted [48]. As a result, wild harvest was prohibited by many governmental legislations. In addition, fucoidan production and chemical structure are greatly

affected by many other factors, such as seasonal and geographical factors as well as extraction methods which affect its pharmacological activities as a result. Therefore, production of a GMP-compliant product that could be investigated clinically is impossible without establishment of innovative and competitive techniques which guarantee a structurally-homogenous and eco-friendly supply.

1.4. Goals of the work

As seen in **Fig. 3**, The present dissertation deals with various aspects of fucoidan production, including optimization of fucoidan classical extraction and purification from marine crude algal extract to obtain a high-quality and native product, development of new biotechnological techniques without harmful effects on the global ecosystem through either callus and protoplast culture from brown algae or heterologous expression of enzymes involved in fucoidan biosynthesis (e.g., FucTs and STs). These routes of production should guarantee an improved yield of fucoidan with minimal structural differences in a commercial scale.

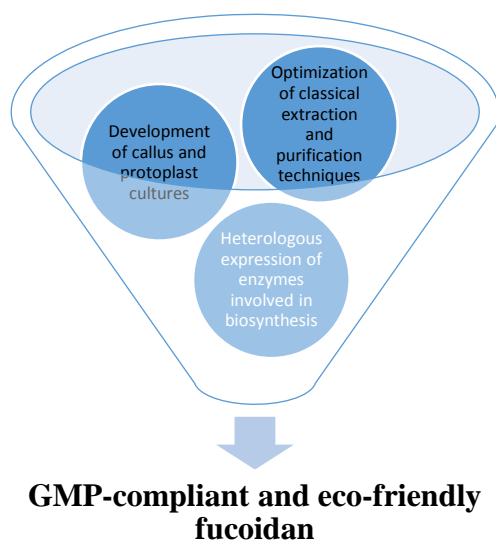


Fig. 3: Overview of the different strategies dealt in the present work

The techniques aimed to produce fucoidan that is compliant with GMP guidelines and from eco-friendly resources.

In details, the following aspects will be discussed within this thesis.

- Production of a GMP high-quality and native fucoidan in a simple, time-saving and cheap protocol is a challenging. To date, a standard and optimized protocol for extraction and

purification techniques of fucoidan have not been developed yet. Recently, immobilized thiazine dyes succeeded in capture of fucoidan from a raw synthetic extract in a simple and fast procedure. However, this procedure has not been applied to real crude extracts and its effect on physico-chemical and pharmacological properties of fucoidan was not investigated. In **Chapter 2**, downstream processes applying different extraction and purification parameters (e.g., temperature, pH, time) of fucoidan from *F. vesiculosus* were studied to isolate different fucoidan fractions applying the recently developed thiazine dyes-derivatized beads. These fractions were characterized physico-chemically (e.g., melting point, monomeric composition, and molecular weight) and pharmacologically (e.g., anti-coagulant, and anti-viral activities) afterwards. These studies aimed to reveal and understand some of fucoidan's SAR. In addition and for more effective purification, immobilization of the sensitive Heparin Red[®] (Redprobes UG) chemically-related PDD would be performed and applied to capture of fucoidan from a crude algal extract.

- In **Chapter 3**, growing of various cell cultures derived from *F. vesiculosus* was discussed. Development of closed-system bioreactors for seaweeds cultivation is a particularly challenging opportunity for marine bioprocess engineers [71]; where, cultivation in a closed-system bioreactors ensures the growth of seaweeds at optimum conditions and production of consistent and homogenous value-added fucoidan as well. This type of production may minimize the structural heterogeneity, which are greatly affected with harvesting time and place, producing species and method of extraction. Since removal of marine microbes from macroalgae represents a rate-limiting step in the development of axenic tissue culture systems, a combination of various as well as delicate reagents should be optimally applied to establish a surface sterilization protocol and at the same time maintain explant viability. These axenic explants would be used in establishment of various types of growing cell phototrophic cultures.
- A novel technique for fucoidan production should be put into consideration; it is enzymatic synthesis. Heterologous expression of the enzymes involved in its biosynthesis in a bacterial cell line could open new chances to produce a high-quality and homogenous engineered fucoidan *in vitro* instead of classical extraction from its biogenic resources. The research in **Chapter 4** aimed to clone some genes from the brown macroalga *E. siliculosus* to heterologous express their corresponding enzymes that are involved in fucoidan biosynthesis in *E. coli* BL21 (DE3) (e.g., FucTs and STs)

2. Optimization of Fucoidan Extraction and Purification from Brown Macroalgae

2.1. Introduction

2.1.1. Definition and functions

Fucoidan is defined as a class of fucose-rich, water-soluble and sulphated homo- or heteropolysaccharides or fucose-containing sulphated polysaccharides (FCSPs) as it is commonly abbreviated. It exists mainly in the fibrillar cell walls and intercellular spaces especially of brown seaweeds (Phaeophyta) [65], urchins and marine invertebrates as well. It presumably functions in brown algae as a cross linker between cellulose and hemicellulose, and therefore is always accompanied with the polyphenolic phlorotannin to give the cell wall its integrity. Moreover, it has other roles in cell polarity and development, cell-to-cell communication and brown macroalgae defense mechanism, as shown in **Fig. 4** [46,72]. Furthermore, fucoidan content was observed to be greatly affected by seasonal variations and tides level in the same organism, suggesting a possible protection role against organism desiccation [58,73,74].

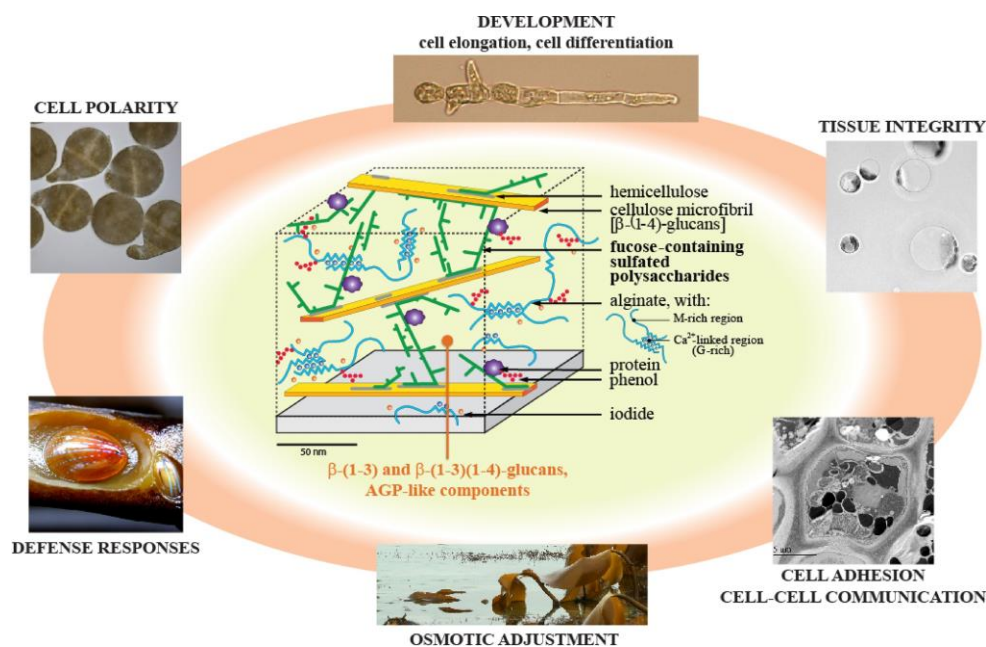


Fig. 4: Cell wall model in a brown macroalgae showing various fucoidan physiological functions

Fucoidan is involved in cell wall integrity, cell development, cell polarity, organism defense mechanism, osmotic adjustment and cell-to-cell communication [46].

In 1913, the Swedish scholar Kylin isolated fucoidan as a polymer of fucose for the first time (or fucoidin as he named it at this time) during his researches in the field of sea algae and fucosan content in different *Fucus* and *Laminaria* sp. extracts [75,76]. According to ISI web of knowledge (Clarivate Analytics), researches performed on fucoidan were scarce till 1980s. However, interest in fucoidan as a drug candidate has dramatically increased in the last few decades due to its chemical diversity, cheap and available resources and promising pharmacological activities, as shown in **Fig. 5**. This interest has resulted in 1833 published articles till July 2017 dealing with various aspects of fucoidan.

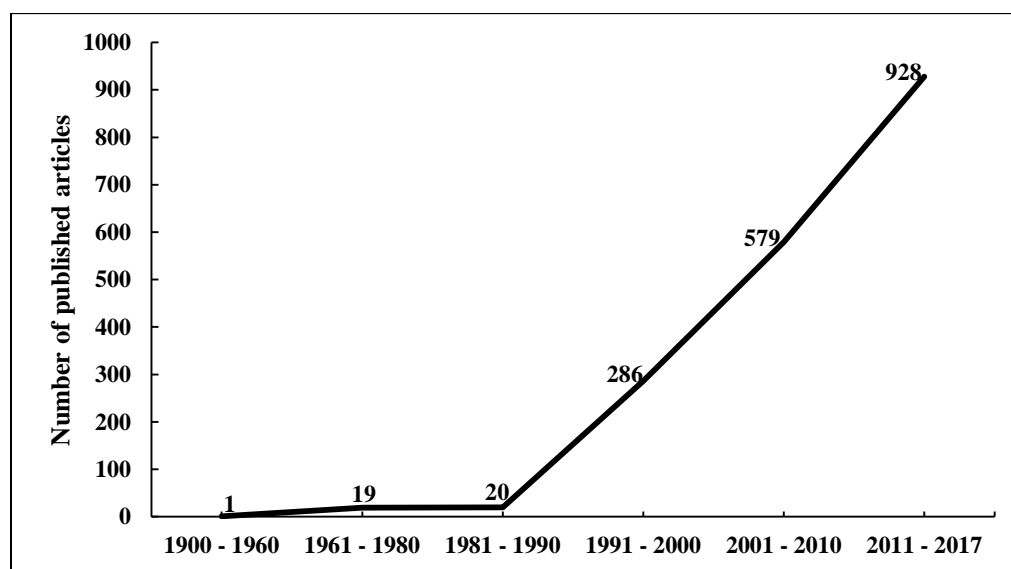


Fig. 5: Published articles on fucoidan since 1900 till July 2017, according to ISI web of knowledge (Clarivate Analytics)

It shows that a great interest has drawn in fucoidan since 1990s.

2.1.2. Fucoidan chemistry

Structural complexity and homogeneity of isolated fucoidan vary with its biological origin, for example; fucoidan of seaweeds showed commonly branching and more sulphated backbone with the presence of sugar monomers other than β -L-fucose. However, marine invertebrates' fucoidan such as sea cucumber is more simple, homogenous and composed of a linear-chain of repeating units [46,77,78]. These differences resulted in multiple biological activities of seaweeds' fucoidan making them a more preferable biogenic resource than marine invertebrates [79].

Literally, Cumashi *et al.* proposed that seaweeds' fucoidan is composed mainly from either α -(1-3) or alternating α -(1-3) with α -(1-4)-linked sulphated linear or branched L-fucopyranoside backbone, based on their study of the chemical structures isolated from different brown seaweeds species. Other

sugar units could be also present like mannose, xylose, galactose or even glucose in addition to uronic acids, but their positions and binding mode are still unclear. In addition, its fundamental subunit L-fucose is further mono- or di- sulphated or acetylated imparting a negative charge and anionic character on fucoidan molecular structure [14]. As shown in **Fig. 6**, fucoidan's chemical structures are between the different species of brown seaweeds and heterogenous regarding monomeric composition, glycosidic linkages and sulphation pattern. Moreover, its chemical structure might be affected by the applied extraction methods with the same organism [65,76].

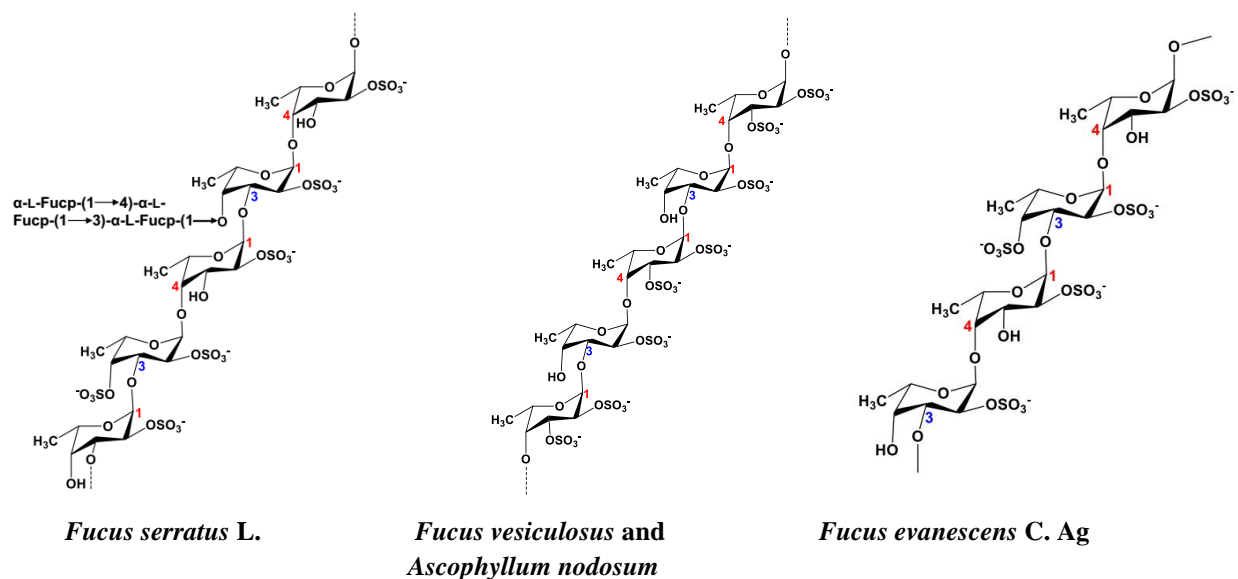


Fig. 6a: Different chemical structures of fucoidan from some Fucales seaweeds [65]

They showed an alternating α -(1-4) and α -(1-3) linked L-fucopyranoside backbone. C-2 is usually substituted with sulphate ester groups in addition to alternating C-3 or C-4 in L-fucopyranoside residue, according to the glycosidic linkages. In addition, branched chain polymers could be also found as in *F. serratus*. Other minor sugar units (e.g., mannose, galactose ...etc..) share in fucoidan structure in certain unknown positions [14].

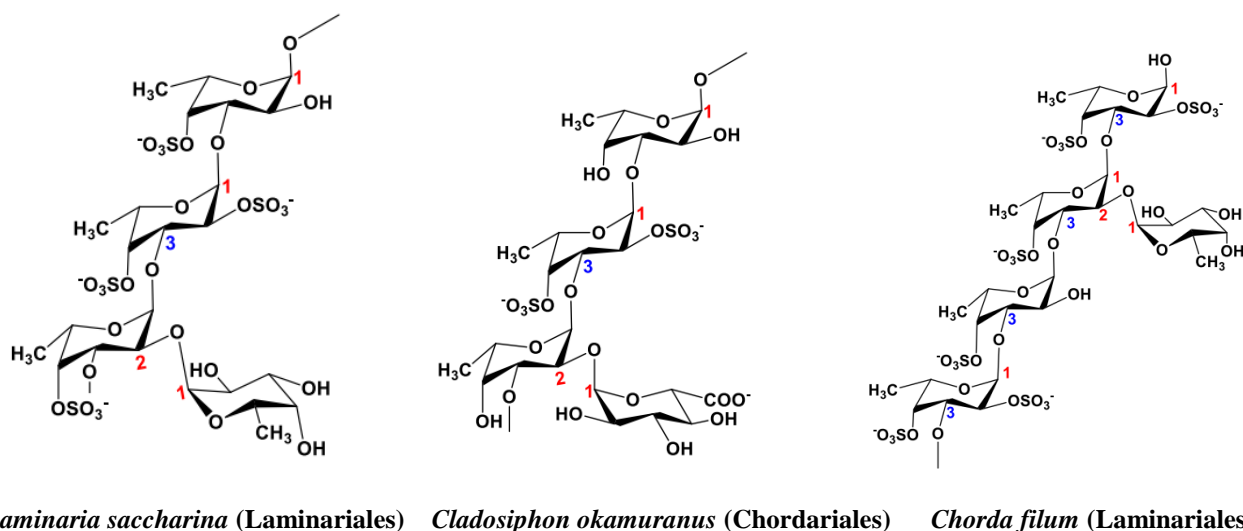


Fig. 6b: Chemical structures of fucoidan from some Laminariales and Chordariales seaweeds [65]

Both orders show repeated α -(1-3) linked branched L-fucopyranoside backbone at C-2. Sulphate ester groups substitute mainly C-4 and sometimes C-2.

Due to its complex chemical structures, several spectroscopical methods (e.g., FTIR, NMR and MS) have been used to elucidate its structural features including position of sulphate groups, glycosidic bonds and molecular weight. Furthermore, application of regio- and stereo-selective enzymatic degrading fucoidanases isolated from marine bacteria provided new insight into the chemical structure of fucoidan [43,74].

2.1.3. Methods of extraction

Since fucoidan is a water soluble polymer and insoluble in ethanol, aqueous extraction then its precipitation with ethanol are always applied. However, the process is not as simple as expected, due to the presence of fucoidan with many other intercalating components of the cell wall matrix (e.g., cellulose, hemicellulose, alginates, laminarin ... etc.). A standard extraction protocol for fucoidan has not yet been established, and therefore, different procedures at different pHs and temperatures, were applied to let protons or hydroxide ions to interfere with hydrogen bonds and then destruct the cell wall's matrix liberating fucoidan from the other polymers to the extraction medium [44,65,78,79]. These trials aimed to optimize extraction conditions and included extraction with hot or cold [80], acidic water (pH 2.0 - 2.3) [81], and alkaline water [82]. Using of CaCl_2 was observed to be also advantageous during extraction for precipitation of alginate as Ca-alginate [46].

Recently, other novel extraction methods were applied utilizing hydrolytic enzymes (e.g., laminarinase, alginate lyase) under moderate conditions (EAE) [79,83], ultrasound (UAE) [84,85], and microwave (MAE) [86,87] for improving the rate, yield and selectivity. These techniques have also succeeded to eliminate the usage of chemicals and harsh extraction conditions and maintain the native nature of fucoïdan.

For a more effective extraction, a pre-treatment step for the algal biomass after collection from beaches and coasts was performed. It included the removal of algal pigments (e.g., chlorophyll and fucoxanthin), lipids and other extraneous compounds which might co-extracted with fucoïdan. This process included the treatment with acetone, methanol or methanol:chloroform:water (4:2:1) [79,88,89].

2.1.4. Purification

Even after pre-treatment, extraction of fucoïdan from either brown macroalgae is, in most cases, accompanied with co-extracted contaminants (e.g., alginate, proteins, polyphenols,...etc.) and needs a purification step later on [79]. The presence of such impurities influences the biological activities of FCSPs, and therefore, it may delay full understanding of the biological activity of FCSPs [89] and physico-chemical properties as well. According to the ISI web of knowledge (accessed on 12.09.2017), only 95 published articles discussed the process of fucoïdan purification from crude brown algae extracts, despite the word fucoïdan was mentioned in 1865 articles representing 5% of the published articles. This survey indicated the difficulty and complexity of fucoïdan purification by the available techniques and the need for other simpler novel techniques. Common examples of purification are described in the following sections.

2.1.4.1. Exchange-based purification (Ion exchange chromatography, IEX)

Anionic properties of fucoïdan are involved in all techniques applied in fucoïdan purification. Anionic resins (e.g., Diethylaminoethyl-cellulose (DEAE-C) or Diethylaminoethyl-sepharose) are usually applied, where negatively charged fucoïdan can be exchanged with negative ions bound on the positively charged quaternary amino group of the diethylaminoethyl [88,90]. For fucoïdan elution, a gradient concentration of NaCl is applied resulting in different fractions of fucoïdan with different molecular weight, sulphate content and variables biological activities.

Disadvantages of this technique included contamination of eluted fucoïdan with high percent of NaCl and other small anionic compounds that could be ionized at used pH such as amino acids,

alginate and polyphenols. These contaminants required a further chromatographic step with GPC technique to remove them. Both chromatographic steps led to increase the costs of purification process. Furthermore, resins to be re-used, it should be regenerated making the process more tedious and time-consuming [91].

2.1.4.2. Biologicals-based affinity chromatography

Biologicals were also successfully applied as a tool for fucoïdan purification, such as anti-thrombin III and heparin co-factor II, depending on the binding affinity of fucoïdan in performing its anti-coagulant function. These compounds were immobilized on concanavalin A-Sepharose and were applied to purify fucoïdan [92]. More recently, fucoïde-specific lectins were applied in a single step to capture fucoïdan similarly to fucoïde-containing proteins [43,93]. However, these techniques suffered also from several disadvantages, such as high expenses and inability of lectins to identify masked fucoïde units due to sulphate ester groups [94].

2.1.4.3. Metachromasia-based affinity chromatography

Thiazine cationic dyes (e.g., methylene blue and toluidine blue) are well-known in cell and tissue staining based on a metachromatic change from its blue to purple colour [95]. Moreover, analytical methods for detection and quantification of anionic polysaccharides were well-established through the formation of a charge transfer complex [96,97,98]. Hahn, *et al.* described the interaction between toluidine blue and the sulphated polysaccharide fucoïdan, that it is strong enough and not only driven by ionic interaction, but also by disperse interactions between the stacked dye molecules [94,98]. In addition, TB was immobilized successfully on an amino derivatized Sepabeads® EC-EA by an innovative immobilization protocol through a glutaraldehyde bridge, as shown in **Fig. 7**. Furthermore, the adsorption kinetics and the binding capacity of the resin were analyzed. A Sips model was used to approximate the adsorption isotherm, resulting in a maximum loading capacity of 127.7 mg fucoïdan per g adsorbent [94]. TB-immobilized adsorbent could capture fucoïdan in a cheaper, in comparison with IEX-GPC and immobilized biologicals, from a synthetic raw extract, in which similar substances to that present in the crude algal extract, such as lactose.H₂O, gluconic acid, gallic acid, and of BSA, were incorporated [94]. Yet, this procedure has not been investigated in crude fucoïdan extracts.

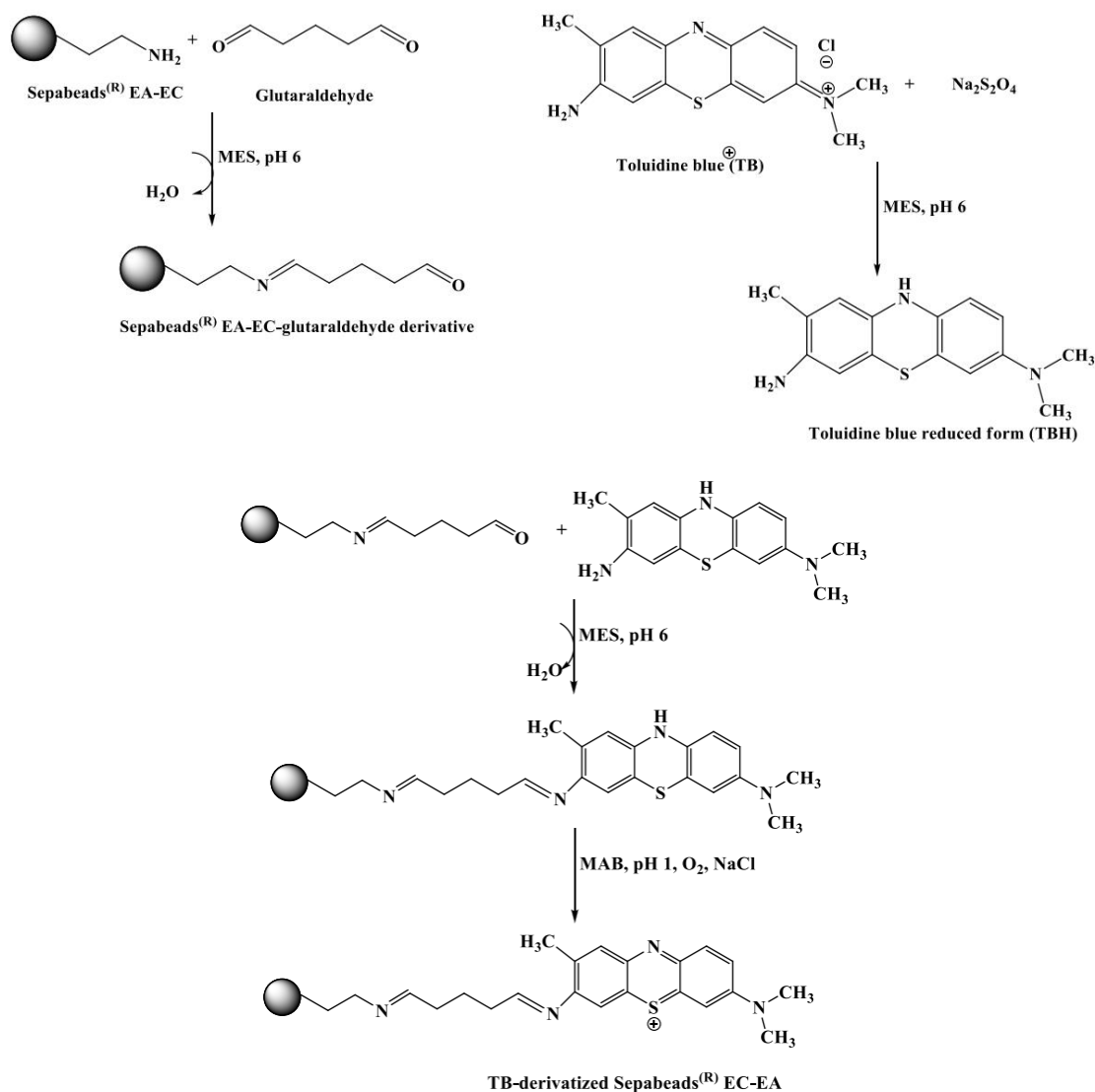


Fig. 7: Steps of TB immobilization protocol on amino derivatized Sepabeads[®] EC-EA [94]

The protocol involved derivatization of the beads with glutaraldehyde, then a nucleophilic attack on carbonyl group of Sepabeads[®] EC-EA-glutaraldehyde derivative was performed by TB in the presence of $\text{Na}_2\text{S}_2\text{O}_4$. Finally, a step of oxidation at highly acidic pH produced the final form of the TB-derivatized beads.

2.1.5. Fucoidan from *F. vesiculosus* or bladder wrack

As an example of fucalcan fucoidan is the fucoidan isolated from *F. vesiculosus* or as commonly named bladder wrack. It is classified as GRAS substance and produced by many companies, such as Marinova (Maritech[®]) [99] and Sigma-Aldrich[®]. In comparison with the other fucoidan isolated from different brown algal species, it is characterized by its relatively simpler chemical structure. It

is composed of 44.1% fucose, 26.3% sulfate and 31.1% ash, in addition to a little aminoglucose [43]. As shown previously in **Fig. 6A**, it is composed from repeating alternating α -(1-3)- with α -(1-4)-linked L-fucopyranose units [14]. Therefore, fucoidan from *F. vesiculosus* was chosen as a model product for this work.

F. vesiculosus inhabits the littoral zone, where the tide changes the depth of the water, and the sublittoral zone, where the organism is constantly submerged around the north Atlantic, in more temperate waters with lower salinity for four to five years old, as shown in **Fig. 8** [100]. In Nordic countries, two types of cultivation are available; onshore cultivation, where cultivation is established in tanks which is more expensive and offshore cultivation, where the cultivation is placed in the ocean with optimization of growth conditions. It is also possible to create the right conditions on the seabeds at intertidal, sheltered place with a wild population to settle and grow [101].



Fig. 8: Habitat of *F. vesiculosus* or bladder wrack across the north Atlantic in more temperate zone [100]

As a marine plant, the organism shows a number of morphological adaptations, such as the presence of a root-like structure holdfast which anchor the thallus to hard substrata such as pebbles, rocks, and dense seabeds. Moreover, fronds survive against sea waves by a flexible stipe and kept near to the water surface by means of vesicles or air bubbles found in lamina blades to continue the photosynthetic process. Fronds have also conceptacles at their tips which contain either one of the reproductive structures; antheridia or oogonia, as demonstrated in **Fig. 9**. Furthermore, taxonomy of *F. vesiculosus* could be described as followed in **Table 2** [102,103].

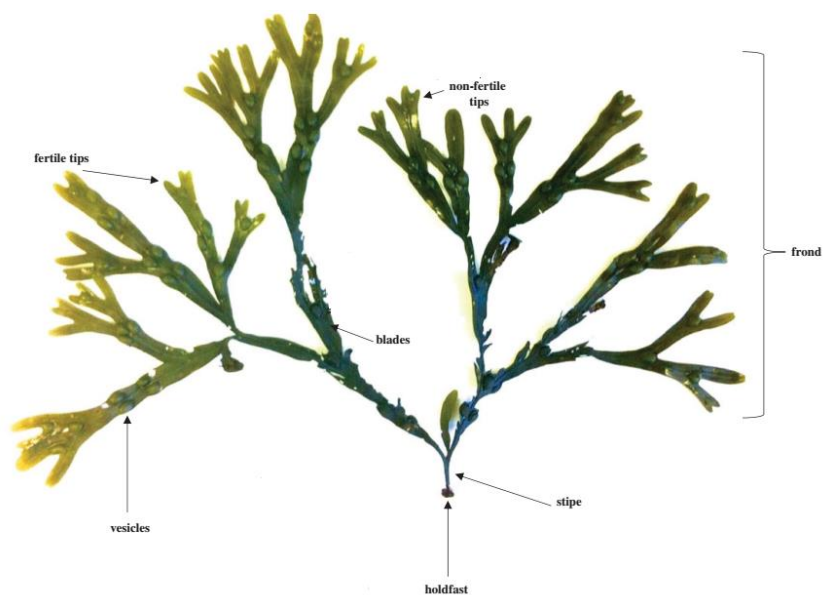


Fig. 9: Morphology and anatomical parts of *F. vesiculosus* thallus (modified after [103])

Table 2: Taxonomy of *F. vesiculosus* [102,103]

Empire	Eukaryota
Kingdom	Chromista
Phylum	Ochrophyta
Class	Phaeophyceae
Subclass	Fucophycidae
Order	Fucales
Family	Fucaceae
Genus	<i>Fucus</i>
Species	<i>vesiculosus</i>

2.2. Material and Methods

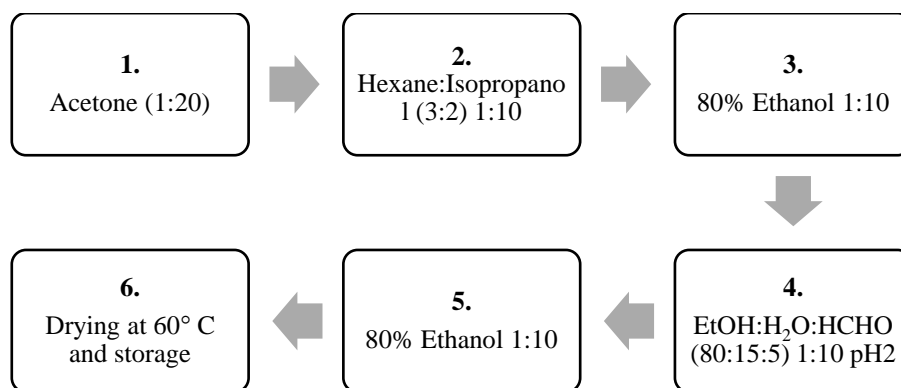
2.2.1. Algae harvesting and pre-treatment

Fresh algal biomass of *F. vesiculosus* was harvested from the North Sea at the region of south beaches of Wilhelmshaven (Germany, 53°31.236N, 8°13.849E), as seen in **Fig. 10**. The algal biomass was washed with tap, and then deionized water, air-dried for few days, then in the drying oven at 50 °C until giving a constant dry weight, and milled afterwards. The milled algal powder was stored in a plastic container at room temperature.



Fig. 10: Growth of the brown macroalgae *F. vesiculosus* at the south beaches of Wilhelmshaven (North Sea, 53°31.236N, 8°13.849E, Germany)

Before the extraction step and in a ration of 1:10 between the algal biomass and used solvent, except acetone step was 1:20, 10 g of a dried algal biomass were handled by several pre-treatment steps successively in a shaker incubator (Infors HT Ecotron) at a constant shaking rate (100 rpm) for overnight each at 25° C with of acetone, hexane : isopropanol (3:2), 80% (v/v) ethanol, ethanol : water : formaldehyde (80:15:5) at pH 2.0, and finally washed again with 80% (v/v) ethanol. After each step, the suspension was centrifuged (4000 rpm, 10 min) by a bench centrifuge, and the supernatant was decanted. The pretreated algal powder was then dried again at 60 °C and stored at room temperature in a well-closed plastic container. **Scheme 1** demonstrates an overview of the major steps of pre-treatment.



Scheme 1: Overview of pre-treatment steps of the dried algae biomass before fucoidan extraction

Steps were performed in a ration of 1:10 between the algal biomass and solvent, except acetone treatment in a shaker incubator a dusted at a constant rate (100 rpm) for overnight each at 25° C.

2.2.2. Optimization of fucoidan extraction

In an extraction set composed of a silicone oil bath over a magnetic heated stirrer and supplied with a thermometer and a temperature control device, as seen in **Fig. 11**, extraction was performed from the pre-treated *F. vesiculosus* biomass.

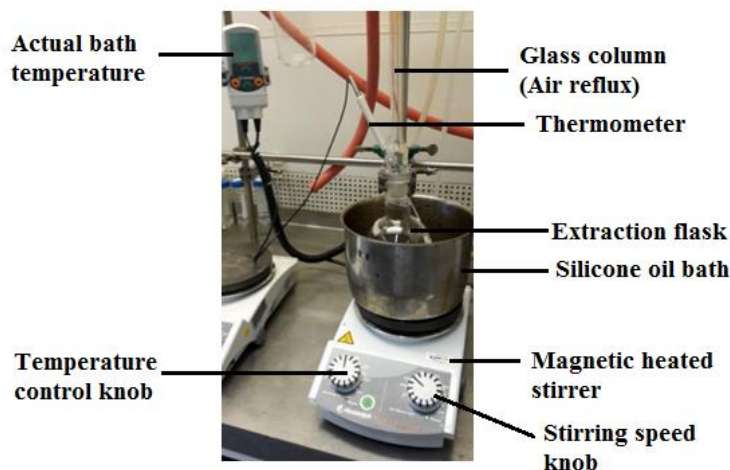


Fig. 11: Extraction set of fucoidan from dried pretreated *F. vesiculosus*

It shows an oil bath on heated magnetic stirrer and provided with a temperature control and thermometer. An air reflux column was applied in extraction Procedure A and B.

Three methods for fucoidan extraction were applied; Procedure A, B and C, which resulted in production of four fractions of crude fucoidan. Procedure A was performed by exhaustion for two times of 7 g of the pre-treated powder with 70 mL of 1% (w/v) aqueous CaCl₂ for 6 h at 70 °C using

a reflux and continuous stirring (500 rpm) at pH 2.0, as described previously by Hahn, *et al.* [94]. The pH was adjusted regularly every 1-2 h at 1 by 1 M HCl, as necessary. After centrifugation (4500 rpm, 15 min), the algal biomass was removed and the supernatant was neutralized to pH 6.0 by 2.0 M ammonium carbonate. Crude fucoidan was then isolated via precipitation by ethanol at a final concentration of 70% (v/v), cooling overnight at 4 °C, centrifugation, and then drying of the precipitate at 50 °C resulting in **Fucoidan_A** production. However, Procedure B administered 1% (w/v) CaCl₂ in 20 mM MAB at pH 1 as an extraction solvent. The extraction was carried out using the same conditions previously mentioned in Procedure A. Centrifugation was then used to separate the supernatant from the algal biomass. The supernatant containing **Fucoidan_B** was stored afterwards at 4 °C until the next step of purification. Procedure C was also performed at moderate conditions at pH 2.7 at 42 °C for 3 h without reflux. **Fucoidan_40%** and **Fucoidan_70%** crude fucoidan fractions were isolated by precipitation with 40% (v/v) and 70% (v/v) ethanol, respectively. As an overview for the extraction process and isolated crude fucoidan, **Fig. 12** illustrated the whole process.

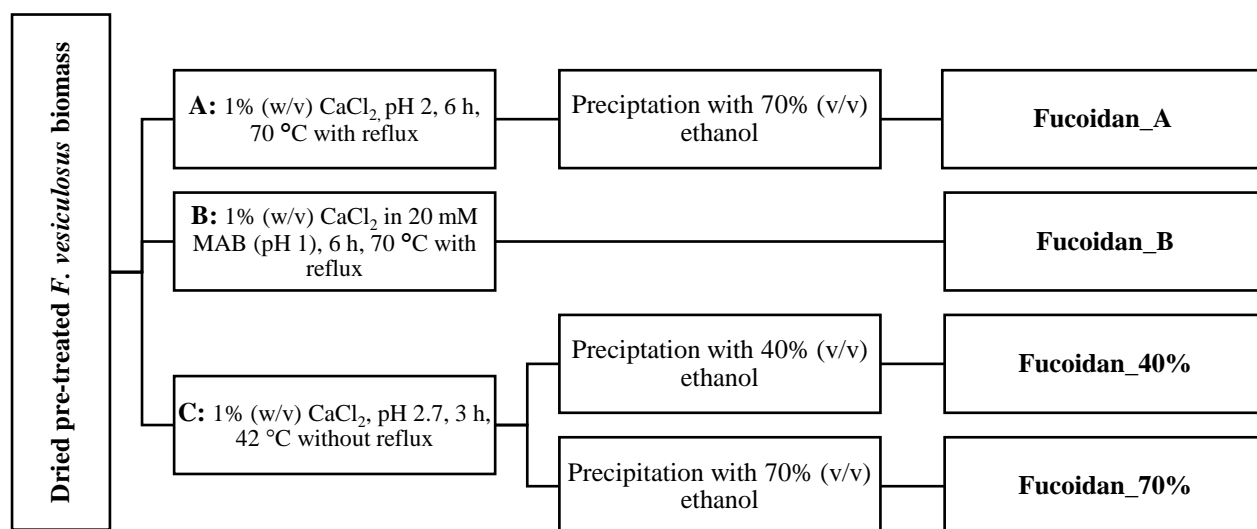


Fig. 12: Overview of fucoidan extraction process from pre-treated *F. vesiculosus* biomass and obtained crude fucoidan

Different fractions of crude fucoidan were isolated; namely **Fucoidan_A**, **Fucoidan_B** and **Fucoidan_40%** and **Fucoidan_70%**.

2.2.3. Quantitative assay for crude fucoidan fractions' contents

Aqueous crude fucoidan solutions; **Fucoidan_A**, **Fucoidan_(40%)** and **Fucoidan_(70%)** were prepared in a concentration of 1 mg mL⁻¹ and several contents were quantified (e.g., sugar, fucoidan, fucose and free sulphate contents) as described in the following sections.

2.2.3.1. Sugar content

According to Dubois and Holtkamp, Dubois or Phenol-Sulphuric acid assay was performed [104,105]. At the beginning, 200 µL of each solutions were mixed with 200 µL of a 5% (w/v) phenol solution gently in a 1.5 mL reaction vessel. Afterwards, 1 mL of concentrated sulphuric acid was added carefully and gently. After 10 min, the samples were mixed vigorously for about 15 sec and 30 min later at room temperature, the absorbance was measured at 490 nm by a Uv/Vis-spectrometer. Different concentrations (0.025 - 0.25 g L⁻¹) of aqueous glucose solution were measured as standards.

2.2.3.2. Fucoidan content

Toluidine blue assay was performed according to Hahn, *et al.* [98]. Briefly, 10 µL of fucoidan containing solutions were mixed with 990 µL of 0.06 mM TB which was prepared in 20 mM MAB (pH 1) for a better reaction sensitivity. Absorbance was afterwards measured at 632 nm using the aqueous solution of commercially-available fucoidan (>95% pure) purchased from Sigma-Aldrich[®] as a reference standard in a concentration range of 0 - 2.5 g L⁻¹.

Moreover, Heparin Red[®] Ultra assay, according to Wartinger, *et al.*, was carried out for **Fucoidan_A** [106] after some modifications. In brief, 5 µL of the fucoidan-containing sample were pipetted into a 96 microplate well. Then, 180 µL of Heparin Red[®] Ultra solution was added as quickly as possible. The microplate was immediately placed in the fluorescence microplate reader adjusted at an excitation λ at 570 nm and emission was recorded at 605 nm with a spectral band width 13.5 nm and read height of 8 mm. Mixing was performed using the plate shaking function (setting "high", 1 min) and fluorescence was measured within one minute after mixing. Fucoidan from Sigma-Aldrich[®] was used as standard (0 – 8 µg mL⁻¹).

2.2.3.3. Fucose content

Dische or cysteine-H₂SO₄ assay was performed to quantify L-fucose content in hydrolyzed fucoidan solutions [105,107]. At first, 400 µL of crude fucoidan solutions were mixed with 1.8 mL diluted sulphuric acid (1:6). The mixtures were subsequently cooked in a silicone oil bath at 100 °C for a period of 10 min and the reaction was stopped by cooling in an ice bath. Thereafter, 40 µL of an

aqueous 3% (w/v) L-cysteine.HCl solution was added and the absorbance was measured at 396 nm and 430 nm. With the difference of those two measurements the influence of other sugars could be neglected. As a standard, aqueous L-fucose solutions were used in a concentration range of 0.03 – 0.21 g L⁻¹.

2.2.3.4. Free sulphate content

Using BaSO₄ assay, free or hydrolyzed sulphate ester content was determined [108]. In a 20 mM MAB (pH 2), aqueous 5 g L⁻¹ crude fucoïdan and 10% (w/v) BaCl₂ solutions were prepared. 250 µL of each crude fucoïdan solutions were mixed with 500 µL of 10% (w/v) BaCl₂. After incubation on ice for 15 min, absorbance at 600 nm was measured. A concentration range (0.1 - 0.6 g L⁻¹) of (NH₄)₂SO₄ was used as a standard for calibration.

2.2.4. Perylene diimide derivative synthesis (PDD)

Synthesis of the red fluorescent PDD was performed at the Institute of Inorganic Chemistry in Heidelberg University by Prof. Dr. Roland Krämer as described previously by Szelke, *et al.* [109]. In brief, 1,7-dibromoperylene-3,4,9,10-tetracarboxylic acid dianhydride was converted to the diimide derivative by reaction with *tris*-(*t*-Butoxycarbonyl) protected by tetraamine spermine. After deprotection with trifluoroacetic acid, the product was isolated as a trifluoroacetate salt.

2.2.5. Immobilization of thiazine dyes and perylene diimide derivative [108]

Thiazine dyes (e.g., toluidine blue and thionin acetate) and PDD were immobilized according to the protocol described by Hahn, *et al.* [94] on Sepabeads[®] EC-EA purchased from Resindion S.R.l, Italy. The beads are porous ethyl amino-derivatized polymethacrylate enzyme carrier [110]. Steps were described in details in **Appendix D: Protocols**.

2.2.6. Adsorption kinetics in crude fucoïdan

Applying the same conditions previously used in section 2.2.6, **Fucoïdan_A** instead of the commercial fucoïdan was incubated with 75 mg of TB- and PDD derivatized beads. After 1080, 1440, 2400 and 2640 min for immobilized TB, and 5, 60 and 960 min for immobilized PDD, a sample volume of 10 µL were analyzed by TB assay and percent of adsorbed fucoïdan was calculated based on the decrease in fucoïdan concentration in the incubation supernatant.

2.2.7. Fucoidan purification and optimization

2.2.7.1. Batch process

Immobilized TB and PDD were applied to purify fucoidan from the isolated **Fucoidan_A** crude fraction following Hahn's previously-described protocol which was applied in a raw synthetic extract [108]. Four phases were executed including adsorption, washing, elution and recovery of fucoidan from eluate. Briefly, 50 mg of derivatized beads in a 2 mL reaction vessel was incubated with 1.5 mL of 2.5 mg mL⁻¹ of crude fucoidan. Then, two steps of washing with deionized water and 0.1 M NaCl in 20 mM MAB (pH 2) and elution with NaCl prepared in 30% (v/v) ethanol in MES (pH 6) were performed. In more details, steps of fucoidan purification and recovery were described in **Appendix D: Protocols**. Moreover, Different factors which may affect fucoidan adsorption and elution were studied. At the same time, different purified fucoidan fractions were produced to investigate the effect of purification conditions on fucoidan's physico-chemical and pharmacological properties. These factors and isolated purified fractions were discussed in the following sections.

a. Incubation pH

Stock solutions of a 2.5 mg mL⁻¹ concentration were prepared in buffers of different pH values, such as 20 mM MAB (pH 1) and 20 mM MES (pH 6) to study the effect of incubation pH on percent capture and molecular weight of isolated fucoidan. The incubation with 50 mg of TB-derivatized beads produced **Fucoidan_1** and **Fucoidan_6** as a result from incubation at pH 1 and pH 6, respectively. However, purification with PDD-derivatized beads at pH 6 resulted in **Fucoidan_PDD**.

b. Type and molarity of thiazine dye

In addition to 2 mM of TB, TA was immobilized for a purpose of comparison. Moreover, different molarities of TB and TA (2, 4 and 6 mM) were immobilized on Sepabeads® EC-EA. Mixed beads were also applied to capture fucoidan. These factors were studied using the same condition applied in pH factor.

c. Presence of interferences and skipping of precipitation step

Fucoidan_B was purified by TB-derivatized beads using the same conditions. This step produced a fourth purified fraction; namely **Fucoidan_M**.

d. Quantity of derivatized beads

Derivatized beads (50 mg and 75 mg) were compared regarding their loading capacity for capturing fucoidan from crude **Fucoidan_A** in MES (pH 6).

e. Multiple use of beads

TB- and PDD-derivatized beads (75 mg) were used for two cycles to compare between beads' loading capacity for 44 h and 16 h, respectively. The 2nd cycle was performed after elution of adsorbed fucoidan from the 1st cycle.

f. NaCl molarity in eluent

Different eluents with 1, 2 and 3 M NaCl were prepared in 30% (v/v) ethanol in 20 mM MES (pH 6). All eluents were applied for 16 h using a thermoshaker at 50 °C and 800 rpm. NaCl molarity was investigated to show its relationship with eluted fucoidan (%) and fucoidan molecular weights.

2.2.7.2. FPLC process

For a scale-up and an automated purification process, a FPLC was used to establish a protocol that had the same optimized phases as in the batch process. 3.2 g of previously-conditioned with MES (pH 6) PDD-derivatized beads were packed in a glass column (XK 16/20, 72x16 mm, 4 cm³), then 1 mL of 50 mg mL⁻¹ in MES of crude **Fucoidan_A** fraction was injected. Afterwards, different flow rates and volumes were applied during the purification phases as shown in **Table 3**.

Table 3: Description of an automated fucoidan purification process by immobilized PDD using FPLC
 Different eluents with different flow rates and volumes were applied during the purification phases.

Step	Eluent used	Flow rate (mL min ⁻¹)	Step volume (mL)
Column conditioning	20 mM MES (PH 6)	1.0	15
Sample injection	50 mg.mL ⁻¹ Fucoidan_A in 20 mM MES (pH 6)	1.0	1.0
Adsorption	20 mM MES (pH6)	0.5	30
Washing	Deionized water	1.0	15
	0.1 M NaCl in 20 mM MAB (pH 2)	1.0	20
Elution	3M NaCl in 30% v/v ethanol in 20 mM MES (pH 6)	2.0	50

Effluents of 2 mL fraction were collected during flow through, washing and elution phases which analyzed by TB assay for fucoidan content. The process was repeated for two times. This process produced two further fractions of purified fucoidan which named **Fucoidan_PDD_1** and **Fucoidan_PDD_2** from the 1st and 2nd cycle, respectively. **Fig. 13** summarized the whole purification process and the different fractions obtained from crude fucoidan fraction.

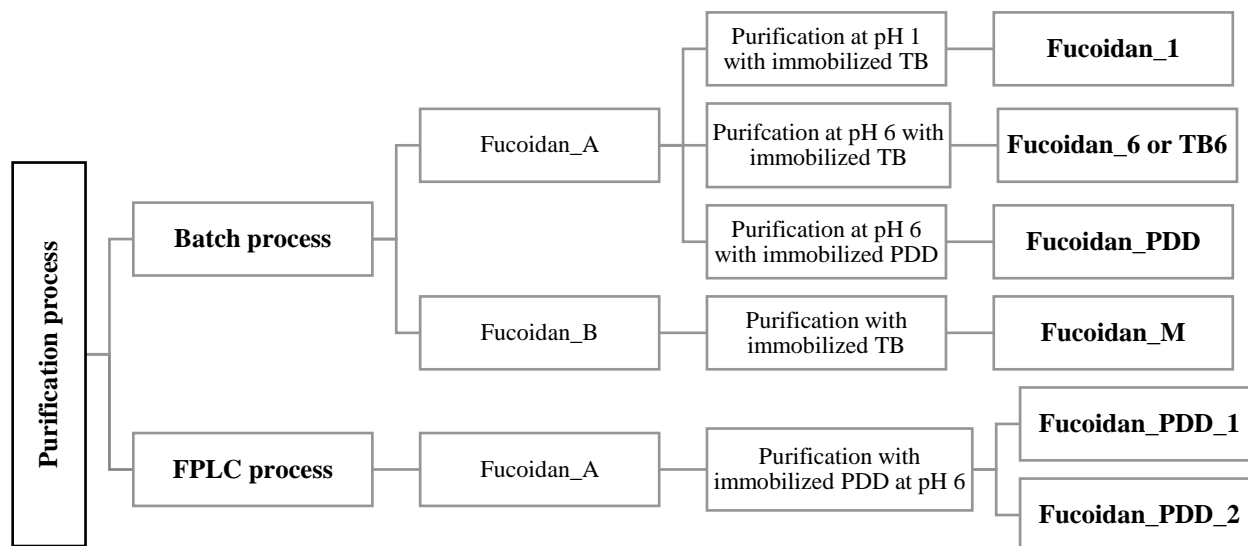


Fig. 13: Overview for isolated fractions of purified fucoïdan

Six fractions were obtained from crude fucoïdan using batch and FPLC processes.

2.2.8. Purified fucoïdan fractions characterization

2.2.8.1. Physico-chemical investigations

Several investigations were carried out to characterize the isolated purified fucoïdan fractions and evaluate the different studied factors in comparison with crude fucoïdan (**Fucoïdan_A**) and the commercially-available fucoïdan (>95%) purchased from Sigma-Aldrich® isolated from *F. vesiculosus*. These investigations were performed as described in the following sections.

a. Elemental (CHNS) analysis

Samples of 1.6 to 1.8 mg or higher, especially in case of low element percent values, in tin boats were combusted. Combustion gases were reduced by hot copper at 830 °C in the reduction oven, then separated in the absorption column into its single components by temperature programmed desorption and the components were transferred sequentially to the thermal conductivity detector. The processor unit calculated afterwards the element concentrations from the measured values and the sample weight based on an instrument calibration. Elemental analysis was performed by the elemental Vario Micro cube apparatus which was calibrated previously with sulphanilic acid.

b. Molecular weight parameters

Molecular weight measurements were performed using an isocratic HPLC-GPC system. Samples were dissolved in phosphate buffer (0.05 M Na₂HPO₄, pH 9.1) in a concentration of 4 mg mL⁻¹ and

then diluted with an equal volume of 1 mg mL⁻¹ ethylene glycol solution as a flow marker. Separation was performed at 25 °C using a GPC_MCX column, which was previously calibrated with dextran of GPC analytical standard grade of different molecular sizes (5.0-670 kDa). The injection volume was 10 µL and the volumetric flow rate 1 mL min⁻¹. The signal detections were performed using RI detector.

c. Melting point

Two mg of each fraction were placed in a capillary tube and placed in the melting point apparatus. Temperature increment was 2 °C min⁻¹ and three temperature points, at which solids started to melt, changed their colour to dark brown, and finally at complete decomposition with charring, were observed and recorded.

d. Specific optical rotation

An aqueous 0.4% (w/v) solution of each fucoïdan fraction was prepared and the specific optical rotation was measured at 22 °C by a digital polarimeter supplied with a sodium spectral adjusted at λ 589 nm.

e. Monomeric composition

Monomeric composition was determined according to protocols developed by Rühmann, *et al.* [111]. Briefly, 1 mg mL⁻¹ aqueous solution of each fucoïdan fractions was prepared and hydrolyzed with 2 M trifluoroacetic acid for 90 min at 121 °C. Sugar monomers were detected, afterwards, as PMP derivatives with a HPLC-UV-ESI-MS system. Tempered column to 50 °C, an autosampler to 20 °C, a flow rate of 0.6 mL min⁻¹ and an injection volume of 10 µL were used. Mobile phase A and B consisted of 5 mM CH₃COONH₄ (pH 5.6) with 15% acetonitrile and pure acetonitrile, respectively. The gradient was programmed as following: start of mobile phase B at 1% (v/v), with increase to 5% over 5 min, hold for 2 min, with following increase to 18% over 1 min. The gradient was further increased to 40 % over 0.3 min, hold for 2 min and returned within 0.2 min to starting conditions for 1.5 min. Before entering ESI-MS the flow was splitted 1:20. Fucoïse, xyloïse, and galactose were detected by the diode array detector, while glucose and uronic acid dimers were detected by MS detector.

f. FT-IR spectrometry

Two to three mg of desiccated fucoïdan fractions were transferred to FT-IR lens and scanned between 4000 - 650 cm⁻¹. Measurements were applied to identify and characterize fucoïdan fractions in comparison with reference fucoïdan.

g. $^1\text{H-NMR}$

Few mg of each samples were dissolved in D_2O to give 5 mL of clear solutions. The samples were scanned at 80°C by a 400 MHz NMR spectrometer.

2.2.8.2. Pharmacological investigations

a. Anti-coagulant activity

Anti-coagulant studies were performed using the blood coagulation system (BCS[®] System) which was completely programmed to mix, pre-warm and incubate the reaction contents at 37°C in addition to measure the coagulation time in s. The experiments were repeated for three times using platelet-poor plasma isolated from healthy patients' blood, reagents purchased from Siemens Healthcare Diagnostics Products GmbH, 0.9% (w/v) NaCl as a negative control and $0.005\ \mu\text{g mL}^{-1}$ as a positive control. Fucoidan fractions were dissolved in an isotonic solution of 0.9% (w/v) NaCl. **Fucoidan_1**, **Fucoidan_6**, **Fucoidan_M** were investigated at a concentration of $0.01\ \text{mg mL}^{-1}$. However, **Fucoidan_PDD** was investigated in a dose-response manner in concentration ranges of $0.01\text{-}0.1\ \text{mg mL}^{-1}$ in aPPT and $0.001\text{-}0.05\ \text{mg mL}^{-1}$ in TT investigations.

i. *Activated Partial Thromboplastin Time (aPTT)*

According to the protocol described by Anderson, *et al.* [112] with few modifications. With each fucoidan fraction, 0.6 mL of plasma was mixed with 0.3 mL of fucoidan solutions. The mixture was then introduced to the blood coagulation system which was programmed to incubate it for 60 s, add 0.5 mL of pre-warmed Pathrombin[®] SL reagent and incubate again for 5 min at 37°C . Afterwards, 0.6 mL of a pre-warmed 0.25 M CaCl_2 solution was added and the time for clot formation recorded. In a dose-dependent method, 50 μL of each spiked **Fucoidan_PDD** platelet-poor plasma solution were mixed equally with Pathromtin SL[®] reagent, incubated then for 2 min, 50 μL CaCl_2 solution was added and the coagulation time recorded. According to the provider, Pathrombin[®] SL reagent consisted of silicon dioxide particles ($1.2\ \text{g L}^{-1}$), plant phospholipids ($0.25\ \text{g L}^{-1}$), NaCl and HEPES (pH 7.6).

ii. *Prothrombin Time (PT)*

PT was determined following the protocol of Quick [113] with some modifications. The blood coagulation system was also programmed to perform the same procedure mentioned previously in APTT determination, but each plasma and fucoidan solution mixture was incubated for 3 min. Afterwards, 0.6 mL pre-warmed Dade[®] Innovin[®] reagent was added and the time for clot formation

was observed. Dade[®] Innovin[®] reagent was a lyophilized product of recombinant human tissue factor and synthetic phospholipids (thromboplastin), calcium ions, a heparin-neutralizing compound, buffers and stabilizers (BSA), as provided by the producer.

iii. Thrombin Time (TT)

TT was measured applying the protocol described by Denson and Bonnnar [114] with some modifications. In a ratio of 3:1, 0.6 mL of plasma was mixed with 0.2 mL of fucoidan solutions. Each mixture was then incubated for 3 min before the addition of 0.2 mL pre-warmed BC Thrombin Reagent (BC THROMBIN) and the time for clot formation was recorded. In addition, 50 μ L of pre-warmed **Fucoidan-PDD**-spiked plasma at different concentrations were mixed with 100 μ L Thrombin Reagent and the time for the coagulation was measured. BC Thrombin Reagent consisted of lyophilized bovine thrombin (≤ 0.8 IU mL⁻¹) and bovine albumin in HEPES (pH 7.4), according the product's data sheet.

b. Anti-viral assay

The anti-viral activity was carried out against a representative of the double stranded DNA (dsDNA) viruses; Herpes Simplex virus-type 1 (HSV-1). The screening assay was based on modified Kleymann and Werling's Tissue Culture Infection Dose 50 (TCID₅₀) protocol for anti-viral candidates [115]. Briefly, a stock solution of 5 mg mL⁻¹ of different fucoidan fractions were dissolved in PBS (pH 7.4), while aciclovir as 10 mM in DMSO. The IC₅₀ was determined using a two-fold serial dilution in the range of 0.2 - 100 and 0.054 - 28 μ g mL⁻¹ for fucoidan solutions and aciclovir, respectively. Each well contained 10,000 cells of Vero B4 cells (50 μ L of a solution with 2×10^5 cells mL⁻¹ provided in Roswell Park Memorial Institute medium (RPMI) containing 10% fetal calf serum (FCS) and penicillin/streptomycin (PS), 50 μ L pathogen with 5 to 500 CFU of HSV-1 (strain HF ATCC-VR-260), the final volume of each well was then completed to 200 μ L by the culture medium. Negative controls were performed by mixing 50 μ L of pathogen, 50 μ L cell suspensions, and 100 μ L medium. After the respective incubation period, the wells of the microplate were washed with 200 μ L PBS and then filled with 200 μ L 10 μ g mL⁻¹ fluorescein diacetate prepared in PBS. Fluorescein diacetate is a non-fluorescent dye and widely used to count viable cells and analyzes their vitality, where viable cells are able to convert the dye enzymatically by a cellular esterase activity releasing the fluorophore from the quenched dye. After 45 min of incubation at room temperature, RFU was measured using 485 nm for excitation and 538 nm for emission.

c. Anti-microbial activity

With the same principle applied in the anti-viral assay, anti-fungal and anti-bacterial activities of fucoidan fractions were investigated. In anti-fungal activity, *Candida albicans*, *C. tropicalis* and *C. glabrata* were chosen as fungal representatives in Vero B4 cell line and amphotericin B was used as a positive control, while *S. aureus* as a Gram +ve and *E. coli* as a Gram –ve in HeLa and CHO-K1 cell lines were used to detect the anti-bacterial activity of fucoidan fractions. The activity investigation applied ciprofloxacin as a bench marker.

d. Free-Radical scavenging anti-oxidant activity

According to Mensor [116] and Paul [117], with some modifications, 2 mL of a freshly prepared methanolic DPPH solution (0.1 mM) was mixed with 0.1 mL of a serial dilution of aqueous fucoidan fraction solutions in a concentration range of 25 - 1000 µg mL⁻¹. The mixtures were incubated at room temperature in a dark place for 30 min, before absorbance measuring with Uv/Vis-spectrometer at 517 nm. Ascorbic acid (6.25 - 200 µg mL⁻¹) was used as a reference. The percent scavenging activity of each fucoidan fraction in addition to ascorbic acid was calculated applying **Eq. 1**.

$$\% \text{ Scavenging activity} = 100 - [(Abs_{\text{sample}} - Abs_{\text{blank}}) \times 100] / Abs_{\text{control}} \dots\dots\dots \text{ (Eq. 1)}$$

Where;

- Abs_{sample} is the Absorbance of fucoidan solution at each concentration
- Abs_{blank} is the Absorbance without DPPH
- Abs_{control} is the Absorbance without fucoidan

2.2.9. Process scaling-up and application of optimized conditions

Starting with 100 g of a dried biomass of *F. vesiculosus*, pre-treatment was performed. Then, the resulted pre-treated biomass was extracted as described previously in Procedure A. Procedures for fucoidan purification and recovery were carried out at the optimized conditions by incubation of both TB- and PDD-derivatized beads (75 mg) with 1.5 mL of the stock solution (2.5 mg mL⁻¹) of **Fucoidan_A** prepared in 20 mM MES (pH 6). The process was performed in a 2 mL reaction vessel at room temperature for 40 h for TB- and 16 h for PDD-deivatized beads, and placed in an overhead shaker adjusted at 30 rpm. The beads were then washed with water and 0.1 M NaCl in 20 mM MAB at pH 2, successively for 3 h and 5 h, respectively. Fucoidan was eluted with 1.5 mL of 3M NaCl

dissolved in 30% (v/v) ethanol in a 20 mM MES (pH 6) with vigorous shaking (800 rpm) at 50 °C for 16 h. To recover fucoidan, a rotary evaporator was utilized to concentrate the eluate and remove ethanol as well (60 °C, 90 mbar). Concentrated solution was then dialyzed using a dialysis membrane with a 3.5 kDa MWCO. During this procedure, deionized water was changed periodically every 2 h and conductivity was measured by a conductivity meter set until the resulting solution had the same conductivity value as deionized water. Finally, freezing at - 20°C for overnight, then lyophilization in a freeze dryer for 48 h adjusted at - 20° C and 1.03 mbar were carried out to obtain a fluffy white product.

2.3. Results and Discussion

2.3.1. Pre-treatment, extraction and preparation of crude extract

Fucoïdan content in *F. vesiculosus* is affected by seasonal and geographical factors and represents a minor component, in relation to other carbohydrates [79,118,119], as shown in **Fig. 14**. Therefore, several steps of pre-treatment were carried out to remove extraneous matters (e.g., mannitol, lipids, polyphenols, etc.), which might be co-extracted with fucoïdan and interfered afterwards with purification processes [120,121].

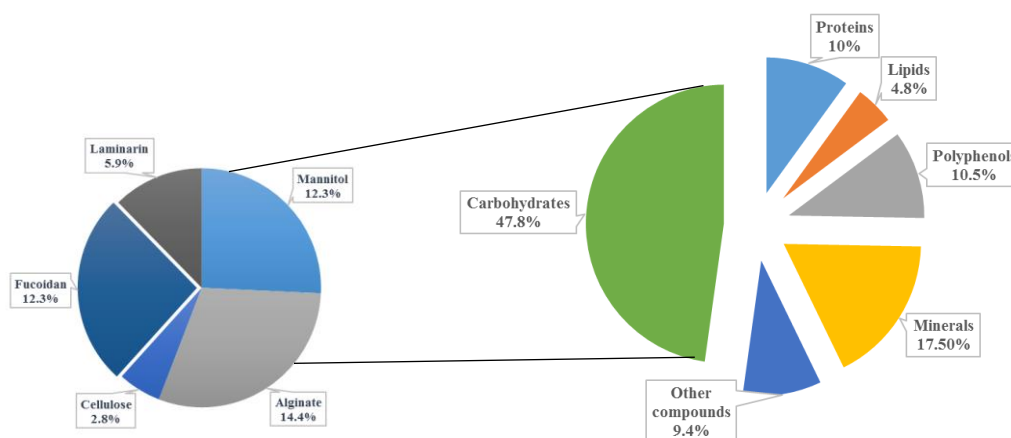


Fig. 14: Average composition of the dried biomass of *F. vesiculosus* [79]

It shows that fucoïdan content represents approx. 12% w/w of the dried algal biomass.

Acetone was applied to remove thallus pigments (e.g., chlorophyll), and non-polar fatty acids, while a hexane/isopropanol mixture removed lipids and more polar fatty acids. An 80% (v/v) ethanol was used to get rid of the major reserve food material mannitol for the algae. An ethanol/water/formaldehyde mixture at pH 2 was used to capture and polymerize polyphenols, which are usually tightly bound to fucoïdan in the cell wall and responsible for the brown colour of contaminated fucoïdan [122], and finally again with 80% (v/v) ethanol for washing and cleaning up the biomass from residual formaldehyde and condensed polyphenol complexes.

An aqueous, acidic conditions and in the presence of calcium ion optimized extraction conditions, and facilitated the precipitation of alginat as Ca salt using several extraction procedures; Procedure_A, Procedure_B and Procedure_C. Besides, a neutralization step with $(\text{NH}_4)_2\text{CO}_3$ was carried out in Procedure_A and Procedure_C after extraction to protect fucoïdan's glycosidic linkages and sulphate esters from acid hydrolysis [120,121]. Moreover, Procedure_B was performed

to study the effect of long incubation of fucoïdan in acidic condition and possibility to purify fucoïdan without the ethanol precipitation step. However, Procedure_C was applied at moderate conditions based on optimized extraction conditions from *F. vesiculosus* previously performed by Hahn, *et al.* [79]. Different crude fucoïdan fractions were precipitated with different volumes of ethanol. In Procedure A, a yield of 2.58 g crude precipitated fucoïdan (**Fucoïdan_A**) was obtained, representing 17.5% (w/w) from the starting dried algal biomass. However, Procedure_C resulted in 0.37 g and 0.38 g as yields from **Fucoïdan_40%** and **Fucoïdan_70%**, respectively. The low yield of crude fucoïdan obtained from Procedure_C indicated that reflux, high temperature and more acidic conditions were critical factors for better extraction. Moreover, extraction conditions used in Procedure_A confirmed its ability to obtain a higher yield than that stated in the literature.

2.3.2. Characterization of crude fucoïdan fractions

Crude fucoïdan fractions; **Fucoïdan_A**, **Fucoïdan_40%** and **Fucoïdan_70%** before purification protocols were characterized regarding its sugar, fucoïdan, fucose and free sulphate contents, according to Dubois (Phenol-Sulphuric acid assay), TB and Heparin Red[®] Ultra assays, Dische (Cysteine-H₂SO₄ assay) and BaSO₄ assay, respectively. Results were summarized in **Table 4**, it shows that **Fucoïdan_A** has the best quality, which had the highest sugar and lowest hydrolyzed free sulphate contents. In addition, its fucoïdan and fucose contents were comparable with **Fucoïdan_70%**. Furthermore, 70% (v/v) ethanol proved its efficiency to precipitate crude fucoïdan with higher fucoïdan and fucose contents. However, the low fucoïdan content (approx. 70% w/w) confirmed that there were still co-extracted contaminants with fucoïdan, despite of the extensive performed pre-treatment steps, and therefore a further step of purification was needed to obtain an improved product. **Fucoïdan_A** was considered as a candidate to give a high-quality fucoïdan and more preferred than the other fractions to perform the further purification process.

Table 4: Sugar, fucoïdan, fucose and sulphate contents in different crude extracted fucoïdan fractions from *F. vesiculosus* by Procedure_A and C

Parameter	Method of Determination	Standard used	Concentration (g/g crude fucoïdan)		
			Fucoïdan_A	Fucoïdan_40%	Fucoïdan_70%
Sugar content	Dubois test (Phenol-Sulphuric acid assay)	D-Glucose	0.2079	0.176	0.14
Fucoïdan content	TB assay	Fucoïdan (>95% pure, Sigma-Aldrich®)	0.731	0.0915	0.76
	Heparin Red® Ultra assay		0.69	n.d*	n.d
Fucose content	Dische assay (Cysteine-H ₂ SO ₄)	L-Fucose	0.165	0.172	0.0654
Free sulphate content	BaSO ₄ assay	Ammonium sulphate	0.0367	0.1559	0.0657

*: not determined

The colour developed in Dubois assay is due to the conversion of the sugars into furfural derivatives by a dehydration reaction with sulphuric acid. The furfural product is condensed with phenol to a coloured compound, which can be detected colorimetry at 490 nm. Colour formation is stable for several hours and proportional to the amount of the sugar present. Its detection limit is 7 µg L⁻¹ [105].

In addition, the Dische assay is a specific-oxidation reaction for methylpentoses like fucose. Cysteine combines with the different breakdown compounds of sugars yielding products with different absorption spectra. Therefore, relative absorbance should be measured at two wavelengths to eliminate possible interferences from other sugars. The detection limit of this test is 10 µg L⁻¹ [105].

Moreover, TB assay was considered a specific test to determine fucoïdan content. The test is based on a metachromatic change of TB due to a charge-transfer complex formation when reacted with polyanionic polymers in acidic or slightly acidic pH, such as fucoïdan [98]. The assay was preferred to be performed in a highly acidic pH (pH 1) to ensure the specificity and sensitivity for sulphated compounds. At pH 1, only sulphate groups of fucoïdan could ionize, because of their lower *pKa* value than other carboxylic and phosphate groups from alginate and nucleic acids, respectively. Moreover, in acidic medium amino groups of thiazine dyes were also protonated and could form a donor-acceptor complex specifically with fucoïdan.

In addition to thiazine dyes, Heparin Red[®] (Redprobes UG) proved its effectiveness in the detection of heparin in plasma [123] and urine [124] and, more recently, for the quantification of fucoïdan in spiked plasma [106]. The reaction is based on the formation of electrostatically-driven aggregates with polyanionic sulphated polysaccharides, such as heparin and fucoïdan followed by fluorescent quenching, as shown in **Fig 15**. To assure test selectivity, Na-alginate samples were analyzed separately, which showed no affinity and fluorescence quenching activity toward Heparin Red[®] probes.

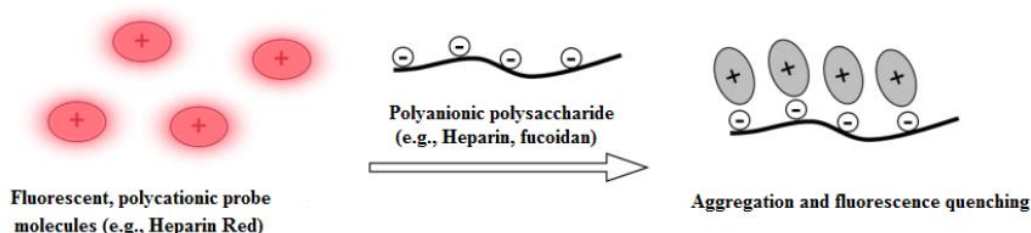


Fig. 15: Representation of the polyanionic polysaccharide reaction with fluorescent Heparin Red[®]

The reaction resulted in formation of electrostatically aggregates and followed by fluorescence quenching (modified according to [125]).

Furthermore, reaction of free sulphate ions with barium ions produced BaSO₄ as a precipitate. The solution turbidity could be measured at a λ of 600 nm. This principle was applied to quantify free sulphate content in crude fucoïdan fractions. Lower free sulphate content is advantageous and indicated lower percent of decomposed or hydrolysed sulphate ester groups during extraction step.

2.3.3. Application and optimization of fucoïdan purification

Fucoïdan_A was used in application and optimization of purification of Hahn's protocol [108] due to its higher production yield and better quality as discussed previously in section 2.3.2. Investigated conditions were classified to be either during fucoïdan's adsorption phase or elution phase. In addition, several fractions of purified fucoïdan were isolated to be characterized afterwards to reach the optimum purification conditions regarding physico-chemical, pharmacological properties in addition to the degree of purity.

2.3.3.1. Adsorption or incubation phase

a. Kinetic, adsorption pH and type of thiazine dye

Fucoïdan adsorption (%) by immobilized 2 mM TB, TA and mixed TA and TB were compared at pH 1 and pH 6. As shown in **Fig. 16**, results revealed that fucoïdan required long incubation periods to be captured significantly confirming the results obtained previously from kinetic and sorption isotherm studies by Hahn [108]. In addition, capture (%) was higher at highly acidic pH 1 than slightly acidic pH 6 conditions. Therefore, it could be concluded that at pH 1, a partial acid hydrolysis of fucoïdan occurred and the diffusion rates (rate limiting step) of the lower molecular weight fucoïdan [94] were possibly improved making the adsorption easier and faster through immobilized dyes found on the beads surface and in pores. In addition, the highly acidic pH may help more sulphate ester groups to be ionized which interacted proportionally with TB. Furthermore, similar adsorption (%) by mixed dyes proved that both beads did not enhance or compete with each other during fucoïdan capturing process.

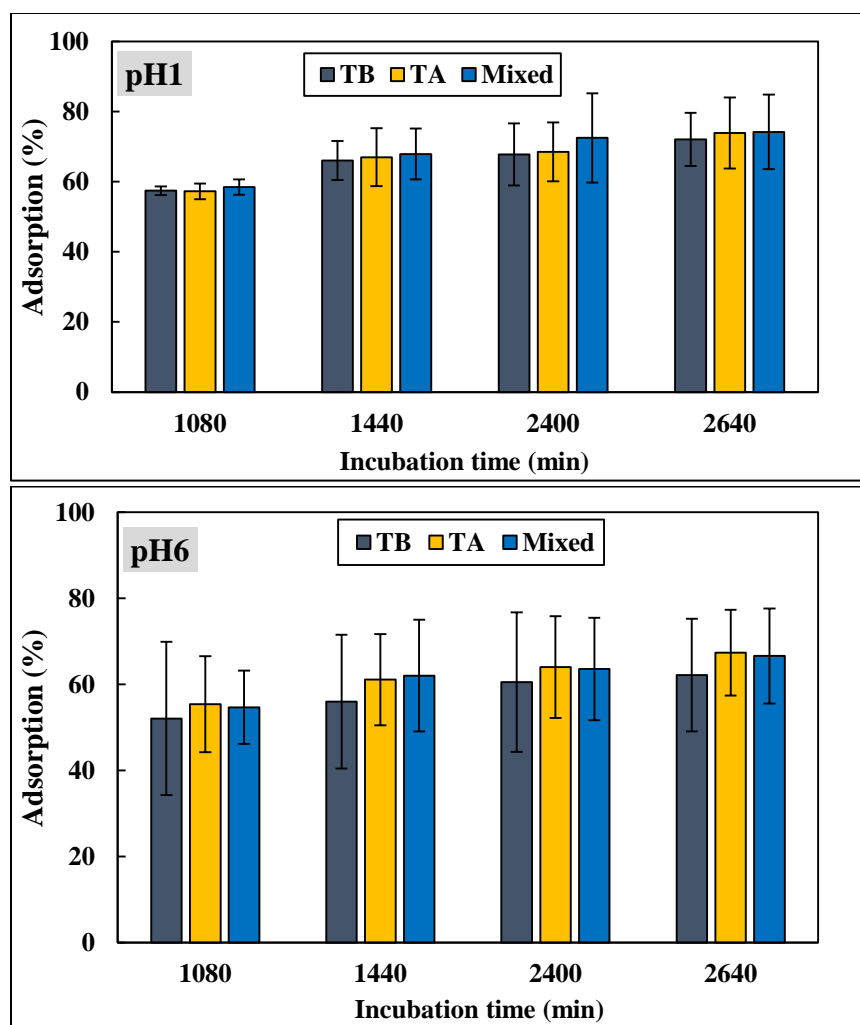


Fig. 16: Adsorption (%) of fucoidan by immobilized 2 mM TB, TA and mixed dyes at pH 1 and pH 6
 The adsorption (%) was determined after incubation of 1.5 mL 2.5 mg mL⁻¹ of **Fucoidan_A** at 1080, 1440, 2400 and 2640 min with 50 mg of derivatized beads at room temperature.

b. Molarity of immobilized dye

As a trial to increase the availability of dyes for fucoidan, and therefore a higher percent of captured fucoidan, immobilization of higher concentrations of dyes; 4 and 6 mM of thiazine dyes, were applied. Results of adsorption at pH 1 showed that, not only the percent of captured fucoidan was not significantly affected by increasing the dye molarity, as shown in **Fig. 17**, but also dyes leaching was higher than immobilized 2 mM. Because of these reasons, 2 mM immobilized TB was preferred in the downstream process for purified fucoidan production.

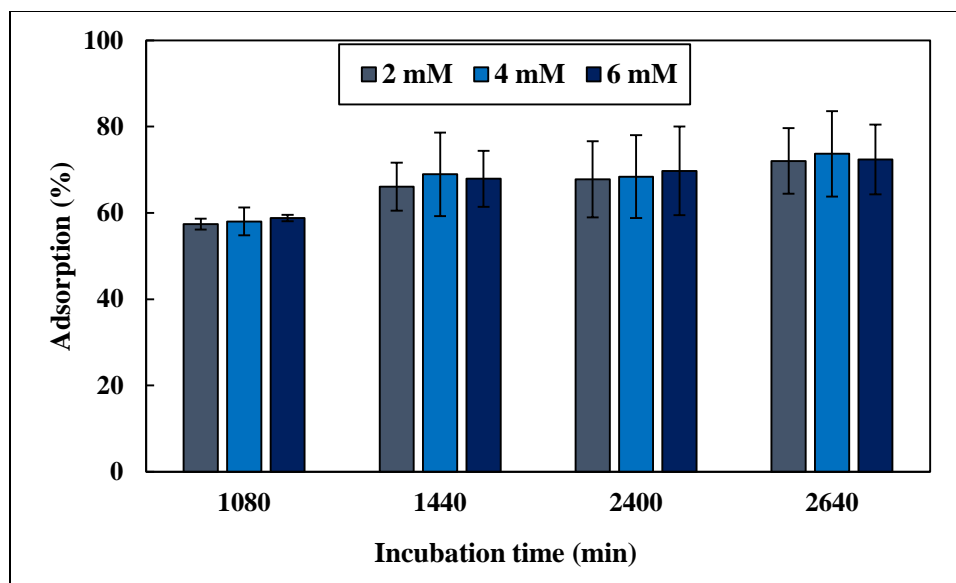


Fig. 17: Comparison between adsorption (%) of fucoïdan by immobilized 2, 4 and 6 mM TB at pH 1

The process was performed after incubation of 1.5 mL 2.5 mg mL⁻¹ of **Fucoïdan_A** with 50 mg of derivatized beads at room temperature. Samples from supernatant were taken at 1080, 1440, 2400 and 2640 min of incubation and analyzed to determine adsorption rates.

c. Incubation time

Adsorption of fucoïdan is a time-dependent process and required at least 30 h of incubation to attain the equilibrium between beads and available fucoïdan [94], and therefore an extended incubation period was studied for 60 h. As shown in **Fig. 18**, captured fucoïdan (%) was increased by time at both pH, especially at pH 1, but the possibility of a non-specific acid hydrolysis for fucoïdan may be occurred, and therefore affected the native molecular weight of fucoïdan at these conditions.

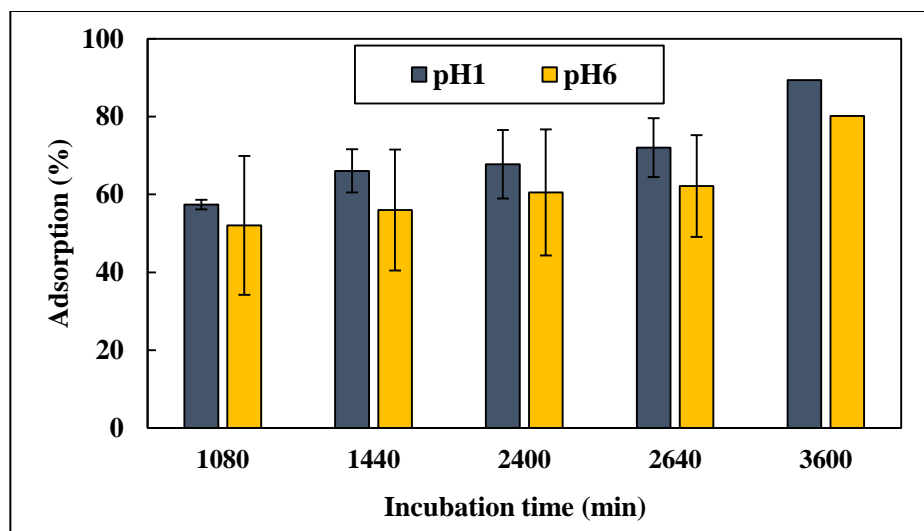


Fig. 18: Adsorption (%) of fucoidan by 2 mM immobilized TB for 60 h of incubation at pH 1 and pH 6

The process was performed by incubation of 1.5 mL 2.5 mg mL⁻¹ of **Fucoidan_A** with 50 mg of derivatized beads at room temperature for 60 h (3600 min). Samples from supernatant were taken at 1080, 1440, 2400, 2640 and 3600 min of incubation and analyzed to determine adsorption rates.

d. Quantity of derivatized beads

As shown in **Fig. 19**, incubation of crude fucoidan at pH 1 and 6 with 75 mg of TB-derivatized beads succeeded to increase adsorption (%) to 99.5% and 83.8%, respectively after 44 h of incubation. This was another proof that the non-completed adsorption, long incubation periods and difficulty to reach the equilibrium state were related to the beads porosity and the slower and variable diffusion rates of fucoidan polymers.

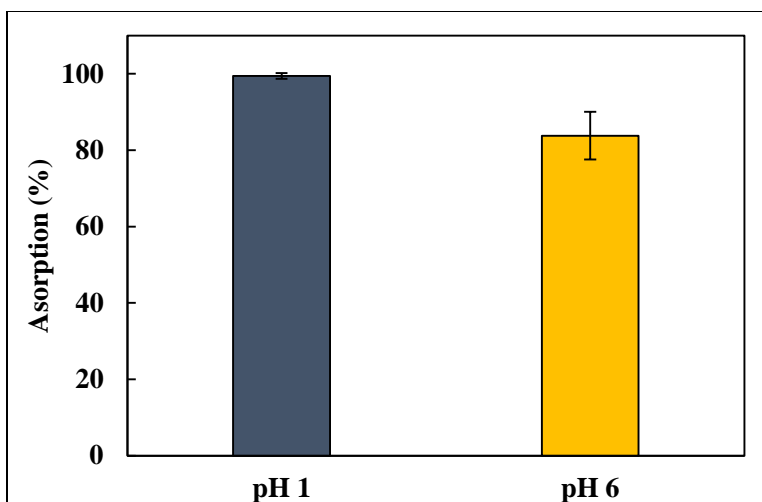


Fig. 19: Adsorption (%) of fucoïdan from Fucoïdan_A by 75 mg of 2 mM immobilized TB at pH 1 and pH 6

The process was performed by incubation of 1.5 mL 2.5 mg mL⁻¹ of **Fucoïdan_A** at room temperature for 44 h in a 2 mL reaction vessel.

e. Effect of multiple use of immobilized beads

TB-derivatized beads were used for several cycles to adsorb fucoïdan from raw synthetic extract efficiently [94]. Similarly, immobilized TB showed reproducible and comparable fucoïdan adsorption (%) from the crude extract of *F. vesiculosus* with multiple use in two cycles, as shown in **Fig. 20**. This factor confirmed also that elution step regenerated the beads' function without the need to an additional regeneration step as in IEX process.

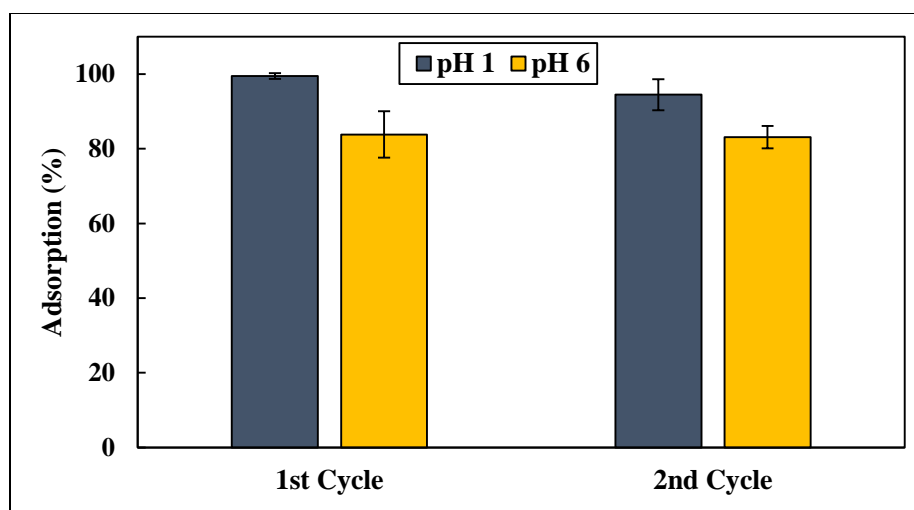


Fig. 20: Adsorbed fucoidan (%) by 75 mg of immobilized TB for two cycles at pH 1 and pH 6

The process was performed by incubation of 1.5 mL 2.5 mg mL^{-1} of **Fucoidan_A** at room temperature for 44 h in a 2 mL reaction vessel.

2.3.3.2. Elution phase

For elution and effective break down of the charge-transfer complex formed between the immobilized TB and the adsorbed fucoidan, high molar concentration of NaCl, ethanol and heating were required. Ethanol was used to enhance the hydrophobic interaction between the stacked dye molecules. In addition, high temperatures e.g., $50 \text{ }^{\circ}\text{C}$ provided the necessary activation energy for desorption and NaCl for suppression of ionic interactions between the dye and the sulphated polysaccharide [94]. Only the effect of NaCl molarity on elution of fucoidan (%) was studied.

As demonstrated in **Fig. 21**, increasing of NaCl molarity in eluent resulted in increasing of eluted fucoidan (%). Molarity of NaCl resulted in obtaining different fractions of fucoidan with different molecular weights (discussed later). The process was tested in adsorbed fucoidan at pH 1 and showed that 3 M NaCl was the best and succeeded to elute 70.3% in average of adsorbed fucoidan. However, non-completed elution could be related to the difficulty of elution of fucoidan present in the beads pores, and therefore further optimization were still required. In addition, leaching of the immobilized dye might be possible which reacted with some the free eluted fucoidan molecules and total eluted fucoidan could not be determined exactly by the TB assay as a result. Non-eluted or strongly bound fucoidan affected negatively on the beads' efficiency with multiple uses as a result, as shown previously in **Fig. 20**. In addition, leached dye from derivatized beads at the elution conditions decreased the number of immobilized molecules with each cycle.

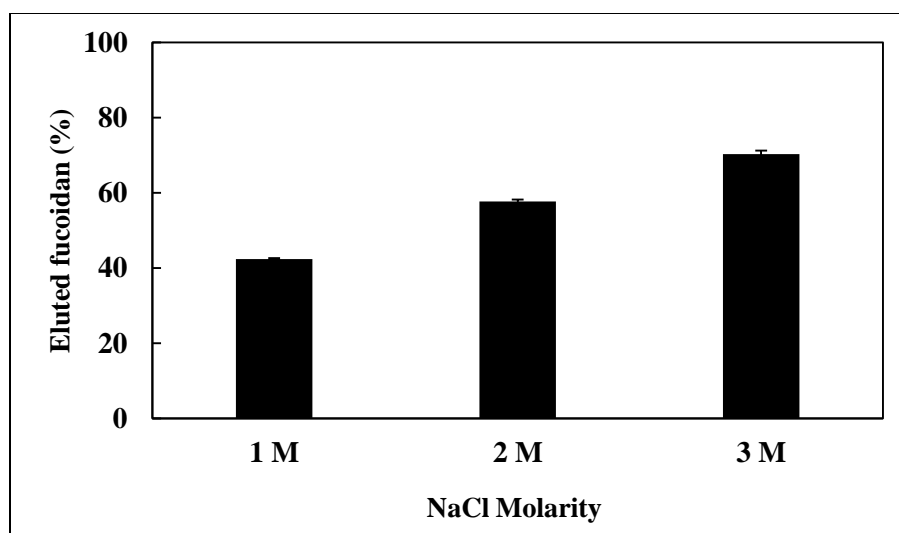


Fig. 21: Effect of NaCl molarity in eluent on eluted fucoidan (%)

Elution (%) was increased by increasing NaCl molarity and performed for 16 h in a thermoshaker at a temperature of 50° C and vigorous shaking at 800 rpm.

Results obtained from investigated factors revealed that neither a completed adsorption of fucoidan nor the maximum loading capacity of immobilized dye were not achieved till 60 h of incubation at both pH values using 50 mg of beads with 2.625 mg of fucoidan. However, the reaction between TB and fucoidan occurred immediately. The previously-studied sorption isotherm concluded that 72 h were required to reach the maximum capacity of beads (127.7 mg g^{-1}) [94]. This might be explained by several reasons including the presence of co-extracted contaminants which delayed fucoidan adsorption or competed for adsorption sites, differences in polymers chain lengths and molecular weights which led to different diffusion rates and beads porosity as well. Moreover, amino groups in thiazine dyes were a limiting factor; i.e., one group per each dye molecule after immobilization, as demonstrated in **Fig. 22**. Based on these arguments, further optimization steps should be performed to overcome these disadvantages.

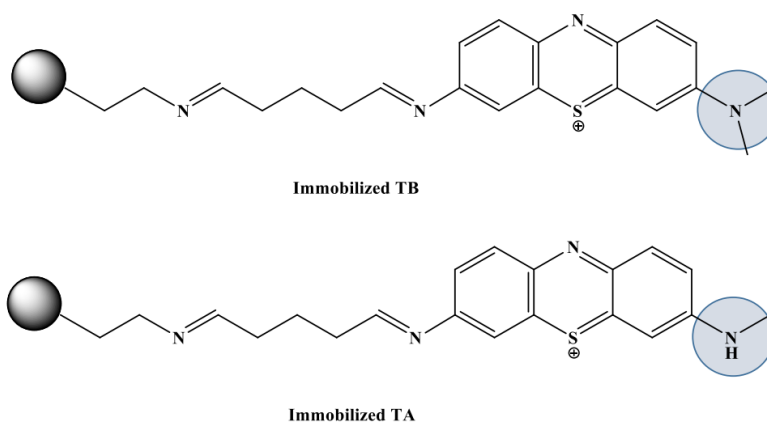


Fig. 22: Immobilized TB and TA on Sepabeads® EC-EA

After immobilization, they showed only one available amino group which could be ionized to capture fucoidan.

2.3.4. Application of PDD for fucoidan purification

Following the high affinity and sensitivity of Heparin Red® to polyanionic polysaccharides [106], a fluorescent structurally-related compound to Heparin Red®; polycationic perylene diimide derivative or PDD (*N,N'*-Bis-(1-amino-4,9-diaza dodecyl)-1,7-di bromo perylene-3,4,9,10-tetracarboxylic acid diimide), as shown in **Fig. 23**, was synthesized and immobilized successfully.

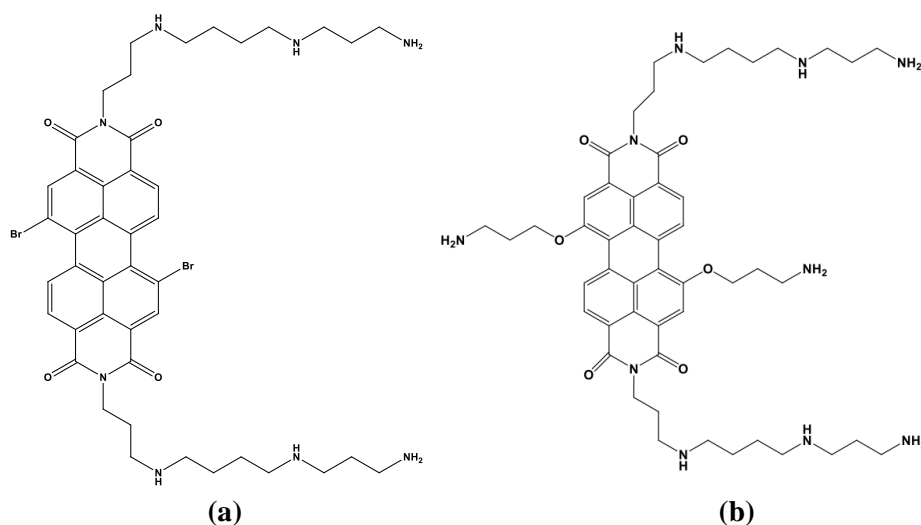


Fig. 23: Molecular structure of a) perylene diimide derivative (*N,N'*-Bis-(1-amino-4,9-diaza dodecyl)-1,7-di bromo perylen-3,4,9,10-tetracarboxylic acid diimide, and b) Heparin Red®

PDD shows different primary and secondary amino groups available for immobilization on amino-derivatized beads through a glutaraldehyde bridge as well as formation of a charge transfer-like aggregate with fucoidan in acidic or neutral pH.

PDD showed a lot of advantages in comparison with thiazine dyes. These advantages include five adsorption amino groups, as shown in **Fig. 24**, in addition to the wide distance between beads and amino groups which may ease their function to hook the huge and slower fucoïdan macromolecules. Moreover, availability of adsorption sites on beads surface overcame the problem of beads porosity.

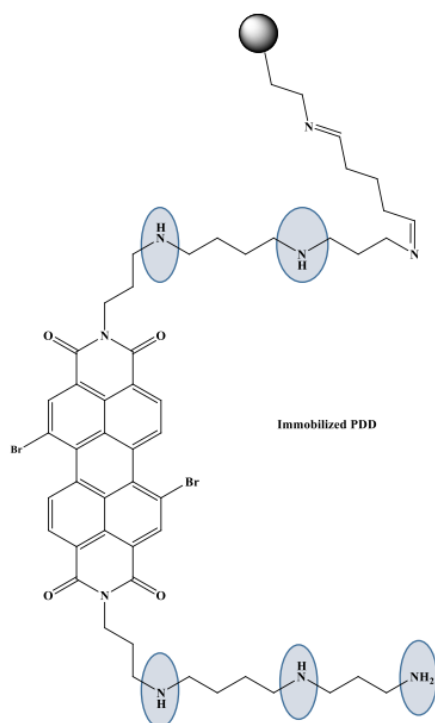


Fig. 24: Immobilized PDD on Sepabeads® EC-EA

It shows five amino groups for fucoïdan binding. The figure is based on a 1:1 ratio of immobilization between beads and PDD molecules.

2.3.4.1. Adsorption kinetic in crude fucoïdan

As shown in **Fig. 25**, application of immobilized PDD at pH 6 proved its efficiency to capture fucoïdan from crude extract and improved purification process drastically. More than 80% (83%) of available fucoïdan was captured in 960 min, compared with 83% in 2640 min with immobilized TB incubated at the same conditions, as shown previously in **Fig. 19**.

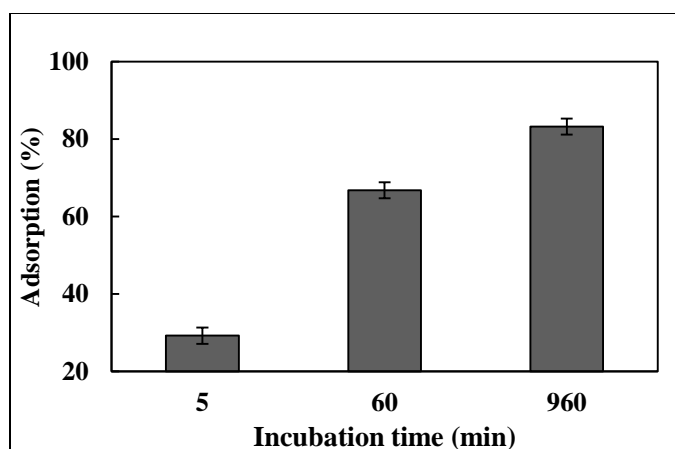


Fig. 25: Time dependence adsorption (%) of fucoïdan from Fucoïdan_A by immobilized PDD

The process was performed using 75 mg derivatized beads with a 2.5 mg mL⁻¹ solution of **Fucoïdan_A** in MES (pH 6) at room temperature and a 2 mL reaction vessel.

2.3.4.2. Multiple use of immobilized PDD

Moreover, PDD-derivatized beads were recycled like immobilized TB without effect on beads efficiency, as shown in **Fig. 26**. Interestingly, it was observed that the beads were able to adsorb much fucoïdan (%) in the 2nd and 3rd cycles, which were constant, than the 1st cycle. This observation might be due to a non-optimized PDD solution used in immobilization step. Much concentrated PDD solution saturated the beads and the additional molecules, despite of the several washing steps, bound to fucoïdan and inhibited its adsorption in the 1st cycle.

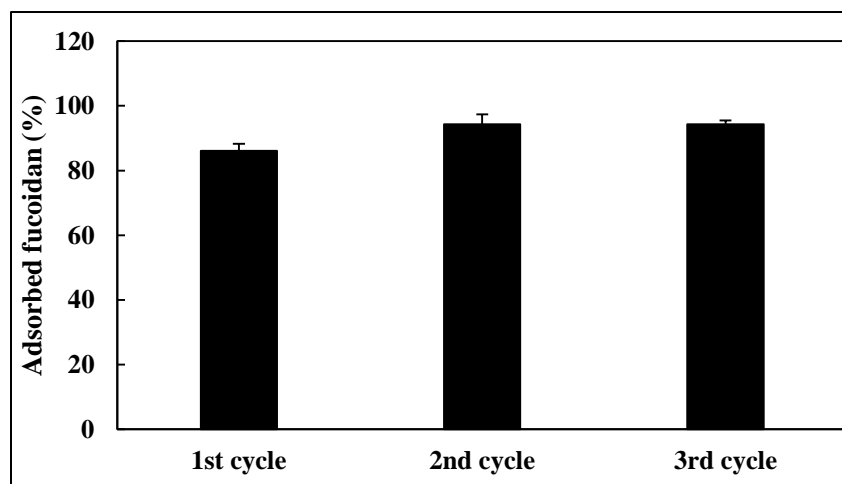


Fig. 26: Multiple use of PDD-derivatized beads for three cycles

Process was performed using 75 mg beads with 2.5 mg mL⁻¹ of **Fucoïdan_A** solution in MES (pH 6) which incubated for 18 h (1080 min) in a 2 mL reaction vessel.

2.3.4.3. FPLC automated purification process

Preliminary results of batch process were a motivation to establish a protocol using FPLC. This could help automation, improve downstream processing, further minimize the time required for the process, and overcome the disadvantages regarding manual solvents exchange during the different purification phases. Furthermore, this process might help in an industrial-scale fucoïdan production. The new protocol was developed to imitate batch process with its four phases and performed in only 150 min. A sample of 50 mg mL⁻¹ was prepared, which was less than the maximum loading capacity of the column material, due to a crude fucoïdan solubility problem. Concentrations more than 50 mg.mL⁻¹ resulted in a turbid solution. First, 20 mM MES buffer (pH 6) was used for column conditioning. Then, a 50 mg mL⁻¹ sample in MES was injected in 1 mL loop, followed by buffer again at a slower flow rate to give adequate time for fucoïdan adsorption by derivatized beads. Deionized water and 0.1 M NaCl in MAB (pH 2) were used afterwards for washing to remove the non-specific bound molecules. Investigation of flow through and washing collected fractions by TB assay confirmed a complete adsorption of fucoïdan. With elution by 3 M NaCl in 30% ethanol, fucoïdan started to leave its complex easily when conductivity and pH were increased to approx. 95 µS/cm and slightly acidic pH 6 (see Appendix), respectively. A similar elution pattern of fucoïdan, as shown in **Fig. 27**, was observed in two cycles.

Fucoïdan was observed to be eluted and reached its maximum concentration earlier with the 2nd application of the derivatized beads. Fractions (6-20) from the 1st and 2nd cycles were pooled (30 mL each) to give yields of **Fucoïdan_PDD_1** and **Fucoïdan_PDD_2** of 16.9 and 16.3 mg, respectively.

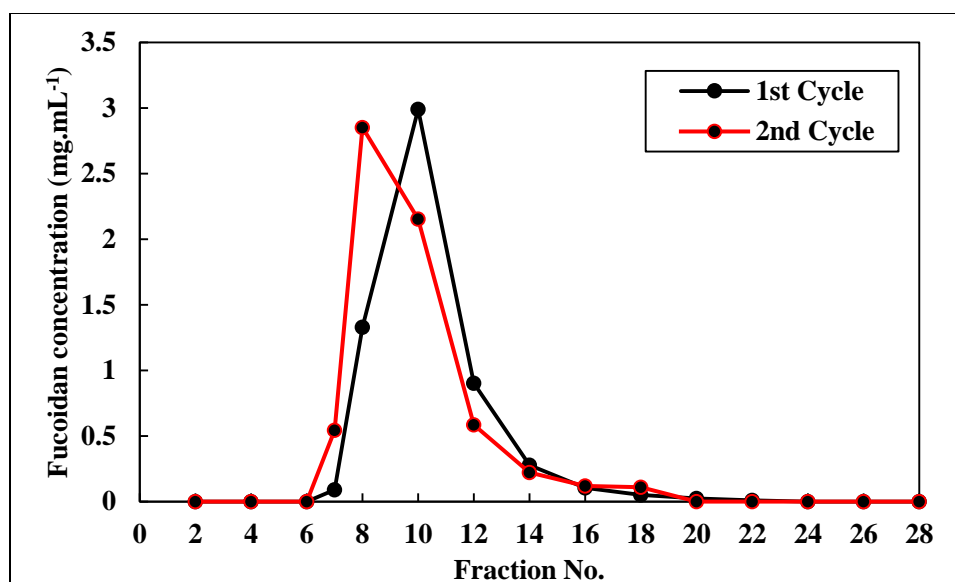


Fig. 27: Fucoidan elution pattern from FPLC column in two successive cycles

Similar pattern of fucoifan elution was observed in the two cycles of fucoifan purification by FPLC. Fucoidan concentrations were determined in column eluates by TB assay.

If the fucoidan content of the injected sample (50 mg mL^{-1}) was considered, only 68% (34 mg) represented fucoidan. This means that the column could elute only 50% of the introduced fucoidan. The low elution (%) might be due to the absence of heating and vigorous shaking applied in batch process.

2.3.5. Physico-chemical characterization of purified fucoidan fractions

After freeze-drying, white and hygroscopic fluffy powders were obtained as in **Fucoidan_1**, **Fucoidan_6** and **Fucoidan_PDD**, while **Fucoidan_M** was white to brownish colour. All of them were soluble in water, sparingly soluble in DMSO, and insoluble in ethanol.

2.3.5.1. Elemental Analysis (CHNS Analysis)

As shown in **Table 5**, the presence of traces of nitrogen content N (%) in all fucoidan types, in contrast with reference fucoidan, suggested the successful removal of a high percent of proteinaceous compounds. These traces were possibly due to the presence of some amino sugars [43,126]. **Fucoidan_PDD** demonstrated the lowest N (%); 0.2% (*m/m*) compared with the other fractions. In contrast, **Fucoidan_M** showed the highest S%; 12.11% (*m/m*), which is critical for some biological activities (e.g., anti-viral activity). Based on CHNS analysis, number of sulphate

ester group per sugar unit and degree of sulphation were calculated using the ratio between C (%) and S (%) contents, as shown in **Eq. 2** and **Eq. 3**, respectively. Fucooidan fractions' degree of sulphation were consistent and interesting compared with literature's values, especially with **Fucooidan_6** and **Fucooidan_PDD** [127].

$$\text{No. of sulphate group per sugar unit} = \left[\frac{\frac{C(\%)}{12}}{\frac{S(\%)}{32}} \right] / 6 \dots\dots\dots (\text{Eq. 2})$$

$$\text{Degree of sulphation} = 1 / \text{No. of sulphate group per sugar unit} \dots\dots\dots (\text{Eq. 3})$$

Where; 12 is the atomic weight of Carbon, 6 is the number of Carbon atoms in the sugar monomer, and 32 is the atomic mass of Sulphur.

Table 5: Elemental analysis (CHNS) and degree of sulphation results of different fucooidan fractions

The results were compared with commercially-available analogue purchased from Sigma-Aldrich® in addition to calculated degree of sulphation.

Sample	N (%)	C (%)	H (%)	S (%)	Degree of sulphation
Reference fucooidan	n.d.*	24.78	4.42	8.89	0.8
Fucooidan_1	0.3	24.14	4.43	11.18	1.09
Fucooidan_6	0.34	26.12	4.63	9.83	0.84
Fucooidan_PDD	0.22	25.35	4.51	8.45	0.75
Fucooidan_PDD_1	0.3	25.77	4.57	8.78	0.766
Fucooidan_PDD_2	0.29	25.95	4.54	8.78	0.761
Fucooidan_M	0.26	23.31	4.28	12.11	1.16
Crude fucooidan (Fucooidan_A)	0.59	22.89	4.54	6.88	0.67

* not detected.

Reference fucooidan (>95% pure isolated from *F. vesiculosus*) was purchased from Sigma-Aldrich®;
 Fucooidan_1 was purified by immobilized TB from crude fucooidan at pH 1;
 Fucooidan_6 was purified by immobilized TB from crude fucooidan at pH 6;
 Fucooidan_PDD was purified by immobilized PDD from crude fucooidan at pH 6;
 Fucooidan_PDD_1 was purified using a FPLC protocol from crude fucooidan at pH 6 (1st cycle);
 Fucooidan_PDD_2 was purified using a FPLC protocol from crude fucooidan at pH 6 (2nd cycle);
 Fucooidan_M was purified from MAB crude extract at pH 1 without crude fucooidan precipitation.

The higher degree of sulphation, especially in **Fucoïdan_1** and **Fucoïdan_M**, were due to lower C(%) to S(%) ration which was affected by highly acidic pH and resulted in polymer hydrolysis, as will be discussed in the following section **2.3.5.2**.

2.3.5.2. Molecular weight parameters

For ideal characterization of any polymer, three different parameters should be calculated, which are **Mw**, **Mn** and **Mp**. **Mn** indicates the number of molecules in a sample of a given weight, while **Mw** takes into account the molecular weight of chains contributing to the molecular weight average [128] and **Mp** determines the polymer molecular weight at the top of peak or the most prominent molecular weight. In addition, the **PDI** measures the broadness of molecular weight distribution of polymers; the larger the PDI, the broader the molecular weight. According to Agilent Technologies [128], the following equations (**Eq. 4 – 6**) were applied.

$$Mn = \frac{\sum N_i M_i}{\sum N_i} \dots\dots\dots (\text{Eq. 4}) \qquad Mw = \frac{\sum N_i M_i^2}{\sum N_i M_i} \dots\dots\dots (\text{Eq. 5})$$

$$PDI = \frac{Mw}{Mn} \dots\dots\dots (\text{Eq. 6})$$

Where; M_i is the molecular weight of a chain, and N_i is the number of chains of that molecular weight.

Natural polymers like proteins and polysaccharides are monodisperse and therefore have PDI near to 1. As demonstrated in **Table 6a**, purification processes either by immobilized TB or PDD improved molecular weight parameters and its quality as well. **Fucoïdan_1** and **Fucoïdan_M** showed the lowest- measured Mw and this proved that long incubation periods in acidic conditions during adsorption phase had a strong hydrolytic effect on fucoïdan polymer, despite of higher adsorption rates. Moreover, low molecular weight obtained from FPLC method suggested that elution conditions were only able to elute low molecular weight fucoïdan (LMWF).

Not only % eluted fucoïdan, but also molecular weight averages of eluted fucoïdan fractions were affected by the NaCl molarity. **Table 6b** shows that molecular weight of fucoïdan purified at the same conditions could be sub-fractionated by gradient elution using different molarities of NaCl. The higher NaCl molarity applied, the more fucoïdan molecular weight is obtained.

Table 6a: Molecular weight parameters and polydispersity index (PDI) of different purified fucoïdan fractions.

The fucoïdan fractions were compared with reference fucoïdan purchased from Sigma-Aldrich® and crude fucoïdan before purification

Fucoïdan type	Mwx10 ⁴	Mnx10 ⁴	Mpx10 ⁴	PDI
Reference fucoïdan	9.5	4.2	5.1	2.2
Fucoïdan_1	5.8	3.9	3.3	1.4
Fucoïdan_6	9.8	5.4	5.7	1.8
Fucoïdan_PDD	8.6	4.2	3.2	2.04
Fucoïdan_PDD_1	5.8	2.5	3.4	2.3
Fucoïdan_PDD_2	6.6	3.98	4.02	1.66
Fucoïdan_M	4.8	1.8	2.6	2.6
Crude fucoïdan	6.6	3.1	4.2	2.1

Mw: weight average molecular weight, **Mn**: Number average molecular weight, and **Mp**: peak molecular weight

Table 6b: Molecular weight parameters of fractions obtained by different NaCl molarity

Fractionation was performed by applying different 1, 2 and 3 M NaCl in eluent.

Molarity of NaCl (M)	Molecular weight averages (x10 ⁴) Da		
	Mw	Mn	Mp
1	5.7	4.1	3.7
2	6.6	4.8	4.9
3	9.2	4.9	4.4

2.3.5.3. Melting point

Since the melting point of crystallized compounds assesses also sample purity and is affected by molecular weight, melting points were measured for some fractions to proof relations with the previously measured molecular weight parameters [129]. All organic polymers like fucoïdan melt and decompose when exposed to heat in an analysis called combustion analysis. Fucoïdan fractions followed the same pattern with increasing the temperature; namely colour changing: yellow, brown and then to black and was reflected by a gas development. The temperature ranges between starting of melting till complete decomposition were 5-6 °C degrees for **Fucoïdan_1** and **Fucoïdan_M**, while they were wide (20 °C) for **Fucoïdan_6**. These data indicated and confirmed higher molecular weight of **Fucoïdan_6** and results obtained from molecular weight measurement. **Table 7** summarizes a comparison among the phases at which the different fractions of fucoïdan purified by

immobilized TB changed their colour, melted and then decomposed with charring at higher temperatures.

Table 7: Comparison among the different fucoïdan fractions purified by immobilized TB, regarding start, colour change and decomposition temperature points

Fucoïdan fraction	Start (°C)	Color Change (°C)	Decomposition (°C)
Fucoïdan_1	130	132–133	135
Fucoïdan_6	140	153–156	161
Fucoïdan_M	130	133–134	136

2.3.5.4. Specific optical rotation

Specific optical rotation $[\alpha]_{589}^{22}$ results, as shown also in **Table 8**, proved the levorotatory (*l*) and asymmetric nature of fucoïdan fractions. This confirmed the presence of *l*-fucose as a major stereoisomer of fucose monomer in fucoïdan. Fucoïdan fractions in addition to commercial analogue showed similar, $[\alpha]_{589}^{22}$ values in the range from -117° for **Fucoïdan_6** to -130° for **Fucoïdan_M**. These values could be related also to fucoïdan molecular weight and fucose content as an indirect relationship. Furthermore, these values are also consistent with the data reported previously in literature: -123° [43].

Table 8: Comparison among the different fractions of fucoïdan regarding specific optical rotation

All fucoïdan fractions are *l*-form polymers.

Fucoïdan fraction	Specific optical rotation $[\alpha]_{589}^{22}$
Reference Fucoïdan	- 121
Fucoïdan_1	- 128
Fucoïdan_6	- 117
Fucoïdan_M	- 130

2.3.5.5. Monomeric composition

Monomeric composition affects significantly fucoïdan biological activities [43]. As **Table 9** shows, fucose is the major monomer in all fucoïdan fractions and represents more than 80% of the total monomers. Other monomers, such as galactose, uronic acid/glucose dimers were also detected. Yet, xylose was detected only in **Fucoïdan_1** and **Fucoïdan_6**. Uronic acids/glucose dimers were only detected by MS; nevertheless, their quantities could not be accurately determined since there were

no standards available in addition to their poor retention behaviors. These results confirmed that the monomeric composition of fucooidan was also dependent on the purification method and its molecular structure as well.

Table 9: Monomeric composition (%) of different purified fucooidan fractions

Composition	% Galactose	% Xylose	% Fucose
Fucooidan_1	7.4 ± 0.06	4.0 ± 0.06	88.59 ± 0.03
Fucooidan_6	8.99 ± 0.25	4.2 ± 0.45	86.8 ± 0.45
Fucooidan_M	7.56 ± 0.2	- *	92.43 ± 0.2

*: not detected

2.3.6. Spectroscopical identification of purified fucooidan fractions

2.3.6.1. FT-IR

Because of the complex and diverse structure of fucooidan, identification of fucooidan functional groups is always performed by IR [43,87,130,131]. Generally, it shows characteristic and typical IR bands for its functional structural building blocks, (e.g., OH group of its monomeric monosaccharides, S=O and C-S-O of sulphate ester groups, O-C-O and C-O-C of glycosidic and intra-molecular linkages, at 3430, 1220, 830, 1620, 1020 cm⁻¹, respectively).

FT-IR was used as an identification tool for fucooidan before and after application of the purification protocol. As revealed in **Fig. 28**, as an example, a comparison between IR bands for **Fucooidan-PDD**, crude fucooidan and the commercially-available pure fucooidan purchased from Sigma-Aldrich® (>95% pure). Obviously, crude fucooidan showed an additional band at 1418 cm⁻¹ which may belong to co-extracted impurities, e.g., alginate [132]. Being purified, fucooidan fractions had not any more this band as shown in **Fucooidan_PDD**.

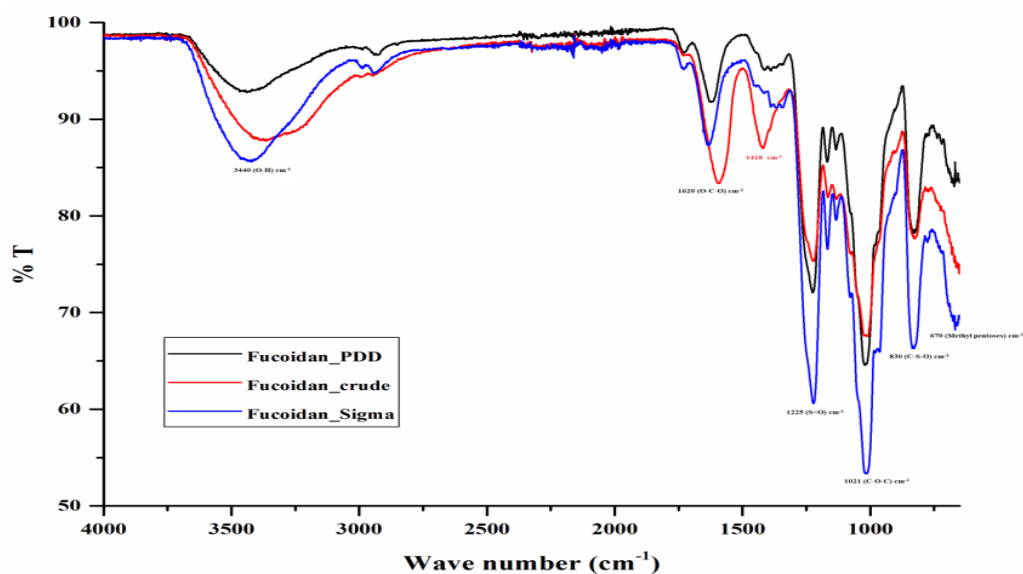


Fig. 28: FT-IR spectra of fucoïdan before (Fucoïdan_crude) and after (Fucoïdan_PDD) in comparison with the commercially-available reference fucoïdan purchased from Sigma-Aldrich® (>95% pure)

Fucoïdan_PDD showed typical IR bands for OH, O-C-O, S=O, C-O-C, C-S-O groups as well as methyl pentoses of fucoïdan. FT-IR of **Fucoïdan_PDD** is only shown, as an example, for a simple overview.

2.3.6.2. ¹H-NMR

¹H-NMR of fucoïdan fractions demonstrated poorly-translated spectra including commercially-available purified fucoïdan purchased from Sigma-Aldrich®. Supposing that fucoïdan is a polymer α -(1-3)-linked L-fucopyranoside repeating unit, as previously hypothesized by Cumashi, *et al.* [14], as shown in **Fig. 29**, some structural features could be elucidated from NMR spectra. All fractions showed peaks of the shielded protons at around 1.2 and 2.15 ppm as singlets (did not appear in commercial fucoïdan), which could be assigned to CH₃- of L-fucose monomer and acetyl groups, respectively. Other peaks appeared slightly shifted between 3.8 and 4.5 ppm assigned to H₂, H₃, H₄ and H₅. Anomeric proton H₁ appeared highly down fielded at 5.2 ppm, confirmed α -linked sugar monomers.

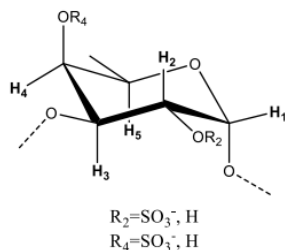


Fig. 29: Representation of an α -(1-3)-linked L-fucopyranoside repeating unit of fucoidan, as previously described by Cumashi, *et al.* [14]

Fucoidan required further pre-treatment before NMR analysis for better and high quality spectra. This pre-treatment includes polymer hydrolysis to oligomers to simplify its structure which could be analyzed afterwards by different 1D and 2D-NMR techniques.

2.3.7. Pharmacological activities

2.3.7.1. Anti-coagulant activity

a. Activated partial thromboplastin time (aPTT)

Normally, aPTT records between 30-40 s, evaluates mainly the effect of anti-coagulants on the intrinsic pathway of blood coagulation system and to monitor patient's response to heparin therapy [133]. Results proved that fucoidan has a potential heparin-like or a heparinoid [134] anti-coagulant activity and interfered with intrinsic coagulation cascade. Coagulation times were significantly prolonged in comparison with the negative control (0.9% NaCl) which recorded 41.8 s.

Fig. 30 a shows that the purification process improved the anti-coagulant activity of crude fucoidan through prolongation of aPTT, where, in a concentration of 0.01 mg mL^{-1} , **Fucoidan_1** and **Fucoidan_6** prolonged coagulation times to 73 and 75 s, respectively, in comparison with 44.8 s for crude fucoidan. **Fucoidan_M** extended coagulation time, as well, but to a lesser extent to just only 51 s which was nearly similar to the reference analogue: 48.3 s. The effect on aPTT did not help discriminate between the LMWF **Fucoidan_1** and the HMWF **Fucoidan_6**. However, heparin of 0.005 mg mL^{-1} recorded 89.3 s indicating more than two times effectiveness than **Fucoidan_6**. In other experimental conditions, effect of **Fucoidan_PDD** was investigated on aPTT, as shown in **Fig. 30 b**. **Fucoidan_PDD** prolonged also aPTT significantly in a dose-dependent manner.

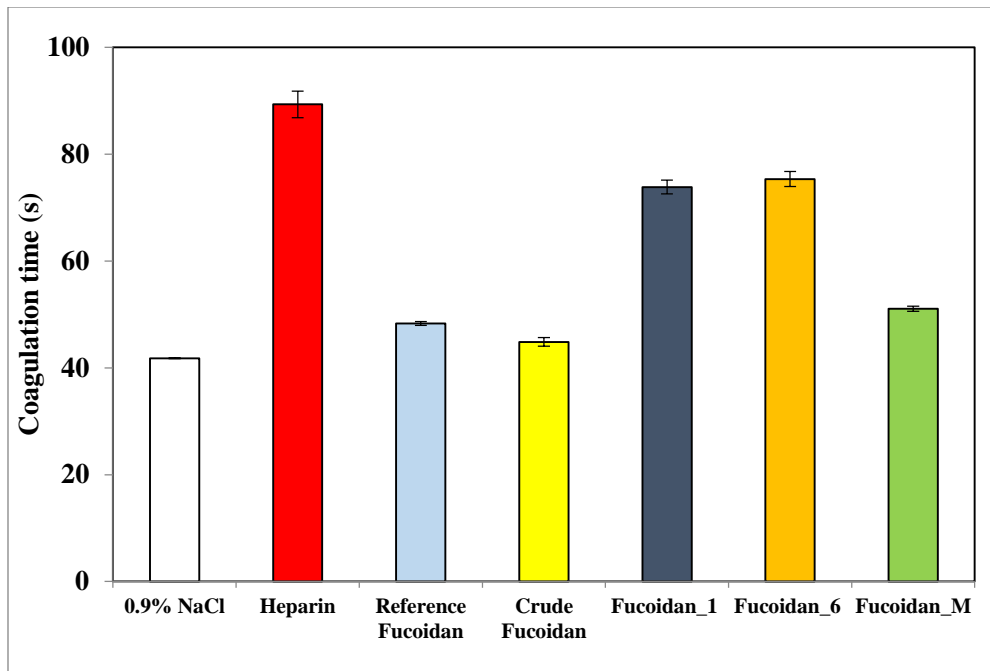


Fig. 30 a: Effect of different fucoidan fractions on aPTT at a concentration of 0.01 mg mL⁻¹
 0.9% NaCl and 0.005 mg mL⁻¹ heparin were chosen as negative and positive controls, respectively (n=3).

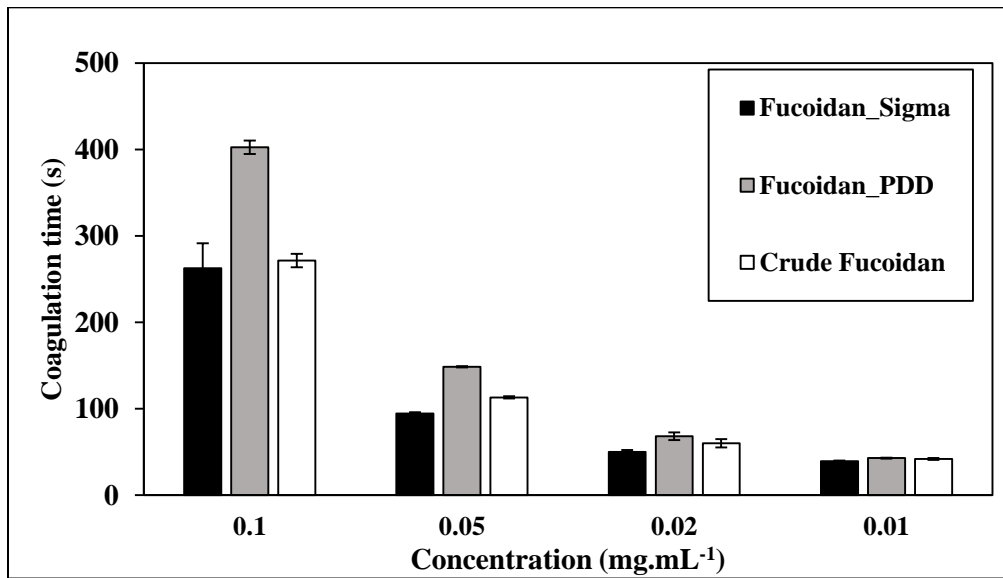


Fig. 30 b: A dose-dependent effect of Fucoidan_PDD on aPTT
 Effect was compared with crude fucoidan and reference fucoidan (Fucoian_Sigma) (n=3).

b. Prothrombin Time (PT)

PT is usually used to evaluate the effect of anti-coagulants (e.g., warfarin) on the blood extrinsic coagulation pathway. It is obvious in **Fig. 31** that all types of fucoidan were not able to prolong PT significantly in comparison with the negative control. These data were consistent with the mechanism of fucoidan as an anti-coagulant, which has a heparin-like effect and mediated by serine protease thrombin enzyme and/or heparin cofactor II inhibition [135] present in common and intrinsic pathways.

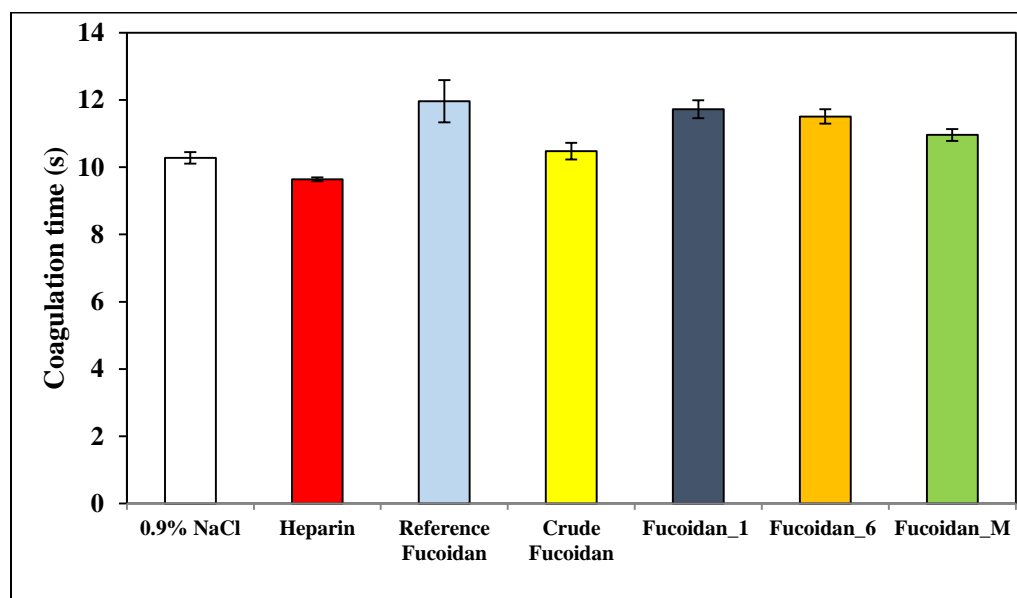


Fig. 31: Effect of different types of fucoidan on PT at a concentration of 0.01 mg mL^{-1}

0.9% NaCl and 0.005 mg mL^{-1} heparin were used as negative and positive control, respectively (n=3).

c. Thrombin Time (TT)

TT studies specifically thrombin function and the effect of anticoagulants against fibrinogen transformation into non-soluble fibrin threads. This step is enzymatically catalyzed by thrombin (Factor IIa). The reference range for the thrombin time is usually less than 20 s [136]. Results, as shown in **Fig. 32**, revealed a similar pattern as in **Fig. 30 a**, where **Fucoidan_6** also demonstrated the highest activity and recorded the longest time required for blood coagulation. **Fucoidan_1** and **Fucoidan_6** prolonged coagulation time significantly to 47 and 66 s, respectively, compared to 19.27 s for the negative control, while **Fucoidan_M** showed the weakest effect on coagulation time.

It increased the coagulation time only to 23.5 s compared with 31.3 and 29.2 s for reference and crude fucoïdan, respectively.

The anti-thrombin differences revealed the importance of sugar composition, molecular weights, and structural comfortability, where higher galactose, an enough long sugar chain and comfortable structure found in **Fucoïdan_6** were more critical than sulphate content for thrombin inhibition [43,137]. These conclusions could be confirmed by the weak effect of the low molecular weight of **Fucoïdan_1** and **Fucoïdan_M**, despite of their higher sulphate contents. More sulphate content than the required threshold could also lead to a decrease in the anti-thrombin activity [138,139,140]. Moreover, in a dose dependent manner, the effect of **Fucoïdan_PDD** as an anti-thrombin was investigated separately, as shown in **Fig. 32 b**. Results confirmed previous conclusions regarding the importance of polymer molecular weight and chain comfortability for anti-thrombin activity.

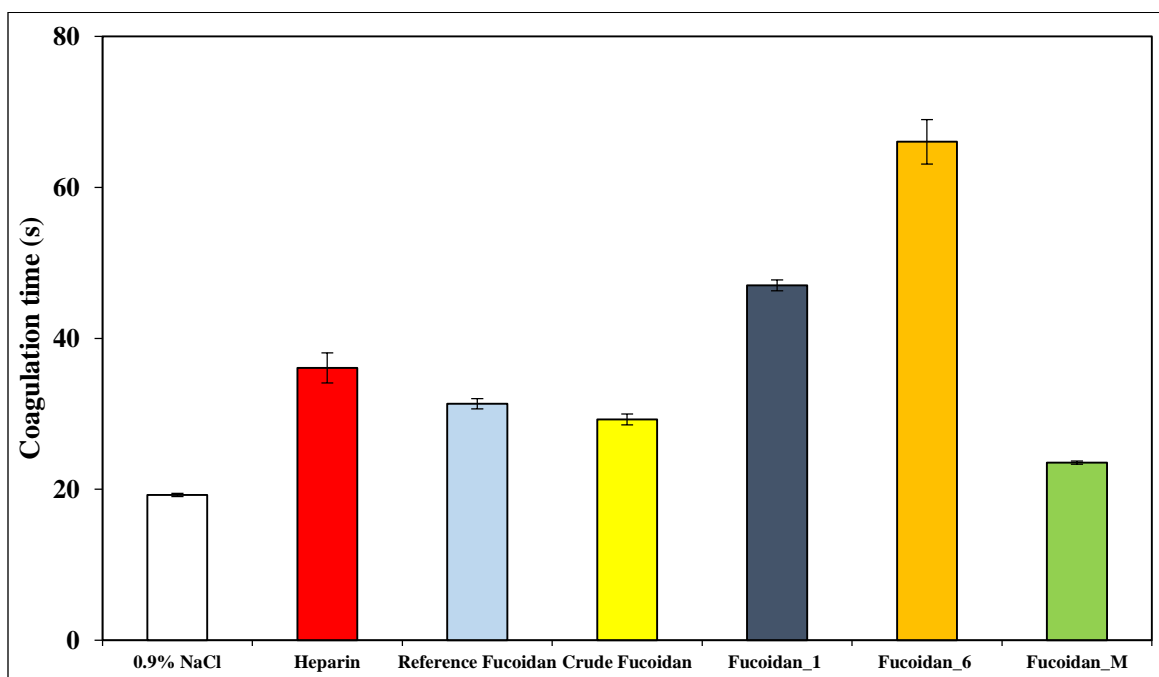


Fig. 32 a: Effect of different fucoïdan fractions on TT at a concentration of 0.01 mg mL⁻¹

0.9% NaCl and 0.005 mg mL⁻¹ heparin were tested as negative and positive control, respectively (n=3)

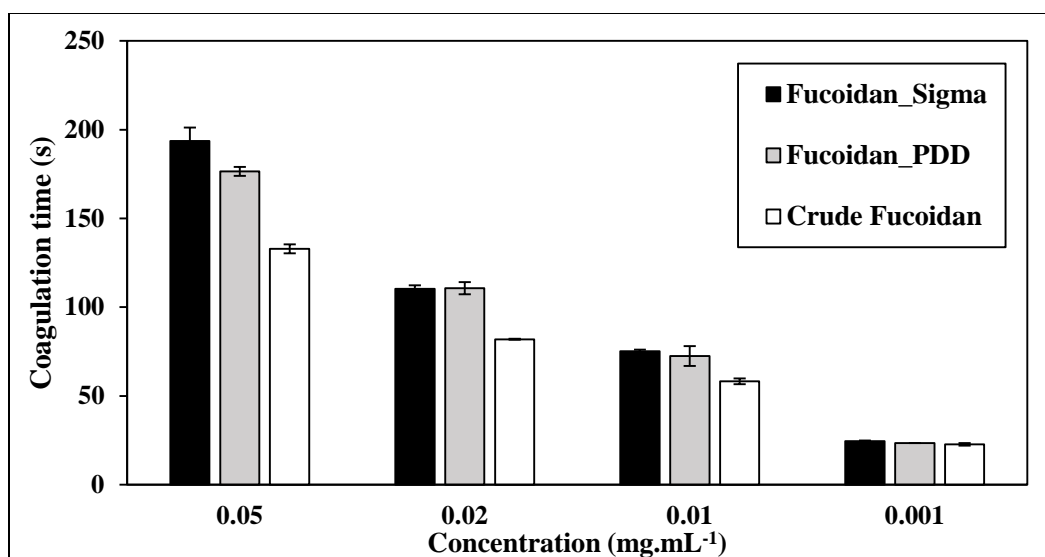


Fig. 32 b: A dose-dependent anti-thrombin effect of Fucoïdan_PDD

The effect on TT was studied in a comparison with crude and commercially-pure fucoïdan (Fucoïdan_Sigma) (n=3).

2.3.7.2. Anti-viral activity

Herpes simplex virus type 1 or HSV-1 is a human dsDNA virus that infects human and transmitted through oral-to-oral contact and causes cold sores. According to WHO, 67% of world population whose age under 50, have HSV-1 [141]. Fucoïdan exhibits its anti-viral activity against HSV-1 mainly through interference with viral replication [134], adsorption and penetration through cellular surface modification, and subsequently, it prevents the viral syncytium formation [63]. For this action, sulphate ester groups' position and content are critical for the anti-HSV-1 activity [134]. Consistent with literature, the fraction with the highest sulphate content, **Fucoïdan_M**, exerted a highly potent anti-viral effect in comparison with other types. **Fig. 33** demonstrates the anti-viral activity (%) with different serial dilutions for the different fucoïdan fractions against HSV-1 and followed by calculated IC₅₀ values in **Table 10**. IC₅₀ varied among different fucoïdan fractions from 2.41 µg mL⁻¹ for **Fucoïdan_M** to 5.69 µg mL⁻¹ for **Fucoïdan_6**. Furthermore, fucoïdan had an advantageous less cytotoxic effect against Vero B cell culture than the commercially-used reference anti-viral aciclovir.

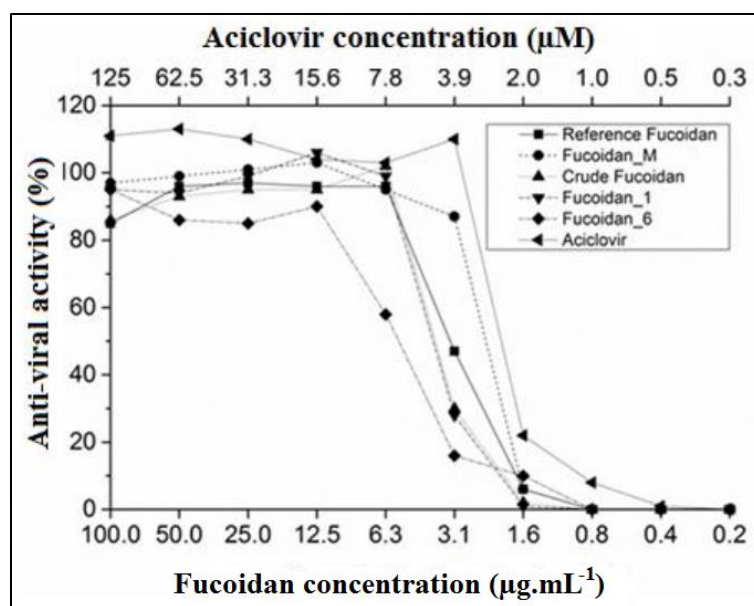


Fig. 33: Comparison between the anti-viral activities of fucoidan fractions against HSV-1

The activity was compared with the commercial analogue purchased from Sigma-Aldrich® (Reference fucoidan) against HSV-1. Aciclovir was used as a positive control.

Table 10: IC₅₀ (µg mL⁻¹) of different fucoidan fractions isolated and purified from *F. vesiculosus* against HSV-1 in comparison with aciclovir

	IC ₅₀ (µg mL ⁻¹)
Reference Fucoidan	3.3
Fucoidan_1	4.09
Fucoidan_6	5.69
Fucoidan_M	2.41
Crude fucoidan	3.99
Aciclovir	0.52

2.3.7.3. Anti-oxidant activity (DPPH Radical scavenging activity)

Radicle scavenging anti-oxidant activity of fucoidan was investigated its ability to capture the free radical DPPH. As shown in **Fig. 34**, all fractions of fucoidan, including crude and reference fucoidan, were DPPH inactive scavengers. The results are inconsistent with literature that confirmed the DPPH radicle antioxidant activity of fucoidan of *F. vesiculosus* [87,88]. Most of the published articles discussed the potential anti-oxidant activity of fucoidan applied a pre-treatment step with acetone, water/chloroform/methanol mixture and did not use formaldehyde, because of its toxicity. Formaldehyde functions to polymerize polyphenols which have a strong relationship with the

potential anti-oxidant activity of fucoïdan. Diaz-Rubio *et al.* have determined significant polyphenol content (960 mg phloroglucinol 100 g⁻¹ dry weight) in commercial fucoïdan from *F. vesiculosus* (Sigma-Aldrich, Spain) [89]. Since formaldehyde was applied in pre-treatment steps, anti-oxidant inactivity results for all fucoïdan fractions are reasonable.

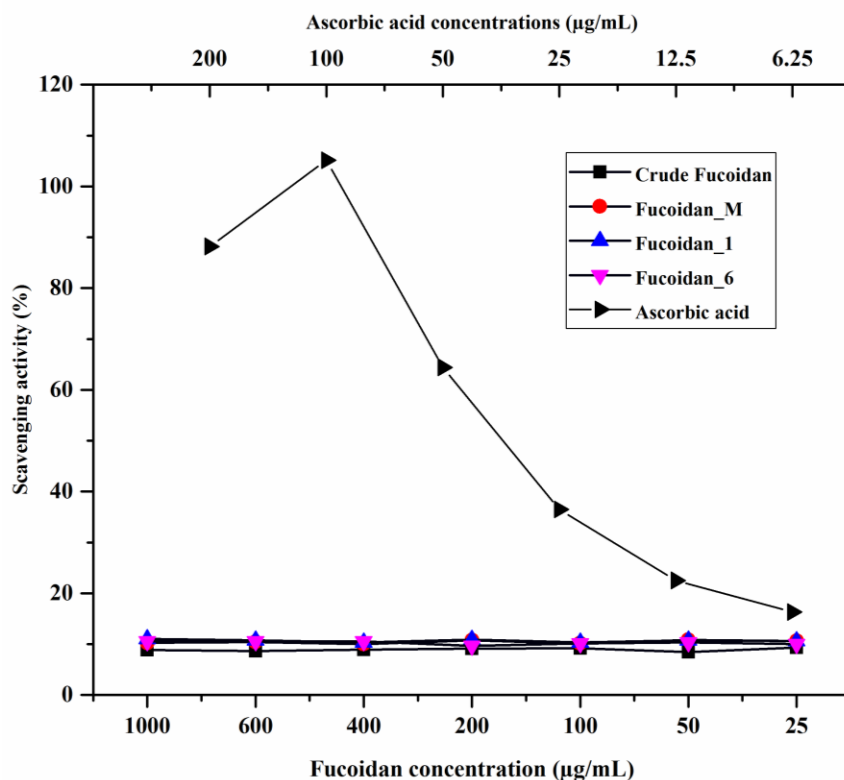


Fig. 34: Antioxidant activity of different fucoïdan fractions in comparison with ascorbic acid

The figure demonstrates the potential DPPH radical scavenging activity of ascorbic acid. However there is no activity for all fucoïdan fractions.

2.3.7.4. Anti-microbial activities

a. Anti-fungal activity

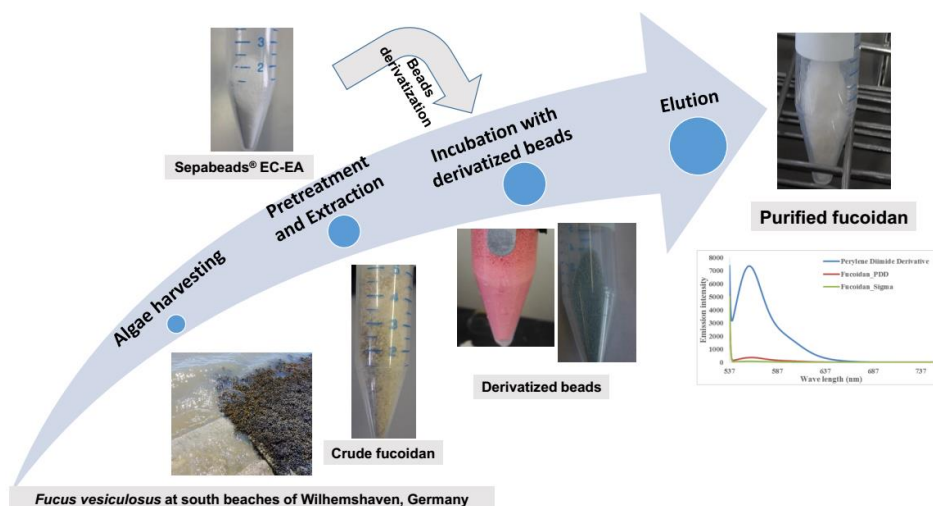
Fucoïdan's anti-fungal activity was investigated against a number of *candida* species, such as *C. albicans*, *C. glabrata* and *C. tropicalis*. All fucoïdan fractions did not show any activity and failed to eradicate the fungal growth. This means that fucoïdan could not affect sites of actions of common anti-fungal agents, such as sterols synthesis in cell membrane like polyene anti-fungal drugs or inhibition of cytochrome P₄₅₀-dependent enzymes as in azole anti-fungal drugs.

b. Anti-bacterial activity

As in anti-oxidant and anti-fungal investigations, fucoïdan was non-toxic to either Gram +ve as *S. aureus* or Gram -ve bacteria such as *E. coli*.

2.3.8. Process scaling-up and application of optimized conditions

Scheme 2 demonstrates the downstream fucoïdan extraction and purification processes. The process initiated with algae harvesting from its natural habitat, then pre-treatment, extraction of crude fucoïdan and finally purification with immobilized TB and PDD at pH 6. In addition, obtained yields from the different fucoïdan fractions are mentioned in **Fig. 35**.



Scheme 2: Graphical summary for fucoïdan purification process from *F. vesiculosus*

The downstream process includes algae harvesting, pre-treatment, extraction and purification with either TB- or PDD-derivatized beads.

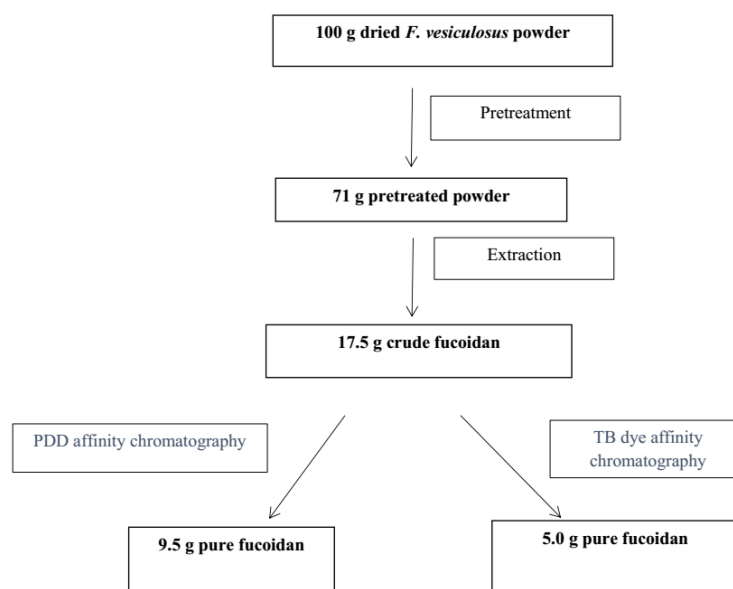


Fig. 35: Downstream process for fucoïdan extraction and purification by either TB- or PDD-derivatized beads at pH 6

The processes resulted in production of 5.0 g and 9.5 g of purified fucoïdan after purification with TB- and PDD-derivatized beads, respectively.

Moreover, fucoïdan content (%) or purity was investigated using TB and Heparin Red[®] Ultra assay methods. Fucoïdan purity was improved in comparison with crude fucoïdan by 1.69 and 1.4 fold after purification through TB- and PDD-immobilized beads, respectively. **Fig. 36** shows that after purification by PDD-immobilized beads, the investigated concentrations of **Fucoïdan_PDD** were similar to the commercial product regarding fucoïdan content. Concentration of **Fucoïdan_PDD** relative to standard was derived from the calibration curve. Purified fucoïdan (Fucoïdan_PDD) showed 97% purity relative to the reference fucoïdan (Fucoïdan_Sigma). Furthermore, alginate, the major contaminant in fucoïdan crude extract, did not show with Heparin Red[®] any fluorescence quenching behavior (**Fig. 77**). Since the response of Heparin Red is sensitive to the charge density of the polysulphated polysaccharide and the sulphation degree of **Fucoïdan_PDD** is lower than that of the reference fucoïdan (**Table 5**), the actual purity of **Fucoïdan_PDD** could be even higher.

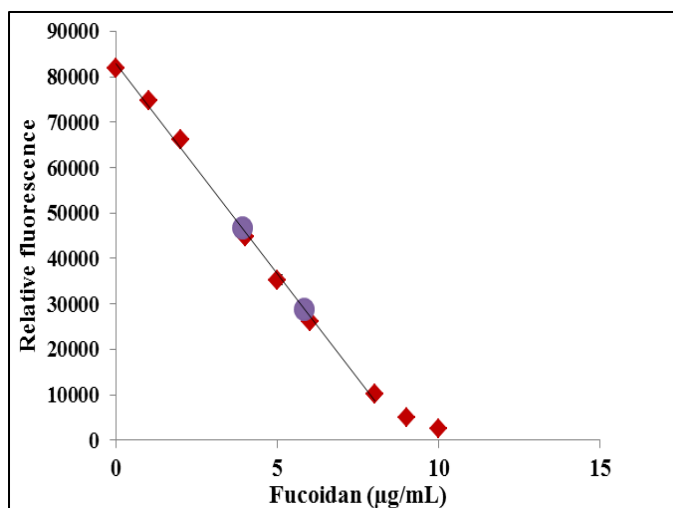


Fig. 36: Determination of Fucoïdan_PDD purity using Heparin Red[®] Ultra assay, in comparison with the commercial standard product (>95% pure) purchased from Sigma-Aldrich[®]

Fucoïdan content recorded 97% relative to the standard product. However, it was 69% in case of crude fucoïdan (Fucoïdan_A). Determination was compared with a calibration curve of the reference fucoïdan (red diamonds), using linear regression for the range 0.0-8.0 µg mL⁻¹ (R²=0.9974). **Fucoïdan_PDD** samples (0.4 and 0.6 µg.mL⁻¹) were prepared and the fluorescence determined (violet circles).

2.4. Conclusion and Prospectives

Pre-treatment with different solvents succeeded to reduce the co-extraction of other extraneous algal constituents (e.g., lipids, pigments, mannitol, and polyphenols). In addition, extraction in acidic condition at higher temperature with reflux improved the production yield of extracted crude fucoidan. Interestingly, application of the recently-developed dye affinity chromatography protocol was possible to purify fucoidan from its crude extract. Different conditions and factors were studied to optimize the process. Moreover, TB-derivatized beads had the selectivity to capture fucoidan even without fucoidan precipitation with ethanol. This procedure resulted in production of a new fucoidan fraction; **Fucoidan_M**. However, the results revealed that the process suffered from some disadvantages, such as long incubation periods and acidic pH were required to achieve the maximum loading capacity of the immobilized dyes, in addition to the inherent problems related to both thiazine dyes represented by limited number of adsorption sites and fucoidan as slower and different diffusion rates of fucoidan polymers and beads porosity, as well.

These challenges were overcome by synthesis and immobilization of a Heparin Red[®]-structurally related PDD which has more available adsorption sites than thiazine dyes. Immobilized PDD succeeded to capture similar quantities of fucoidan in a shorter incubation period at a slightly acidic condition. The second challenge with fucoidan diffusion rates was resolved by performing of the adsorption phase under an external pressure to push the fucoidan molecules much faster to the adsorption sites by developing a FPLC protocol. The last technique helped also to automate and scale-up of the purification process.

Future work should focus on using non-porous beads with more surface reactive sites. In addition, optimization of FPLC protocol in adsorption phase and in elution phase should be performed. It was clear that the maximum loading capacity of the column was not reached and this means that there were still available adsorption sites. The concentration of injected sample could be increased using a 5 mL injection loop to load the column with much fucoidan content considering the breakthrough curve of the purification process. Moreover, elution and fucoidan recovery (%) could be optimized by varying the eluent flow rates, applying warmer temperatures and another force instead of the vigorous shaking used in the batch process. Furthermore, application of such sensitive technique could be performed in fucoidan capture and analysis in different raw synthetic dosage forms in the presence of other drug excipients. These experiments could achieve great success in pharmacokinetic studies toward a FDA approval of fucoidan as a medicament.

3. Development of Axenic Protoplast and Callus-like Cultures from *F. vesiculosus*

3.1. Introduction

3.1.1. Marine biotechnology challenges

Seaweed farming through aquaculture (e.g., tanks, cages) was established to provide the expanding global market with its demands. However, major problems, such as control of epiphytes, fouling algae, grazing animals, and low levels of planting stock are greatly limiting industrial-scale seaweed cultivation. Moreover, seaweed farms occupy large areas hampering shipping and fishing and creating a lot of social problems as a result. Furthermore, seaweeds harvesting affects natural marine and terrestrial ecosystems negatively [143]. Expansion of market requirements from seaweeds and their valuable products needs new technologies, especially these eco-friendly techniques (e.g., marine biotechnology), as alternative tools.

Marine biotechnology has drawn a special interest in the last few decades following advances developed in plant and animal fields [1,145] as a potential tool for the discovery and development, of marine-derived compounds with biomedical applications. It involves tissue culture, protoplast isolation, cell fusion and gene transfer [146]. Its advantages include the production of a high-yield with improved quality products from fast growing and diseases-free strains [147]. However, the challenge facing the marine biotechnology industry in the next millennium is to:

- identify new sources of marine bioproducts;
- develop novel screening technologies;
- provide a sustainable source of supply; and
- optimize production and recovery of the bioproducts [148].

Microalgae have rapid growth rates, simple structures and ability to adapt in different cultivation conditions [149]. These factors led to interesting advances in cultivation techniques including isolation and purification of microalgae from natural habitat and well-characterized nutritional requirements. As a result, a possible establishment of a lot of microalgae single strain cultures either in a closed or open system. Therefore, microalgae have been seen as potential candidates in biotechnological researches and industrial applications for production of biofuels and valuable bioactive compounds. These achievements encouraged the performance of similar techniques for the more developed and complicated seaweeds in the last few decades.

3.1.2. Marine microbes and macroalgae tissue culture

Adding to the complex structure of marine macroalgae, marine microbes live in a symbiotic relationship with seaweeds. They produce vital compounds for macroalgae immune system resulting in improving the host resistance [150,151] or function in the food chain cycle, as well as nutrients assimilation. Macroalgae host various marine microbes and diatoms providing them protection from tides and predators. Moreover, marine bacteria are very important for macroalgae development and morphogenesis, such as the green algae *Ulva mutabilis* through a cell to cell communication signals [152,153].

A crucial requirement for bioprocess technologies for production of valuable marine products is the development of an axenic, fast-growing culture before scale-up to various bioreactor cultivations [145,154]. The surface of seaweeds is heavily infested by various microbial and larger epiphytes. Some of these organisms are implanted in cell walls and between meristematic cells which are frequently located on the surface and will be impaired upon chemical treatment [132]. Meristematic cells are highly divided cells and seen as a potential tissue for starting various marine biotechnology techniques. Due to microbes' diversity, an efficient and easily-applicable surface sterilization protocol is needed. This protocol should combine more than one strategy to combat against the different marine populations. In contrast to terrestrial plant, thallus tissue is mainly composed of delicate parenchyma tissues. Application of sodium hypochlorite (NaOCl) and 70% (v/v) ethanol are commonly-used as disinfectants in terrestrial plant surface sterilization protocols eradicating most of the symbiotically-lived microorganisms. However, they could bleach and destroy macroalgae parenchymal tissues and thereby reducing photosynthetic ability and viability.

Several strategies could be applied to obtain marine aseptic cultures, such as using ultraviolet radiation [155], povidone iodine and broad spectra antibiotics [154]. Nevertheless, these strategies are ineffective, time-consuming; especially, when used as separate procedures and their doses should be further controlled. Moreover, the effect of surface sterilization procedures on tissue vitality should be evaluated afterwards before starting cultivation as well. Trials to develop marine STC are still in their infancy compared to PTC for production of valuable compounds [156]. This status could be related to tissue structure complexity found in macroalgae in addition to nutritional and long-term aseptic requirements. These factors determine the part within the thalli from which the explant is excised and the degree of relationship between marine microbiomes and macroalgae.

3.1.3. Development of marine macroalgal cultures

Callus-like cultures are well-known cell lines for decades as friable totipotent non-differentiated cells. These lines used as production systems for a lot of bioactive compounds in PTC (e.g., paclitaxel and Scopolamine) [157]. However, marine callus-like growth appears usually as filaments originating from exposed cut meristematic active cells, as shown in **Fig. 37**. Through further culture optimization (i.e., medium solidity, photoperiod regime and phytohormones), organogenesis and development into a plantlet were possible [158].

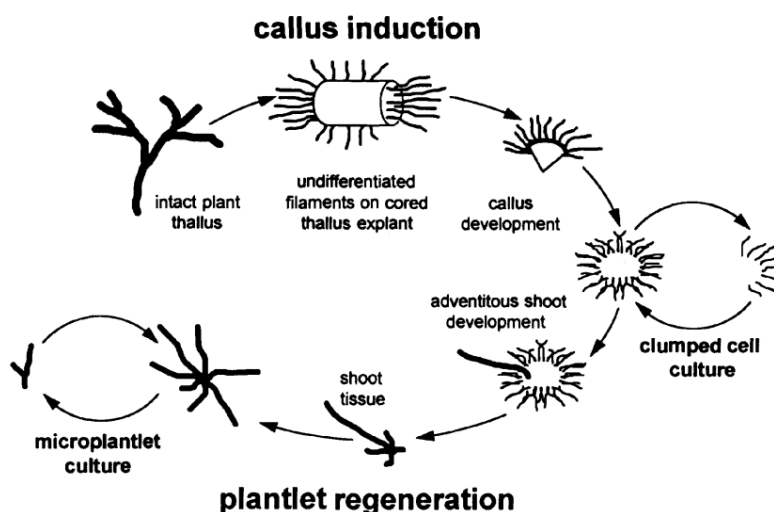


Fig. 37: Callus and plantlet regeneration from an intact marine macroalgae thallus of *Agardhiella subulata* [158]

Moreover, Huang and Rorrer established a microplantlet suspension culture from the red algae *Agardhiella subulata* in a stirred tank photobioreactor [159]. Such achievements could lead to elicitation of a diverse array of valuable natural compounds from a reliable supply of a macroalgae cell biomass.

Another relatively new biotechnological strategy to develop a marine biomass culture is protoplast cultivation. Although, protoplast isolation in terrestrial plants was known since 1960s, it has only been recently shown in seaweeds. Marine protoplasts have cell membranes but lack their polysaccharide cell walls. Macroalgae cell walls could be removed through a specifically enzymatic attack to both the microfibrillar and polysaccharide matrix components (i.e., alginate, galactans and fucoidan) [160,161]. Isolation of protoplasts from red and brown algae are more difficult than in green algae, because of their cell wall resistance to cellulase and pectinase [162]. Reddy and Fujita

isolated protoplast from three species of green algae and succeeded to regenerate plantlet from axenic protoplast culture of *Enteromorpha linza* [163].

3.1.4. Growth requirements and previously-performed trials

Axenic as well as vital explants could be cultivated and induced to give a callus-like growth and continue further to develop a cultivation in a closed system bioreactor. Different growth conditions and factors could be applied and affect culture growth, as demonstrated in **Fig. 38**.

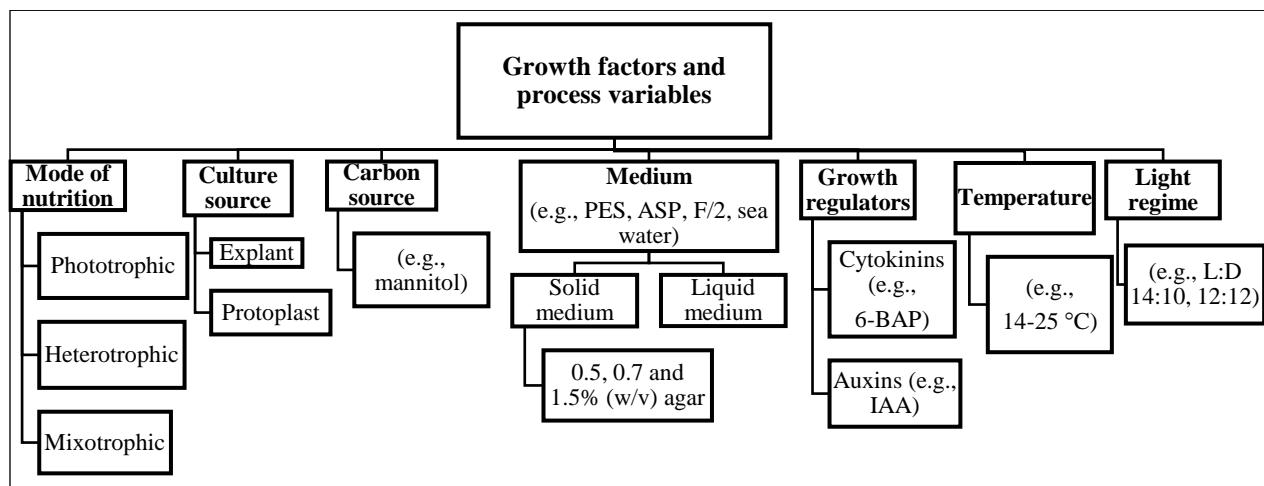


Fig. 38: Summary of previously-applied growth conditions and variables to develop marine macroalgal cultures

In more details, several experiments were previously mentioned for development of a callus-like growth and plantlet regeneration from seaweeds, as shown in **Table 11**. Nevertheless, few of them could succeed to produce valuable products in bioreactor systems (e.g., *Laminaria saccharina* suspension culture system) which biosynthesized three bioactive hydroxy fatty acids deriving from ω -6 lipoxygenase oxidation [158].

Table 11: Some selected trials with callus cultures and plant regeneration in marine macroalgae organisms

Macroalgae class	Parameters	Organism	Medium	Ref.
1. Brown algae	<ul style="list-style-type: none"> • T: 12 °C, • L:D (8:14) 	Apical meristematic cells of <i>F. vesiculosus</i>	Sterile sea water	[164]
	<ul style="list-style-type: none"> • T: 14 °C, • L:D (14:10), 2000 Lux • 3% Mannitol 	<i>Dictyosiphon foeniculaceus</i>	ASP 12-NTA, 0.1% yeast, 1.5% agar (ASP-C-1 medium)	[165]
	<ul style="list-style-type: none"> • T: 20-22 °C, • L:D (12:12), 30 $\mu\text{E m}^{-2} \text{s}^{-1}$ 	Phycocolloid yielding seaweeds (e.g., <i>Turbinaria conoides</i>)	PES for red seaweeds or modified PES with 0.4% KI (PESI) for brown seaweeds with 1.5% Bacto agar	[166]
	<ul style="list-style-type: none"> • T: 15 °C, • L:D (16:8), 100 $\mu\text{E m}^{-2} \text{s}^{-1}$ 	<i>Sargassum heterophyllum</i>	ASP-12 NTA	[167]
	<ul style="list-style-type: none"> • T: 15 to 25 °C • L:D (12:12), 20-200 $\mu\text{E m}^{-2} \text{s}^{-1}$ (Blue light) 	<i>Sargassum horneri</i>	ESL medium supplemented with 5 μM uniconazole (a triazole-type inhibitor of cytochrome P ₄₅₀ enzymes)	[168]
	<ul style="list-style-type: none"> • T: 14 °C, • L:D (14:10), 2000 Lux, cool white fluorescent lamps 	Medullary tissues of <i>Laminaria angustata</i>	ASP 12-NTA medium solidified with 1.0% agar	[169]

Cont., Table 11: Some selected trials with callus cultures and plant regeneration in marine macroalgae organisms

Macroalgae class	Growth parameters	Organism	Medium	Ref.
2. Green and Red algae	<ul style="list-style-type: none"> • T: 18 °C, • L:D (12:12), 60 $\mu\text{E m}^{-2} \text{s}^{-1}$ 	Different species of green and red macroalgae	Seven different media in liquid form and as gels (e.g., sea water, PES, ASP-C-1) (agar 0.3-1.5%, or carrageenans 0.5-3%).	[170]
	<ul style="list-style-type: none"> • T: 20 °C, • L:D (12:12), 10-20 $\mu\text{E m}^{-2} \text{s}^{-1}$ 	Some species of red algae	ASP-12 NTA solid medium (1.5% agar) supplemented with IAA and BAP	[171]
	<p>For solid medium:</p> <ul style="list-style-type: none"> • T: 19 °C, • L:D (14:10), 25 $\mu\text{E m}^{-2} \text{s}^{-1}$ <p>For liquid medium:</p> <ul style="list-style-type: none"> • T: 19 °C, • L:D (14:10), 98 $\mu\text{E m}^{-2} \text{s}^{-1}$ 	Green algae (<i>Ulva pertusa</i>)	Artificial sea water (0.7% agar) supplemented with different plant growth regulators, organic acids and sugars	[172]
	<ul style="list-style-type: none"> • T: 20-22 °C, • L:D (12:12), 5 $\mu\text{E m}^{-2} \text{s}^{-1}$ 	Red algae (<i>Gelidiella acerosa</i>)	PES medium solidified with 1.5% agar	[173]

3.2. Materials and Methods

3.2.1. Harvest and pre-treatment of algae

The brown algae *F. vesiculosus* was chosen also as a model for the brown macroalgae tissue culture development. Algae was harvested by Alfred Wegner Institute-Helmholtz Institute for Polar and Marine Research (Helgoland, Germany) from the North Sea in summer 2015. It was kept wet with sea water in ice-cooled boxes during transportation to the laboratory which was performed directly after collection.

As soon as algae had reached the laboratory, the thalli were washed thoroughly with tap water for 2-3 min removing visible symbionts with hands and brush, and then 1-2 min using sterile sea water or normal saline. Cleaned thalli were stored afterwards in wet hand tissues at 4 °C.

3.2.2. Surface sterilization

All the following steps were performed in a laminar flow cabinet and with sterile reagents and materials. In addition, reagents were prepared in a sterile sea water. Thalli were cut into 7-10 cm pieces which divided afterwards into six groups to evaluate different surface sterilization protocols.

a. Protocol 1: 2% (w/v) Povidone iodine and 70% (v/v) ethanol

Thallus pieces were dipped in 70% (v/v) ethanol for 3-5 s, dried on filter paper, and washed with deionized water for 2 min to rinse the alcohol. Then, they were rubbed smoothly with Kleenex® for cleansing before being immersed in 2% (w/v) povidone iodine solution for 4 min. Povidone iodine was then removed with a filter paper and washed out for several times with deionized water for 2 min.

b. Protocol 2: 2% (w/v) Povidone iodine, 70% ethanol and UV radiation

The same steps were performed as in **Protocol 1**. Pieces were then cultured in MB50 and LB agar plates which further exposed to UV radiation for 15 min.

c. Protocol 3: 2% (w/v) Povidone iodine, 70% ethanol, 10 µM GeO₂ and 1% (v/v) Triton X-100

The same steps were performed as in **Protocol 1**, except that 10 µM GeO₂ was added to the povidone iodine solution, which was prepared in 1% (v/v) Triton X-100.

c. Protocol 4: Ultrasound, 5% (w/v) povidone iodine, 10 µM GeO₂ and antibiotics

In the following **Protocols (4-6)**, other mechanical and chemical treatments (e.g., ultrasound and antibiotics) were performed. The 7-10 cm pieces were thoroughly washed in PESA medium (PES

medium without vitamins) three times (2 min each), and stored overnight in a fresh medium at 4 °C. These pieces were then treated for 10 s in an ultrasound bath (40%) at room temperature, and then rinsed once with water and once with medium. Pieces were then immersed in groups of 3-5 in a solution of 10 mL of 1% (v/v) Triton X-100, 10 mL 5% (w/v) povidone iodine and 30 mL PESA medium. The suspension was shaken vigorously with hand for 5 min and then treated in an ultrasound bath for 5 s again. To remove the brown colour of iodine, pieces were washed five times in a PESA medium. The next step utilized a concentrated antibiotic treatment. Thallus pieces were incubated for 1 h at 4 °C with 5 mL 1% (v/v) Triton X-100, 15 mL 30x filter-sterilized antibiotic mixture (constituents of antibiotic stock solution are described in **Table 12**) and 20 mL of PESA medium. Thallus pieces were washed several times with medium before a second antibiotic treatment with 5 mL of antibiotic stock solution in 45 mL PESA medium. This treatment was applied for 48 h without shaking in conditions similar to cultivation conditions (e.g., a photoincubator adjusted to 17 °C, photoperiod of L:D (16:8) and 35 $\mu\text{E m}^{-2} \text{s}^{-1}$ as a light intensity). Finally, pieces were thoroughly washed several times with PESA medium to remove antibiotic residuals before sterility and viability assessments.

Table 12: Antibiotic stock solution (30x) composition [274]

Antibiotics were used in **Protocol 4-6**.

Component	Quantity (mg) /100 mL
Ampicillin sodium	360.0
Kanamycin sulphate	600.0
Tetracycline hydrochloride	360.0
Chloramphenicol **	300.0
Gentamycin sulphate	240.0
Penicillin G sodium	600.0
Erythromycin**	600.0
Nystatin***	300.0

* After preparation, the stock suspension was filter-sterilized and stored at - 20 °C.

** Prepared in 5 mL in 70% ethanol before addition to the stock solution.

*** Prepared in 5 mL in DMF before addition to the stock solution and used only in **Protocol 6**.

d. Protocol 5: Ultrasound, 5% (w/v) povidone iodine, 10 μM GeO_2 , antibiotics and UV radiation

The same steps as **Protocol 4** were performed, but cultured pieces were incubated in LB and MB50 media plates and then exposed to UV light for 15 min.

e. Protocol 6: Ultrasound, povidone iodine, 10 µM GeO₂, antibiotics and Nystatin

Protocol 6 was performed similarly as **Protocol 4**, except that 300 mg of Nystatin as an anti-fungal agent was mixed with the 30x antibiotic stock solution. Due to its poor water solubility of Nystatin, it was prepared in 5 mL DMF before addition to the antibiotic stock solution. Performed processes of **Protocols (1-6)** could be summarized in **Table 13**.

Table 13: Summary of processes performed in all surface sterilization protocols

Steps are described after algae harvesting, washing with sterile sea water and cutting into 7-10 cm pieces.

Type of treatment	Protocol 1	Protocol 2	Protocol 3	Protocol 4	Protocol 5	Protocol 6
2% (w/v) Povidone iodine	+	+	+	-	-	-
70% (v/v) ethanol	+	+	+	-	-	-
UV radiation	-	+	-	-	+	-
5% (w/v) Povidone iodine	-	-	-	+	+	+
Ultrasound radiation	-	-	-	+	+	+
10 µM GeO ₂	-	-	+	+	+	+
1% Triton X-100	-	-	+	+	+	+
Antibiotic without Nystatin	-	-	-	+	+	-
Antibiotic with Nystatin	-	-	-	-	-	+

+: applied; -: not applied

3.2.3. Sterility investigation

After each protocol, treated thalli pieces were further cut into 2-3 cm pieces and cultured on MB50 and LB (Miller) solid media for sterility investigation. They were incubated in groups of 2-3 pieces for 2 weeks at 17 °C and 26 °C, respectively, in dark to check for any type of microbial growth. Incubation was performed in a static shaker incubator.

3.2.4. Genotyping of microbial contaminants

As described by AllPrep[®] DNA/RNA mini Kit (Qiagen, Germany) manual, genetic materials from contaminated explants were extracted and purified [174]. Samples were ground and put in sterile E-Matrix-tubes (MP Biomedicals GmbH, Germany) which were filled with 600 µL RLT lysis buffer

and 6 μ L mercaptoethanol. Then, tissue and cell lysis was performed in a tissuelyzer for 2 min at 30 Hz and frozen at -70 °C for 5 min in liquid nitrogen and repeated for three times. 18S SSU rRNA genes were identified and amplified from DNA and cDNA using the universal eukaryotic primers Euk-A (5'-AACCTGGTTGATCCTGCCAGT-3') and Euk-B (5'-GATCCTTCTGCAGGTTACCTAC-3') [175]. An initial denaturation at 98 °C for 30 s, followed by 35 cycles at 98 °C for 10 s, 67 °C for 30 s and 72 °C for 30 s and finally at 72 °C for 5 min were carried out. PCR products were checked by gel electrophoresis using 1% (w/v) agarose and then purified by MinElute PCR Purification Kit (Qiagen, Germany). Afterwards, a nested PCR experiment was performed for the purified products using the Euk82F (5'-GAAAGTCTGCTGAACTGGCTC-3') and Euk1517R (5'-ACGGCTACCTTGTTACGACTT-3') primers following the protocol which consisted of 98 °C for 30 s for denaturation, 30 cycles of 98 °C for 10 s, 53 °C for 30 s, and 72 °C for 30 s and finally at 72 °C for 5 min. Amplicons were checked and purified again as described before. Ligation and cloning of the PCR products were achieved as described in manual of NEB PCR cloning kit using pMiniT as a vector, before the isolated constructs were sent for sequencing by Seq-It GmbH (Kaiserslautern, Germany). Alignment of sequencing results were performed by NCBI-blast database in order to identify the microbial contamination.

3.2.5. Vitality investigation (2,3,5-Triphenyltetrazolium chloride (TTC) assay)

According to a previously described protocol by Nam, *et al.* [176], 0.8% (w/v) TTC was prepared in a 50 mM Tris-HCl buffer (pH 7) in PESA medium. Triplicates of 0.1 g pieces of treated as well as non-treated thalli were each incubated in 15 mL capped test tubes with 4 mL of TTC colorless solution and two drops of mineral oil. After 1 h incubation in the dark at 20 °C without shaking, thalli were washed with sterile PESA medium 3 times. To extract the red and water insoluble reduction product triphenylformazan (TPF) from tissues, 2 mL of 0.2 M KOH prepared in 25% (v/v) ethanol was incubated with the thalli for 15 min in a drying oven at 60 °C. For a quantitative determination of TPF, hexane (2 mL) was added to a cooled extract, the sample was then vortexed for 10 s and centrifuged (4500 rpm) for 1 min. Finally, the upper red hexane layer was measured by colorimetry at 545 nm, using hexane as a blank.

3.2.6. Protoplast isolation and culture development

Protoplasts from *F. vesiculosus* were isolated and purified as described previously by Mussio and Rusig [177]. Briefly, 0.7 g of previously-sterilized explant with **Protocol 6** was digested with 20 mL of a filter-sterilized enzyme solution (see **Appendix C: Medium composition and preparations**) for 20 h in the dark at room temperature in addition to 1 h in an overhead shaker (F1 mode, 30 rpm). After tissue digestion, the cell suspension was filtered by an autoclaved sieve with a 40 μm mesh size. Isolated protoplasts were washed for two times in a sterile washing solution (5 mL each) containing 0.4 M NaCl and 5 mM CaCl_2 . A sample of isolated protoplasts was detected by UV light using 10 $\mu\text{g mL}^{-1}$ Calcofluor white stain and a microscope.

3.2.7. Development of protoplast and callus-like cultures

Several growth variables were investigated to check their ability to induce callus and protoplast cultures either in solid, suspension cultures in addition to bioreactors. Cultures were incubated in a photoincubator at controlled parameters including temperatures and light regimes and intensities. Applied growth conditions were summarized, as shown in **Fig. 39**.

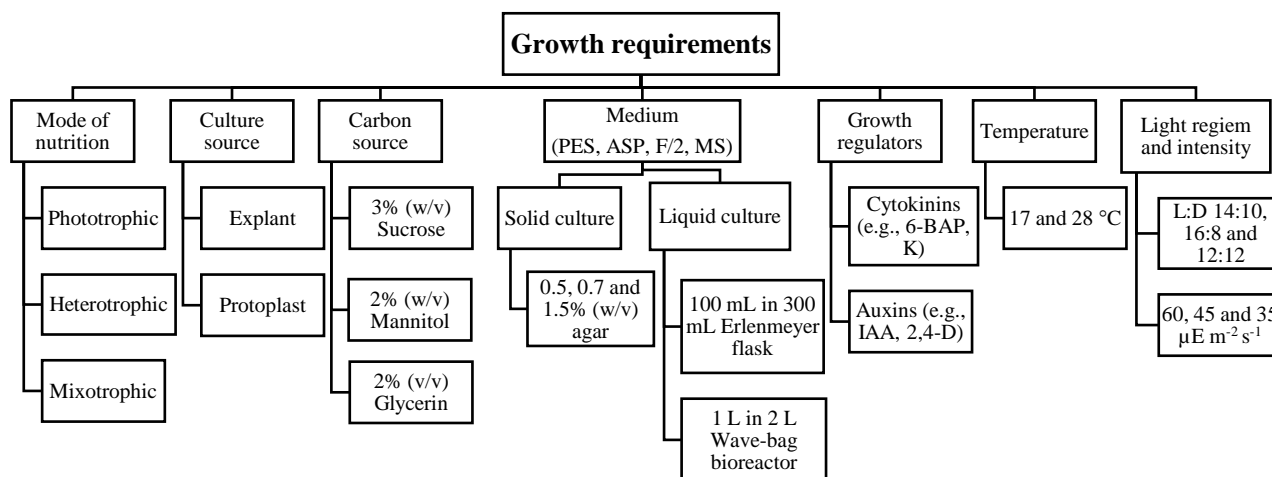


Fig. 39: Applied growth conditions and variables to induce callus-like and protoplast cultures

These conditions were applied separately and in combinations during callus development.

In more details, the different culture types were induced, as described in the following sections.

3.2.7.1 Protoplast culture

Induction of cell wall reformation and cell reproduction were performed as follows: 1 mL of washed isolated protoplasts was cultured in 2 steps, for one week as a heterotroph in a 50 mL protoplast medium containing 2 mM HEPES, 1% (v/v) PES with 3.8% sea salt, 0.25 M glucose, 0.15 M sucrose, 0.025% (w/v) casein hydrolysate, 20 μ M ornithine and supplemented with a combination of 45 μ M 2,4-D and 40 μ M CPPU as plant growth regulators [178]. Afterwards, in a 50 mL PES medium, 10 mL of cultured protoplasts were sub-cultured as phototroph at 17 °C with a shaking rate (130 rpm) using an orbital shaker and L:D 14:10, 35 μ E m⁻² s⁻¹. Mixotrophic and heterotrophic cultivation using 2% (v/v) glycerin as a carbon source were also investigated. In parallel, cultivation in solid medium supplemented with 0.5% (w/v) agar at the same previously conditions were applied.

3.2.7.2 Callus induction

a. Solid cultures

ASP-12-NTA, according to Provasoli [165], PES [155] and F/2 (Guillard's (F/2) Marine Enrichment medium purchased from Sigma-Aldrich® 50x stock solution) media supplemented with 0.5, 0.7 and 1.5 % (w/v) agar were incubated with 2-3 explants that were previously surface sterilized with **Protocol 6**. The cultures were cultivated as phototrophs, mixotrophs and heterotrophs in different light regimes including intensities at 60, 45 and 35 μ E m⁻² s⁻¹ and with photoperiods L:D of (16:8, 14:10 and 12:12) at 17 °C and 28 °C. In mixotrophic and heterotrophic cultivation, either 3% (w/v) sucrose or 2% (w/v) mannitol or 2% (v/v) glycerin were used as a carbon source.

In addition, different growth regulators, such as auxins (e.g., 2,4-D and IAA) and cytokinins (e.g., K and BAP) were supplemented some cultivation medium to study their effect on callus induction from explants. They were applied in concentrations of 0.1 mg mL⁻¹ for IAA and BAP [171], 4 μ M for 2,4-D and 2 μ M for K.

b. Liquid suspension cultures

i. Cultivation in Erlenmeyer flasks

Applying the same conditions in solid cultures, two-three explant pieces were cultivated in 100 mL media in 300 mL Erlenmeyer flasks. The flasks were incubated for a week at static condition, then

agitated at 130 rpm using an orbital shaker. Sub-culturing was performed regularly at 6-8 weeks intervals.

ii. *Cultivation in wave bag photobioreactor (PBR)*

Rhythmic, wave-like movement of the wave bag bioreactor was attempted to induce callus growth directly from explants. In a 2 L bag, 20 algae explants of *F. vesiculosus* were incubated in phototrophic growth conditions in a 1 L PES medium at 18 °C with a rocking speed 15 r min⁻¹, a 10° angle and an air flow rate of 90 m.min⁻¹ with a photoperiod of L:D (16:8) and light intensity of 30-50 μE m⁻² s⁻¹. Regularly, 100 mL of medium were replaced weekly with a fresh medium under sterile conditions.

3.3. Results and Discussion

3.3.1. Sterility investigations

3.3.4.1 Surface sterilization procedures

Complex interrelationships between marine organisms resulted in difficult complete removal of marine microbes and production of axenic cultures. Such features limit advances in *in vitro* marine biotechnology. Collection of clean and healthy algae from regions of low contamination or from deep water is recommended to ease the process of sterilization and obtain an axenic culture. Different treatments were investigated to produce axenic or unialgal cultures, for example:

- a. **70% (v/v) Ethanol** had a harmful effect on microorganisms' cell wall leading to protein denaturation and precipitation. A major disadvantage of ethyl alcohol was its bleaching and nonspecific tissue destructive effect (i.e., immersion of explants for more than 10 s) resulted in a pale green colored explant.
- b. **UV radiation** had a germicidal effect. It penetrates microorganisms' cell wall and cytoplasmic membrane causing a molecular rearrangement of the microorganism's DNA that prevents it from reproducing.
- c. **GeO₂** was applied to suppress the growth of diatoms. GeO₂ competes with SiO₂ in diatoms biochemical metabolic reactions. It was reported that the presence of GeO₂ could inhibit growth of brown algae contrary to green and red algae [179]. Therefore, washing with sterilized sea water for several times was performed immediately after this step to remove Ge residuals.
- d. **Povidone iodine or Betadine[®]** is a surface disinfectant against a broad spectrum of germs. Such treatment is well-known to establish axenic marine cultures [166,180].
- e. **Ultrasound radiation and Triton X-100** were effective tools to disintegrate and dislodge associated adherent microorganisms [181].
- f. **Broad-spectrum antibiotics** with bactericidal and bacteriostatic effect were applied in two steps as the main tool to remove marine bacteria including cyanobacterial contamination [181,182]. Because the nature of marine bacterial flora is variable and not well-characterized, a mixture of broad-spectrum antibiotics was effectively applied.
- g. **Anti-fungal agent** like Nystatin was used to control the fungal contamination [154].

Results showed that cultured explants sterilized by all protocols, except **Protocol 6**, suffered from contamination in all cultured plates in LB and MB50 plates. The best results were obtained from **Protocol 6**, which showed that more than 90% of cultivated explants were sterile. In **Protocol 6**, the

cultured explants on MB50 and LB media still showed contamination until the second treatment of antibiotics, as reported in **Fig. 40**.

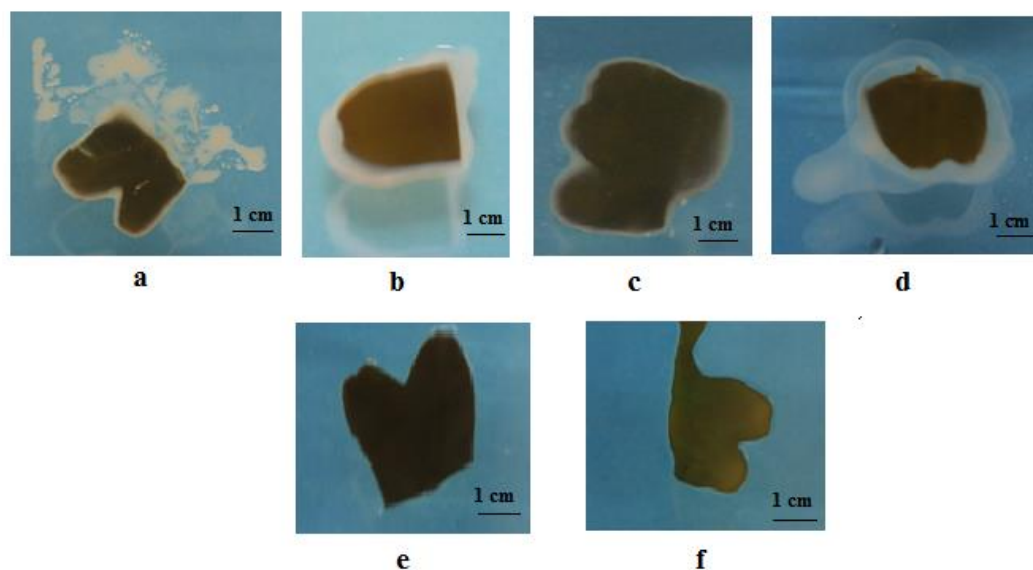


Fig. 40: Different explants of *F. vesiculosus* incubated on MB50 (a, b, c, d and e) and LB (f) media at 17 °C and 26 °C, respectively, after different steps of Protocol 6
a: non-treated explant; **b:** after washing with sterilized PESA medium step; **c:** after sonication step; **d:** after treatment with povidone iodine and Triton X-100; **e:** after a 2nd treatment with broad-spectrum antibiotics including Nystatin; **f:** after a 2nd treatment step with antibiotics including Nystatin on LB medium.

3.3.4.1 Genotyping of microbial contaminants

Results of 18S rRNA nucleotide sequencing which was isolated from contaminated explants revealed the presence of *Aplanochytrium* sp. with an identity of 97%. *Aplanochytrium* sp. (Labryinthulomycota) are marine heterotrophic stramenopiles that associate often in a parasitic relationship with dead and decay marine algae [183]. These findings showed the importance of the addition of an anti-fungal agent during surface sterilization procedures.

3.3.2. Vitality investigation

Enzymatic reduction of TTC was investigated to determine quantitatively axenic explants vitality and their metabolic activity, in comparison with non-sterilized thallus tissues. TTC is a colourless, water-soluble reagent that enzymatically-transformed to red, water-insoluble TPF through a

reduction reaction [184]. This biotransformation reaction occurred through a tetrazolium radicle, as shown in **Fig. 41**, and thus tissue dehydrogenase activity and vitality could be quantitatively determined. The enzymatic conversion was evaluated by absorbance measurement at 545 nm to prevent interferences from other pigments [185]. Since TTC is oxygen- [186] and light-sensitive [184], mineral oil was added to cover the reaction surface without shaking and performed in darkness, respectively.

In optimized protocol (i.e., **Protocol 6**), tissue vitality (%) after the washing step with sterilized sea water or PESA medium, after ultrasound treatment and by the end of the protocol recorded 78 ± 1.01 , 51 ± 1.13 and 29 ± 0.026 %, respectively, relative to vitality of a non-sterile thallus. Before complete axenic conditions, marine microbes interfered also with this reaction results, because they had also the ability to reduce TTC. Therefore, by the end of protocol, the explants were only responsible for the 29% vitality detected during the TTC conversion to TPF.

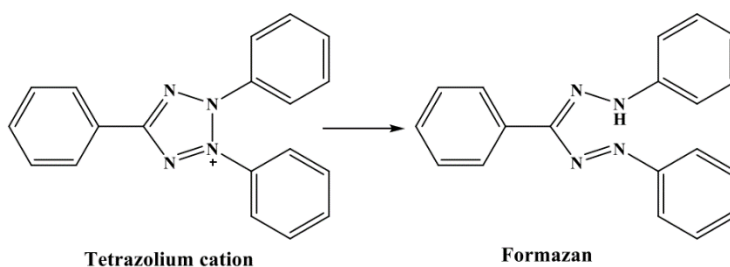


Fig. 41: Enzymatic reduction of tetrazolium chloride (TTC) (Tetrazolium cation, colorless) to triphenylformazan (TPF) (Formazan, red color)

3.3.3. Protoplasts isolation and culture development

After protoplasts isolation from *F. vesiculosus* axenic explant, protoplasts protected themselves from destruction [156] and were elicited to reform their cell walls and then reproduce normally. This was performed by incubation of them in the protoplast cultivation medium which was a highly osmotic medium. Therefore, protoplast cultivation medium was supplemented with 250 mM glucose, 150 mM sucrose and 3.8% (w/v) sea salts, that increased medium osmotic pressure. As **Fig. 42** demonstrates, protoplasts after isolation were scattered irregularly without any specific arrangement, but upon culturing, they began to reproduce with clumps or aggregates formation.

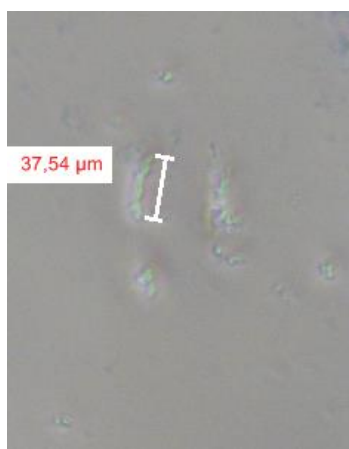


Fig. 42: Protoplasts after 72 h heterotroph cultivation in the protoplast medium showing start of cell multiplication and aggregation

Isolated protoplasts were identified by UV light with the aid of Calcofluor white stain [177] (not shown). However, cell aggregates were detected normally using white light.

The results were highly promising for the transfer of such reformed cells to specific PES solid medium with 0.5% (w/v) agar and liquid marine media supplemented with 2% (v/v) glycerin to develop either mixotrophic or heterotrophic protoplast cultures of *F. vesiculosus*. Unfortunately, cells stopped their reproduction with sub-culturing.

3.3.4. Callus-like development from *F. vesiculosus* explant

3.3.4.1. Solid medium

Another strategy to develop a callus-like growth from brown seaweeds was carried out. Different combinations of nutrition mode, media, light regime and phytohormones were applied. A phototrophic callus-like structure was successfully induced on ASP-12-NTA medium supplemented with 0.5% (w/v) agar using a light regime of L:D (14:10), $35 \mu\text{E m}^{-2} \text{s}^{-1}$ at 17°C after five weeks of cultivation. The callus showed colourless with friable to filamentous-like cell mass, as demonstrated in **Fig. 43**. The callus was sub-cultured afterwards regularly every six-to-eight weeks on the same medium composition solidified with 0.7% (w/v) agar.

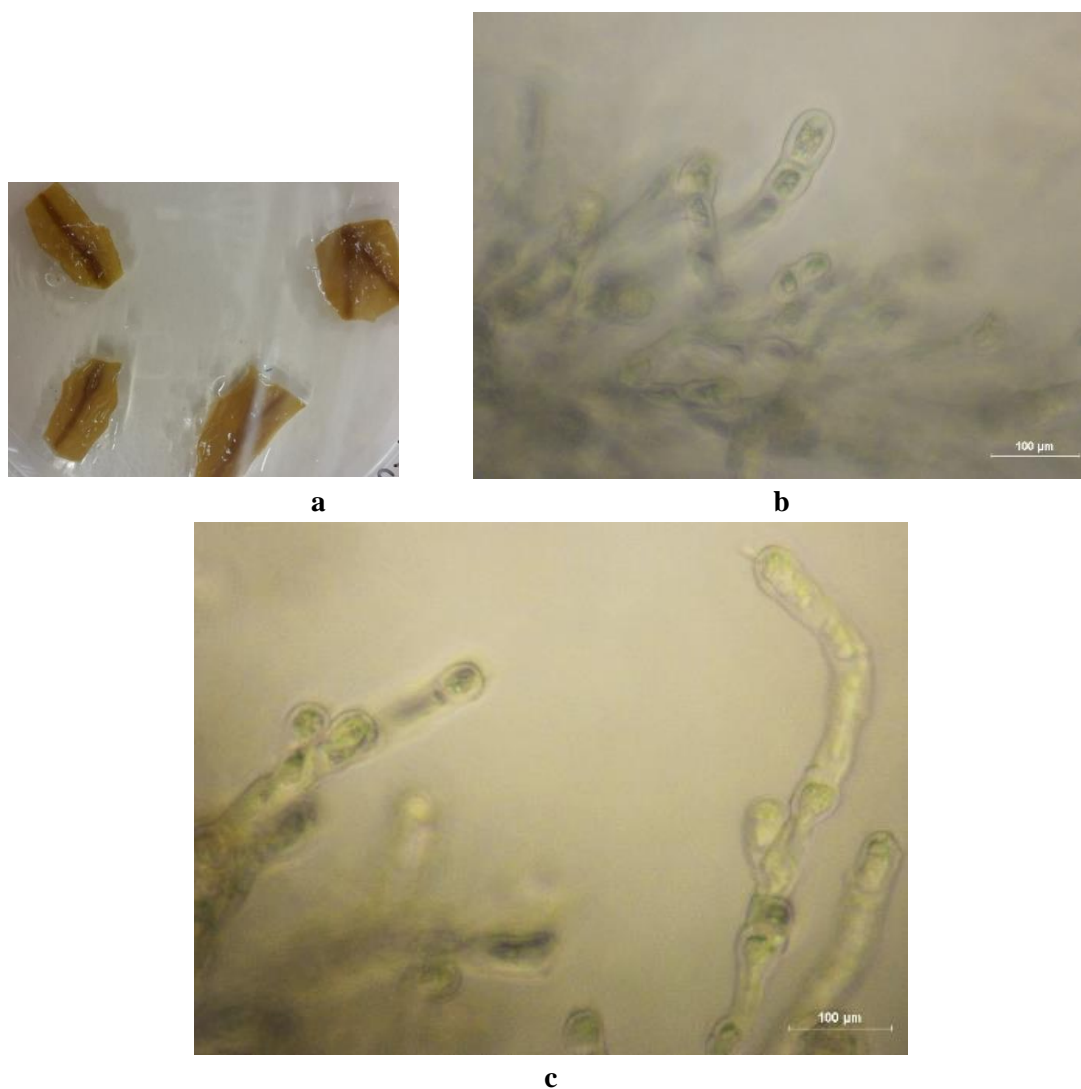


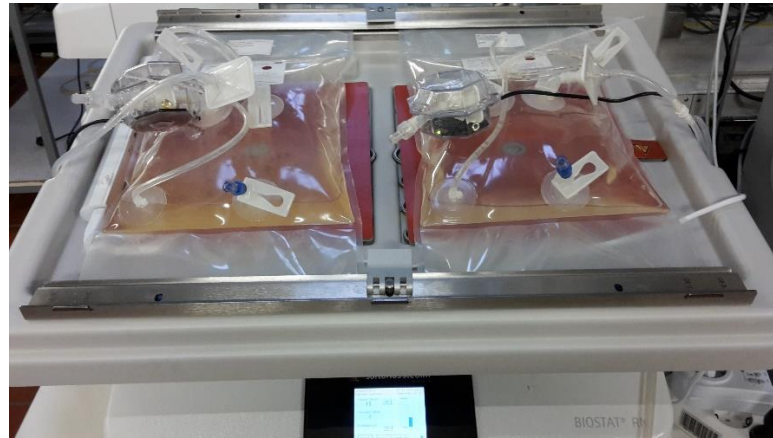
Fig. 43: Development of a phototrophic callus-like growth from *F. vesiculosus* explant in ASP-12-NTA medium

(a) Axenic *F. vesiculosus* explants in ASP-12-NTA medium supplemented with 0.5% (w/v) agar. Phototrophic cultivation after three weeks led to the disappearance of the explant greenish colour. After five weeks of a phototroph cultivation applying L:D (14:10) light regime, $35 \mu\text{E m}^{-2} \text{s}^{-1}$ at a temperature of $17 \text{ }^\circ\text{C}$, a callus-like growth was developed and sub-cultured on the same medium supplemented with 0.7% (w/v) agar. (b,c) Filamentous callus-like growth after six months of sub-culturing developed into a plantlet-like growth.

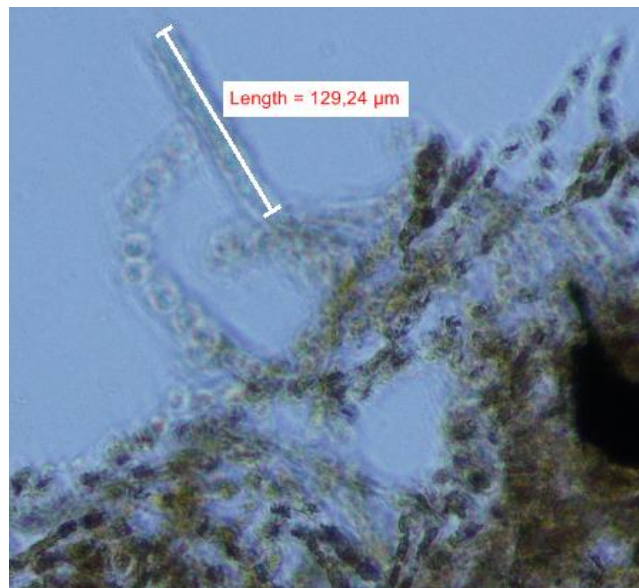
3.3.4.2. Cultivation in liquid suspension cultures

Induction of callus-like growth in normal shaking flasks applying different conditions was not possible. Fortunately, cultivation in a wave bag-mixed bioreactor successfully utilized its advantage of rhythmic wave-like movement and produced a callus-like growth in a shorter cultivation time than classical techniques. After four weeks in a PES medium of phototrophic cultivation, explants

of *F. vesiculosus* showed a filamentous, callus-like growth similar to that developed on solid medium, as shown in **Fig. 44 (b)**. Application of a wave bag bioreactor in the field of seaweeds tissue culture was used for the first time. It is often used in cultivation of animal, insect and plant cell lines [145].



a



b

Fig. 44: (a) Cultivation of *F. vesiculosus* explants in a wave bag bioreactor, (b) Filamentous callus-like growth from *F. vesiculosus* explant developed after four weeks of phototrophic cultivation in PES medium

3.4. Conclusion and Prospectives

Development of axenic protoplast and callus-like phototrophic cultures were possible. A time-saving and efficient surface sterilization protocol was established for marine macroalgae in only three days. The protocol combined different mechanical and chemical treatments, instead of ineffective separately-applied sterilization techniques. In comparison with different sterilization protocols, results showed that more than 90% of cultivated explants demonstrated unialgal cultures, when an anti-fungal agent was added to the broad spectra antibiotics. Moreover, the optimized protocol did not greatly affect the explant viability and had 29% vitality relative to a non-sterile tissue.

Furthermore, induction of protoplast, callus-like were performed either in a solid medium or a wave bag bioreactor from brown macroalgae. Moreover, in comparison with terrestrial plants, phytohormones did not have a significant effect on callus induction confirming its debatably role in marine biotechnology [145]. Interestingly, algal farming through tissue culture in a wave bag bioreactor was applied for the first time in marine biotechnology. Unfortunately, maintenance of callus-like and protoplasts cultures sterile and undefined nutrition requirements were limiting factors to continue their further growing and durability.

Future work should focus on maintenance of cultures' axenic conditions and defining of nutritional requirements to obtain a high-weighted biomass that could be induced to produce their secondary metabolites including fucoidan. Different variables including dehydration stress and cultivation using warm conditions might induce fucoidan production as a trial preventing algae desiccation [74]. In addition, development of a fast growing hairy root system has not been known or performed yet in marine biotechnology of brown macroalgae. However, transformation of tissues from terrestrial plants with the "natural genetic engineer" *Agrobacterium rhizogenes*, has been successfully performed for more than three decades as a tool for plant cultivation. So far, hairy root cultures have been developed from more than 100 plant species, including several endangered medicinal plants, giving opportunities to produce important phytochemicals in environment-friendly conditions [187]. In nature ecosystem, wounded plants secrete simple phenolic compounds, such as acetosyringone, which induce the plasmid-localized *vir* (virulence) genes of *A. tumefaciens* transferring the T-DNA fragments of the *Ti*-(tumor inducing) plasmid to plant cells. This transfer results in a rapidly-dividing tumor cell or hairy-root-like growth [188].

Interestingly, it was reported that photosynthetic dinoflagellates (e.g. *Symbiodinium* sp.) were susceptible to be transformed by *A. tumefaciens* [189]. This was a motivation to start transfection of *F. vesiculosus* explant with *A. tumefaciens* and development of a hairy-root culture.

3.4.1. Crown gall-like growth development in *F. vesiculosus*

Rhizopium radiobacter (previously, *Agrobacterium tumefaciens* DSM 30147) was ordered from the Leibniz Institute DSMZ-German Collection of Microorganisms and Cell Cultures. The lyophilized bacterial strain was then regenerated and cultured on nutrient agar medium at 30 °C for two days, as described by the supplier's protocol. A liquid culture was afterwards prepared from a bacterial colony previously grown on solid medium.

As mentioned before by Georgiev, *et. al.* in hairy-root induction in terrestrial plants [187], previously two-to-three wounded aseptic explants of *F. vesiculosus* were then transfected by incubation with *R. radiobacter* in a nutrient liquid, and then solid media with 1.5% (w/v) agar each of 72 h at 30 °C. Transgenic explants were, afterwards, transferred to an agar medium supplemented with 1x antibiotic solution for another 72 h. Sterile transformed tissues were then cultivate as phototroph using PES, Guillard's F/2 and ASP-12 NTA supplemented with 0.7% (w/v) agar.

As shown in **Fig. 45**, a crown gall or a hairy-root disease was detected in transformed *F. vesiculosus* tissues after six days of incubation of wounded explants with *A. tumefaciens* in a nutrient liquid and agar media each of three days.

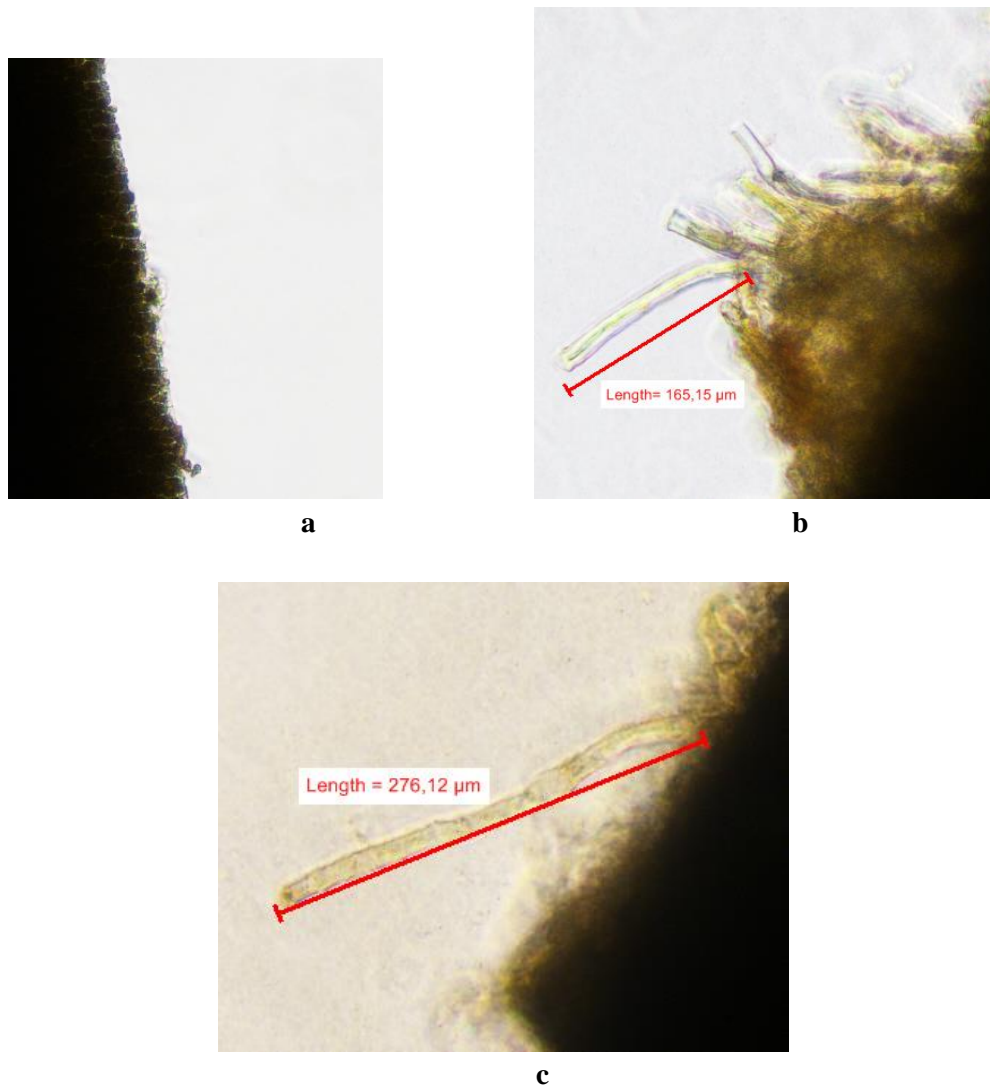


Fig. 45: Development of crown gall or hairy-root in *F. vesiculosus* explants after transfection with *R. radiobacter* or *A. tumefaciens* DSM 30147

(a): Non-infected intact smooth surface of *F. vesiculosus*; (b and c): Developed crown gall and hairy-root disease from a wounded explant after incubation with *R. radiobacter* liquid and agar nutrient media each of three days.

Unfortunately, excised hairy-root growth was deteriorated and not able to accommodate after phototrophic sub-culturing in PES, Guillard's F/2 and ASP-12 NTA solid media. In addition, transfer of *Ti*-plasmid to algal cells has not been confirmed genetically yet. Further experiments should be also performed to investigate the required cultivation conditions for accommodation and growth of the newly-born crown gall-like growth from *F. vesiculosus*. Moreover, genomic DNA should be identified to confirm the presence of the *Ti*-plasmid of *R. radiobacter* in infected tissues [190].

4. Heterologous Expression of Enzymes Involved in Fucoïdan Biosynthesis

4.1. Introduction

Problematic cultivation of brown seaweeds through tissue culture discussed previously in **Chapter 3**, in addition to structure heterogeneity of extracted fucoïdan discussed in **Chapter 2** created a novel strategy to produce an engineered fucoïdan by its enzymatic synthesis. Enzymatic synthesis of a GMP-compliant fucoïdan is a novel technique that has not been discussed in literature yet. An advantage for this strategy is a product that can be easily manipulated without being affected by algae species, extraction method, seasonal and geographical variations. Systematic chemical synthesis of low molecular weight fucoïdan was performed successfully [191]; nevertheless specific synthesis by regio-specific and stereo-selective enzymes is still a challenge to provide a high-quality, consistent and long chain product in a short and time saving protocol.

Recent extensive bioinformatics and phylogenetic analyses have been performed in the brown macroalgae *Ectocarpus siliculosus*. They succeeded to reveal a lot of biosynthetic and remodeling information concerning the extracellular matrix (ECM) polysaccharides including fucoïdan, cellulose and alginate [192]. Furthermore, performed genome analysis revealed the genes encode for enzymes that involved in fucoïdan biosynthesis.

Fucoïdan, as a high molecular weight homo- or hetero- sulphated polysaccharides, several enzymes contribute to its biosynthetic pathway. As shown in **Fig. 46**, it was postulated that fucoïdan or sulphated fucan is synthesized in brown algae from the precursor GDP-L-fucose, which is obtained either by a *de novo* pathway from GDP-mannose or a salvage pathway from L-fucose. *De novo* synthesis of GDP-L-fucose is carried out in 2 steps catalyzed by GDP-mannose 4,6-dehydratase (GM46D) (1) and a bifunctional GDP-L-fucose synthetase (GFS) or GDP-4-keto-6-deoxy-D-mannose epimerase-reductase (2). However, salvage pathway is minor and catalyzed by the bifunctional l-fucokinase (FK) and GDP-fucose pyrophosphorylase (GFPP) with an aid from the GHMP kinase [192] from cytosolic L-fucose. GDP-L-fucose is further polymerized and elongated by different fucosyltransferases (FucTs) related to Glycosyltransferases families GT10, 23 and 65 to fucan polymer (5). The polymer is afterwards sulphated in a specific pattern by another group of enzymes; namely carbohydrate sulphotransferases (STs) to the final product sulphated fucan or fucoïdan (6).

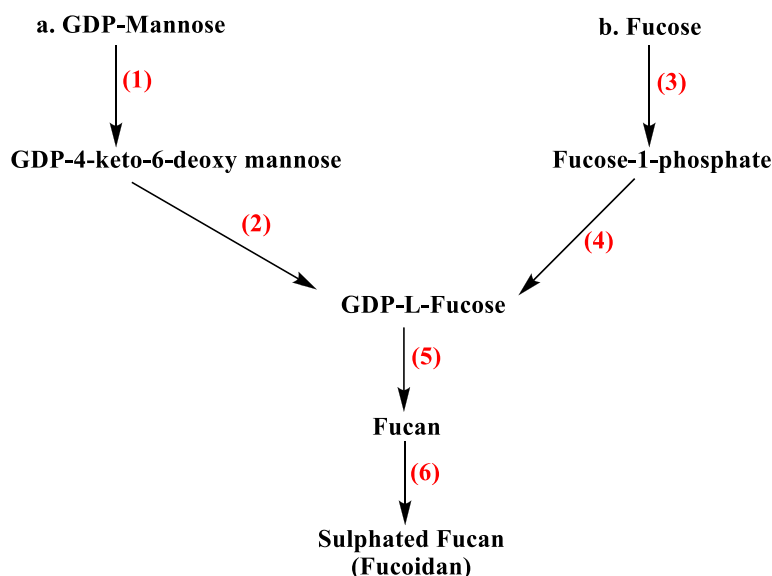


Fig. 46: The two different possible pathways for fucoidan biosynthesis in the brown algae *Ectocarpus siliculosus* (a) *De novo* pathway and b) salvage pathway

1) GDP-mannose 4,6-dehydratase (GM46D); 2) GDP-L-Fucose synthetase (GFS) or GDP-4-keto-6-deoxy-D-mannose epimerase-reductase (GMER); 3) L-Fucokinase (FK); 4) GDP-fucose pyrophosphorylase (GFPP); 5) Fucosyltransferases (FuTs); 6) Sulphotransferases (STs). Modified after Michel, G. *et al.* [192].

In more details, **Fig. 47** illustrates the *de novo* and salvage pathways for GDP-L-fucose synthesis from GDP-mannose and L-fucose, respectively, according to Yan Ren, *et al.*, in the filamentous fungus *Mortierella alpina* [193].

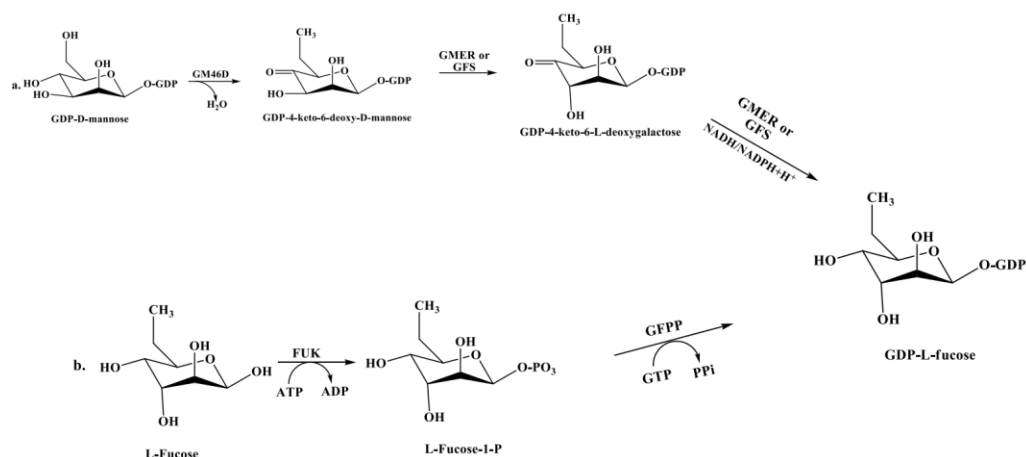


Fig. 47: Detailed *de novo* (a) and salvage pathway (b) for GDP-L-fucose biosynthesis either from GDP-mannose or cytosolic L-fucose, respectively (modified according to [193])

Alternatively, heterologous expression of such enzymes in fast growing cell lines such as bacteria, yeast or even mammalian cell lines could be a potential technique for fucoidan production. Enzymes with similar functions were successfully over-expressed in bacteria and other cell lines which encouraged performing and starting similar experiments in the production cell factory *E. coli*. **Table 14** summarizes some of the previously-performed heterologous expression experiments of similar enzymes from different biogenic sources in bacteria, yeast and mammalian cell lines.

Table 14: Examples of previous trials with heterologous expression to overexpress similar enzymes from different resources to that involved in fucoidan biosynthesis

Name of the enzyme	Name of gene	Source	Expression system	Ref.
a. de novo GDP-L-Fucose synthesis				
GM46D and GFS or GMER	cDNA	<i>Mortierella alpine</i>	<i>E. coli</i> BL21 (DE3)	[193]
	<i>gmd</i> (GM46D) and <i>wcaG</i> (GFS or GMER)	<i>E. coli</i> K-12	<i>S. cerevisiae</i>	[194]
			<i>E. coli</i> BL21(DE3)	[195]
	BT_1224 (GM46D) and BT_1225 (GFS or GMER)	<i>Bacteroides thetaiotaomicron</i>		[196]
	<i>gmd</i>	<i>E. coli</i> (INVF1)	<i>E. coli</i>	[197]
	Human cDNA	Human	Defective Lec13, a CHO cell line deficient in GM46D activity	[198]
	<i>bceN</i>	<i>Burkholderia cenocepacia</i> J2315	<i>E. coli</i> BL21 (DE3)	[199]
	cDNA	<i>Homo sapiens</i>	human hepatocarcinoma cell line HepG2	[200]
	HP0044 and HP0045	<i>Helicobacter pylori</i>	<i>E. coli</i> BL21 (DE3)	[201]
	<i>MUR1</i> (GM46D)	<i>Arabidopsis thaliana</i>	<i>E. coli</i>	[202] [203]
A118R (GM46D) and A295L (GMER)	<i>Paramecium bursaria</i> <i>Chlorella</i> Virus 1 (PBCV-1)	<i>E. coli</i> K803	[204]	

Cont., Table 14: Examples of previous trials with heterologous expression to overexpress similar enzymes from different resources to that involved in fucoidan biosynthesis

Name of the enzyme	Name of gene	Source	Expression system	Ref.
b. Salvage GDP-L-fucose synthesis				
FK and GMER	<i>fk/gfpp</i>	<i>Bacteroides</i>	<i>S. cerevisiae</i>	[205]
	<i>fkp</i>	<i>fragilis</i>	<i>E. coli</i> BL21(DE3)	[206] [207]
	<i>AtFKGP</i>	<i>A. thaliana</i>	<i>E. coli</i> BL21(DE3)	[208]
	<i>FUK</i>	<i>M. alpina</i>	<i>E. coli</i>	[209]
	<i>GFPP</i>		<i>E. coli</i> BL21(DE3)	[210]
Fucosyltransferases (FucTs)				
α 1,3-fucosyltransferase	<i>HpfucT</i>	<i>H. pylori</i>	<i>E. coli</i> CSRDE3	[211]
	fucT (<i>HP0379</i>)		<i>E. coli</i>	[212]
	human (1,3/4) (<i>FUT3</i>)	Human <i>FUT3</i> cDNA	<i>Pichia pastoris</i>	[213]
	<i>FucT</i>	Maize (<i>Zea mays</i>)	<i>Spodoptera frugiperda</i> Sf21 cells by baculovirus mediated infection	[214]
	<i>fucT VI</i>	Human	<i>Pichia pastoris</i>	[215]
α 1,6-fucosyltransferase	<i>nodZ</i>	<i>Rhizobium sp.</i> NGR234	<i>E. coli</i> XL1-Blue MRF'	[216]
α 1,2-fucosyltransferase	<i>WbgL</i>	<i>E. coli</i> O126	<i>E. coli</i> BL21(DE3)	[206]
	<i>WbsJ</i>	<i>E. coli</i> O128		[217]
	<i>wbnK</i> and <i>wbwK</i>	<i>E. coli</i> O86		[218]
	<i>wbiQ</i>	<i>E. coli</i> O127		[219]
	<i>fucT2</i>	<i>H. pylori</i> NCTC 364	<i>E. coli</i> JM 109 (DE3)	[220]
		<i>H. pylori</i> UA802	<i>E. coli</i> CLM4 (pGP1-2)	[221]
	<i>futC</i>	<i>H. pylori</i> NCTC11639	<i>E. coli</i> BL21 (DE3)	[222]
<i>wcfB</i>	<i>Bacteroides fragilis</i>	<i>E. coli</i> BL21star (DE3)	[223]	
Sulphotransferases (STs)				
Arylsulphate sulphotransferase (ASST)	HAST1 and HAST3	Human cDNA	<i>E. coli</i> DH5 α F'IQ TM	[224]
	<i>astA</i>	<i>Klebsiella</i> K-36	<i>E. coli</i> BL21 (DE3)	[225]
	Hoch_5094	<i>Haliangium ochraceum</i>		[226]

Cont., Table 14: Examples of previous trials with heterologous expression to overexpress similar enzymes from different resources to that involved in fucoidan biosynthesis

Name of the enzyme	Name of gene	Source	Expression system	Ref.
Heparan sulfate O- sulphotransferase (OST)	A truncate version (human <i>r-3-OST1</i>)	Human cDNA		[227]
	<i>NST</i> , <i>2-OST</i> , <i>3-OST-1</i> , <i>6-OST-1</i> and <i>6-OST-3</i>		Yeast cells (<i>Kluyveromyces lactis</i>)	[228]
	<i>6-OST-1</i> , <i>6-OST-2</i> and <i>6-OST-3</i>	Mouse liver cDNA	Human Embryonic Kidney 293 Cells (HEK 293 cells)	[229]
	<i>dHS6ST</i>	<i>Drosophila melanogaster</i> cDNA	COS-7 cells	[230]
Heparan sulphate N- sulphotransferase (NST)	A truncated version of Heparan sulfate/heparin N-deacetylase/N- sulphotransferase-1 (NDST-1) (<i>rNDST-1</i>)	Rat liver cDNA	<i>S. cerevisiae</i>	[231]
	NDST-1	Mouse cDNA	HEK 293 cells	[232, 233]
	NDST-2	Murine cDNA		[234]
Phenol sulphotransferase	Hydroxyarylamine (or acetylaminofluorene) sulphotransferases (SULT1C)	Human cDNA	<i>E. coli</i> BL21 (DE3)	[235]
	(rabSULT1C2) cDNA	Rabbit stomach	<i>E. coli</i> HB101 and COS-7 cells	[236]
	Different human SULTs (SULT1A3, SULT1C4, and SULT1E1)	Human	<i>E. coli</i> BL21 (DE3)	[237]
Dopa/Tyrosine- Ester Sulphotransferase	PST-1 cDNA	Rat liver	<i>E. coli</i> BL21 (DE3)	[238]
	cDNA	Rat liver	COS-7 Cells	[239]
	SULT1A3 cDNA	Human	<i>S. cerevisiae</i> and <i>E. coli</i> BL21(DE3)	[240]

This part of the work focused on heterologous expression of some algal fucosyltransferases (FucTs) and sulphotransferases (STs) from genes isolated from *E. siliculosus* in *E. coli* BL21 (DE3) as a trial to produce active and right-folded over-expressed enzymes.

4.2. Heterologous expression of algal fucosyltransferases (FucTs)

FucTs are a subfamily of the super family glycosyltransferases (GTs) according to Carbohydrate-Active enZymes (CAZy) [241]. GTs catalyze different glycosidic bonds formation using mainly an active sugar containing a nucleoside phosphate or a lipid phosphate leaving group as donor substrates [242]. They are further classified into five classes according to the glycosidic linkages they synthesize; namely α -1,2-, α -1,3-, α -1,4-, α -1,6-, and *O*-fucosyltransferases [243]. They function L-fucose transfer specifically from GDP-L-fucose to protein [244] and glycan forming fucosides or fucosylated glycoconjugates [245].

FucTs are involved in a number of potential and versatile functions through synthesis of compounds that are involved in different physiological and pathological processes in prokaryotic or eukaryotic organisms. They include fertilization, neuronal development, immune responses, and cell adhesion [246], such as synthesis of Lewis (Le) antigens which are glycoproteins associated with the human ABO blood group system [247]. They are expressed on red blood cells, kidney and gastrointestinal epithelium by contribution from FUT3 (α -1,3) and FUT2 (α -1,2). Even in terrestrial plants, it was observed an increment in Fuc-T (α -1,4) in plant life cycle during flower development resulting in pollen maturation and pollen tube elongation [248]. On the other side, expression of FucTs is increased, especially *FUT4* (α -1,3), in some cancer cell lines resulting in cancer promotion and metastasis [249]. Therefore, fucosylated molecules are considered as cancer biomarkers and beneficial in cancer diagnosis and potential targets in treatment [250]. Besides, different *H. pylori* FucTs such as α -1,2 and α -1,3/4 FucTs participate in the biosynthesis of its carbohydrate complex Lewis antigen which plays an important role in the bacterial pathogenesis including cell adaptation, adhesion and colonization [221,251].

Few bacterial FucTs (e.g., α -1,3/4-FucTs from *H. pylori*) and human (*H. sapiens*) analogues were well identified and specified by expression in different cell lines [211,246], as previously demonstrated in **Table 14**. Since oceans and seas represent 70% of our planet surface, enzyme analogues from aquatic organisms could be also possible, if their genomic maps are well analyzed.

Recently, genome analysis of *E. siliculosus* revealed the presence of different kinds of FucTs including α -1,3-FucTs (GT10) such as Esi_0050_0098, α -1,6-FucTs (GT23) (e.g., Esi0135_0016 and Esi0540_0004) as well as *O*-FucTs (GT65) like Esi0021_0026 [192]. This diversity in algal FucTs proved that marine life has still treasures which have not been discovered yet.

Heterologous expression is a well-documented tool in verifying bioinformatics results and gene functions, this part aimed to over-express representatives from algal FucTs; FucTs_21 and FucTs_50 in *E. coli* BL21 (DE3) via cloning of Esi0021_0026 and Esi0050_0098 genes, respectively.

4.2.1. Material and Methods

4.2.1.1. *In silico* analysis of FucTs analogues, synthetic gene materials and bacterial transformation

Amino acids sequences of human and bacterial FucTs analogues were aligned using DNASTAR® (Lasergene v7, MegAlign) software. Clustal W algorithm was applied to investigate the different homology studies, including percent identity and motifs in aligned sequences. *H. pylori* α -1,3-FucTs (HP0651 and HP0379) and human FUT (P51993) were aligned with algal putative FucTs_50 and FucTs_21.

Synthetic Esi0050_0098 and Esi0021_0026 genes were supplied by Invitrogen GeneArt® as described by Michel, *et al.* [252,253] as lyophilized samples. They were inserted into pMK and pMA-T plasmid vectors, as shown in **Fig. 48**. *E. coli* JM83 competent cells hosted the foreign DNA inserts through a heat shock protocol to produce gene copies. The bacterial growth was performed at 37° C in LB medium containing their corresponding selection markers; ampicillin sodium and kanamycin sulphate. DNA constructs were afterwards extracted by NucleoSpin® Plasmid EasyPure kits (Macherey-Nagel GmbH & Co. KG, Düren, Germany) and concentrations were measured by Nanodrop Spectrophotometer

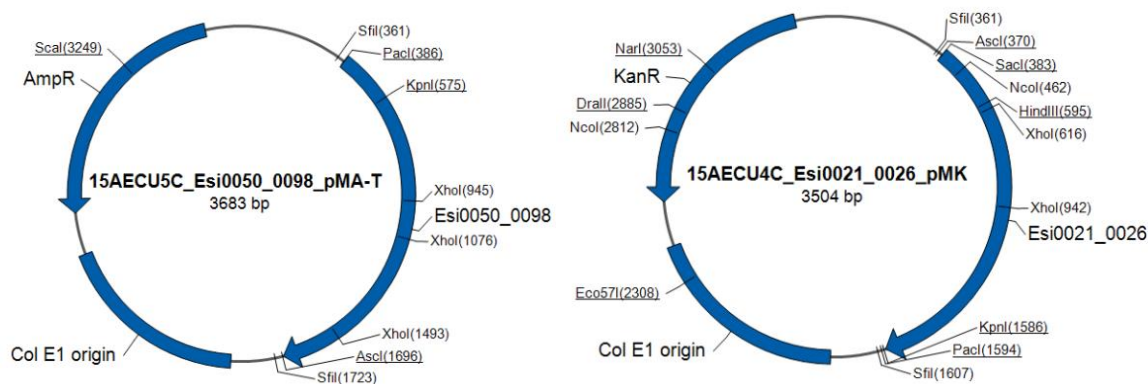


Fig. 48: Synthetic and cloned Esi0050_0098 and Esi0021_0026 in pMA-T and pMK plasmid vectors, respectively

Both DNA constructs were synthesized and provided by Invitrogen GeneArt®.

4.2.1.2. Cloning by Gibson assembly

As shown in **Fig. 49**, between *EcoRI* and *BamHI* sites of the vector plasmid pASK-IBA 45(+) (IBA GmbH, Germany), Esi0050_0098 and Esi0021_0026 were cloned to produce *Strep*®-tag fusion proteins. Steps were performed according to NEBuilder HiFi DNA® Assembly Master Mix and

Gibson Assembly[®] Cloning Kit instruction manuals [254,255]. Primers were designed by the online service provided by New England Biolabs[®] (NEBuilder[®] Assembly Tool), as demonstrated in **Table 15**, and PCR experiments were performed in a PCR thermocycler to amplify both inserts.

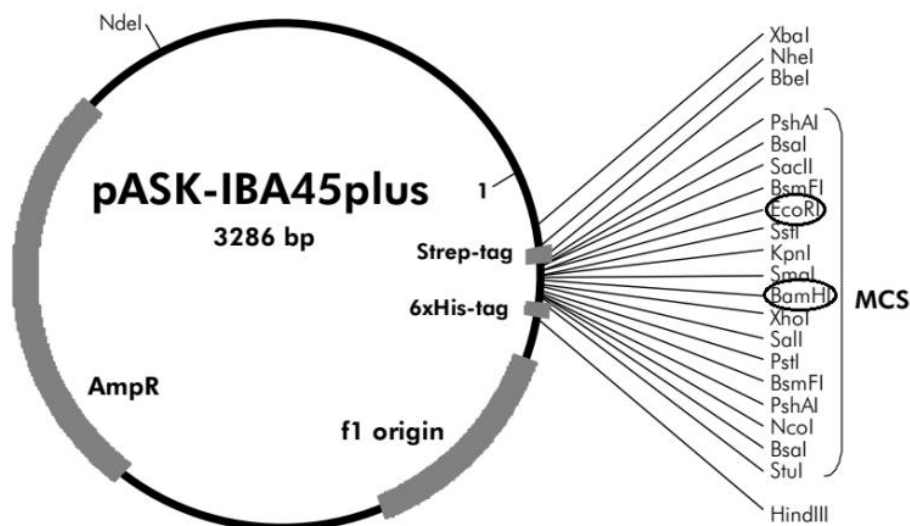


Fig. 49: Features of pASK-IBA 45(+) plasmid vector as described by IBA GmbH [256]

Esi0050_0098 and Esi0021_0026 were cloned between *EcoRI* and *BamHI* site of the plasmid multiple cloning site (MCS) using Gibson assembly.

Table 15: Designed primers for cloning of Esi0050_0098 and Esi0021_0026 in pASK-IBA 45(+), according to NEBuilder[®] Assembly Tool

The capital and small letters denoted for nucleotides from inserts and vector, respectively.

DNA constructs	Primer		Annealing temperature (°C)
pASK-IBA 45(+)_Esi0050_0098	fwd	5'-gcgccgagaccgcgtcccgATGGACAAGGAGGGCAGC-3'	61.3
	rev	5'-cctgcaggtcgacctcgaggTCACCGCAGTGACTCTTG-3'	
pASK-IBA 45(+)_Esi0021_0026	fwd	5'-gcgccgagaccgcgtcccgATGGCCTTCGAGACCGTGGTCGTG-3'	72.0
	rev	5'-cctgcaggtcgacctcgaggTCACCCCCGGGGCGGGG-3'	

The molecular sizes of amplified inserts with overlapping ends were then confirmed by gel electrophoresis, detected using Gel iX20 Imager and then purified by NucleoSpin[®] Gel and PCR Clean-up kits (MACHEREY-NAGEL GmbH & Co. KG).

In parallel, pASK-IBA 45(+) was opened by *EcoRI* and *BamHI* endonucleases. The purified doubly-digested plasmid in addition to PCR products were incubated in a ratio of 1:2 with 10 μ L NEBuilder[®]

HiFi DNA Assembly Master Mix in a total volume of 20 μL for 15 min at 50 $^{\circ}\text{C}$ following the protocol of the provider (New England BioLabs[®] Inc.) [254]. Chemically competent cells of the supplier hosted then the recombinant DNA constructs before growing on LB solid followed by liquid media supplemented with 100 $\mu\text{g mL}^{-1}$ ampicillin sodium as a selection marker for 18 h at 37 $^{\circ}\text{C}$.

4.2.1.3. DNA sequencing of recombinant DNA constructs

To check accuracy of molecular cloning experiments, recombinant DNA constructs were afterwards extracted by NucleoSpin[®] Plasmid EasyPure kits (Macherey-Nagel GmbH & Co. KG, Düren, Germany). Isolated pASK-IBA 45(+)_Esi0021_0026 (4458 bp) was doubly digested by *StuI* and *XbaI*, while pASK-IBA 45(+)_Esi0050_0098 (4566 bp) was only linearized by a single digestion with *XbaI*. All of digested constructs were checked by gel electrophoresis.

Right constructs were sent for sequencing and compared their results with the designed templates by GATC Biotech AG (Konstanz, Germany), after preparing them for a light run sequencing in a 1.5 mL reaction tube which consisted of 100 ng DNA, 5 μL fwd/rev plasmid primer (20 pmol) and sterile water up to 10 μL . Alignment analysis was performed then with the online service of Clustal Omega (EMBL-EBI).

4.2.1.4. Transformation of *E. coli* BL21 (DE3) and gene expression

Both sequenced DNA constructs and empty vector plasmid were applied to transform *E. coli* BL21 (DE3) (Agilent Technologies, Inc.). In shaking flasks using a shaker incubator (Innova[®] 44), transformed *E. coli* were cultivated in 1 L LB culture medium supplemented with 100 $\mu\text{g mL}^{-1}$ ampicillin sodium at 37 $^{\circ}\text{C}$ as a pilot experiment. Proteins expression was induced by 150 $\mu\text{g L}^{-1}$ AHT, when bacterial growth log phase was reached (i.e., $\text{OD}_{578\text{nm}}$ between 0.6 – 0.8). The cultivation temperature was then decreased to 17 $^{\circ}\text{C}$ and held for overnight (18 h). Cells were harvested by superspeed centrifuge at 4 $^{\circ}\text{C}$ (10 min at 17600 x g) and stored at -20 $^{\circ}\text{C}$ until purification. Scaling-up of FucTs_50 production was carried out in 44 L of cultivation medium applying the same conditions.

4.2.1.5. Proteins purification by affinity chromatography

Expressed *Strep*[®]-tag fusion proteins were purified according to the protocol described by IBA Lifesciences (Göttingen, Germany) [257] after some modifications. Cells were reconstituted in buffer W without EDTA (100 mM Tris, 150 mM NaCl, pH 8.0). Afterwards, cells were lysed with a microfluidizer adjusted at 15000 psi after incubation with of DNaseI and lysozyme for 30 min. The step of cell disruption was repeated for three times. To isolate cell debris from cell lysates, cell

suspensions were centrifuged again at 4° C for 1 h at 43000 x g. Clear lysates were then filtered by a 0.45 µm regenerated cellulose syringe filter and purified with a *Strep*-Tactin® Sepharose® affinity column. The column was pre-conditioned with buffer W and bound proteins were eluted with five column volume (CV) of buffer E (2.5 mM desthiobiotin in buffer W) before a step of washing with buffer W.

4.2.1.6. Protein detection by SDS-PAGE and Western blot

Column fractions were plotted on SDS-PAGE (12.5 %) using Vertical electrophoresis cell for SDS-PAGE and proteins were stained by Coomassie brilliant blue solution. Moreover, recombinant *Strep*®-tag fusion proteins were detected by Western blot using monoclonal *Strep*®-Tactin® AP conjugate (IBA Lifesciences, Göttingen, Germany) according to manufacturer's instructions[258].

4.2.1.7. Activity assays

a. Glycosyltransferase activity kit

Activity assays were performed according to the protocol of Glycosyltransferase activity kit (Catalog # EA001) described by Bio-Techne GmbH [259]. Briefly, purified enzymes were dialyzed against the reaction buffer (25 mM Tris, 150 mM NaCl, 10 mM MnCl₂, 10 mM CaCl₂, pH 7.5) for overnight and concentrated using Vivaspin centrifugal concentrators (MWCO 10 kDa, VWR). The reaction was initiated by incubation of 25 µL a serial dilution of purified protein in a working solution consisting of 10 µL 8 mM GlucNAc, 10 µL 3 mM GDP-L-fucose (Carbosynth Limited, Berkshire, United Kingdom), 5 µL 20 ng µL⁻¹ coupling phosphatase for 1 h at 37 °C. Afterwards, 30 µL malachite green A (ammonium molybdate in 3 M sulphuric acid), 100 µL water and 30 µL malachite green B (malachite green oxalate and polyvinyl alcohol) were added before another incubation at room temperature for 20 min. Finally the absorbance was measured at 620 nm with reaction buffer as a blank to measure the reaction background.

b. Multiplexed Capillary Electrophoresis (MP-CE)

MP-CE was carried out as described previously by Wahl, *et al.* [260]. Briefly, samples were diluted with a stock solution, containing 14 mM SDS, 2 mM *para*-amino benzoic acid (PABA) and 2 mM *para*-amino phthalic acid (PAPA), to a final concentration of 7 mM SDS, 1 mM PABA and 1 mM PAPA. SDS was used to denature the enzyme, while PABA and PAPA were internal standards. Precipitated enzyme was removed by centrifugation and the supernatants were applied with a vacuum injection at -0.7 psi for 10 s. Separation was carried out with a capillary electrophoresis (cePRO 9600™) system with a 96 fused silica capillary array and a UV-detection at 254 nm.

Capillary tubes with a total length of 80 cm, i.d. of 50 μm and 55 cm as an effective length were used. Analytes were separated with an applied voltage of 12 kV and the used running buffer contained 1 mM EDTA and 50 mM ammonium acetate at pH 9.2. Integrated analytical areas were normalized to the internal standard peak area of PABA.

4.2.2. Results and Discussion

According to Cumashi, *et. al.*, α -1,3 linked L-fucopyranoside is principally found in fucoidan backbone among different studied molecular structures from brown macroalgae species. However, other linkages such as α -1,4 linkage might also alternate with α -1,3 [14]. Moreover, branched chain fucoidan contains further α -1,2 or even α -1,6 residues as branching sites. Genome analysis of *E. siliculosus* proved the presence of different genes encoded for different FucTs involved in different glycosidic linkages like α -1,3 and α -1,6 [192].

4.2.2.1. Homology and phylogenetic relationships with relative FucTs

Results from NCBI database showed that amino acid sequences of both algal FucTs are novel and different from other known glycosyltransferases [240,241]. As demonstrated in **Fig. 50**, homology studies of amino acids sequences of both algal FucTs; FucTs_50 (Esi0050_0098 (D7G396)) and FucTs_21 (Esi0021_0026 (D7FR32)) with the well specified *H. pylori* α -1,3/4-FucTs (HP0651 and HP0379) [211,263] in addition to the human analogue FUT6 (P51993), revealed that FucTs_50 was more related to bacterial α -1,3/4-analogues than FucTs_21, where identity (%) to HP0651 and HP0379 was 14.7% and 15.4%, respectively, however, it was only 9.8% and 9.7% with FucTs_21, respectively. This result was likely due to the fact that FucTs_21 is a *O*-FucTs rather than and a α -1,3-FucTs. Furthermore, the comparison between algal FucTs_50, *H. pylori* and human α -1,3-FucTs demonstrated more relations of algal enzymes to the human analogue than the bacterial one.

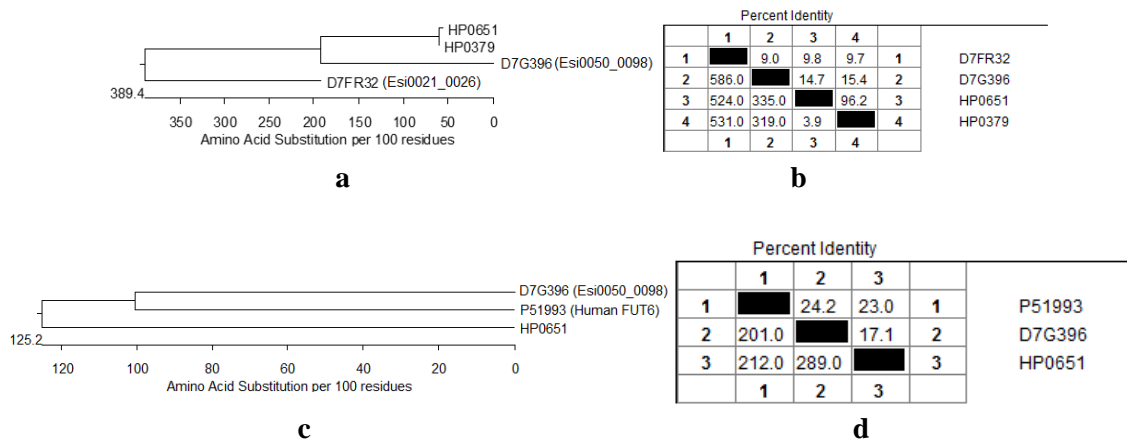


Fig. 50: Homology and phylogenetic relationships of algal FucTs₂₁ and FucTs₅₀ with other bacterial and human FucTs

(a) Phylogenetic tree shows more similarity of FucTs₅₀ (Esi0050_0098, D7G396) with *H. pylori* enzymes than FucTs₂₁ (Esi0021_0026, D7FR32). (b) Sequence distance matrix confirmed phylogenetic tree regarding identity (%). (c&d) Phylogenetic tree and sequence distance matrix of algal FucTs₅₀ (Esi0050_0098, D7G369) in comparison with bacterial *H. pylori* (HP0651) and human (P51993) analogues. DNASTAR[®] (Lasergene v7, MegAlign) software and Clustal W algorithm were applied to investigate the different homology studies, including percent identity, phylogenetic tree and motifs in aligned sequences

These lower percentages of identity might indicate different enzymatic functions. However, different enzymes' resources should be taken into consideration. Furthermore, amino acid sequence of FucTs₅₀ revealed the presence of the conserved stretch of 17 amino acids; **FLAFENNNQIRDYVTEK**. This consensus sequence is referred as a α 3-FucTs structural motif after alignment of several α 3-FucTs from bacteria and human [264]. It is believed that this sequence is essential for enzyme activity and related to GDP-L-fucose binding site. In addition, alignment of FucTs₂₁ amino acid sequence with other protein-*O*-fucosyltransferases family 1 (POFUT1), revealed the presence of some conserved peptide motifs for example **LxYIATD** and **SSFxA**). These POFUT1 include enzymes present in *H. sapiens*, *S. scrofa*, *G. gallus* ...etc. genome [265].

4.2.2.2. Molecular cloning by Gibson assembly

Gibson assembly performed, as shown in **Fig. 51**, by three successive enzymatic activities in a single-tube reaction: 5' exonuclease, DNA polymerase and DNA ligase activities. The 5' exonuclease chews back the 5' end sequences resulting in exposed complementary sequence to be annealed. The polymerase activity then fills in the gaps on the annealed regions. A DNA ligase afterwards seals

the nick and connects the DNA fragments together. An advantage of Gibson assembly is that the overlapping sequence of the connecting fragments is longer than those used in previous assemblies (e.g., Golden Gate Assembly), which leads to a higher percentage of correct assemblies [266].

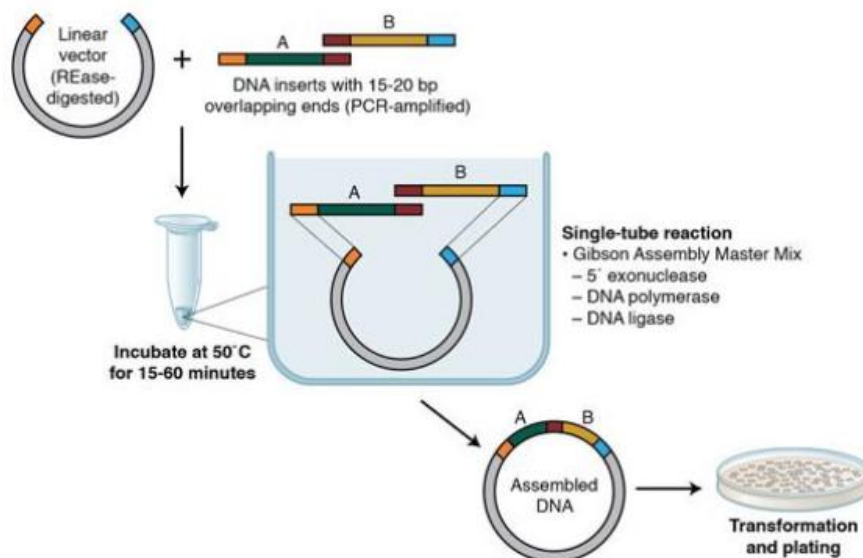


Fig. 51: Gibson Assembly work flow; an example [266]

As shown in **Fig. 52**, both inserts; Esi0021_0026 (1197 bp) and Esi0050_0098 (1305 bp) were amplified successfully with designed PCR primers. The ends of both amplicons included *EcoRI* and *BamHI* restriction site sequences from pASK-IBA 45(+) to facilitate ligation to the vector in subsequent steps.

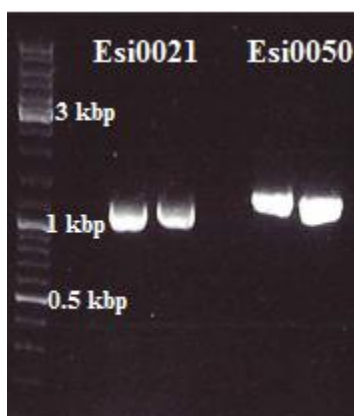


Fig. 52: Agarose gel electrophoresis of amplified PCR products of Esi0021_0026 and Esi0050_0098

Esi0021_0026 and Esi0050_0098 amplicons were detected at 1197 bp and 1305 bp, respectively with their overlapping ends.

4.2.2.3. DNA extraction, digestion and sequencing

Extracted DNA constructs were singly or doubly digested to confirm their right constructions. **Fig. 53** and **54** describe the comparison between designed constructs by pDRAW32 DNA analysis software and obtained results from gel electrophoresis. In pASK-IBA 45(+)_Esi0021_0026, only recombinant DNA from replicate 3 showed two fragments at 3129 and 1329 bp, upon digestion with *StuI* and *XbaI*, as predicted. However, in pASK-IBA 45(+)_Esi0050_0098, recombinant DNA from replicate 3 and 8 showed a typical gel electrophoresis profile with a single band at 4566 bp after a digestion with *XbaI*.

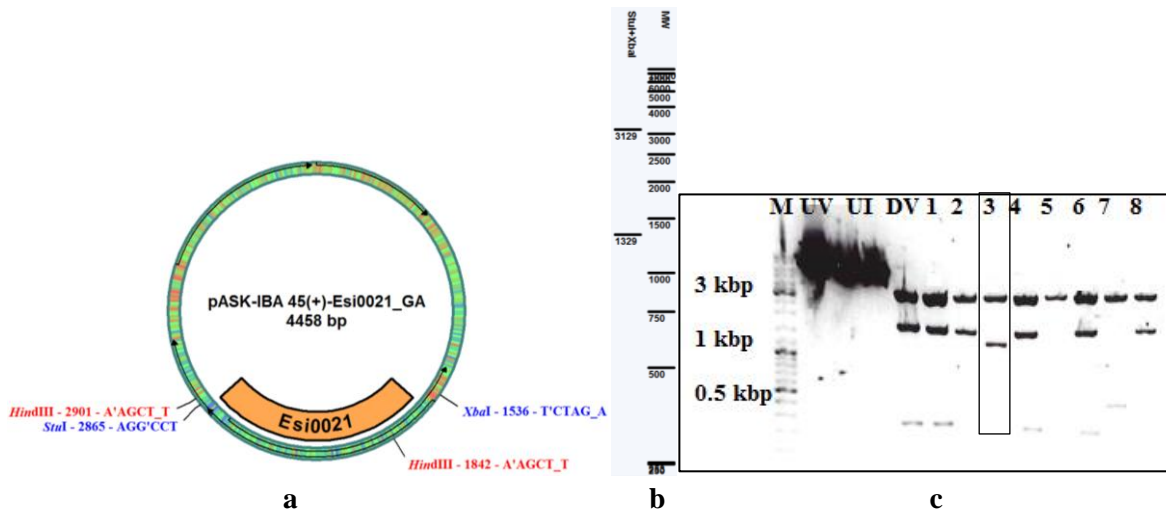


Fig. 53: Design of pASK-IBA 45(+)_Esi0021_0026 DNA construct showing some possible restriction sites and gel electrophoresis results after its digestion with *StuI* and *XbaI*
a) Designed construct by pDRAW32 DNA analysis software; **b)** Expected produced fragments after double digestion with *StuI* and *XbaI* at 3129 and 1329 bp, **c)** Gel electrophoresis of recombinant DNA digested by *StuI* and *XbaI* obtained from different replicates in comparison with undigested vector, undigested insert, digested vector and DNA marker. Only replicate 3 produced two fragments at 3129 and 1329 bp. M= size marker, UV=undigested vector, UI=undigested insert, DV= digested vector.

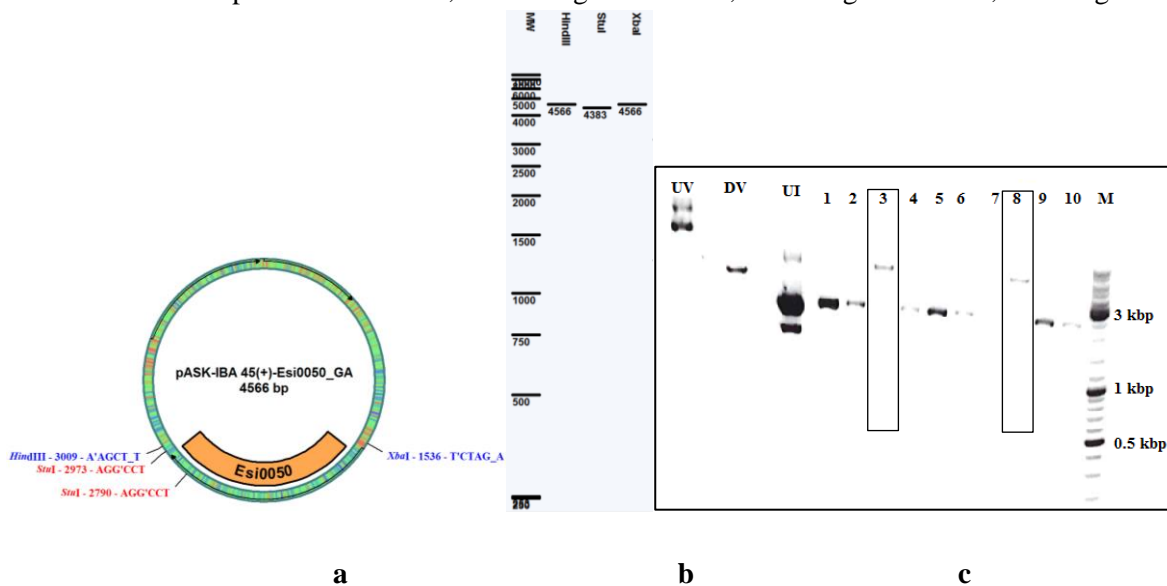


Fig. 54: Design of pASK-IBA 45(+)_Esi0050_0098 DNA construct showing some possible restriction enzymes and gel electrophoresis results after digestion *XbaI*
a) Designed pASK-IBA 45(+)_Esi0050_0098 construct pDRAW32 DNA analysis software; **b)** Expected fragments after single digestion with *XbaI* at 4566 bp; **c)** Gel electrophoresis of recombinant DNA digested by *XbaI* obtained from different prep in comparison with undigested vector, undigested insert, digested vector and a DNA size marker. Digested DNA from replicates 3 and 8 showed slower migration rates than digested vector, this referred to higher molecular weight of

recombinant DNA construct. M= size marker, UV=undigested vector, UI=undigested insert, DV= digested vector.

Recombinant DNA constructs of replicate 3 from pASK-IBA 45(+)_Esi0021_0026 and pASK-IBA 45(+)_Esi0050_0098 were sent to be sequenced. As demonstrated in **Fig. 55 a** and **b**, alignment with designed constructs revealed higher percentages of similarity with sequencing results.

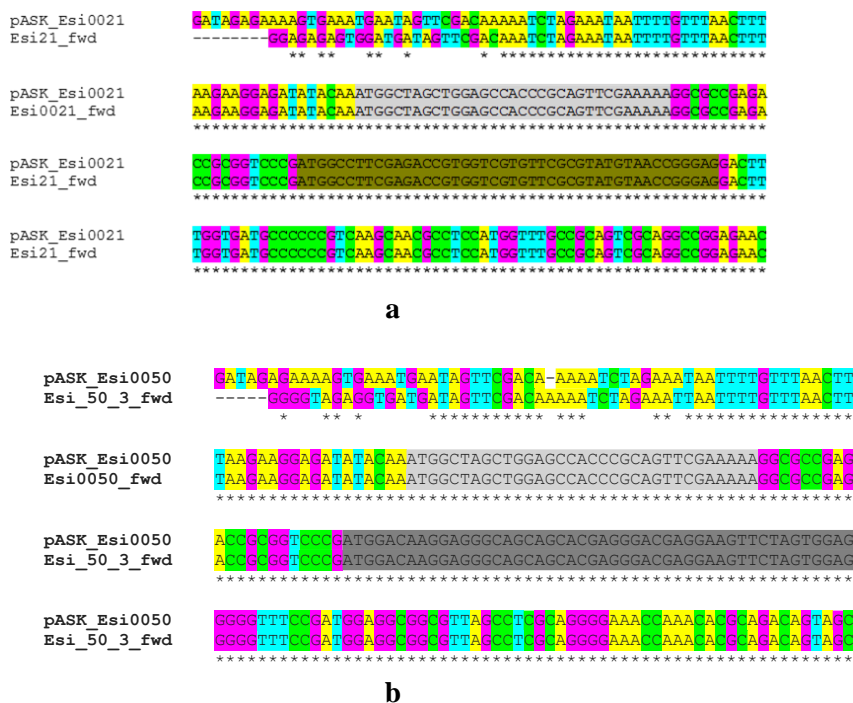


Fig. 55: Alignment of DNA templates (pASK_Esi0021 and pASK_0050) with the forward (fwd) sequence of the sequencing results

a) Alignment of DNA sequencing result of pASK-IBA 45 (+)_Esi0021_0026; **b)** Alignment of DNA sequencing result of pASK-IBA 45 (+)_Esi0050_0098 in comparison with their DNA templates. They showed *Strep*[®]-tag (in grey) and the gene start sequence (in green, **a** and dark grey, **b**) and the right insertion of both genes in the cloning site of pASK-IBA 45(+) vector.

4.2.2.4. Enzymes production (pilot experiment)

As seen in **Fig. 56 a** and **b**, SDS-PAGE showed poor detections of recombinants proteins at predicted molecular sizes for both proteins. However, Western blot results demonstrated that enzymes were successfully produced in fermentation flasks, using empty plasmid vector as a control. Both proteins were detected in intact cells and cell pellets as inclusion bodies. Nevertheless, FucTs_50 was present only in bacterial cell lysate.

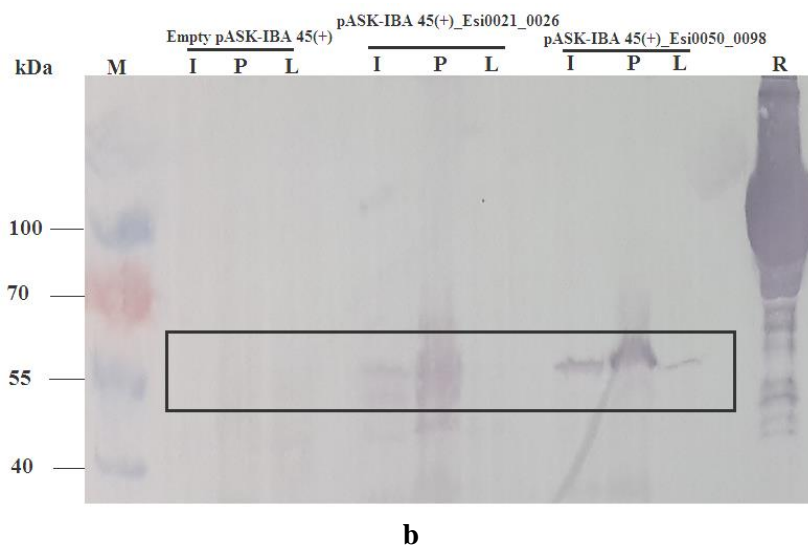
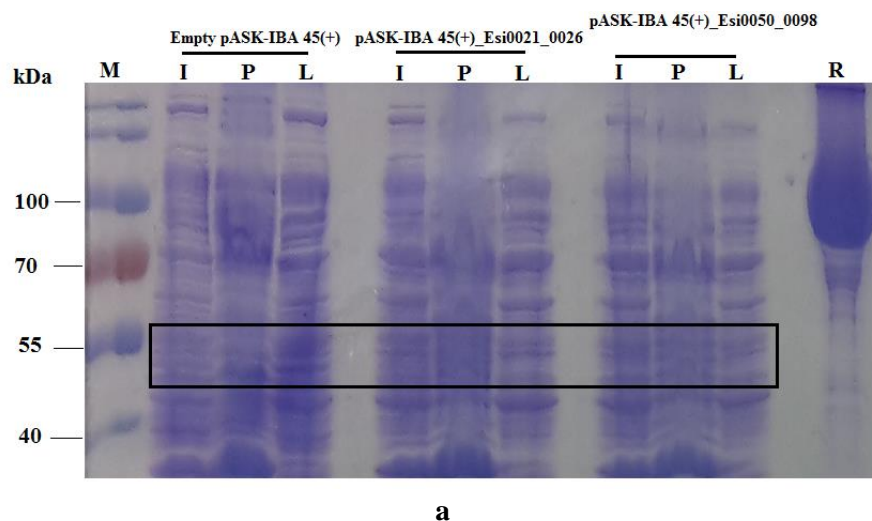


Fig. 56: SDS-PAGE (a) and Western blot (b) of overexpressed recombinant proteins from pASK_IBA 45(+)_Esi0021_0026 and pASK_IBA 45(+)_Esi0050_0098 DNA constructs, in comparison with an empty vector plasmid in a 2 L of LB medium of *E. coli* BL21(DE3)

Proteins were detected in Western blot by *Strep*[®] antibodies, according to IBA[258]. M= size marker – PageRuler™ Prestained (Thermo Fisher); I= intact cells; P= cell pellets; L= cell lysate; R= external reference *Strep*[®]-tag protein of molecular size 100 kDa used to check the the detection procedure.

4.2.2.5. FucTs_50 production and purification

Based on preliminary results, scaling-up of FucTs_50 production and purification was only performed and its activity was evaluated, afterwards. Over-expressed FucTs_50 crude lysate, produced from a 44 L cultivation medium, was pooled and purified by affinity chromatography depending on interaction with the immobilized engineered streptavidin named *Strep-Tactin*[®]. After

a washing step, elution of recombinant protein was performed by adding 2.5 mM desthiobiotin in buffer W. Application of desthiobiotin depends on structural similarity to biotin which is the natural ligand of streptavidin. Finally after eluate dialysis and concentration, the experiment resulted in production of 175 μ g of purified FucTs_50 protein, after its measurement by Bradford assay [267]. **Fig. 57** shows the cascade of FucTs_50 protein purification and its detection in column eluates in comparison with expressed proteins at the same fermentation conditions from empty plasmid vector pASK-IBA 45(+).

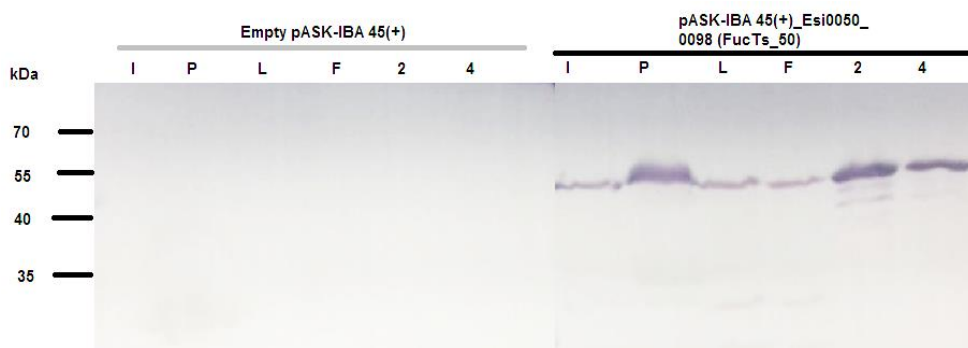


Fig. 57: Western blot of expressed recombinant FucTs_50 from the pASK-IBA 45(+)_Esi0050_0098 construct in comparison with empty vector plasmid during purification cascade

It showed that proteins were present in intact cells, cell pellets, lysate, and flow through, in addition to eluate fractions. All fractions of expressed empty vector at the same conditions did not show any presence of *strep*[®]-tag proteins. R= external reference *Strep*[®]-tag protein of molecular size 100 kDa; I=Intact cells; P=cell pellets; L=cell lysate; F=flow through; 2, 4= eluate fractions.

4.2.2.6. Activity assay

Catalytic activity of purified FucTs_50 using GDP-L-fucose as a donor substrate form was investigated by Glycosyltransferase activity kit and MP-CE analytics.

a. Glycosyltransferase activity kit

As shown in **Fig. 58**, the principle of the reaction depends on a cascade of steps which initiated with hydrolysis of GDP-L-fucose with the FucTs and terminated with free phosphate detection. The step of GDP-L-fucose hydrolysis was accompanied by liberation of a free GDP moiety, which was further hydrolyzed by coupling phosphatase activity to give free phosphate and guanosine monophosphate. Malachite green reagents (malachite green A and malachite green B) reacted afterwards with these free phosphates and the products were quantified by measuring the absorbance at 620 nm, as

described by Wu, *et al.* [259]. Denser green colour means much liberated free phosphates and consequently higher fucosyl transfer enzymatic activity.

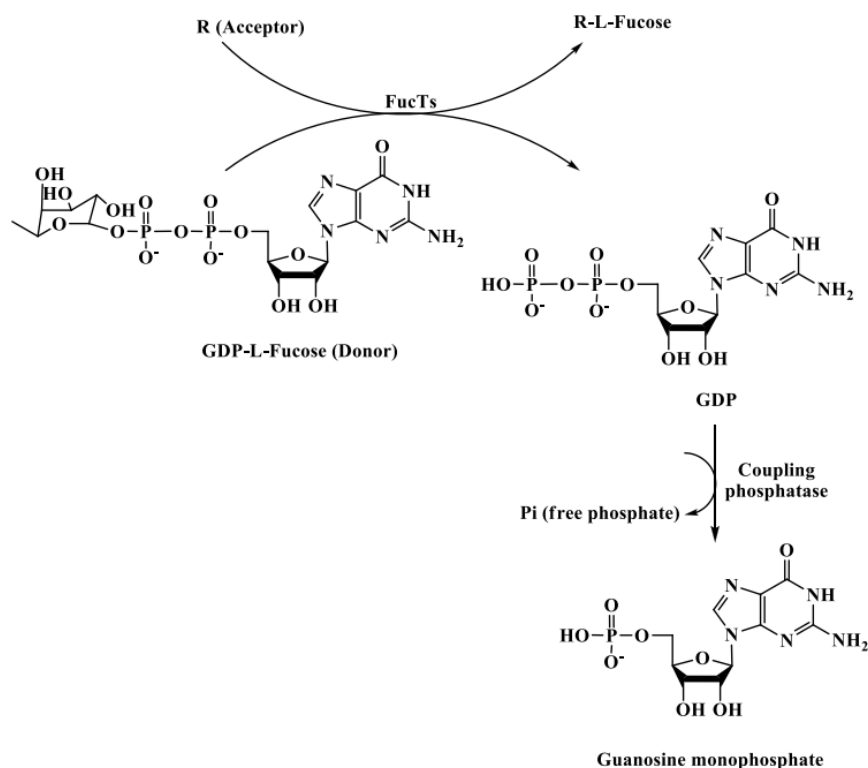


Fig. 58: Glycosyltransferase activity kit principle, as described by the supplier (Bio-Techne®)

Steps are initiated with hydrolysis of GDP-L-fucose with an active FucTs and terminated with free phosphate detection

FucTs₅₀ was determined in comparison with empty plasmid expressed proteins. FucTs₅₀ showed an activity towards GDP-L-fucose of 0.47 pmol min⁻¹ μg⁻¹. It was determined according to the **Eq. 7** [259], where; **S** is the slope of **Fig. 59** and **CF** is the conversion factor determined from phosphate concentration calibration curve (see Appendix).

$$\text{Specific activity} = \frac{S \left(\frac{\text{OD}}{\mu\text{g}} \right) \times \text{CF} \left(\frac{\text{pmol}}{\text{OD}} \right)}{\text{Time (min.)}} \dots\dots\dots \text{(Eq. 7)}$$

$$\text{Specific activity of FucTs}_{50} = \frac{0.008 \times 3509.8}{60} = 0.47 \text{ pmol min}^{-1} \mu\text{g}^{-1}$$

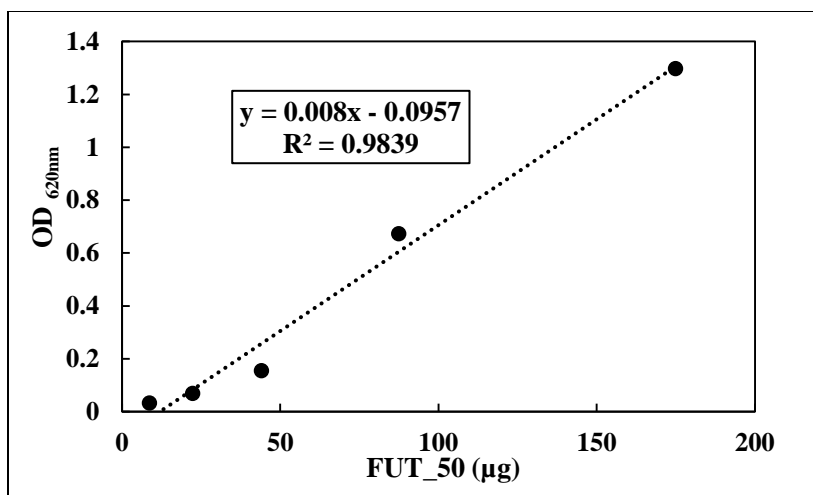


Fig. 59: Measurement of catalytic activity of FucTs_50 on the donor substrate GDP-L-fucose by Glycosyltransferase activity kit

OD values were measured at 620 nm to determine free liberated phosphate from GDP moiety. All absorbance values were subtracted from background value.

b. MP-CE analysis

Another hydrolytic activity was performed to investigate the putative function of FucTs_50 toward its substrate GDP-L-fucose in the absence of a suitable fucose acceptor. It was investigated by measuring GDP-L-fucose concentration after incubation with FucTs at optimum conditions. After 24 h incubation, as shown in **Fig. 60**, approx. 40% of GDP-L-fucose was hydrolyzed in the presence of the enzyme. However, GDP-L-fucose concentration remained intact in the absence of the enzyme confirming an enzymatic catalytic activity of FucTs_50.

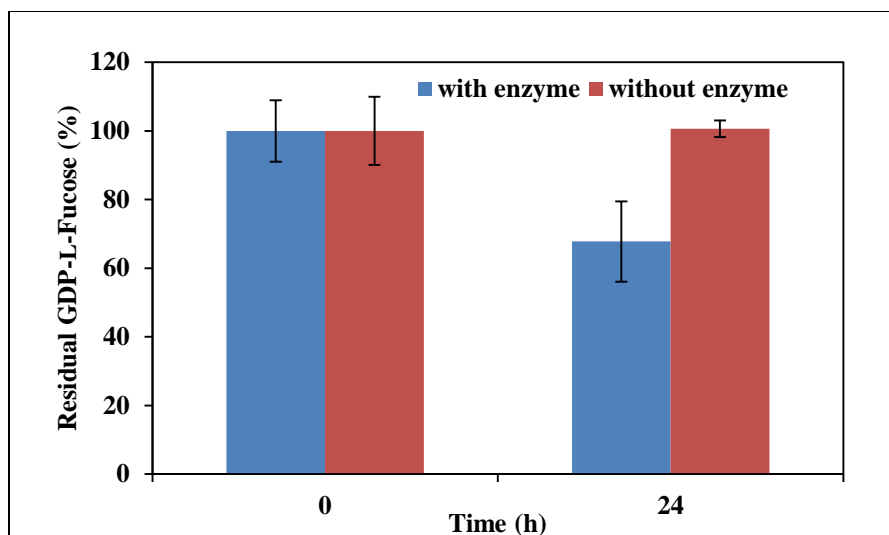


Fig. 60: FucTs_50 hydrolytic activity toward GDP-L-fucose as determined by MP-CE

Results showed that after 24 h, FucTs_50 could cleavage approx. 40% of GDP-L-fucose, in comparison with the enzyme-free condition.

4.3. Carbohydrate sulphotransferases (STs)

Sulphotransferases (STs) catalyze the sulphonation reaction which is involved in many biological activities (e.g., detoxification and drug metabolism) [251]. They transfer sulphonate ester group (SO_3^-) from the donor activated substrate 3'-phosphoadenosine 5'-phospho-sulphate (PAPS) to a hydroxyl group acceptor of specific compounds, such as phenolic and complex carbohydrates molecules in a regio- and stereo-selective reaction creating a sulphate ester (SO_4^-). Their activity are often regulated by supply of PAPS which acts as also a cofactor, as shown in **Fig. 61** [268].

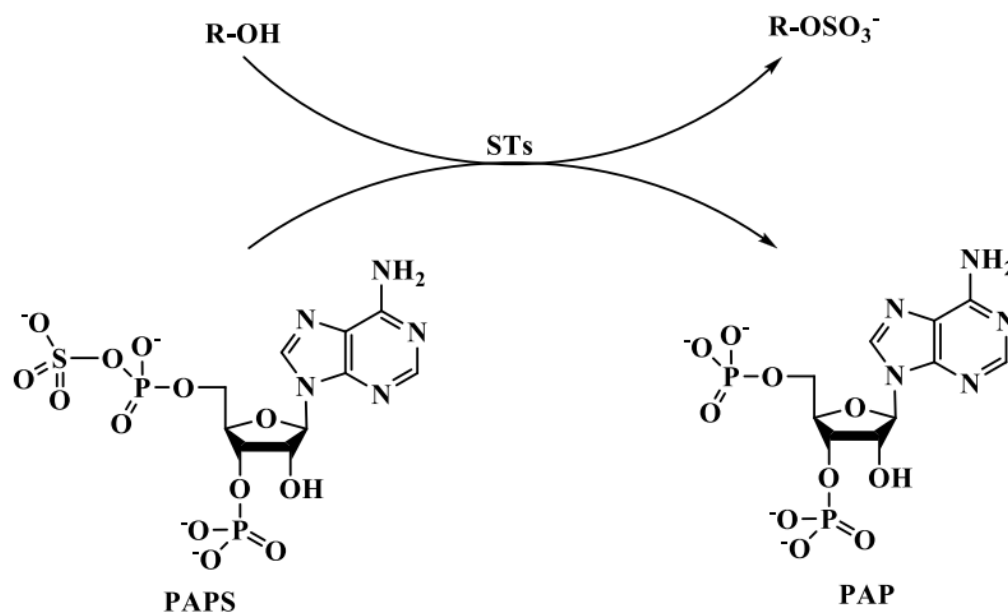


Fig. 61: Catalysis of sulphonate group (SO_3^-) transfer to a hydroxyl group-containing compound by Sulphotransferases (STs) using PAPS as a donor substrate

E. siliculosus genome has, in addition, a gene cluster of more than 10 genes encode for different classes of carbohydrate sulphotransferases (STs). Some of these enzymes are speculated to be involved in fucoidan biosynthesis in brown macroalgae [192]. Nevertheless, the others contribute in synthesis of other unknown compounds or detoxification of water pollutants. Exact specificity and functions of most of these enzymes are still uncertain. Therefore further characterizations are required regarding to confirm their ability to sulphonate sugar monomers and contribution to fucoidan synthesis. **Table 16** summarizes the different algal STs regarding their encoded genes, amino acids and putative functions [192].

Table 16: Overview of different algal STs, regarding their names, sizes of encoded genes, number of amino acids and putative functions

STs name	Encoded gene	Size of gene (nucleotides)	No. of amino acids	Putative functions
STs_28	Esi0028_0011	1026	342	Aryl sulphotransferase
STs_411	Esi0411_0021	837	279	
STs_442	Esi0442_0008	1026	342	
STs_197	Esi0197_0025	1002	334	
STs_289	Esi0289_0025	1044	348	Transfer of sulphate group to specific compounds (unclear specificity)
STs_210	Esi0210_0041	1392	464	Related to Chondroitin 6-sulphotransferase and keratan sulphate Gal-6 sulfotransferase (unclear specificity)
STs_312	Esi0312_0029	1272	424	
STs_32	Esi0032_0064	1386	462	Related to Galactose-3- <i>O</i> -sulphotransferase 2 (unclear specificity)
STs_283	Esi0283_0018	1032	344	
STs_57	Esi0057_0043	939	313	
STs_118	Esi0118_0049	1029	343	
STs_37	Esi0037_0054	1458	486	Related to heparan sulfate glucosamine 3- <i>O</i> -sulphotransferase (unclear specificity)
STs_80	Esi0080_0060	1044	348	
STs_26	Esi0026_0167	1644	548	
STs_239	Esi0239_0035	1680	560	

Esi0032_0064 and Esi0283_0018 encode for STs_32 and STs_283 respectively are distantly related to Galactose-3-*O*-sulfotransferase 2 (EC 2.8.2.-) [269,270]. However, the other genes are more related to phenol, heparan and chondroitin sulphonation. As a pilot experiment, they were chosen to be cloned and expressed in *E. coli* after optimization of their nucleotides' sequence to *E. coli*. This experiments aimed to reveal the role of this class in fucoidan biosynthesis.

4.3.1. Material and Methods

4.3.1.1. Synthetic gene materials

Both *E. coli*-opt. genes (Esi0032_0064 and Esi0283_0018) were synthesized by Invitrogen GeneArt®, as described by Michel, *et al.* [180,181]. These constructs were delivered as inserts in pMA-T plasmid, as shown in **Fig. 62**. As mentioned previously in FucTs section (section 4.2.1.1), *E. coli* JM83 competent cells were transformed and incubated with specified medium (LB supplemented with ampicillin) to produce several genes copies.

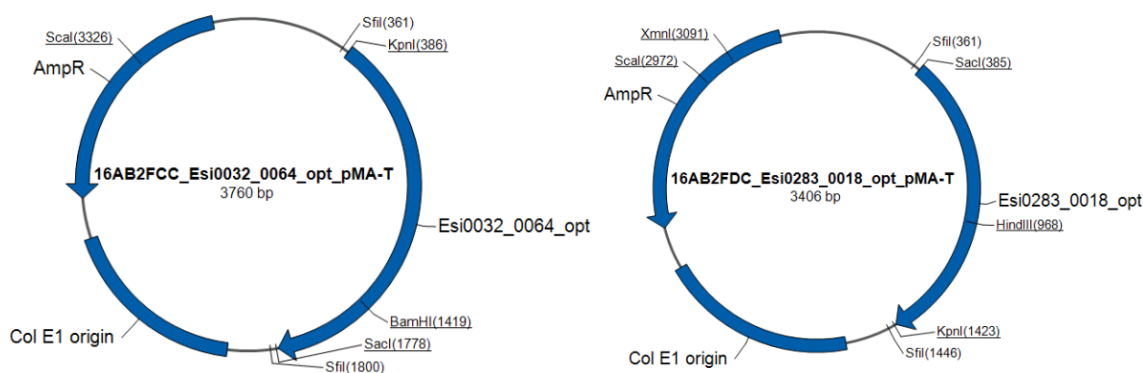


Fig. 62: Cloned *E. coli*-opt. Esi0032_0064 and Esi0283_0018 in pMA-T plasmid vector

Both DNA constructs were synthesized and delivered by Invitrogen GeneArt®, according to Michel, *et al.* [180,181].

4.3.1.2. Cloning by Gibson assembly and sequencing

As previously described in section 4.2.1.2, *E. coli*-adapted Esi0032_0064 and Esi0283_0018 genes were cloned inside its multiple cloning site (MCS) specifically between *EcoRI* and *SacI* restriction sites of the vector plasmid pASK-IBA 45(+). Primers were designed and optimized by the online service provided by New England Biolabs® so as to make genes translation in the same frame of *Strep*®-tag sequence present in the vector plasmid, as demonstrated in **Table 17**.

Table 17: Designed primers for cloning of *E. coli*-adapted Esi0032_0064 and Esi0283_0018 in pASK-IBA 45(+), according to NEBuilder® Assembly Tool

DNA constructs	Primer		Annealing temperature (°C)
pASK-IBA 45(+)_Esi0032_0064	fwd	5'- gcgccgagaccgcggtcccgATGCGTCGTGCACAGGGT -3'	60.0
	rev	5'- ggatccccgggtaccgagctTTAAAAGGCCAGAATAGGCGGTG -3'	
pASK-IBA 45(+)_Esi0283_0018	fwd	5'- gcgccgagaccgcggtcccgATGGCAGGTAATGCAATG -3'	60.0
	rev	5'- ggatccccgggtaccgagctTTAAAACGGCTGAACCGG -3'	

The amplified inserts were afterwards confirmed by gel electrophoresis and PCR products were purified by NucleoSpin® Gel and PCR Clean-up kits (Macherey-Nagel GmbH & Co. KG) and their concentrations were measured by Nanodrop spectrophotometer.

EcoRI and *SacI* restriction endonucleases digestion products with PCR products were incubated in a ratio of 1:2 with 10 µL NEBuilder® HiFi DNA Assembly MasterMix in a total volume of 20 µL for 15 min at 50 °C following the protocol of the provider (New England BioLabs® Inc.) [254]. Recombinant DNA constructs were extracted from culture replicates by NucleoSpin® Plasmid EasyPure (Macherey-Nagel GmbH & Co. KG), and then digested by *XbaI* to give single linearized fragments of the original molecular sizes for verification. The constructs with a right gel electrophoresis profile was then sent for sequencing following protocol described in sections 4.2.1.3.

4.3.1.3. Transformation of *E. coli* BL21 (DE3), enzymes expression and purification

Both sequenced DNA constructs in addition to an empty vector plasmid were applied to transform *E. coli* BL21 (DE3) by heat shock. A pilot experiment with cultivation, protein expression, detection and purification were performed as previously mentioned in pASK-IBA 45(+)_Esi0021_0026 and Esi0050_0098 transformed *E. coli* (section 4.2.1.5 and 4.2.1.6).

4.3.1.4. Activity assay (*Universal sulphotransferase activity kit*)

According to the kit protocol (Catalog # EA003) described by Bio-Techne GmbH, enzymes' activity was investigated [271,272]. Briefly, purified enzymes were dialyzed in a reaction buffer (50 mM Tris, 15 mM MgCl₂, pH 7.5). Reaction was initiated by incubation of 25 µL of serial dilutions of the enzymes in a 25 µL working solution, which was consisted of 10 µL 5 mM GlucNac, 10 µL 1 mM PAPS (as triethylammonium salt) purchased from Sirius fine chemicals (SiChem GmbH) and 5 µL 100 ng µL⁻¹ coupling phosphatase 3 for 20 min at 37 °C. Afterwards, 30 µL of malachite green A,

100 μ L deionized water and 30 μ L malachite green B were added, before an incubation step at room temperature again for 20 min. Finally the absorbance was measured at 620 nm and reaction buffer was used as a blank.

4.3.2. Results and Discussion

Fucan backbone shows different sulphation patterns (e.g., 2- and/or, 3- and/or, 4- sulphated fucan), which is confirmed by the presence of several encoding genes for algal STs [192]. Unlike to fucan synthesis formation site, it is still unclear whether the final fucan sulphonation step is performed in cell cytosol by cytosolic STs and then transported to macroalgal cell wall or inside the cell wall *in situ* by membrane STs.

4.3.2.1. Homology with other STs

Conserved peptide motifs were observed with alignment of STs_32 and STs_283 amino acids, such as **NIAFxKTHKTAStTxAxxLYRYGxRHD** and **VTVxREPVAHYxSYYYYFLxP** which may be related to the enzyme active sites. Moreover, a comparison of the two representatives with the human Galactose-3-*O*-sulfotransferase 2 (G3ST2) revealed 21.9 and 20.9 identity (%), respectively, as shown in **Fig. 63**. Lower percentages of homology may be problematic, but the presence of these motifs proved their putative functions.

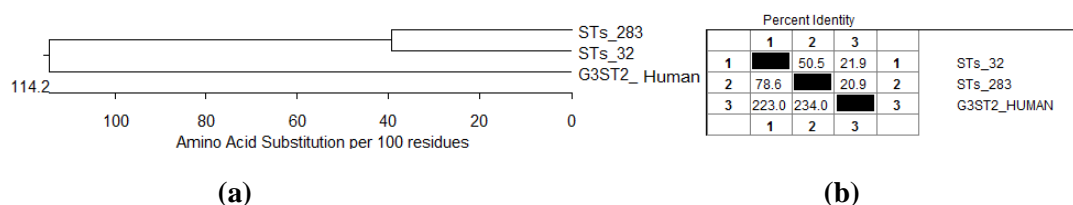


Fig. 63: A homology study between algal STs_283, STs_32 and the human Galactose-3-*O*-sulfotransferase 2 (G3ST2)

(a) Phylogenetic tree; (b) percent identity of algal STs_32 and STs_283 with the human enzyme is of 21.9 and 20.9%, respectively. DNASTAR® (Lasergene v7, MegAlign) software and Clustal W algorithm were applied to investigate the different homology studies, including percent identity, phylogenetic tree and motifs in aligned sequences

4.3.2.2. PCR of Esi0032_0064 and Esi0283_0018 with overlapping ends

To design PCR primers with overlapping sequences between plasmid vector pASK-IBA 45(+) and the two DNA fragments for their assembly, the Web Tool of NEBuilder® was applied. Plasmid vector was opened by a double digestion step with *EcoRI/SacI*; therefore, PCR primers were designed to have an overlapping sequence from plasmid and a gene specific sequence for template priming. Amplified PCR products were verified by agarose gel electrophoresis. As shown in **Fig. 64**, Esi0032_0064 and Esi0283_0064 were detected at 1386 and 1032 bp, respectively.

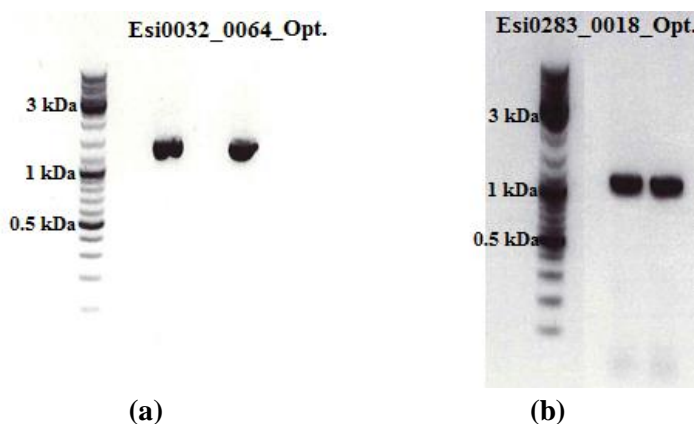
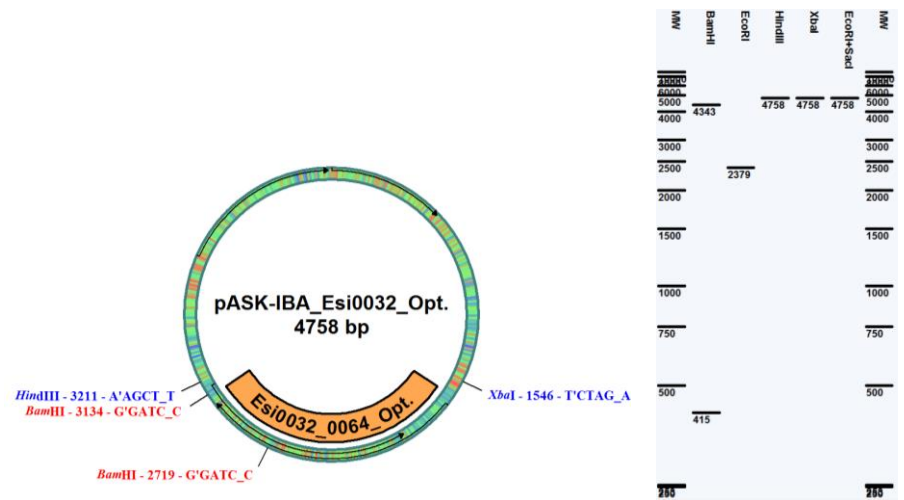


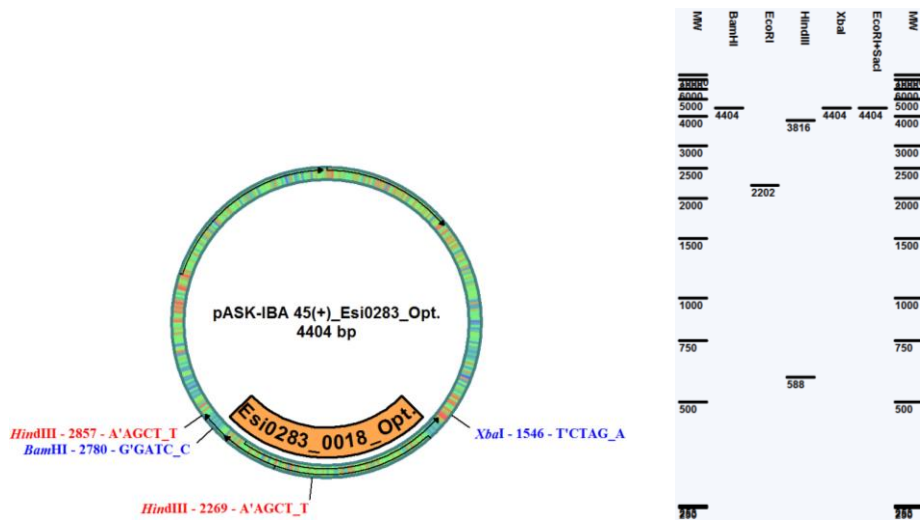
Fig. 64: Agarose gel electrophoresis of (a) amplified Esi0032_0064 (1386 bp) and (b) Esi0283_0018 (1032 bp) with their overlapping ends from *EcoRI/SacI* restriction sites of the vector pASK-IBA 45(+)

4.3.2.3. Gibson assembly and constructs sequencing

As shown in **Fig. 65 and 66**, DNA constructs were designed by pDRAW32 DNA analysis Software, as previously performed, and synthesized according to Gibson assembly protocol. Extracted recombinant pASK-IBA 45(+)_Esi0032_0064 construct from replicate 1 and 4 showed after a single digestion by *XbaI* a single fragment at 4758 bp. However, several replicates (1-4 and 6) from Esi0283_0018 were detected at 4404 bp. These results were confirmed by lower migration rates of linearized single bands compared with digested vector at 3286 bp.



(a)



(b)

Fig. 65: Designed pASK-IBA 45(+)_Esi0032_0064 (a) and pASK-IBA 45(+)_Esi0283_0018 (b) templates by pDRAW32 DNA analysis software
 Templates showed their sizes in bp and sites of some possible restriction enzymes.

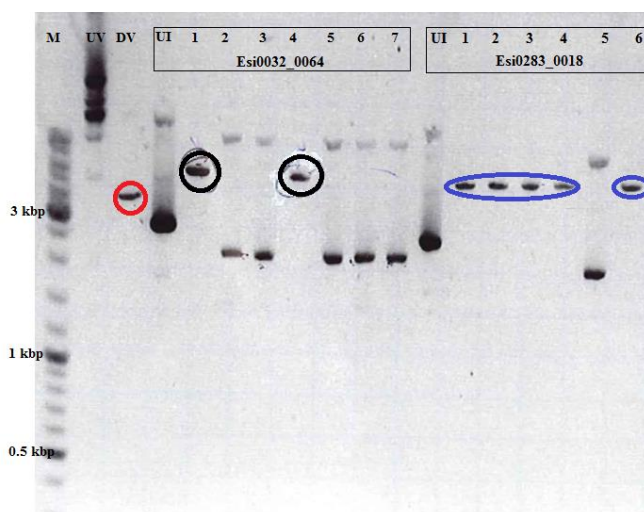


Fig. 66: Agarose gel electrophoresis of extracted DNA constructs; pASK-IBA 45(+)_Esi0032_0064_Opt. and pASK-IBA 45(+)_Esi0283_0018_Opt. after digestion with *Xba*I

They were compared with undigested empty vector, digested vector and undigested inserts. Constructs 1 and 4 from Esi0032_0064 as a single fragment at 4758 bp and 1-4 and 6 from Esi0283_0018 at 4404 bp showed lower migration rates than digested vector at 3286 bp. M= size marker, UV= undigested empty vector, DV= digested vector, UI=undigested insert.

Sequence results were aligned, afterwards, with the designed templates and showed identical sequence in addition to right cloning of synthetic genes in the plasmid vector. Moreover, *Strep*[®]-tag sequence was inserted correctly as N-terminal in front of the expressed proteins, as demonstrated in **Fig. 67**.

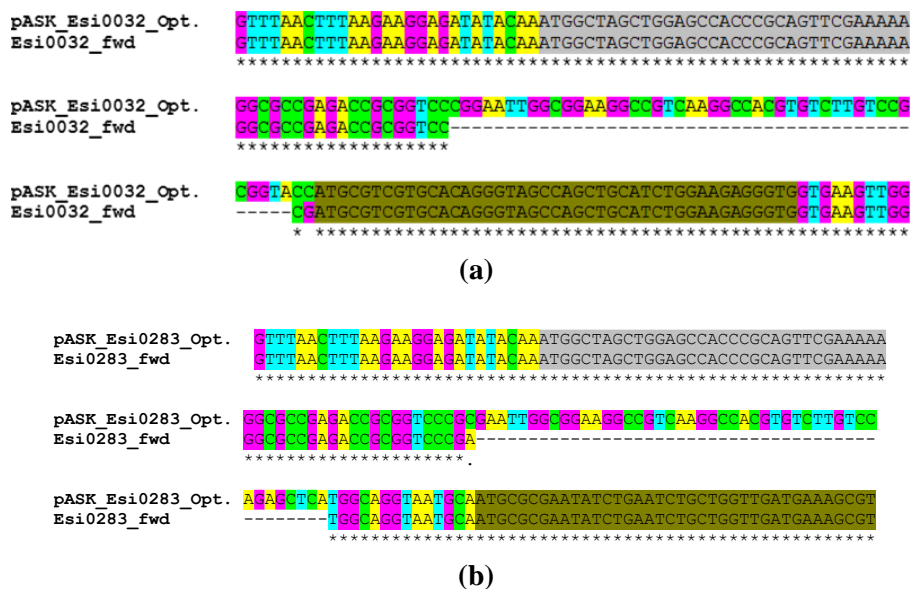


Fig. 67: Alignment of sequencing results of fwd DNA constructs; pASK-IBA 45(+)_Esi0032_0064_Opt. (a) and pASK-IBA 45(+)_Esi0283_0018_Opt. (b) with the designed templates
 The results showed great similarities and insertion of *Strep*-tag sequence (in grey) as N-terminals of expressed proteins.

4.3.2.4. Gene expression and proteins detection by Western blot

Induction of STs over-expression by AHT from cultivated genetically-engineered *E. coli* BL21 (DE3) and further steps of proteins purification and detection in eluates were carried out as previously mentioned with FucTs. As demonstrated in **Fig. 68** and **69**, results confirmed that both STs were expressed as *Strep*[®]-tag proteins at the right expected molecular sizes with yield of 55.1 µg and 60.5 µg from STs_32 and STs_283, respectively, as determined by UV spectrometry at 280 nm.

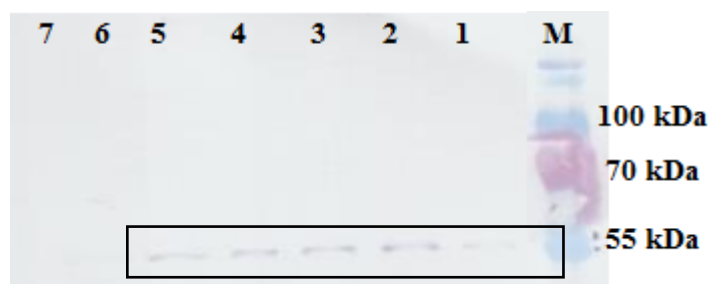


Fig. 68: Western blot of purified heterologously expressed STs_32 by *E. coli* BL21 (DE3)
 Heterologously-expressed STs_32 of a molecular size 55.28 kDa was detected in column fractions 2-5, compared to the size marker. M=size marker – PageRuler[™] Prestained (Thermo Fisher).

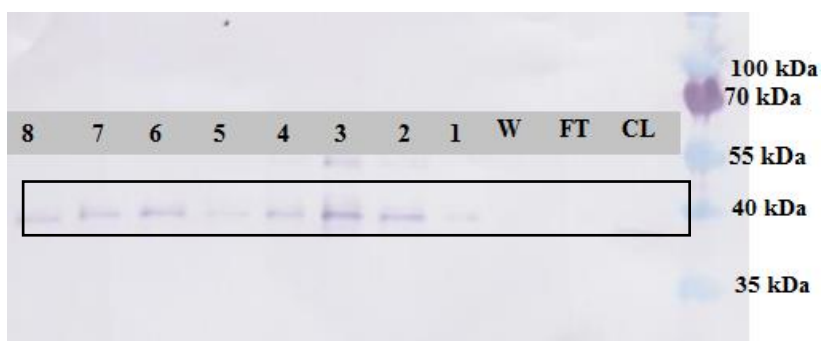


Fig. 69: Western blot of purified heterologously expressed STs_283 by *E. coli* BL21 (DE3)

Protein of a molecular size 40.58 kDa was detected in column fractions (2-8). CL= cell lysate, FT= column flow through, W= wash.

4.3.2.5. Activity assay

Activity of expressed STs was assessed by their ability to transfer the sulphonate group from the activated sulphonate donor PAPS substrate, according to the protocol established by the kit's provider [271,272]. The reaction principle could be summarized as followed in **Fig. 70**. As a result of sulphonate group removal from PAPS, PAP is produced which and further hydrolyzed by a phosphatase enzyme. The last step is accompanied with the liberation of free phosphate which could be measured colorimetry at 620 nm by malachite green reagents.

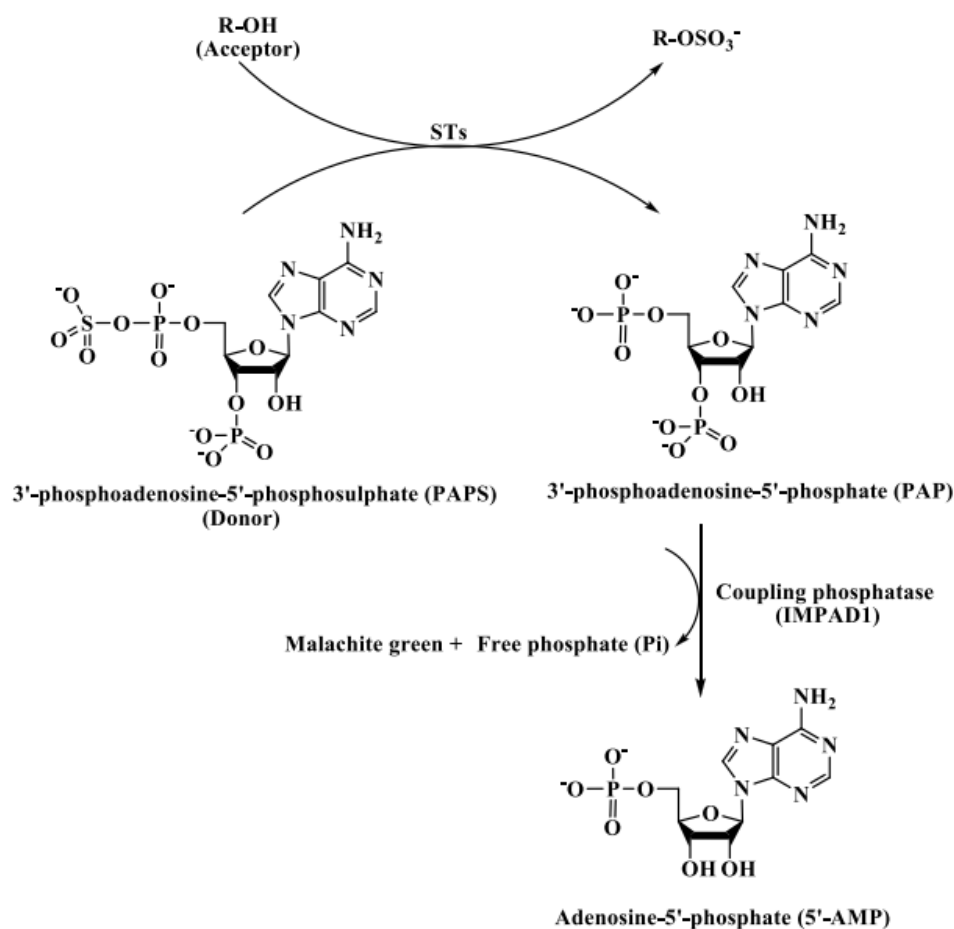


Fig. 70: Principle of the Universal sulphotransferase activity kit as described by the supplier (Bio-Techne®) [271,272]

Results, as shown in **Fig. 71 a** and **b**, proved that STs_32 and STs_283 had a catalytic activity which was directly related with the enzyme concentration. STs_32 and STs_283 recorded similar sulphotransferase activities of 2.38 and 2.29 $\text{pmol min}^{-1} \mu\text{g}^{-1}$, using **Eq. 7**, respectively, where; **S** is the slope of **Fig. 71a** and **b** and **CF** is the conversion factor determined from phosphate concentration calibration curve (see **Appendix E: Calibration curves**).

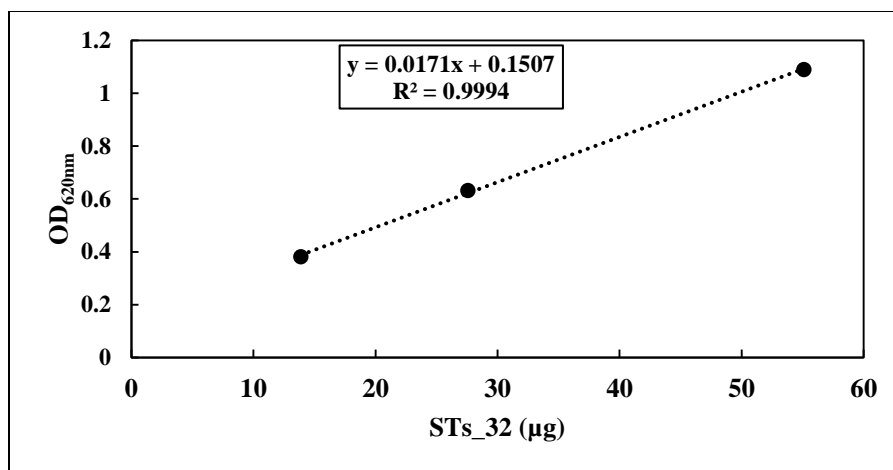


Fig. 71 a: Relationship between purified STs₃₂ at different concentrations and liberated free phosphate from PAPS detected by malachite green and measured at 620 nm
All absorbance values were subtracted from the background value (reaction buffer).

$$\text{Specific activity} = \frac{S \left(\frac{\text{OD}}{\mu\text{g}} \right) \times \text{CF} \left(\frac{\text{pmol}}{\text{OD}} \right)}{\text{Time (min.)}} \dots\dots\dots \text{(Eq. 7)}$$

$$\text{Specific activity of STs}_{32} = \frac{0.0171 \times 2784.1}{20} = 2.38 \text{ pmol min}^{-1} \mu\text{g}^{-1}$$

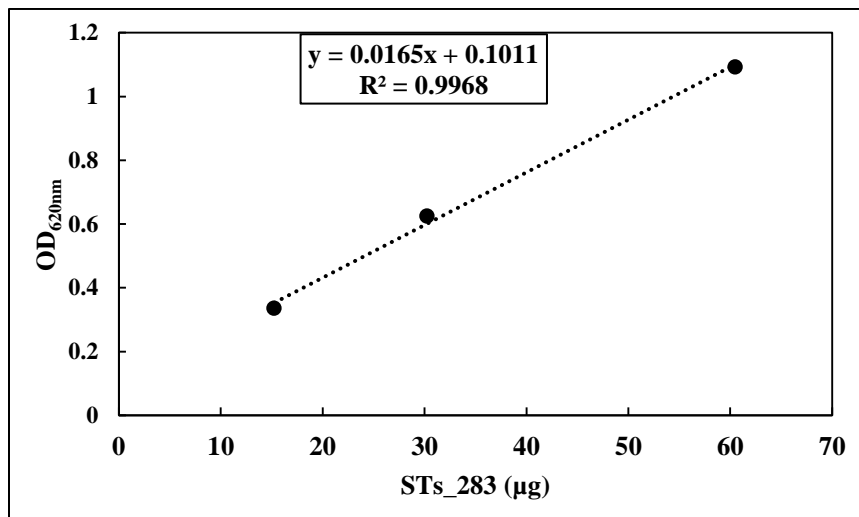


Fig. 71 b: Relationship between purified STs₂₈₃ at different concentrations and liberated free phosphate from PAPS detected by malachite green and measured at 620 nm
All absorbance values were subtracted from the background value (reaction buffer).

$$\text{Specific activity of STs}_{283} = \frac{0.0165 \times 2784.1}{20} = 2.29 \text{ pmol min}^{-1} \mu\text{g}^{-1}$$

4.4. Conclusion and Prospectives

Algal FucTs and STs are involved in fucoidan biosynthesis and considered as potential enzyme classes from eukaryotic sources with better similarities with human than bacterial analogues. These enzymes have not been characterized yet and their exact specificity have not been verified. Therefore, heterologous expression of some FucTs and STs in *E. coli* was performed for the first time.

Overexpressed algal FucTs_50, STS_32 and STs_283 showed a catalytic activity on their donor substrates GDP-L-fucose and PAPS, respectively, as determined by different techniques (e.g., Universal Glycosyltransferase and Sulphotransferase activity kits). These results provided a strong proof for active and correctly-folded enzymes. Nevertheless, overexpression experiments showed proteins with low water solubility and inclusion bodies formation, especially FucTs_21, which affected afterwards on extraction and further purification steps. It might be concluded that these enzymes still needed a post-translational modification which is not present in *E. coli*. This was confirmed by the presence of a number of serine, threonine and asparagine residues which are possible glycosylation sites. Therefore, lower water solubility might be due to lack of protein glycosylation, which was not possible by a glycosylation machinery-deficient *E. coli*.

Further experiments should be performed to specify acceptor substrates including non-modified substrates (e.g., L-fucose, and GlucNAc) and modified analogues (e.g., *N*-acetyl lactosamine (LacNAc-*t*-Boc type I and II). As seen in **Fig. 72**, If GlucNAc is considered as an appropriate fucose acceptor, over-expressed putative FucTs_50 should be able to build up an α -1,3 glycosidic linkage and produce α -1,3 fucosyl *N*-acetyl glucosamine. Product could be detected by different hyphenated spectrometric techniques, such as HPLC-MS [273]. Enzyme kinetics should be addressed applying Michalis-Menten equation to determine K_m and V_{max} kinetic parameters that affect the enzymes' activity in addition to their inhibitors for further characterization.

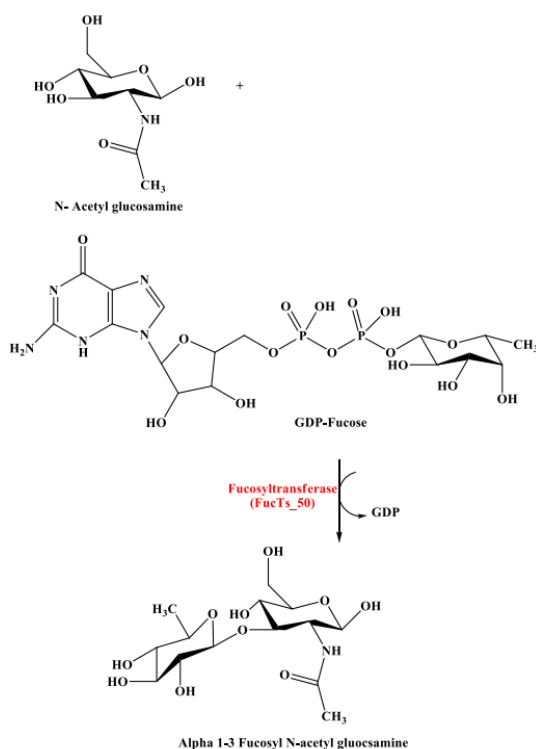


Fig. 72: Simulated fucosylation reaction of GlcNAc catalyzed by heterologously expressed FucTs_50

Furthermore, rate of protein expression and protein water solubility could be increased by their production as GST-fusion proteins or application of eukaryotic expression system with a glycosylation machinery, such as *P. pastoris*.

Moreover, polymer building activity of expressed FucTs should be investigated to be applied in the synthesis of structurally-consistent fucoidan after sulphonation at some positions of polymer backbone with the assist of expressed sulphotransferase (STs). This will help the enzymatic synthesis of a GMP-compliant and eco-friendly product instead of chemical [191] and classical extraction procedures [79].

5. Conclusion

Increasing the global demands from marine-based products (e.g., fucoidan), heterogeneity, seasonality and negatively consequences on ecosystem showed that novel non-traditional eco-friendly techniques for commercial production of a GMP-compliant product are required. Firstly, it was observed that classical extraction and purification of fucoidan from natural habitat have not been optimized yet which necessitate the emergence of new ideas and techniques for optimization to increase the yield and quality as well. Immobilization of PDD improved fucoidan purification from *F. vesiculosus* crude extract drastically, in comparison with the recently-established purification by immobilized thiazine dyes. The batch process was performed in only 16 h instead of 44 h with thiazine dyes and 3 h in case of automated process by FPLC. This confirmed that there is a direct relationship between the number of amino groups and reagent sensitivity resulting in a higher percentages of captured fucoidan. Furthermore, purified products demonstrated improved anti-coagulant and anti-viral activities, compared with >95% pure fucoidan purchased from Sigma-Aldrich®.

Moreover, development of axenic callus-like and protoplast suspension cultures from marine macroalgae as well as cultivation in bioreactors were possible. However, maintenance of cultures growth and induction of fucoidan production were limited by susceptible contamination and undefined nutritional requirements. Induction of hairy root and callus-like growth in wave bag bioreactor were presented for the first time.

In addition, possibility of enzymatic synthesis of marine compounds by heterologous expression of the responsible enzymes was also discussed in the present dissertation showing a novel technique for fucoidan production. Genetically transformed *E. coli* was able to overexpress some enzymes (e.g., FucTs_50, STs_32 and STs_283) which proved their catalytic activities on their substrates. Moreover, overexpression of algal FucTs and STs might give the opportunity to specify these new category of enzymes and verify bioinformatics predictions.

All of these experiments were performed as potential solutions for production of a fucoidan with a high-quality and low heterogeneity without effects on the global ecosystem. This product can be at this stage investigated clinically to give reliable and consistent results with patients and obey the GMP guidelines.

6. Future Outlook

Further work should continue the optimization trials of cultivation techniques for fast growing cultures of marine organisms at reproducible and controlled conditions (e.g., bioreactor cultivation of hairy root) to assure a constant and homogenous supply of marine-based products such as fucoidan. This field of research needs much work and experiments to follow the advances achieved in terrestrial plants and animals fields.

Overexpression of algal enzymes with their more similarities to human analogues might be applied for synthesis of fucosides and sulphated polysaccharides. Algal enzymes could be seen as a source of enzyme biodiversity for more understanding of their roles in physiological and pathophysiological processes (after investigations of their acceptor substrate specificity) such as synthesis of sialyl Lewis^X antigens and bacterial pathogenicity. In addition, *in vitro* enzymatic synthesis of fucoidan could be possible with these active enzymes. Incorporation of fucoidan precursors to cultivation medium of a genetically-modified organisms (either *E. coli* or *P. pastoris*) might enable the organisms to synthesize fucoidan and incorporate it into its cell wall, secret to the medium or even maintained in site of biosynthesis in cell organelles.

In parallel, traditional extraction and purification techniques should be furtherly optimized especially that there is no standardized procedure. Automated processes, such as developed FPLC purification technique might contribute obtaining a high-yield and pure product without negligible effect on its chemical structure in a time-saving and cheap protocol. Additionally, as a step toward fucoidan approval as a medicament, pharmacokinetic and pharmacodynamics studies should be initiated. For example, accurate and robust analytical techniques which are able to determine its concentrations and recovery (%) in different synthetic dosage forms should be addressed including TB and Heparin Red[®] assay. This study determines robustness of fucoidan measurement in the presence of interferences from drug excipients.

References

- [1] National Oceanic and Atmospheric Administration, “Marine microbes are tiny, single-celled organisms that live in the ocean and account for more than 98 percent of ocean biomass” [Online]. Available: <http://oceanexplorer.noaa.gov/facts/marinemicrobes.html>. [Accessed: 21-Nov-2017].
- [2] K. R. Arrigo, “Marine microorganisms and global nutrient cycles,” *Nature*, vol. 437, no. 7057, pp. 349–355, 2005.
- [3] I. Hamed, F. Özogul, Y. Özogul, and J. M. Regenstein, “Marine bioactive compounds and their health benefits: A review,” *Comprehensive Reviews in Food Science and Food Safety*, vol. 14, no. 4, pp. 446–465, 2015.
- [4] C. Tichet, H. K. Nguyen, S. El Yaakoubi, and J. F. Bloch, “Commercial product exploitation from marine microbial biodiversity: Some legal and IP issues: Opinion,” *Microbial Biotechnology*, vol. 3, no. 5, pp. 507–513, 2010.
- [5] X. Wang, H. Yu, R. Xing, and P. Li, “Characterization, preparation, and purification of marine bioactive peptides,” *BioMed Research International*, vol. 2017, 2017.
- [6] Committee on Marine Biotechnology: Biomedical Applications of Marine Natural Products, National Research Council, “Marine biotechnology in the twenty-first century: problems, promise, and products”. National academy press, Washington, D.C., 2002.
- [7] B. Nijampatnam, S. Dutta, and S. E. Velu, “Recent developments in the isolation, synthesis, and bioactivities of bispyrroloquinone alkaloids of marine origin,” *Chinese Journal of Natural Medicines*, vol. 13, no. 8, pp. 561–577, 2015.
- [8] P. M. Murray *et al.*, “Sustainable production of biologically active molecules of marine based origin,” *New Biotechnology*, vol. 30, no. 6, pp. 839–850, 2013.
- [9] U. Lindequist, “Marine-derived pharmaceuticals - challenges and opportunities,” *Biomolecules and Therapeutics*, vol. 24, no. 6, pp. 561–571, 2016.
- [10] S. Sagar, M. Kaur, and K. P. Minneman, “Antiviral lead compounds from marine sponges,” *Marine Drugs*, vol. 8, no. 10, pp. 2619–2638, 2010.
- [11] W. C. Dunlap and Y. Yamamoto, “Small-molecule antioxidants in marine organisms: Antioxidant activity of mycosporine-glycine,” *Comparative Biochemistry and Physiology - Part B: Biochemistry and*, vol. 112, no. 1, pp. 105–114, 1995.
- [12] P. Bermejo, E. Piñero, and Á. M. Villar, “Iron-chelating ability and antioxidant properties of phycocyanin isolated from a protean extract of *Spirulina platensis*,” *Food Chemistry*, vol. 110, no. 2, pp. 436–445, 2008.
- [13] A. Asghari, M. Fazilati, A. M. Latifi, H. Salavati, and A. Choopani, “A review on antioxidant properties of Spirulina,” *Journal of Applied Biotechnology Reports*, vol. 3, no. 1, pp. 345–351, 2016.
- [14] A. Cumashi *et al.*, “A comparative study of the anti-inflammatory, anticoagulant, antiangiogenic, and antiadhesive activities of nine different fucoidans from brown seaweeds,” *Glycobiology*, vol. 17, no. 5, pp. 541–552, 2007.
- [15] Y. González, D. Torres-Mendoza, G. E. Jones, and P. L. Fernandez, “Marine diterpenoids as potential anti-inflammatory agents,” *Mediators of Inflammation*, vol. 2015, Article ID 263543, 2015.
- [16] R. Karthikeyan, S. T. Somasundaram, T. Manivasagam, T. Balasubramanian, and P. Anantharaman, “Hepatoprotective activity of brown alga *Padina boergesenii* against CCl₄ induced oxidative damage in Wistar rats,” *Asian Pacific Journal of Tropical Medicine*, vol. 3, no. 9, pp. 696–701, 2010.
- [17] D. G. Nair, R. Weiskirchen, and S. K. Al-Musharafi, “The use of marine-derived bioactive compounds

- as potential hepatoprotective agents,” *Acta Pharmacologica Sinica*, vol. 36, no. 2, pp. 158–170, 2015.
- [18] Y. Murti and T. Agrawal, “Marine derived pharmaceuticals–development of natural health products from marine biodiversity,” *International Journal of ChemTech Research*, vol. 2, no. 4, pp. 2198–2217, 2010.
- [19] N. Anand, D. Rachel, N. Thangaraju, and P. Anantharaman, “Potential of marine algae (sea weeds) as source of medicinally important compounds,” *Plant Genetic Resources: Characterisation and Utilisation*, vol. 14, no. 4, pp. 303–313, 2016.
- [20] G. Schwartzmann, A. B. da Rocha, R. G. S. Berlinck, and J. Jimeno, “Marine organisms as a source of new anticancer agents,” *The Lancet Oncolog*, vol. 2, no. 4, pp. 221–225, 2001.
- [21] S. R. Kumar, M. Hosokawa, and K. Miyashita, “Fucoxanthin: A marine carotenoid exerting anti-cancer effects by affecting multiple mechanisms,” *Marine Drugs*, vol. 11, no. 12, pp. 5130–5147, 2013.
- [22] N. Sithranga Boopathy and K. Kathiresan, “Anticancer drugs from marine flora: An overview,” *Journal of Oncology*, vol. 2010, Article ID 214186, 2010.
- [23] S. Jiang *et al.*, “Chalcomycins from marine-derived *Streptomyces* sp. and their antimicrobial activities,” *Marine Drugs*, vol. 15, no. 6, pp. 8–13, 2017.
- [24] M. J. Abad, L. M. Bedoya, and P. Bermejo, “Marine compounds and their antimicrobial activities,” *Fortamex*, pp. 1293–1306, 2011.
- [25] D. Lee, *et al.*, “Inhibition of *Candida albicans* isocitrate lyase activity by sesterterpene sulfates from the tropical sponge *Dysidea* sp.,” *Bioorganic and Medicinal Chemistry Letters*, vol. 18, no. 20, pp. 5377–5380, 2008.
- [26] L. Xu, W. Meng, C. Cao, J. Wang, W. Shan, and Q. Wang, “Antibacterial and antifungal compounds from marine fungi,” *Marine Drugs*, vol. 13, no. 6, pp. 3479–3513, 2015.
- [27] I. S. Boziaris, “Food ingredients from the marine environment. Marine biotechnology meets food science and technology,” *Frontiers in Marine Science*, vol. 1, no. November, pp. 1–4, 2014.
- [28] K. Y. Lee and D. J. Mooney, “Alginate: properties and biomedical applications,” *Progress in Polymer Science (Oxford)*, vol. 37, no. 1, pp. 106–126, 2012.
- [29] M. Lahaye and C. Rochas, “Chemical structure and physico-chemical properties of agar,” *Hydrobiologia*, vol. 221, pp. 137–148, 1991.
- [30] E. Tojo and J. Prado, “Chemical composition of carrageenan blends determined by IR spectroscopy combined with a PLS multivariate calibration method,” *Carbohydrate Research*, vol. 338, no. 12, pp. 1309–1312, 2003.
- [31] V. L. Campo, D. F. Kawano, D. B. da Silva, and I. Carvalho, “Carrageenans: Biological properties, chemical modifications and structural analysis - A review,” *Carbohydrate Polymers*, vol. 77, no. 2, pp. 167–180, 2009.
- [32] M. Tsuda, *et al.*, “Speradine A, a new pentacyclic oxindole alkaloid from a marine-derived fungus *Aspergillus tamarii*,” *Tetrahedron*, vol. 59, no. 18, pp. 3227–3230, 2003.
- [33] K. K. Tae and J. A. Fuerst, “Diversity of polyketide synthase genes from bacteria associated with the marine sponge *Pseudoceratina clavata*: Culture-dependent and culture-independent approaches,” *Environmental Microbiology*, vol. 8, no. 8, pp. 1460–1470, 2006.
- [34] Y. Zhu, L. Wu, Y. Chen, H. Ni, A. Xiao, and H. Cai, “Characterization of an extracellular biofunctional alginate lyase from marine *Microbulbifer* sp. ALW1 and antioxidant activity of enzymatic hydrolysates,” *Microbiological Research*, vol. 182, pp. 49–58, 2016.
- [35] Q. Wu, M. Zhang, K. Wu, B. Liu, J. Cai, and R. Pan, “Purification and characteristics of fucoidanase obtained from *Dendryphiella arenaria* TM94,” *Journal of Applied Phycology*, vol. 23, no. 2, pp. 197–

- 203, 2011.
- [36] H. Malve, “Exploring the ocean for new drug developments: Marine pharmacology,” *Journal of Pharmacy and Bioallied Sciences*, vol. 8, no. 2, pp. 83–91, 2016.
- [37] WHO, “InvestigationalPharmaceuticalProductsClinicalTrialsHumansTRS863Annex7.pdf,” 1996. [Online]. Available: http://www.who.int/medicines/areas/quality_safety/quality_assurance/InvestigationalPharmaceuticalProductsClinicalTrialsHumansTRS863Annex7.pdf. [Accessed: 30-Jun-2017].
- [38] N. Rhein-Knudsen, M. T. Ale, and A. S. Meyer, “Seaweed hydrocolloid production: An update on enzyme assisted extraction and modification technologies,” *Marine Drugs*, vol. 13, no. 6, pp. 3340–3359, 2015.
- [39] A. H. Buschmann, *et al.*, “Seaweed production: overview of the global state of exploitation, farming and emerging research activity,” *European Journal of Phycology*, vol. 52, no. 4, pp. 391–406, 2017.
- [40] C. M. Duarte, J. Wu, X. Xiao, A. Bruhn, and D. Krause-Jensen, “Can seaweed farming play a role in climate change mitigation and adaptation?,” *Frontiers in Marine Science*, vol. 4, no. April, 2017.
- [41] D. Hurst, T. Børresen, L. Almesjö, F. De Raedemaeker, and S. Bergseth, Marine biotechnology strategic research and innovation roadmap: Insights to the future direction of European marine biotechnology. Marine Biotechnology ERA-NET: Oostende. September 2016.
- [42] M. F. de Jesus Raposo, A. M. de Morais, and R. M. de Morais, “Marine polysaccharides from algae with potential biomedical applications,” *Marine Drugs*, vol. 13, no. 5, pp. 2967–3028, 2015.
- [43] B. Li, F. Lu, X. Wei, and R. Zhao, “Fucoidan: Structure and bioactivity,” *Molecules*, vol. 13, no. 8, pp. 1671–1695, 2008.
- [44] M. Garcia-vaquero, G. Rajauria, O. J. V Doherty, and T. Sweeney, “Polysaccharides from macroalgae: Recent advances, innovative technologies and challenges in extraction and purification,” *Food Research International*, vol. 99, no. September, pp. 1011–1020, 2016.
- [45] C. M. Dore, *et al.*, “A sulfated polysaccharide, fucans, isolated from brown algae *Sargassum vulgare* with anticoagulant, antithrombotic, antioxidant and anti-inflammatory effects,” *Carbohydrate Polymers*, vol. 91, no. 1, pp. 467–475, 2013.
- [46] E. Deniaud-Bouët, K. Hardouin, P. Potin, B. Kloareg, and C. Hervé, “A review about brown algal cell walls and fucose-containing sulfated polysaccharides: cell wall context, biomedical properties and key research challenges,” *Carbohydrate Polymers*, vol. 175, pp. 395–408, 2017.
- [47] K. Muse, H. Naturelle, and R. Cuvier, “Phylogenetic relationships within the Fucales (Phaeophyceae) assessed by the photosystem I coding psa A sequences,” *Phycologia*, vol. 45, no. September, pp. 512–519, 2006.
- [48] M. Wahl, *et al.*, “The responses of brown macroalgae to environmental change from local to global scales: direct versus ecologically mediated effects,” *Perspectives in Phycology*, vol. 2, no. 1, pp. 11–29, 2015.
- [49] M. R. Irhimeh, J. H. Fitton, and R. M. Lowenthal, “Pilot clinical study to evaluate the anticoagulant activity of fucoidan,” *Blood Coagulation & Fibrinolysis*, vol. 20, no. 7, pp. 607–610, 2009.
- [50] J. Dürig, T. Bruhn, K.-H. Zurbornl, K. Gutensohn, B. Hans D., and L. Beress, “Anticoagulant fucoidan fractions from *Fucus vesiculosus* Induce platelet Activation in vitro,” *Thrombosis Research*, vol. 85, no. 6, pp. 479–491, 1997.
- [51] H. Young *et al.*, “Anti-inflammatory effects of fucoidan through inhibition of NF- κ B, MAPK and Akt activation in lipopolysaccharide-induced BV2 microglia cells,” *Food and Chemical Toxicology*, vol. 49, no. 8, pp. 1745–1752, 2011.
- [52] S. Palanisamy, M. Vinosha, T. Marudhupandi, P. Rajasekar, and P. N. Marimuthu, “Isolation of

- fucoidan from *Sargassum polycystum* brown algae: Structural characterization, *in vitro* antioxidant and anticancer activity,” *International Journal of Biological Macromolecules*, vol. 102, pp. 405–412, 2017.
- [53] S. Sinha, A. Astani, T. Ghosh, P. Schnitzler, and B. Ray, “Phytochemistry polysaccharides from *Sargassum tenerrimum*: Structural features, chemical modification and anti-viral activity,” *Phytochemistry*, vol. 71, no. 2–3, pp. 235–242, 2010.
- [54] J. L. Ee, K. H. Ayashi, M. H. Ashimoto, T. N. Akano, and T. H. Ayashi, “Novel antiviral fucoidan from sporophyll of *Undaria pinnatifida* (Mekabu),” *Chemical Pharmaceutical Bulletin*, vol. 52, no. 9, pp. 1091–1094, 2004.
- [55] S. Dinesh, T. Menon, L. E. Hanna, V. Suresh, M. Sathuvan, and M. Manikannan, “*In vitro* anti-HIV-1 activity of fucoidan from *Sargassum swartzii*,” *International Journal of Biological Macromolecules*, vol. 82, pp. 83–88, 2016.
- [56] G. Jiao, G. Yu, J. Zhang, and H. S. Ewart, “Chemical structures and bioactivities of sulfated polysaccharides from marine algae,” *Marine Drugs*, vol. 9, pp. 196–223, 2011.
- [57] RCR Oliveira, RR Almeida, and TA. Gonçlclves, “A review of plant sulfated polysaccharides and their relations with anticoagulant activities,” *Journal of Developing Drugs*, vol. 5, no. 3, pp. 3–5, 2016.
- [58] B. Matsuhira, “Characterization of a fucoidan from *Lessonia vadosa* (Phaeophyta) and its anticoagulant and elicitor properties,” vol. 42, pp. 235–240, 2008.
- [59] M. Baba, R. Snoeck, R. Pauwels, and E. De Clercq, “Sulfated polysaccharides are potent and selective inhibitors of various enveloped viruses, including herpes simplex virus, cytomegalovirus, vesicular stomatitis virus, and human immunodeficiency virus,” *Antimicrobial Agents and Chemotherapy*, vol. 32, no. 11, pp. 1742–1745, 1988.
- [60] R. Elizondo-Gonzalez, L. E. Cruz-Suarez, D. Ricque-Marie, E. Mendoza-Gamboa, C. Rodriguez-Padilla, and L. M. Trejo-Avila, “*In vitro* characterization of the antiviral activity of fucoidan from *Cladosiphon okamuranus* against Newcastle Disease Virus,” *Virology Journal*, vol. 9, no. 1, p. 307, 2012.
- [61] J. A. Melero and V. Mas, “The Pneumovirinae fusion (F) protein: A common target for vaccines and antivirals,” *Virus Research*, vol. 209, pp. 128–135, 2015.
- [62] H. Li *et al.*, “Fucoidan from *Fucus vesiculosus* suppresses hepatitis B virus replication by enhancing extracellular signal-regulated Kinase activation,” *Virology Journal*, vol. 14, no. 1, p. 178, 2017.
- [63] P. Mandal, C. G. Mateu, K. Chattopadhyay, C. A. Pujol, E. B. Damonte, and B. Ray, “Structural features and antiviral activity of sulphated fucans from the brown seaweed *Cystoseira indica*,” *Antiviral Chemistry Chemotherapy*, vol. 18, no. 3, pp. 153–162, 2007.
- [64] K. K. A. Sanjeewa, J. S. Lee, W. S. Kim, and Y. J. Jeon, “The potential of brown-algae polysaccharides for the development of anticancer agents: An update on anticancer effects reported for fucoidan and laminaran,” *Carbohydrate Polymers*, vol. 177, no. August, pp. 451–459, 2017.
- [65] M. T. Ale, J. D. Mikkelsen, and A. S. Meyer, “Important determinants for fucoidan bioactivity: A critical review of structure-function relations and extraction methods for fucose-containing sulfated polysaccharides from brown seaweeds,” *Marine Drugs*, vol. 9, pp. 2106–2130, 2011.
- [66] M. C. Rocha De Souza, C. T. Marques, C. M. Guerra Dore, F. R. Ferreira Da Silva, H. A. Oliveira Rocha, and E. L. Leite, “Antioxidant activities of sulfated polysaccharides from brown and red seaweeds,” *Journal of Applied Phycology*, vol. 19, no. 2, pp. 153–160, 2007.
- [67] C. Y. Wang, T. C. Wu, S. L. Hsieh, Y. H. Tsai, C. W. Yeh, and C. Y. Huang, “Antioxidant activity and growth inhibition of human colon cancer cells by crude and purified fucoidan preparations extracted from *Sargassum cristaefolium*,” *Journal of Food and Drug Analysis*, vol. 23, no. 4, pp. 766–

- 777, 2015.
- [68] C. Y. Huang, S. J. Wu, W. N. Yang, A. W. Kuan, and C. Y. Chen, "Antioxidant activities of crude extracts of fucoidan extracted from *Sargassum glaucescens* by a compressional-puffing-hydrothermal extraction process," *Food Chemistry*, vol. 197, pp. 1121-1129, 2016.
- [69] G. Qu, X. Liu, D. Wang, Y. Yuan, and L. Han, "Isolation and characterization of fucoidans from five brown algae and evaluation of their antioxidant activity," *Journal of Ocean University of China*, vol. 13, no. 5, pp. 851-856, 2014.
- [70] W. Mak, N. Hamid, T. Liu, J. Lu, and W. L. White, "Fucoidan from New Zealand *Undaria pinnatifida*: Monthly variations and determination of antioxidant activities," *Carbohydrate Polymers*, vol. 95, no. 1, pp. 606-614, 2013.
- [71] G. L. Rorrer and D. P. Cheney, "Bioprocess engineering of cell and tissue cultures for marine seaweeds," *Aquacultural Engineering*, vol. 32, no. 1, pp. 11-41, 2004.
- [72] N. Kervarec, G. Michel, T. Tonon, B. Kloareg, and E. Deniaud-boue, "Chemical and enzymatic fractionation of cell walls from Fucales: insights into the structure of the extracellular matrix of brown algae," *Annals of Botany*, vol. 114, no. 6, pp. 1203-1216, 2014.
- [73] H. R. Fletcher, P. Biller, A. B. Ross, and J. M. M. Adams, "The seasonal variation of fucoidan within three species of brown macroalgae," *Algal Research*, vol. 22, pp. 79-86, 2017.
- [74] A. D. Holtkamp, S. Kelly, R. Ulber, and S. Lang, "Fucoidans and fucoidanases - focus on techniques for molecular structure elucidation and modification of marine polysaccharides," *Applied Microbiology and Biotechnology*, vol. 82, pp. 1-11, 2009.
- [75] H. Kylin, "Zur Biochemie der Meeresalgen," *Zeitschrift für Physiologische Chemie*, vol. 83, pp. 171-197, 1913.
- [76] M. T. Ale and A. S. Meyer, "Fucoidans from brown seaweeds: an update on structures, extraction techniques and use of enzymes as tools for structural elucidation," *RSC Advances*, vol. 22, pp. 8131-8141, 2013.
- [77] P. A. S. Mourão and M. S. Pereira, "Searching for alternatives to heparin sulfated fucans from marine invertebrates," *Trends in Cardiovascular Medicine: Discoveries in Cardiology* vol. 9, no. 8, pp. 1647-1654, 2000.
- [78] S. Li, *et al.*, "4-O-Sulfation in sea cucumber fucodians contribute to reversing dyslipidaemia caused by HFD," *International Journal of Biological Macromolecules*, vol. 99, pp. 96-104, 2017.
- [79] T. Hahn, S. Lang, R. Ulber, and K. Muffler, "Novel procedures for the extraction of fucoidan from brown algae," *Process Biochemistry*, vol. 47, no. 12, pp. 1691-1698, 2012.
- [80] X. Liu, B. Liu, X. Wei, Z. Sun, and C. Wang, "Extraction, fractionation, and chemical characterisation of fucoidans from the brown seaweed *Sargassum pallidum*," *Czech Journal of Food Sciences*, vol. 34, no. 5, pp. 406-413, 2016.
- [81] T. I. Imbs, N. M. Shevchenko, and S. V. Sukhoverkhov, "Seasonal variations of the composition and structural characteristics of polysaccharides from the brown alga *Costaria costata*," *Chemistry of Natural compounds*, vol. 45, no. 6, pp. 661-665, 2009.
- [82] E. Percival, "Glucuronoxylifucan, a cell-wall component of *Ascophyllum nodosum*," *Carbohydrate Research*, vol. 7, pp. 272-283, 1968.
- [83] A. M. Hammed, I. Jaswir, S. Simsek, Z. Alam, and A. Amid, "Enzyme aided extraction of sulfated polysaccharides from *Turbinaria turbinata* brown seaweed," *International Food Research Journal*, vol. 24, no. 4, pp. 1660-1666, 2017.
- [84] N. Flórez-Fernández, M. López-García, M. J. González-Muñoz, J. M. L. Vilariño, and H. Domínguez, "Ultrasound-assisted extraction of fucoidan from *Sargassum muticum*," *Journal of Applied*

- Phycology*, vol. 29, no. 3, pp. 1553–1561, 2017.
- [85] A. B. Hmelkov, T. N. Zvyagintseva, & N. M. Shevchenko, A. B. Rasin, and S. P. Ermakova, “Ultrasound-assisted extraction of polysaccharides from brown alga *Fucus evanescens*. Structure and biological activity of the new fucoidan fractions,” *Journal of Applied Phycology*, 2017.
- [86] R. M. Rodriguez-jasso, S. I. Mussatto, L. Pastrana, C. N. Aguilar, and J. A. Teixeira, “Microwave-assisted extraction of sulfated polysaccharides (fucoidan) from brown seaweed,” *Carbohydrate Polymers*, vol. 86, no. 3, pp. 1137–1144, 2011.
- [87] Y. Yuan and D. Macquarrie, “Microwave assisted extraction of sulfated polysaccharides (fucoidan) from *Ascophyllum nodosum* and its antioxidant activity,” *Carbohydrate Polymers*, vol. 129, pp. 101–107, 2015.
- [88] E. Sinurat and R. Peranginangin, “Purification and characterization of fucoidan from the brown seaweed *Sargassum binderi* sonder,” *Squalen Bulletin of Marine & Fisheries Postharvest & Biotechnology*, vol. 10, no. 2, pp. 79–87, 2015.
- [89] T. I. Imbs, A. V. Skriptsova, and T. N. Zvyagintseva, “Antioxidant activity of fucose-containing sulfated polysaccharides obtained from *Fucus evanescens* by different extraction methods,” *Journal of Applied Phycology*, vol. 27, no. 1, pp. 545–553, 2014.
- [90] A. Isnansetyo, F. Nor, L. Lutfia, M. Nursid, R. A. Susidarti, and A. Isnansetyo, “Cytotoxicity of fucoidan from three tropical brown algae against breast and colon cancer cell lines,” vol. 9, no. 1, pp. 14–20, 2017.
- [91] A. A. El Gamal, “Biological importance of marine algae,” *Saudi Pharmaceutical Journal*, vol. 18, no. 1, pp. 1–25, 2010.
- [92] V. Sinniger and J. Tapon-Bretonnière, C. Milien, D. Muller, J. Jozefonvicz and AM. Fischer, “Affinity chromatography of sulphated polysaccharides separately fractionated on antithrombin III and heparin cofactor II immobilized on concanavalin A-Sepharose,” *Journal of Chromatography*, vol. 615, no. 2, pp. 215–223, 1993.
- [93] K. Matsumura *et al.*, “Carbohydrate binding specificity of a fucose-specific lectin from *Aspergillus oryzae*: A novel probe for core fucose,” *Journal of Biological Chemistry*, vol. 282, no. 21, pp. 15700–15708, 2007.
- [94] T. Hahn *et al.*, “Dye affinity chromatography for fast and simple purification of fucoidan from marine brown algae,” *Engineering in Life Sciences*, vol. 16, no. 1, pp. 78–87, 2016.
- [95] A. X. P. D’Mello, T. V. Sylvester, V. Ramya, F. P. Britto, P. K. Shetty, and S. Jasphin, “Metachromasia and metachromatic dyes: A review,” *International Journal of Advanced Health Sciences*, vol. 2, no. 10, pp. 12–17, 2016.
- [96] Q. Jiao and Q. Liu, “Simple spectrophotometric method for the estimation of algal polysaccharide concentrations,” *Journal of Agricultural and Food Chemistry*, vol. 47, no. 3, pp. 996–998, 1999.
- [97] H. S. Soedjak, “Colorimetric determination of carrageenans and other anionic hydrocolloids with methylene blue,” *Analytical Chemistry*, vol. 66, no. 24, pp. 4514–4518, 1994.
- [98] T. Hahn *et al.*, “Cationic dye for the specific determination of sulfated polysaccharides,” *Analytical Letters*, vol. 49, no. 12, pp. 1948–1962, 2016.
- [99] L. M. Pty., GRAS notification for fucoidan concentrate from *Fucus vesiculosus*, [Online]. <https://www.fda.gov/downloads/Food/IngredientsPackagingLabeling/GRAS/NoticeInventory/ucm520974.pdf>. [Accessed: 9-March-2018], no. 477. 2016.
- [100] B. Harris, “*Fucus vesiculosus* (Bladder wrack).” [Online]. Available: http://bioweb.uwlax.edu/bio203/2011/harris_benj/habitat.htm. [Accessed: 13-Mar-2018].
- [101] D. B. Hermund, “Extraction, characterization and application of antioxidants from the Nordic brown

- alga *Fucus vesiculosus*,” Technical University of Denmark, 2016.
- [102] “*Fucus vesiculosus* Linnaeus.” [Online]. Available: http://www.algaebase.org/search/species/detail/?species_id=Ta869fe1da130ab10. [Accessed: 06-Dec-2017].
- [103] B. Racionero-Gómez, A. D. Sproson, D. Selby, D. R. Gröcke, H. Redden, and H. C. Greenwell, “Rhenium uptake and distribution in phaeophyceae macroalgae, *Fucus vesiculosus*,” *Royal Society Open Science*, vol. 3, no. 5, p. 160161, 2016.
- [104] M. Dubois, K. A. Gilles, J. K. Hamilton, P. A. Rebers, and F. Smith, “Colorimetric Method for Determination of Sugars and Related Substances,” *Analytical Chemistry*, vol. 28, no. 3, pp. 350–356, 1956.
- [105] A. D. Holtkamp, “Isolation , characterisation , modification and application of fucoidan from *Fucus vesiculosus*,” Technical University of Braunschweig, 2009.
- [106] U. Warttinger, C. Giese, J. Harenberg, and R. Krämer, “Direct quantification of brown algae-derived fucoidans in human plasma by a fluorescent probe assay,” 2016. arXiv:1608.00108 [q-bio.QM]
- [107] Z. Dische and L. B. Shettles, “A specific color reaction of methylpentoses and a spectrophotometric micromethod for their determination,” *The Journal of Biological Chemistry*, vol. 175, pp. 595-603, 1948.
- [108] T. Hahn, “Extraktion von Fucoidan aus Braunalgen,” Technical University of Kaiserslautern, 2012.
- [109] H. Szelke, S. Schübel, J. Harenberg, and R. Krämer, “A fluorescent probe for the quantification of heparin in clinical samples with minimal matrix interference.,” *Chemical communications (Cambridge, England)*, vol. 46, no. 10, pp. 1667–9, 2010.
- [110] Resindion S.r.l., “Relizyme™ and Sepabeads EC - Ready-to-use Enzyme carriers,” *Product brochure*, 2011.
- [111] B. Rühmann, J. Schmid, and V. Sieber, “Fast carbohydrate analysis via liquid chromatography coupled with ultra violet and electrospray ionization ion trap detection in 96-well format,” *Journal of Chromatography A*, vol. 1350, pp. 44-50, 2014.
- [112] L. O. Andersson, T. W. Barrowcliffe, E. Holmer, E. A. Johnson, and G. E. Simms “Anticoagulant properties of heparin fractionated by affinity chromatography on matrix-bound antithrombin III and by gel filtration,” *Thrombosis Research*, vol. 9, pp. 575–583, 1976.
- [113] A. J. Quick, “The clinical application of the hippuric acid and the prothrombin test,” *American Journal of Clinical Pathology*, vol. 10, pp. 222-233, 1940.
- [114] J. Denson, K. W. E., Bonner, “The measurement of heparin: method based on the potentiation of anti-factor Xa,” *Thrombosis et diathesis haemorrhagica*, vol. 30, no. 3, pp. 471–479, 1974.
- [115] G. Kleymann, and H. O. Werling, “A generally applicable, high-throughput screening-compatible assay to identify, evaluate, and optimize antimicrobial agents for drug therapy,” *Journal of Biomolecular Screening*, vol. 9, no. 7, pp. 578-587, 2004.
- [116] F. Boylan, S. Menezes, and G. G. Leita, “Screening of Brazilian plant extracts for antioxidant activity by the use of DPPH free radical method,” *Phytotherapy Research*, vol. 130, no. August, pp. 127-130, 2001.
- [117] J. John Peter Paul, “*In Vitro* anti-oxidant activity of fucoidan extracted from *Padina distromatica* Hauck (brown seaweed) from Hare Island, Thoothukudi, Tamil Nadu, India,” *American Journal of Biological and Pharmaceutical Research*, vol. 1, no. 3, pp. 151-155, 2014.
- [118] S. Park, Y.H., Jang, D.S., Kim, *Utilization of Marine Products*, 2nd edition. Seoul, South Korea: Hyongsul Press, 1997.
- [119] E. D. Obluchinskaya, G. M. Voskoboinikov, and V. A. Galynkin, “Contents of alginic acid and

- fucoidan in fucus algae of the Barents Sea,” *Applied Biochemistry and Microbiology*, vol. 38, pp. 186–188, 2002.
- [120] S. Colin; *et al.*, “Cloning and biochemical characterization of the fucanase FcnA: Definition of a novel glycoside hydrolase family specific for sulfated fucans,” *Glycobiology*, vol. 16, no. 11, pp. 1021-1032, 2006.
- [121] V. Descamps; *et al.*, “Isolation and culture of a marine bacterium degrading the sulfated fucans from marine brown algae,” *Marine Biotechnology*, vol. 8, no. 1, pp. 27-39, 2006.
- [122] B. de Reviere, “Fucans and alginates without phenolic compounds,” *Journal of Applied Phycology*, vol. 1, no. 1, pp. 75-76, 1989.
- [123] U. Wartinger, C. Giese, J. Harenberg, E. Holmer, and R. Krämer, “A fluorescent probe assay (Heparin Red) for direct detection of heparins in human plasma,” *Analytical and Bioanalytical Chemistry*, vol. 408, no. 28, pp. 8241-8251, 2016.
- [124] U. Wartinger, and R. Krämer, “Quantification of heparin in complex matrices (including urine) using a mix-and-read fluorescence assay,” 2016. arXiv:1611.02482 [q-bio.QM]
- [125] M. Rappold, U. Wartinger, and R. Krämer, “A fluorescent probe for glycosaminoglycans applied to the detection of dermatan sulfate by a mix-and-read assay,” *Molecules*, vol. 22, no. 5, pp. 1-11, 2017.
- [126] C. Y. Wang and Y. C. Chen, “Extraction and characterization of fucoidan from six brown macroalgae,” *Journal of Marine Science and Technology (Taiwan)*, vol. 24, no. 2, pp. 319-328, 2016.
- [127] J. H. Fitton, D. N. Stringer, and S. S. Karpinić, “Therapies from fucoidan: An update,” *Marine Drugs*, vol. 13, no. 9, pp. 5920-5946, 2015.
- [128] Agilent Technologies, “Polymer Molecular Weight Distribution and Definitions of MW Averages,” 2015. [Online]. Available: <https://www.agilent.com/cs/library/technicaloverviews/Public/5990-7890EN.pdf>. [Accessed: 19-Oct-2017].
- [129] J. B. Austin, “A relation between the molecular weights and melting points of organic compounds,” *Journal of the American Chemical Society*, vol. 52, no. 3, pp. 1049-1053, 1930.
- [130] E. Sinurat, P. Rosmawaty, and E. Saepudin, “Characterization of fucoidan extracts Binuangeun’s brown seaweed,” *International Journal of Chemical, Environmental and Biological Sciences*, vol. 3, no. 4, pp. 329–332, 2015.
- [131] N. M. Shevchenko, *et al.*, “Further studies on structure of fucoidan from brown alga *Saccharina gurjanovae*,” *Carbohydrate Polymers*, vol. 121, pp. 207–216, 2015.
- [132] P. Li, Y.-N. Dai, J.-P. Zhang, A.-Q. Wang, and Q. Wei, “Chitosan-alginate nanoparticles as a novel drug delivery system for nifedipine,” *International Journal of Biomedical Science*, vol. 4, no. 3, pp. 221-228, 2008.
- [133] M. B. Hammami, “Partial Thromboplastin Time, Activated,” 2015. [Online]. Available: <https://emedicine.medscape.com/article/2085837-overview>. [Accessed: 23-Oct-2017].
- [134] K. Se-kwon, T.-S. Vo, and D.-H. Ngo, *Marine Nutraceuticals: Prospects and Perspectives*. New York: CRC Taylor & Francis Group, LLC, 2013.
- [135] P. A. S. Mourao, “Use of sulfated Fucans as anticoagulant and antithrombotic agents: Future perspectives,” *Current Pharmaceutical Design*, vol. 10, no. 9, pp. 967–981, 2004.
- [136] J. Teruya, “Thrombin Time,” 2014. [Online]. Available: <https://emedicine.medscape.com/article/2086278-overview>.
- [137] K. Dobashi, T. Nishino, M. Fujihara, and T. Nagumo, “Isolation and preliminary characterization of fucose-containing sulfated polysaccharides with blood-anticoagulant activity from the brown seaweed *Hizikia fusiforme*,” *Carbohydrate Research*, vol. 194, no. C, pp. 315–320, 1989.
- [138] T. Nishino and T. Nagumo, “Anticoagulant and antithrombin activities of oversulfated fucans,”

- Carbohydrate Research*, vol. 229, no. 2, pp. 355–362, 1992.
- [139] T. Nishino, H. Ura, and T. Nagumo, “The relationship between the sulfate content and the antithrombin activity of an $\alpha(1\rightarrow2)$ -fucoidan purified from a commercial fucoidan Fraction,” *Botanica Marina*, vol. 38, pp. 187–194, 2009.
- [140] T. Nishino, G. Yokoyama, K. Dobashi, M. Fujihara, and T. Nagumo, “Isolation, purification, and characterization of fucose-containing sulphated polysaccharides from the brown seaweed *Ecklonia kurome* and their blood-anticoagulant activities,” *Carbohydrate Research*, vol. 186, pp. 119–129, 1989.
- [141] WHO, “Herpes simplex virus,” 2017. [Online]. Available: <http://www.who.int/mediacentre/factsheets/fs400/en/>. [Accessed: 24-Oct-2017].
- [142] W. Saburi, H. M. Ueno, H. Matsui, and H. Mori, “Acidophilic β -galactosidase from *Aspergillus niger* AHU7120 with lactose hydrolytic activity under simulated gastric conditions,” *Journal of Applied Glycoscience*, vol. 61, pp. 53–57, 2014.
- [143] E. A. Titlyanov and T. V. Titlyanova, “Seaweed cultivation: Methods and problems,” *Russian Journal of Marine Biology*, vol. 36, no. 4, pp. 227–242, 2010.
- [144] K. Se-kwon and J. Venkatesan, *Handbook of Marine Biotechnology*. Springer-Verlag Berlin Heidelberg, 2015.
- [145] C. R. K. Reddy, B. Jha, Y. Fujita, and M. Ohno, “Seaweed micropropagation techniques and their potentials: An overview,” *Journal of Applied Phycology*, vol. 20, no. 5, pp. 609–617, 2008.
- [146] T. Masakazu, “A simple method of seaweed axenic culture,” *The Korean Journal of Phycology*, vol. 4, no. 2, pp. 183–189, 1989.
- [147] N. Kaliaperfomal, “Sea weed biotechnology,” *Proc. Firts Nayl Semi Mar Biotech*, pp. 91–98, 1998.
- [148] S. A. Pomponi, “The potential for the marine biotechnology industry,” *Industry-Driven Changes and Policy Responses*, pp. 101–104, 1996.
- [149] P. Singh, S. K. Gupta, A. Guldhe, I. Rawat, and F. Bux, “Microalgae isolation and basic culturing techniques,” in *Handbook of Marine Microalgae: Biotechnology Advances*, K. Se-kwon, Ed. Elsevier Inc., 2015, pp. 43–54.
- [150] C. Munn, “Microbes in the marine environment,” *Marine Microbiology Ecology and Applications*, pp. 1–24, 2011.
- [151] J. Kubanek, P. R. Jensen, P. A. Keifer, M. C. Sullards, D. O. Collins, and W. Fenical, “Seaweed resistance to microbial attack: A targeted chemical defense against marine fungi,” *Pnas*, vol. 100, no. 12, pp. 6916–6921, 2003.
- [152] T. Wichard and C. Katsaros, “Phycomorph: Macroalgal development and morphogenesis,” *Botanica Marina*, vol. 60, no. 2, pp. 85–87, 2017.
- [153] I. Joint, “Cell-to-cell communication across the prokaryote-eukaryote boundary,” *Science*, vol. 298, no. 5596, p. 1207, 2002.
- [154] L. Xuewu and B. Kloareg, “Explant axenisation for tissue culture in marine macroalgae,” *Chinese Journal of Ocean and Liminology*, vol. 10, no. 3, pp. 268–277, 1992.
- [155] R. A. Andersen, Ed., *Algal Culturing Techniques*. MA: Elsevier Academic Press, 2005.
- [156] P. Baweja, D. Sahoo, P. García-Jiménez, and R. R. Robaina, “Review: Seaweed tissue culture as applied to biotechnology: Problems, achievements and prospects,” *Phycological Research*, vol. 57, no. 1, pp. 45–58, 2009.
- [157] M. Ochoa-Villarreal, *et al.*, “Plant cell culture strategies for the production of natural products,” *BMB Reports*, vol. 49, no. 3, pp. 149–158, 2016.
- [158] T.-J. Fu, G. Singh, and W. R. Curtis, *Plant Cell and Tissue Culture for the Production of Food*

- Ingredients*, 1st ed. New York, 1999.
- [159] Y. Huang and G. L. Rorrer, "Cultivation of microplantlets derived from the marine red alga *Agardhiella subulata* in a stirred tank photobioreactor," *Biotechnology Progress*, vol. 19, pp. 418-427, 2003.
- [160] J. G. Modrell, "Bioreactor development and cell culture of the marine macroalgae *Porphyra* (sp.) and *Laminaria saccharina*," 1994.
[http://ir.library.oregonstate.edu/concern/graduate_thesis_or_dissertations/44558h09k]
- [161] N. Saga, "Isolation of protoplasts from edible seaweeds," *The Botanical Magazine, Tokyo*, vol. 97, pp. 423-427, 1984.
- [162] N. Saga and Y. Sakai, "Isolation of protoplasts from *Laminaria paper* and *Porphyra*," *Bulletin of the Japanese Society of Scientific Fisheries*, vol. 50, no. 6, p. 1085, 1984.
- [163] C. R. K. Reddy and Y. Fujita, "Regeneration of plantlets from *Enteromorpha* (Ulvales, Chlorophyta) protoplasts in axenic culture," *Journal of Applied Phycology*, vol. 3, no. 3, pp. 265-275, 1991.
- [164] B. Moss, "Apical dominance in *Fucus vesiculosus*," *New Phytologist*, vol. 64, no. 3, pp. 387-392, 1964.
- [165] N. Saga, T. Motomura, and Y. Sakai, "Induction of callus from the marine brown alga *Dictyosiphon foeniculaceus*," *Plant & Cell Physiology*, vol. 23, no. 4, pp. 727-730, 1982.
- [166] G. R. Kumar, C. R. K. Reddy, and B. Jha, "Callus induction and thallus regeneration from callus of phycocolloid yielding seaweeds from the Indian coast," *Journal of Applied Phycology*, vol. 19, no. 1, pp. 15-25, 2007.
- [167] P. A. Mooney and J. van Staden, "*In vitro* plantlet formation and multiple shoot induction in *Sargassum heterophyllum*," *South African Journal of Botany*, vol. 51, no. 1, pp. 41-44, 1985.
- [168] T. Uji, D. Nanaumi, C. Kawagoe, N. Saga, and K. Miyashita, "Factors influencing the induction of adventitious bud and callus in the brown alga *Sargassum horneri* (Turner) C. Agardh," *Journal of Applied Phycology*, vol. 28, no. 4, pp. 2435-2443, 2016.
- [169] N. Saga and Y. Sakai, "Axenic tissue culture and callus formation of the marine brown alga *Laminaria angustata*," *Bulletin of the Japanese Society of Scientific Fisheries*, vol. 49, no. 10, pp. 1561-1563, 1983.
- [170] M. Polne-Fuller and A. Gibor, "Calluses and callus-like growth in seaweeds: Induction and culture," *Hydrobiologia*, vol. 151-152, no. 1, pp. 131-138, 1987.
- [171] W. Huang and Y. Fujita, "Callus induction and thallus regeneration in some species of red algae," *Phycological Research*, vol. 45, pp. 105-111, 1997.
- [172] H. Amano and H. Noda, "Effects of plant growth regulators, constituents in the tissue culture organic acids, and sugars of sea lettuce *Ulva pertusa*," *Fisheries Science*, vol. 60, no. 4, pp. 449-454, 1994.
- [173] G. Rajakrishna Kumar, *et al.*, "Tissue culture and regeneration of thallus from callus of *Gelidiella acerosa* (Gelidiales, Rhodophyta)," *Phycologia*, vol. 43, no. 5, pp. 596-602, 2004.
- [174] Qiagen, "AllPrep DNA/ RNA Mini Handbook For simultaneous purification of genomic DNA and total RNA from the same animal," no. November, pp. 1-56, 2005.
- [175] A. Koid, W. C. Nelson, A. Mraz, and K. B. Heidelberg, "Comparative analysis of eukaryotic marine microbial assemblages from 18s rRNA gene and gene transcript clone libraries by using different methods of extraction," *Applied and Environmental Microbiology*, vol. 78, no. 11, pp. 3958-3965, 2012.
- [176] B. H. Nam, H. J. Jin, S. K. Kim, and Y. K. Hong, "Quantitative viability of seaweed tissues assessed with 2,3,5-triphenyltetrazolium chloride," *Journal of Applied Phycology*, vol. 10, no. 1, pp. 31-36, 1998.

- [177] I. Mussio and A. M. Rusig, "Isolation of protoplasts from *Fucus serratus* and *F. vesiculosus* (Fucales, Phaeophyceae): Factors affecting protoplast yield," *Journal of Applied Phycology*, vol. 18, no. 6, pp. 733–740, 2006.
- [178] I. Mussio and A. M. Rusig, "Morphogenetic responses from protoplasts and tissue culture of *Laminaria digitata* (Linnaeus) J. V. Lamouroux (Laminariales, Phaeophyta): Callus and thalloid-like structures regeneration," *Journal of Applied Phycology*, vol. 21, no. 2, pp. 255–264, 2009.
- [179] P. J. Harrison and J. A. Berges, "Marine culture media," in *Algal Culturing Techniques*, 2005, pp. 21–33.
- [180] N. Sahidin, "Establishment of axenic culture of *Kappaphycus alvarezii* and optimum culture system for germings production," *Malaysian Fisheries Journal*, vol. 13, pp. 33–38, 2014.
- [181] S. M. Shishlyannikov, Y. R. Zakharova, N. A. Volokitina, I. S. Mikhailov, D. P. Petrova, and Y. V. Likhoshway, "A procedure for establishing an axenic culture of the diatom *Synedra acus* subsp. *radians* (Kütz.) Skabibitsch. from Lake Baikal," *Limnology and Oceanography: Methods*, vol. 9, pp. 478–484, 2011.
- [182] C. G. Bruckner and P. G. Kroth, "Protocols for the removal of bacteria from freshwater benthic diatom cultures," *Journal of Phycology*, vol. 45, no. 4, pp. 981–986, 2009.
- [183] C. A. Leander, D. Porter, and B. S. Leander, "Comparative morphology and molecular phylogeny of aplanochytrids (Labyrinthulomycota)," *European Journal of Protistology*, vol. 40, no. 4, pp. 317–328, 2004.
- [184] G. A. Jones and B. A. Humphrey, "Evaluation of a dehydrogenase assay based on tetrazolium reduction for rapid *in vitro* estimation of fermentation activity in rumen content," *Canadian Journal of Animal Science*, vol. 58, pp. 501–511, 1978.
- [185] W. Chang and M. Chen, "2,3,5-Triphenyltetrazolium reduction in the viability assay of *Ulva fasciata* (Chlorophyta) in response to salinity stress," *Botanical Bulletin of Academia Sinica*, vol. 40, pp. 207–212, 1999.
- [186] F. P. Altman, "On the oxygen-sensitivity of various tetrazolium salts," *Histochemie*, vol. 22, no. 3, pp. 256–261, 1970.
- [187] M. I. Georgiev, A. I. Pavlov, and T. Bley, "Hairy root type plant *in vitro* systems as sources of bioactive substances," *Applied Microbiology and Biotechnology*, vol. 74, no. 6, pp. 1175–1185, 2007.
- [188] O. Nilsson and O. Olsson, "Getting to the root: The role of the *Agrobacterium rhizogenes* rol genes in the formation of hairy roots," *Physiologia Plantarum*, vol. 100, no. 3, pp. 463–473, 1997.
- [189] M. F. Ortiz-Matamoros, T. Islas-Flores, B. Voigt, D. Menzel, F. Baluška, and M. A. Villanueva, "Heterologous DNA uptake in cultured *Symbiodinium* spp. aided by *Agrobacterium tumefaciens*," *PLoS ONE*, vol. 10, no. 7, pp. 1–16, 2015.
- [190] J. H. Haas, L. W. Moore, W. Ream, and S. Manulis, "Universal PCR primers for detection of phytopathogenic *Agrobacterium* strains," *Applied and Environmental Microbiology*, vol. 61, no. 8, pp. 2879–2884, 1995.
- [191] A. Kasai, S. Arafuka, N. Koshiba, D. Takahashi, and K. Toshima, "Systematic synthesis of low-molecular weight fucoidan derivatives and their effect on cancer cells," *Organic & Biomolecular Chemistry*, vol. 13, no. 42, pp. 10556–10568, 2015.
- [192] G. Michel, T. Tonon, D. Scornet, J. M. Cock, and B. Kloareg, "The cell wall polysaccharide metabolism of the brown alga *Ectocarpus siliculosus*. Insights into the evolution of extracellular matrix polysaccharides in Eukaryotes," *New Phytologist*, vol. 188, pp. 82–97, 2010.
- [193] Y. Ren *et al.*, "Biochemical characterization of GDP-L-fucose de novo synthesis pathway in fungus *Mortierella alpina*," *Biochemical and Biophysical Research Communications*, vol. 391, pp. 1663–

- 1669, 2010.
- [194] P. Mattila, J. Rabinä, S. Hortling, J. Helin, and R. Renkonen, "Functional expression of *Escherichia coli* enzymes synthesizing GDP-L-fucose from inherent GDP-D-mannose in *Saccharomyces cerevisiae*," *Glycobiology*, vol. 10, no. 10, pp. 1041-1047, 2000.
- [195] S. G. Byun, M. D. Kim, W. H. Lee, K. J. Lee, N. S. Han, and J. H. Seo, "Production of GDP-L-fucose, L-fucose donor for fucosyloligosaccharide synthesis, in recombinant *Escherichia coli*," *Applied Microbiology and Biotechnology*, vol. 74, no. 4, pp. 768-775, 2007.
- [196] M. H. Jang, W. H. Lee, S. Y. Shin, N. S. Han, J. H. Seo, and M. D. Kim, "Molecular cloning of the genes for GDP-mannose 4,6-dehydratase and GDP-L-fucose synthetase from *Bacteroides thetaiotaomicron*," *Food Science and Biotechnology*, vol. 19, no. 3, pp. 849-855, 2010.
- [197] L. Sturla, A. Bisso, D. Zanardi, U. Benatti, A. De Flora, and M. Tonetti, "Expression, purification and characterization of GDP-D-mannose 4,6-dehydratase from *Escherichia coli*," *FEBS Letters*, vol. 412, no. 1, pp. 126-130, 1997.
- [198] F. X. Sullivan *et al.*, "Molecular cloning of human reconstitution of GDP-fucose biosynthesis *in vitro* molecular cloning of human GDP-mannose 4,6-dehydratase and reconstitution of GDP-fucose biosynthesis *in vitro*," *The Journal of biological chemistry*, vol. 273, no. 14, pp. 8193-8202, 1998.
- [199] S. A. Sousa, J. R. Feliciano, P. F. Pinheiro, and J. H. Leitão, "Biochemical and functional studies on the *Burkholderia cepacia* complex *bceN* gene, encoding a GDP-D-mannose 4,6-dehydratase," *PLoS ONE*, vol. 8, no. 2, e56902, 2013.
- [200] M. Tonetti, L. Sturla, A. Bisso, U. Benatti, and A. De Flora, "Synthesis of GDP-L-fucose by the human FX protein," *The Journal of Biological Chemistry*, vol. 271, no. 44, pp. 27274-27279, 1996.
- [201] B. Wu, Y. Zhang, and P. G. Wang, "Identification and characterization of GDP-d-mannose 4,6-dehydratase and GDP-l-fucose synthetase in a GDP-l-fucose biosynthetic gene cluster from *Helicobacter pylori*," *Biochemical and Biophysical Research Communications*, vol. 285, no. 2, pp. 364-71, 2001.
- [202] C. P. Bonin, I. Potter, G. F. Vanzin, and W.-D. Reiter, "The *MURI* gene of *Arabidopsis thaliana* encodes an isoform of GDP-D-mannose-4,6-dehydratase, catalyzing the first step in the *de novo* synthesis of GDP-L-fucose," *Plant Biology*, vol. 94, no. March, pp. 2085-2090, 1997.
- [203] C. P. Bonin and W. D. Reiter, "A bifunctional epimerase-reductase acts downstream of the *MURI* gene product and completes the *de novo* synthesis of GDP-L-fucose in *Arabidopsis*," *Plant Journal*, vol. 21, no. 5, pp. 445-454, 2000.
- [204] M. Tonetti, *et al.*, "*Paramecium bursaria* *Chlorella* virus 1 encodes two enzymes involved in the biosynthesis of GDP-L-fucose and GDP-D-rhamnose," *Journal of Biological Chemistry*, vol. 278, no. 24, pp. 21559-21565, 2003.
- [205] T. W. Liu, H. Ito, Y. Chiba, T. Kubota, T. Sato, and H. Narimatsu, "Functional expression of L-fucokinase/guanosine 5'-diphosphate-L-fucose pyrophosphorylase from *Bacteroides fragilis* in *Saccharomyces cerevisiae* for the production of nucleotide sugars from exogenous monosaccharides," *Glycobiology*, vol. 21, no. 9, pp. 1228-1236, 2011.
- [206] L. Engels and L. Elling, "WbgL: a novel bacterial α 1,2-fucosyltransferase for the synthesis of 2'-fucosyllactose," *Glycobiology*, vol. 24, no. 2, pp. 170-178, 2014.
- [207] H. Ohashi, C. Wahl, T. Ohashi, L. Elling, and K. Fujiyama, "Effective synthesis of guanosine 5'-diphospho- β -l-galactose using bacterial l-Fucokinase/Guanosine 5'-diphosphate-l-fucose pyrophosphorylase," *Advanced Synthesis & Catalysis*, vol. 359, pp. 4227-4234, 2017.
- [208] T. Kotake, S. Hojo, N. Tajima, K. Matsuoka, T. Koyama, and Y. Tsumuraya, "A bifunctional enzyme with L-fucokinase and GDP-L-fucose pyrophosphorylase activities salvages free L-fucose in

- Arabidopsis,” *Journal of Biological Chemistry*, vol. 283, no. 13, pp. 8125-8135, 2008.
- [209] H. Wang, *et al.*, “Characterization of a fungal *l*-fucokinase involved in *Mortierella alpina* GDP-L-fucose salvage pathway,” *Glycobiology*, vol. 26, no. 8, pp. 880-887, 2016.
- [210] H. Wang, *et al.*, “Production of GDP-L-fucose from exogenous fucose through the salvage pathway in *Mortierella alpina*,” *RSC Advances*, vol. 6, no. 52, pp. 46308–46316, 2016.
- [211] Z. Ge, N. W. Chan, M. M. Palcic, and D. E. Taylor, “Cloning and heterologous expression of an alpha1,3-fucosyltransferase gene from the gastric pathogen *Helicobacter pylori*,” *The Journal of Biological Chemistry*, vol. 272, no. 34, pp. 21357–21363, 1997.
- [212] C. Dumon, B. Priem, S. L. Martin, A. Heyraud, C. Bosso, and E. Samain, “*In vivo* fucosylation of lacto-*N*-neotetraose and lacto-*N*-neohexaose by heterologous expression of *Helicobacter pylori* α -1,3 fucosyltransferase in engineered *Escherichia coli*,” *Glycoconjugate Journal*, vol. 18, no. 6, pp. 465-474, 2001.
- [213] P. F. Gallet, *et al.*, “Heterologous expression of an engineered truncated form of human Lewis fucosyltransferase (Fuc-TIII) by the methylotrophic yeast *Pichia pastoris*,” *Glycobiology*, vol. 8, no. 9, pp. 919-925, 1998.
- [214] J. S. Bondili, *et al.*, “Molecular cloning and heterologous expression of β 1,2-xylosyltransferase and core α 1,3-fucosyltransferase from maize,” *Phytochemistry*, vol. 67, no. 20, pp. 2215-2224, 2006.
- [215] M. Malissard, S. Zeng, and E. G. Berger, “Expression of functional soluble forms of human beta-1,4-galactosyltransferase I, alpha-2,6-sialyltransferase, and alpha-1, 3-fucosyltransferase VI in the methylotrophic yeast *Pichia pastoris*,” *Biochemical and Biophysical Research Communications*, vol. 267, no. 1, pp. 169-173, 2000.
- [216] A. Bastida, A. Fernández-Mayoralas, R. Gómez Arrayás, F. Iradier, J. C. Carretero, and E. García-Junceda, “Heterologous over-expression of α -1,6-fucosyltransferase from *Rhizobium* sp.: Application to the synthesis of the trisaccharide β -D-GlcNAc(1 \rightarrow 4)- [α -L-Fuc-(1 \rightarrow 6)]-D-GlcNAc, study of the acceptor specificity and evaluation of polyhydroxylated indolizidines as inhibitors,” *Chemistry – A European Journal*, vol. 7, no. 11, pp. 2390-2397, 2001.
- [217] J. Shao, M. Li, Q. Jia, Y. Lu, and P. G. Wang, “Sequence of *Escherichia coli* O128 antigen biosynthesis cluster and functional identification of an α -1,2-fucosyltransferase,” *FEBS Letters*, vol. 553, no. 1-2, pp. 99-103, 2003.
- [218] W. Yi, *et al.*, “*Escherichia coli* O86 O-antigen biosynthetic gene cluster and stepwise enzymatic synthesis of human blood group B antigen tetrasaccharide,” *Journal of the American Chemical Society*, vol. 127, no. 7, pp. 2040-2041, 2005.
- [219] N. Pettit, T. Styslinger, Z. Mei, W. Han, G. Zhao, and P. G. Wang, “Characterization of WbiQ: An α 1,2-fucosyltransferase from *Escherichia coli* O127:K63(B8), and synthesis of H-type 3 blood group antigen,” *Biochemical and Biophysical Research Communications*, vol. 402, no. 2, pp. 190-195, 2010.
- [220] C. Albermann, W. Piepersberg, and U. F. Wehmeier, “Synthesis of the milk oligosaccharide 2'-fucosyllactose using recombinant bacterial enzymes,” *Carbohydrate Research*, vol. 334, no. 2, pp. 97-103, 2001.
- [221] G. Wang, P. G. Boulton, N. W. C. Chan, M. M. Palcic, and D. E. Taylor, “Novel *Helicobacter pylori* α 1,2- fucosyltransferase, a key enzyme in the synthesis of Lewis antigens,” *Microbiology*, vol. 145, no. 11, pp. 3245–3253, 1999.
- [222] D. B. Stein, Y. N. Lin, and C. H. Lina, “Characterization of *Helicobacter pylori* α 1,2-fucosyltransferase for enzymatic synthesis of tumor-associated antigens,” *Advanced Synthesis and Catalysis*, vol. 350, no. 14-15, pp. 2313-2321, 2008.
- [223] Y. W. Chin, J. Y. Kim, J. H. Kim, S. M. Jung, and J. H. Seo, “Improved production of 2'-fucosyllactose

- in engineered *Escherichia coli* by expressing putative α -1,2-fucosyltransferase, WcfB from *Bacteroides fragilis*,” *Journal of Biotechnology*, vol. 257, pp. 192-198, 2017.
- [224] L. M. Bidwell, E. M. J. Gillam, A. Gaedigk, X. Zhu, D. Grant, and M. E. McManus, “Bacterial expression of two human aryl sulfotransferases,” *Chemico-Biological Interactions*, vol. 109, no. 1-3, pp. 137-141, 1998.
- [225] M. C. Baek, K. H. Choi, T. G. Oh, D. H. Kim, and E. C. Choi, “Overexpression of arylsulfate sulfotransferase as fusion protein with glutathione S-transferase,” *Protein Expression and Purification*, vol. 11, no. 3, pp. 257-262, 1997.
- [226] I. Ayuso-Fernández, M. A. Galmés, A. Bastida, and E. García-Junceda, “Aryl sulfotransferase from *Haliangium ochraceum*: A versatile tool for the sulfation of small molecules,” *ChemCatChem*, vol. 6, no. 4, pp. 1059–1065, 2014.
- [227] J. R. Myette, Z. Shriver, J. Liu, G. Venkataraman, R. Rosenberg, and R. Sasisekharan, “Expression in *Escherichia coli*, purification and kinetic characterization of human heparan sulfate 3-*O*-sulfotransferase-1,” *Biochemical and biophysical research communications*, vol. 290, no. 4, pp. 1206-13, 2002.
- [228] X. Zhou, K. Chandarajoti, T. Q. Pham, R. Liu, and J. Liu, “Expression of heparan sulfate sulfotransferases in *Kluyveromyces lactis* and preparation of 3'-phosphoadenosine-5'-phosphosulfate,” *Glycobiology*, vol. 21, no. 6, pp. 771–780, 2011.
- [229] A. T. Do, E. Smeds, D. Spillmann, and M. Kusche-Gullberg, “Overexpression of heparan sulfate 6-*O*-sulfotransferases in human embryonic kidney 293 cells results in increased *N*-acetylglucosaminyl 6-*O*-sulfation,” *Journal of Biological Chemistry*, vol. 281, no. 9, pp. 5348-5356, 2006.
- [230] K. Kamimura, *et al.*, “Drosophila heparan sulfate 6-*O*-sulfotransferase (dHS6ST) gene. Structure, expression, and function in the formation of the tracheal system,” *Journal of Biological Chemistry*, vol. 276, no. 20, pp. 17014-17021, 2001.
- [231] A. S. Saribaş, *et al.*, “Production of *N*-sulfated polysaccharides using yeast-expressed *N*-deacetylase/*N*-sulfotransferase-1 (NDST-1),” *Glycobiology*, vol. 14, no. 12, pp. 1217–1228, 2004.
- [232] D. S. Pikas, I. Eriksson, and L. Kjellén, “Overexpression of different isoforms of glucosaminyl *N*-deacetylase/*N*-sulfotransferase results in distinct heparan sulfate *N*-sulfation patterns,” *Biochemistry*, vol. 39, no. 15, pp. 4552-4558, 2000.
- [233] J. Presto, *et al.*, “Heparan sulfate biosynthesis enzymes EXT1 and EXT2 affect NDST1 expression and heparan sulfate sulfation,” *Proceedings of the National Academy of Sciences*, vol. 105, no. 12, pp. 4751-4756, 2008.
- [234] A. Deligny, *et al.*, “NDST2 (*N*-deacetylase/*N*-sulfotransferase-2) enzyme regulates heparan sulfate chain length,” *Journal of Biological Chemistry*, vol. 291, no. 36, pp. 18600-18607, 2016.
- [235] Y. Sakakibara, *et al.*, “Molecular cloning, expression, and characterization of novel human SULT1C sulfotransferases that catalyze the sulfonation of *N*-hydroxy-2-acetylaminofluorene,” *The Journal of Biological Chemistry*, vol. 273, no. 51, pp. 33929-35, 1998.
- [236] N. Hehonah, *et al.*, “Molecular cloning, expression, localisation and functional characterisation of a rabbit SULT1C2 sulfotransferase,” *International Journal of Biochemistry and Cell Biology*, vol. 31, no. 8, pp. 869–882, 1999.
- [237] T. Shimohira, K. Kurogi, T. Hashiguchi, M. C. Liu, M. Suiko, and Y. Sakakibara, “Regioselective production of sulfated polyphenols using human cytosolic sulfotransferase-expressing *Escherichia coli* cells,” *Journal of Bioscience and Bioengineering*, vol. 124, no. 1, pp. 84-90, 2017.
- [238] X. Chen, Y.-S. Yang, Y. Zheng, B. M. Martin, M. W. Duffel, and W. B. Jakoby, “Tyrosine-Ester Sulfotransferase from Rat Liver: Bacterial Expression and Identification,” *Protein Expression and*

- Purification*, vol. 3, pp. 421-426, 1992.
- [239] Y. Sakakibara, *et al.*, “Purification, characterization, and molecular cloning of a novel rat liver Dopa/tyrosine sulfotransferase,” vol. 270, no. 51, pp. 30470,30478, 1995.
- [240] R. Dajani, *et al.*, “Kinetic properties of human dopamine sulfotransferase (SULT1A3) expressed in prokaryotic and eukaryotic systems: Comparison with the recombinant enzyme purified from *Escherichia coli*,” *Protein Expression and Purification*, vol. 16, no. 1, pp. 11-18, 1999.
- [241] B. I. Cantarel, P. M. Coutinho, C. Rancurel, T. Bernard, V. Lombard, and B. Henrissat, “The Carbohydrate-Active EnZymes database (CAZy): An expert resource for glycogenomics,” *Nucleic Acids Research*, vol. 37, no. SUPPL. 1, pp. 233-238, 2009.
- [242] L. L. Lairson, B. Henrissat, G. J. Davies, and S. G. Withers, “Glycosyltransferases: Structures, Functions, and mechanisms,” *Annual Review of Biochemistry*, vol. 77, no. 1, pp. 521-555, 2008.
- [243] B. Ma, J. L. Simala-Grant, and D. E. Taylor, “Fucosylation in prokaryotes and eukaryotes,” *Glycobiology*, vol. 16, no. 12, pp. 158R-184R, 2006.
- [244] L. Muinelo-Romay, S. Villar-Portela, E. Cuevas, E. Gil-Martin, and A. Fernandez-Briera, “Identification of alpha(1,6)fucosylated proteins differentially expressed in human colorectal cancer,” *BMC Cancer*, vol. 11, no. 1, p. 508, 2011.
- [245] G. Fabini, A. Freilinger, F. Altmann, and I. B. H. Wilson, “Identification of core α 1,3-fucosylated glycans and cloning of the requisite fucosyltransferase cDNA from *Drosophila melanogaster*: Potential basis of the neural anti-horseradish peroxidase epitope,” *Journal of Biological Chemistry*, vol. 276, no. 30, pp. 28058-28067, 2001.
- [246] H. Kajiwara, M. Toda, T. Mine, H. Nakada, and T. Yamamoto, “Isolation of fucosyltransferase-producing bacteria from marine environments,” *Microbes and Environments*, vol. 27, no. 4, pp. 515-518, 2012.
- [247] P. A. Prieto, *et al.*, “Expression of human H-type α 1,2-fucosyltransferase encoding for blood group H (O) antigen in chinese hamster ovary cells,” vol. 272, no. 4, pp. 2089-2097, 1997.
- [248] C. Joly, R. Leonard, A. Maftah, and C. Riou-Khamlichi, “alpha4-Fucosyltransferase is regulated during flower development: increases in activity are targeted to pollen maturation and pollen tube elongation,” *Journal of Experimental Botany*, vol. 53, no. 373, pp. 1429-1436, 2002.
- [249] X. Yang, S. Liu, and Q. Yan, “Role of fucosyltransferase IV in epithelial-mesenchymal transition in breast cancer cells,” *Cell Death and Disease*, vol. 4, no. 7, pp. e735-9, 2013.
- [250] E. Miyoshi, *et al.*, “Fucosylation is a promising target for cancer diagnosis and therapy,” *Biomolecules*, vol. 2, no. 4, pp. 34-45, 2012.
- [251] A. P. Moran, “Relevance of fucosylation and Lewis antigen expression in the bacterial gastroduodenal pathogen *Helicobacter pylori*,” *Carbohydrate Research*, vol. 343, no. 12, pp. 1952-1965, 2008.
- [252] G. Michel, “Online Resource for Community Annotation of Eukaryotes.” [Online]. Available: http://bioinformatics.psb.ugent.be/orcae/annotation/Ectsi/current/Esi0050_0098. [Accessed: 20-Nov-2015].
- [253] G. Michel, “Online Resource for Community Annotation of Eukaryotes.” [Online]. Available: http://bioinformatics.psb.ugent.be/orcae/annotation/Ectsi/current/Esi0021_0026. [Accessed: 20-Nov-2015].
- [254] New England Biolabs, “NEBuilder HiFi DNA Assembly Master Mix,” *Instruction Manual*, vol. 1, no. 10, pp. 1-23, 2014.
- [255] New England Biolabs, “Gibson Assembly™ Cloning Kit,” *Instruction Manual*, vol. 3.2, 2017.
- [256] IBABioTAGnology, “pASK-IBA 45(+) Data Sheet,” vol. 402, pp. 1-8, 2005.
- [257] IBA, “Expression and purification of proteins using 6x Histidine -tag A comprehensive manual,” *IBA*

- Solutions for Life Sciences*, no. October, pp. 1-36, 2012.
- [258] IBABioTAGnology, “Strep-tag[®] detection in Western blots,” *Instruction Manual*, vol. PR07-0012, p. 7, 2016.
- [259] Z. L. Wu, C. M. Ethen, B. Prather, M. MacHacek, and W. Jiang, “Universal phosphatase-coupled glycosyltransferase assay,” *Glycobiology*, vol. 21, no. 6, pp. 727-733, 2011.
- [260] C. Wahl, D. Hirtz, and L. Elling, “Multiplexed capillary electrophoresis as analytical tool for fast optimization of multi-enzyme cascade reactions—synthesis of nucleotide sugars: Dedicated to Prof. Dr. Vladimir Křen on the occasion of his 60th birthday,” *Biotechnology Journal*, vol. 11, no. 10, pp. 1298-1308, 2016.
- [261] NCBI, “NCBI blast protein sequence.” [Online]. Available: <https://blast.ncbi.nlm.nih.gov/Blast.cgi#563472779>. [Accessed: 02-Feb-2018].
- [262] NCBI, “NCBI blast protein sequence.” [Online]. Available: <https://blast.ncbi.nlm.nih.gov/Blast.cgi>. [Accessed: 02-Feb-2018].
- [263] C. Dumon, E. Samain, and B. Priem, “Assessment of the two *Helicobacter pylori* α -1,3-fucosyltransferase ortholog genes for the large-scale synthesis of lewisx human milk oligosaccharides by metabolically engineered *Escherichia coli*,” *Biotechnology Progress*, vol. 20, no. 2, pp. 412-419, 2004.
- [264] T. De Vries, R. M. A. Knegtel, E. H. Holmes, and B. A. Macher, “Fucosyltransferases: structure/function studies,” *Glycobiology*, vol. 11, no. 10, pp. 119-128, 2001.
- [265] I. Martinez-Duncker, R. Mollicone, J. J. Candelier, C. Breton, and R. Oriol, “A new superfamily of protein-*O*-fucosyltransferases, α 2-fucosyltransferases, and α 6-fucosyltransferases: Phylogeny and identification of conserved peptide motifs,” *Glycobiology*, vol. 13, no. 12, pp. 1–5, 2003.
- [266] New England Biolabs, “Gibson Assembly[®].” [Online]. Available: <https://www.neb.com/applications/cloning-and-synthetic-biology/dna-assembly-and-cloning/gibson-assembly>.
- [267] M. M. Bradford, “A rapid and sensitive method for the quantitation of microgram quantities of protein utilizing the principle of protein-dye binding,” *Analytical Biochemistry*, vol. 72, no. 1–2, pp. 248–254, 1976.
- [268] E. Chapman, M. D. Best, S. R. Hanson, and C. H. Wong, “Sulfotransferases: Structure, mechanism, biological activity, inhibition, and synthetic utility,” *Angewandte Chemie - International Edition*, vol. 43, no. 27, pp. 3526-3548, 2004.
- [269] G. Michel, “Online resource for community annotation of eukaryotes.” [Online]. Available: http://bioinformatics.psb.ugent.be/orcae/annotation/Ectsi/current/Esi0032_0064. [Accessed: 16-Oct-2015].
- [270] G. Michel, “Online resource for community annotation of eukaryotes.” [Online]. Available: http://bioinformatics.psb.ugent.be/orcae/annotation/Ectsi/current/Esi0283_0018. [Accessed: 16-Oct-2015].
- [271] B. Prather, C. M. Ethen, M. MacHacek, and Z. L. Wu, “Golgi-resident PAP-specific 3’-phosphatase-coupled sulfotransferase assays,” *Analytical Biochemistry*, vol. 423, no. 1, pp. 86–92, 2012.
- [272] Z. L. Wu, “Phosphatase-coupled universal kinase assay and kinetics for first-order-rate coupling reaction,” *PLoS ONE*, vol. 6, no. 8, p. e23172, 2011.
- [273] T. Fischöder, D. Laaf, C. Dey, and L. Elling, “Enzymatic synthesis of *N*-acetyllactosamine (LacNAc) type 1 oligomers and characterization as multivalent galectin ligands,” *Molecules*, vol. 22, no. 8, pp. 1-15, 2017.
- [274] M. Kovacheva, “Kultivierung von Makroalgen,” TU Kaiserslautern, 2012.

Appendix

Appendix A

Chemical structures of some marine-derived bioactive compounds

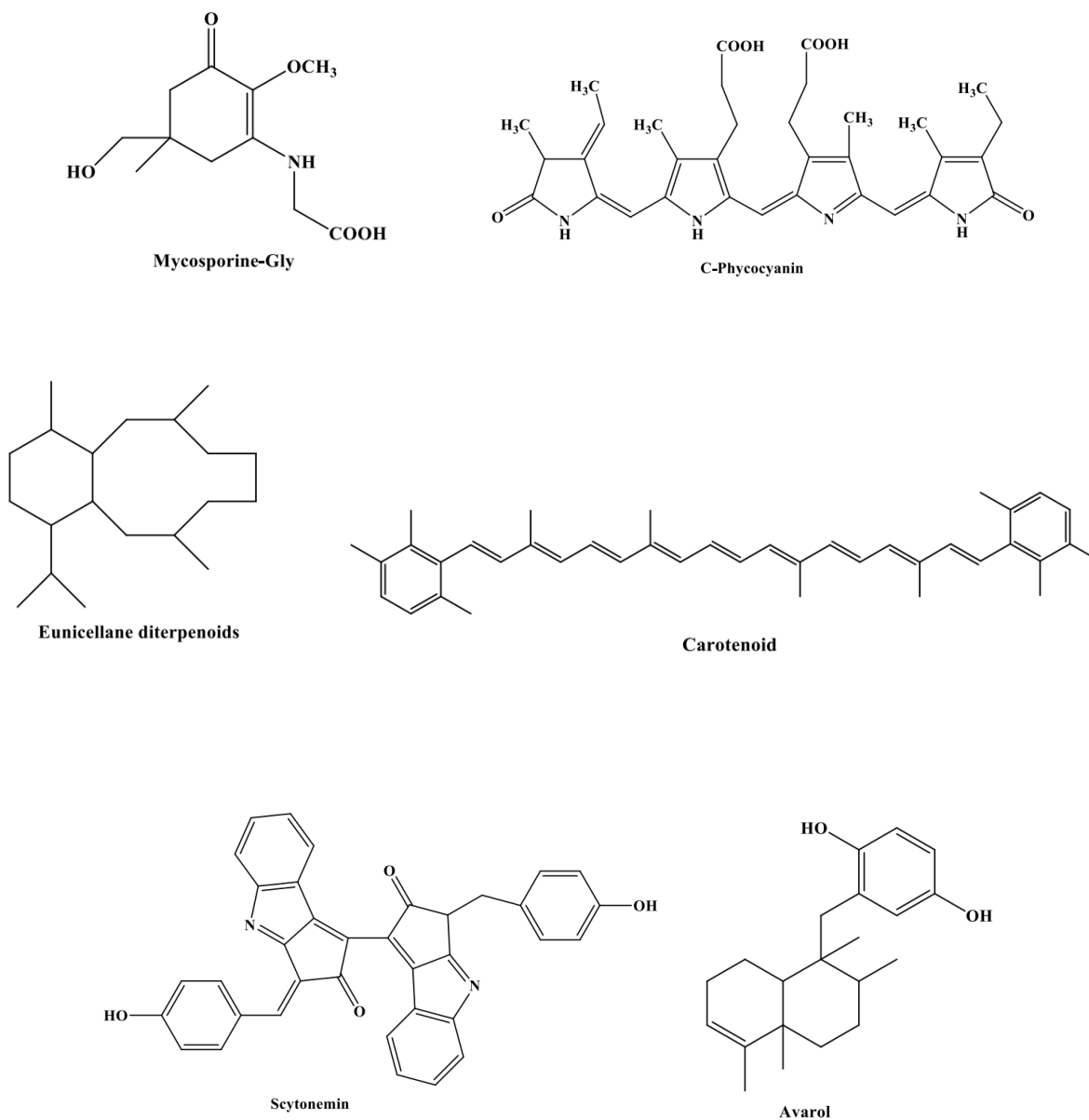
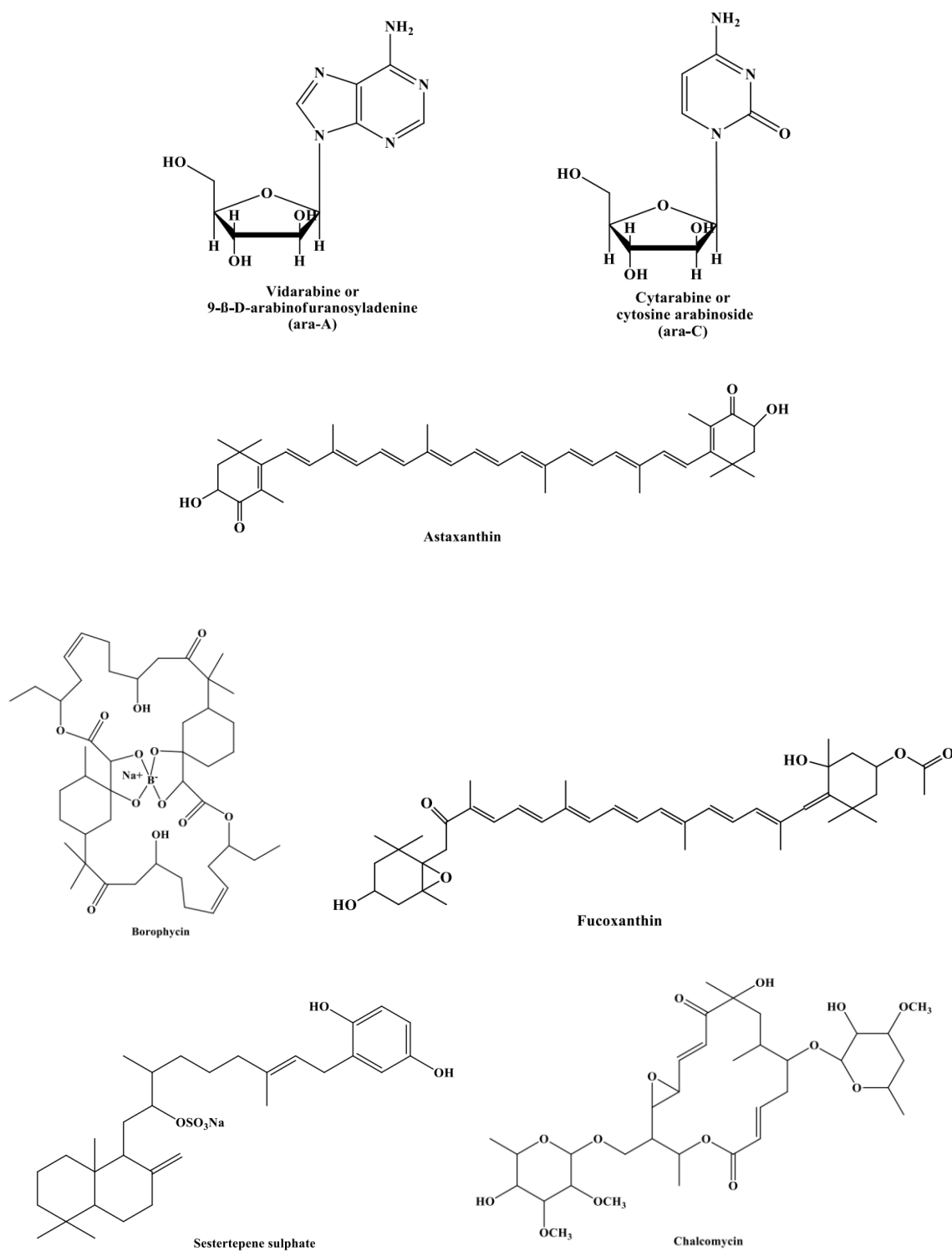


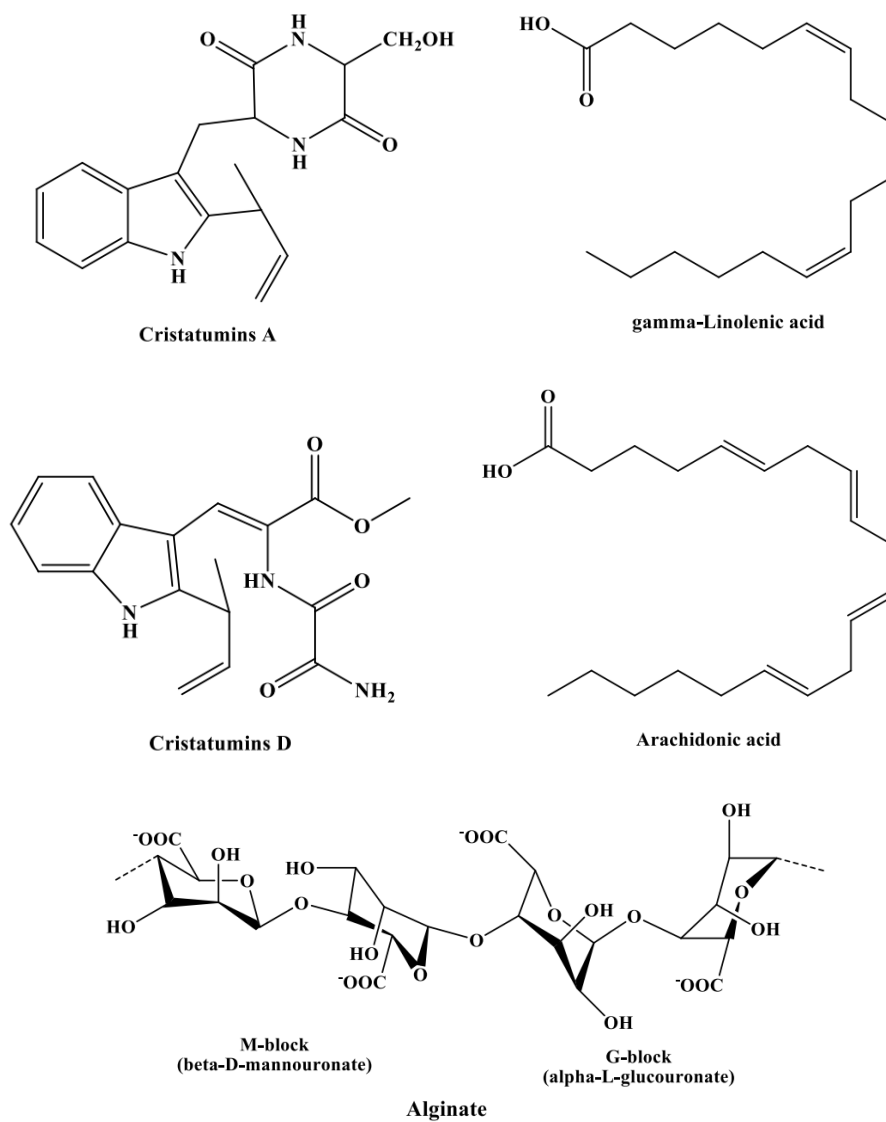
Fig. 73: Chemical structures of some selected marine-derived compounds previously-mentioned in Table 1

Different products could find great interest in medical fields and were able to be produced and marketed globally.



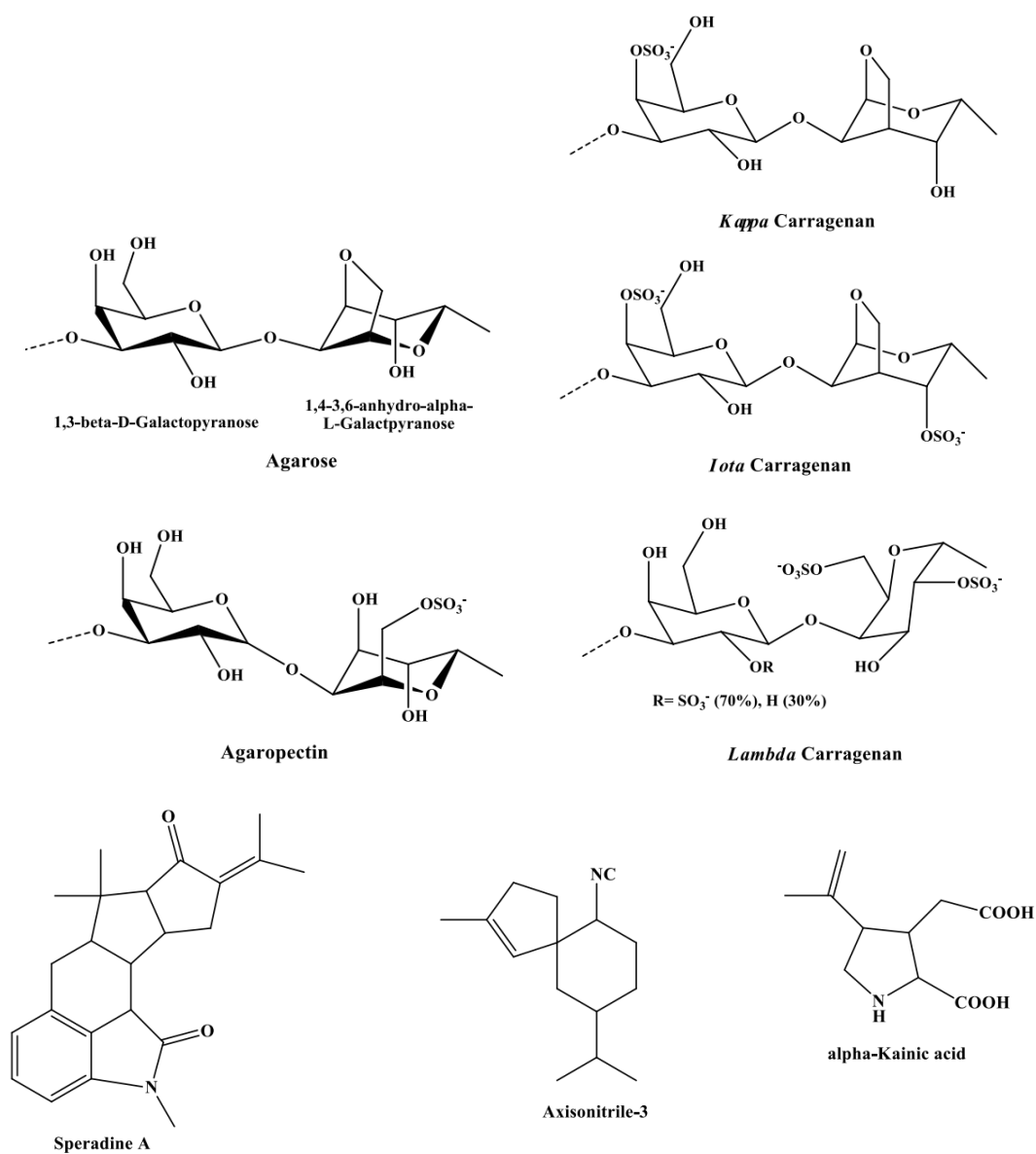
Cont., Fig. 73: Chemical structures of some selected marine-derived compounds which were mentioned in Table 1.

Different products could find great interest in medical fields and were able to be produced and marketed globally.



Cont., Fig. 73: Chemical structures of some selected marine-derived compounds which were mentioned in Table 1.

Different products could find great interest in medical fields and were able to be produced and marketed globally.



Cont., Fig. 73: Chemical structures of some selected marine-derived compounds which were mentioned in Table 1.

Different products could find great interest in medical fields and were able to be produced and marketed globally.

Appendix B

Reagents and buffers

1. 20 mM Maleic acid buffer (MAB) (pH 1)

Component	Quantity	Producer
- Maleic acid	2.32 g	TU Kaiserslautern (Chemistry Department)
- Deionized water	900 mL	

The solution was adjusted at pH 1 before the volume had been completed to 1 L.

2. 0.06 mM Toluidine blue O

Component	Quantity	Producer
- Toluidine blue O	0.018 g	Sigma-Aldrich®
- Maleic acid buffer (pH 1)	to 1 L	

3. 20 mM 2-(N-morpholino) ethanesulfonic acid (MES) (pH 6)

Component	Quantity	Producer
- MES monohydrate	2.32 g	Carl-Roth®
- Deionized water	900 mL	

The solution was adjusted at pH 6 before the volume had been completed to 1 L.

4. Phosphate-buffered saline (1x) (PBS buffer) (pH 7.4)

Component	Molarity (mM)	Quantity (g)	Producer
- Na ₂ HPO ₄ ·2H ₂ O	5.0	12.0	Sigma-Aldrich®
- NaHPO ₄ ·H ₂ O	1.5	0.21	
- KCl	2.7	0.2	Carl-Roth®
- NaCl	137	8.01	Sigma-Aldrich®
- Deionized water		900 mL	

The solution was adjusted at pH 7.4 before the volume had been completed with deionized water to 1 L.

5. Toluidine blue, thionin acetate and perylene diimide derivative (as TFA salt) (CF₃CO₂H)₈ for immobilization

Component	Toluidine blue O			Thionin acetate		Perylene diimide derivative
Molarity (mM)	2	4	6	2	4	2
Quantity (g)	0.61	1.22	1.8	0.57	1.15	3.66 g
Producer	Sigma-Aldrich®					University of Heidelberg (Institute of inorganic chemistry)

The different powders had been dissolved with 1 L deionized water.

6. 50 mM Na₂HPO₄ (eluent for molecular weight investigations)

Component	Quantity	Producer
- Na ₂ HPO ₄	7.1 g	Sigma-Aldrich®
- Deionized water	1 L	

pH was only measured directly after powder dissolution and it was 9.1 at room temperature (23 °C).

7. 0.9% (w/v) NaCl

Component	Quantity	Producer
- NaCl	9 g	Sigma-Aldrich®
- Deionized water	1 L	

8. 100 mM Na₂S₂O₄ in 20 mM MES (pH 6)

Component	Quantity	Producer
- Na ₂ S ₂ O ₄	17.4 g	TU Kaiserslautern (Chemistry Department)
- MES (pH 6)	1 L	

9. Enzyme solution for protoplast isolation

According to Mussio and Rusig [177], protoplast from *F. vesiculosus* was isolated by the following solution.

Component	Molarity (M) or %w/v	Quantity (g)/100 mL	Producer
- Mannitol	0.5	9.1	- Sigma-Aldrich® - TU Kaiserslautern
- Trisodium citrate	0.11	2.8	(Chemistry Department)
- BSA	0.3 %	0.3	- Sigma-Aldrich®
- Cellulase R-10	2%	2.0	- Duchefa Biochemie
- Alginate lyase	0.05%	0.05	- Sigma-Aldrich®
- Macerozyme	0.5%	0.5	- Duchefa Biochemie
- MES	0.08%	0.08	- Carl-Roth®

All constituents should be dissolved in autoclaved sea water and then filter sterilized and stored at 4 °C.

10. Protoplast washing solution

Component	Molarity (M)	Quantity (g) /L	Producer
- NaCl	0.4	23.38	Sigma-Aldrich®
- CaCl ₂ .2H ₂ O	0.005	0.74	

pH was adjusted at 7.0 before autoclaving.

11. Antibiotic stock solutions (1000x) in LB cultivation medium

Antibiotic	Concentration (mg.mL ⁻¹)	Producer
- Ampicillin sodium	100.0 in water	AppliChem GmbH
- Kanamycin sulphate	50.0 in water	Carl-Roth®
- Chloramphenicol	34.0 in 70% v/v ethanol	AppliChem GmbH

Prepared stock antibiotic solutions should be sterile-filtered then stored at -20 °C.

Other antibiotics used in surface sterilization protocol were purchased from AppliChem GmbH.

12. Agarose gel electrophoresis: 50x TAE buffer

Component	Molarity (M)	Quantity (g)/L	Producer
- Tris-acetate (pH 8.5)	2	242.28	Carl-Roth®
- Na ₂ EDTA	0.05	18.61	

13. Stock solutions in protein expression, detection and purification**13.1. General solutions**

Compound	Concentration
- Anhydrotetracycline (AHT)	2 mg.mL ⁻¹ in DMF or ethanol
- Ammonium Persulphate (APS)	10 % (w/v) 1 g.10 mL ⁻¹ deionized water
- Avidin	2 mg.mL ⁻¹ deionized water
- 5-Bromo-4-chloro-3-indolyl phosphate (BCIP)	50 mg.mL ⁻¹ in DMF
- Nitro blue tetrazolium (NBT)	100 mg.mL ⁻¹ in 70% (v/v) DMF

Prepared and stored at – 20 °C.

13.2. SDS-PAGE and Western blot solutions*13.2.1. 10x SDS Running buffer*

Component	Molarity (M)	Quantity (g)/L	Producer
- Tris-HCl (pH 8.3)	0.25	30.28	Carl-Roth®
- Glycine	1.92	144.0	Sigma-Aldrich®
- SDS (1% w/v)	0.035	10.0	Carl-Roth®

13.2.2. 4x Stacking gel buffer

Component	Molarity (M)	Quantity (g)/200 mL
- Tris-HCl (pH 6.8)	0.5	12.114
- SDS (4% w/v)	0.138	8.0

13.2.3. 4x Separation gel buffer

Component	Molarity (M)	Quantity (g)/200 mL
- Tris-HCl (pH 8.8)	1.5	36.34
- SDS (0.4% w/v)	0.0138	0.8

13.2.4. 4x SDS sample buffer

Component	Molarity (M)/%w/v	Quantity (g)/10 mL	Producer
- Tris-HCl (pH 6.8)	0.1	0.121	All products were purchased from Sigma-Aldrich®
- SDS (8% w/v)	0.28	0.8	
- Glycerol	40% v/v	4 mL	
- β -Mercaptoethanol	10% v/v	1 mL	
- Bromophenol blue	0.015 (1% w/v)	0.1	

13.2.5. SDS-Gel plate (12.5%)

In the beginning, the following reagents and gel should be prepared, as follows:

Reagent	Separation gel (12.5%)	Stacking gel (5.25%)	Stop gel
- Acrylamide 30%	6.7 mL	1.4 mL	420 μ L
- Buffer	4.0 mL	2.0 mL	250 μ L
- D.W	5.3 mL	4.6 mL	330 μ L
- 10% APS	80 μ L	30 μ L	13 μ L
- TEMED	8 μ L	20 μ L	2 μ L

As shown in **Fig. 74**, each plate consists of 500 μ L of stop gel should be poured in between fitted glass plates in its casting chamber to form the basal guard layer of the gel. Afterwards, 3 mL of separation gel form the main part of gel then 1 mL of stacking buffer to be appeared as in the following figure. Prepared plates should be then stored in wet tissues at 4 °C till time of use.

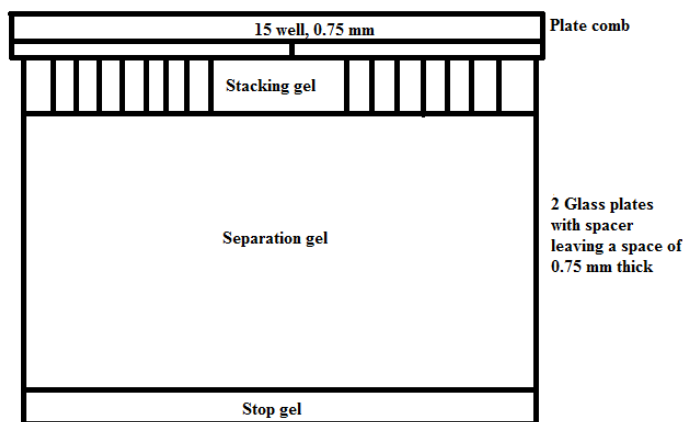


Fig. 74: SDS-PAGE plate showing its building components

13.2.6. Coomassie blue staining solution

Component	% v/v	Volume mL/ L	Producer
- Acetic acid (P. A., 99.8%)	10	100	TU Kaiserslautern
- Ethanol (Analytical grade, $\geq 99.8\%$)	30	300	(Chemistry Department)
- Coomassie Brilliant Blue G-250 Dye	0.5% w/v	5.0 g	AppliChem GmbH

13.2.7. Coomassie blue bleaching solution

Component	% v/v	Volume mL/ L
- Acetic acid (P. A., 99.8%)	10	100
- Ethanol (Analytical grade, $\geq 99.8\%$)	30	300

13.2.8. Western Blot

i. Towbin buffer

Component	Molarity (M)	Quantity (g/L)
- Tris (pH 8.3)	0.025	3.028
- Glycine	0.192	14.4

pH should not be adjusted with acids or alkali.

ii. Alkaline phosphatase (AP buffer) pH 9.5

Component	Molarity (M)	Quantity (g)/L	Producer
- Tris-HCl	0.1	3.028	Carl-Roth®
- NaCl	0.1	5.85	Sigma-Aldrich®
- MgCl ₂	0.005	1.02	Carl-Roth®

iii. PBS-T buffer

Component	Volume (mL)	Producer
- PBS	999.0	
- Tween-20 (0.1% v/v)	1.0	Carl-Roth®

iv. Blocking solution in PBS-T buffer

Component	Quantity (g)/ 100 mL	Producer
- Albumin fraction V from BSA	3.0	Carl-Roth®
- Complete volume to 100 mL by PBS-T		

v. Purification buffer (Buffer W (pH 8.0))

Component	Molarity (M)	Quantity (g)/L
- Tris-HCl	0.1	12.14
- NaCl	0.15	8.76

1 mM EDTA was excluded from IBA GmbH formula

vi. Elution buffer (Buffer E)

Component	Molarity (M)	Quantity (g)/L	Producer
- Desthiobiotin	0.0025	0.54	Sigma-Aldrich®
- Buffer W was added to 1 L			

vii. Regeneration buffer (Buffer R)

Component	Molarity (M)	Quantity (g/L)
- 2-[4-hydroxy-benzeneazo]benzoic acid (HABA)	0.001	0.24
- Buffer W was added to 1 L		

14. Description of Sepabeads® EC-EA [98]

Item	Description
Grade	S (small)
Particle size range	100-300 µm
Matrix	Polymethacrylate
Appearance	Perfect spherical white opaque beads
Functional group	Ethylenediamino
Functional group density	Min. 600 µmol/g wet
Median pore diameter	10 – 20 nm
True density	>1.1 g/mL
Water retention	55 – 65 %
Temperature stability range	2 – 60° C
pH stability	1 - 14
Recommended storage temperature	Room temperature

Appendix C

Medium composition and preparations

1. Lysogeny Broth-Miller (LB)-agar medium [Tissue culture chapter]

Component	Quantity (g/L)	Producer
- Tryptone	10.0	AppliChem GmbH
- Yeast extract	5.0	
- NaCl	10.0	
- Agar	15.0	Carl-Roth®

Medium components (without agar) had been dissolved in deionized water (pH 6.8 – 7.0, 24.0 °C), then it was autoclaved after the addition of agar.

2. Marine Boullion (MB50)-Agar medium

Component	Quantity (g/L)	Producer
- Marine Broth (Carl Roth®)	20.0	Carl-Roth®
- NaCl	9.7	
- Agar (1.5 % w/v)	15.0	

Medium components (without agar) had been dissolved in deionized water (pH 6.8 – 7.0, 24.0 °C), then it was autoclaved after the addition of agar.

3. Murashige and Skoog (MS) medium (pH 5.8) supplemented with 3% (w/v) sucrose

Component	Quantity (g/L)	Producer
- Sucrose	30.0	Carl-Roth®
- MS	4.4	AppliChem GmbH
- Agar	5.5	Carl-Roth®

4. Nutrient agar medium for cultivation of *Rhizopium radiobacter* DSM30147

(as described by Leibniz Institute DSMZ-German Collection of Microorganisms and Cell Cultures)

Component	Quantity (g/L)	Producer
- Pepton (Soya)	5.0	Sigma-Aldrich®
- Meat extract	3.0	AppliChem GmbH
- Agar (for solid medium)	15.0	Carl-Roth®

Constituents were dissolved in 900 mL deionized water and pH was adjusted to 7.0, before the addition of agar. Volume was then completed to 1 L before autoclaving.

5. **LB Broth medium (Liquid and solid media) [Lennox] [for heterologous expression chapter]**

Component	Quantity (g/L)	Producer
- Tryptone	10.0	Carl-Roth®
- Yeast extract	5.0	
- NaCl	5.0	
- Agar (for solid medium)	15.0	
Complete volume to 1000		

Prepared medium was also purchased from Carl-Roth®. In this case, 20 g of the medium powder was dissolved in 1 L deionized water. 1000x Sterile-filtered antibiotic solution (1 mL) should be added to a cooled autoclaved medium.

6. **PES medium**

In a ratio of 1:50, 20 mL of Enrichment Stock Solution (ESS) was diluted to 1 L using 0.45 µm filtered seawater to produce PES medium. pH should be adjusted at 7.8 before autoclaving. In addition, vitamins should be added to cooled autoclaved medium. In washing steps, an alternative medium was used (PESA), in which PES medium was used without vitamins.

6.1. **Enrichment Stock Solution (ESS) (50x)**

Component	Quantity (g) /L	Producer
- Tris base	5.0	Carl-Roth®
- NaNO ₃	3.5	Merck
- Na ₂ β-glycerophosphate.H ₂ O	0.5	AppliChem GmbH
- Iron-EDTA solution (see 14.2)	250 mL	
- Trace metal solution (see below)	25 mL	
- Vitamin B1 (Thiamine.HCl)	5x10 ⁻⁴	Carl-Roth®
- Vitamin H (Biotin)	5x10 ⁻⁶	Sigma-Aldrich®
- Vitamin B12 (Cyanocobalamin)	1x10 ⁻⁵	Carl-Roth®

6.2. **Iron-EDTA solution**

Component	Quantity (g) /L	Producer
- Na ₂ EDTA.2H ₂ O	6.0	Carl-Roth®
- Fe(NH ₄) ₂ (SO ₄) ₂ .6H ₂ O	7.0	Merck

6.3. Trace metal solution

Component	Quantity (g/L)	Producer
- Na ₂ EDTA.2H ₂ O	2.54	Carl-Roth®
- H ₃ BO ₃	2.24	Merck
- MgSO ₄ .7H ₂ O	0.24	Merck
- ZnSO ₄ .7H ₂ O	0.044	TU Kaiserslauern
- CoSO ₄ .7H ₂ O	0.01	(Chemistry Department)

7. ASP-12-NTA medium

Medium constituents were completely dissolved in deionized water with aid of ultrasound. The medium pH was adjusted to 7.8 before autoclaved (20 min, 121° C, 2 bar). Sterile-filtered vitamin solutions were added to a room-temperature autoclaved medium.

Component	Quantity (g) /L	Producer
- NaCl	20	Sigma-Aldrich®
- KCl	0.7	Sigma-Aldrich®
- MgSO ₄ .7H ₂ O	7.0	Merck
- MgCl ₂ .6H ₂ O	4.0	Sigma-Aldrich®
- CaCl ₂ .2H ₂ O	0.4	Sigma-Aldrich®
- NaNO ₃	0.1	Merck
- K ₃ PO ₄	0.01	Sigma-Aldrich®
- Na ₂ β-glycerophosphate.H ₂ O	0.01	AppliChem GmbH
- Na ₂ SiO ₃ .9H ₂ O	0.15	Sigma-Aldrich®
- PII metal solution	10 mL	
- SII metal solution	10 mL	
- Nitrilotriacetic acid	0.1	TU Kaiserslauern (Chemistry Department)
- Tris	1.0	Carl-Roth®
- Vitamin B1 (Thiamine.HCl)	0.1	Carl-Roth®
- Vitamin H (Biotin)	1x10 ⁻³	Sigma-Aldrich®
- Vitamin B12 (Cyanocobalamin)	2x10 ⁻⁴	Carl-Roth®

7.1. PII metal solution

Component	Quantity (g) /100 mL	Producer
- Na ₂ EDTA.2H ₂ O	0.1	Carl-Roth®
- FeCl ₃	0.001	TU Kaiserslauern (Chemistry Department)
- H ₃ BO ₃	0.02	Meck
- MgCl ₂ .2H ₂ O	0.004	Carl-Roth®
- ZnCl ₂ .7H ₂ O	0.0005	TU Kaiserslauern (Chemistry Department)
- CoCl ₂	0.0001	TU Kaiserslauern (Chemistry Department)

7.2. SII metal solution

Component	Quantity (g) /100 mL	Producer
- NaBr	0.1	TU Kaiserslauern (Chemistry Department)
- SrCl ₂	0.02	Sigma-Aldrich®
- RbCl	0.002	Sigma-Aldrich®
- LiCl	0.002	TU Kaiserslauern (Chemistry Department)
- Na ₂ MoO ₄	0.005	Sigma-Aldrich®
- KI	0.0001	TU Kaiserslauern (Chemistry Department)

8. F/2 medium

A sterile-filtered 50x Guillard's (F/2) Marine Enrichment medium was purchased from Sigma-Aldrich®. For the production of a 1 L medium, 20 mL of medium was diluted by 980 mL 0.45 µm filtered and autoclaved sea water.

9. Protoplast cultivation medium [177]

Component	Molarity / %w/v	Quantity (g) /100 mL	Producer
- HEPES	2 mM	0.047	Carl-Roth®
- PESA (3.8 % sea salt)	1% v/v	1.0 mL	
- Glucose	250 mM	4.5	Sigma-Aldrich®
- Sucrose	150 mM	5.1	Carl-Roth®
- Casein hydrolysate	0.025 %	0.025	Sigma-Aldrich®
- Ornithine hydrochloride	20 µM	3.3x10 ⁻⁴	Duchefa Biochemie
- CPPU	0.4 µM	9.9x10 ⁻³	Duchefa Biochemie
- 2,4-D	0.45 µM	1 x 10 ⁻⁵	Duchefa Biochemie

Appendix D

Protocols

1. Heat shock bacterial transformation protocol

- i. *E. coli* JM83 and BL21 (DE3) competent cells were provided from Prof. Dr. Nicole Frankenberg-Dinkel's lab. (Institute of Microbiology, TU Kaiserslautern) in a 1.5 mL reaction vessel as 0.5 mL samples. The cells were preserved in a cryopreservation refrigerator. Cells were thawed on ice, firstly for 5 min. 1 μ L of 100 ng μ L⁻¹ dissolved DNA constructs was added afterwards.
- ii. Cells were incubated with constructs on ice for 30 min.
- iii. The mixtures were then heat shocked at 42 °C for 120 s.
- iv. 700 μ L of LB broth was added afterwards to the tube and the transformation reactions placed in a shaker incubator at 37 °C for 45-60 min.
- v. At the end of this incubation, centrifugation was carried out for 1 min. at 13200 rpm and/or spread 100 μ L of the cell suspension on LB agar plates supplemented with the suitable antibiotic.
- vi. Finally, plates were incubated overnight for approx. 16 h at 37 °C to get colonies of genetically transformed *E. coli* with corresponding required DNA.

2. PCR protocol (Thermo Fisher Scientific®)

Each reaction tube should be incubated in ice, while constituents were added:

- 25 μ L Dream-Tag™ green PCR Master Mix (2x),
- 2 μ L fwd primer (20 μ M),
- 2 μ L rev primer (20 μ M),
- 1 μ L DNA template (50 ng), and
- 20 μ L sterile highly pure water.

The PCR reaction afterwards was performed, according **Table 18**.

Table 18: PCR steps used in amplification of synthetic Esi0021_0026, Esi0050_0098, Esi0283_0018 and Esi0032_0064

Step	Temperature (°C)	Time	No. of cycles
Initial denaturation	95	3 min	1
Denaturation	95	30 s	30
Annealing	Depend on primer's T _m	30 s	
Extension	72	1 min	
Final extension	72	10 min	1
Storage	4	forever	

3. Gibson assembly transformation protocol, according to Gibson assembly cloning kit instruction manual [254]

- i. Thaw chemically competent cells on ice.
- ii. Add 2 μ L of the chilled assembly product to the competent cells. Mix gently by pipetting up and down for 4–5 times. Do not vortex.
- iii. Place the mixture on ice for 30 min. Do not mix.
- iv. Heat shock at 42 °C for 30 s. Do not mix.

- v. Transfer tubes to ice for 2 min.
- vi. Add 950 μL of room-temperature SOC media to the tube.
- vii. Incubate the tube at 37°C for 60 min. Shake vigorously (250 rpm) or rotate.
- viii. Spread 100 μl of the cells onto the selection plates.
- ix. Incubate overnight at 37 °C.

4. **Chromogenic detection of *Strep-tag*[®] fusion proteins with alkaline phosphatase (Western blot)**

According to the protocol described by IBA BioTAGnology [258] with some modifications, steps of protocols were performed as follow:

- i. After SDS-PAGE, electro-transfer of proteins via Semi Dry-Blot technique to a PVDF membrane (previously activated by incubation with MeOH for 5 min) was performed firstly. Membrane and Whatman filter papers were equilibrated with Towbin buffer, before protein transfer, which is carried out for 20 min at 15 V using an electrotansfer cell.
- ii. Block the membrane with 20 ml PBS-blocking buffer (3% w/v albumin Fraction V in PBS-T buffer) by incubation for 1 h (room temperature; with gentle shaking) or overnight (4°C).
- iii. Wash three times with 20 ml PBS-T buffer (each step: 5 min., room temperature, gentle shaking).
- iv. After the last washing step, add 10 ml 2 $\mu\text{g}\cdot\text{mL}^{-1}$ avidine in PBS-T buffer to the membrane (10 minutes, room temperature, gentle shaking). This blocks endogenously biotinylated proteins (e.g. the biotin carboxyl carrier protein (BCCP, 22 kDa) in case of *E. coli*) which will otherwise stain sensitively.
- v. Add 2.5 μL *Strep-Tactin*[®] labeled with alkaline phosphatase conjugate to 10 mL PBS-T buffer (1:4000). Incubate 60 min. at room temperature with gentle shaking.
- vi. Wash three times with PBS-T buffer (each step: 5 min, room temperature, gentle shaking).
- vii. Wash three times with PBS-buffer (each step: 5 min, room temperature, gentle shaking).
- viii. Equilibrate the membrane with 10 mL alkaline phosphatase buffer for 5 min with gentle shaking. Add 33 μL nitrotetrazolium blue (NBT; 100 $\text{mg}\cdot\text{mL}^{-1}$) and 66 μL 5-bromo-4-chloro-3-indolyl-phosphate (BCIP; 50 $\text{mg}\cdot\text{mL}^{-1}$) to a 10 mL fresh alkaline phosphatase buffer.
- ix. Proceed the chromogenic reaction under shaking until optimal signal:background ratio is achieved.
- x. Stop reaction by washing several times with deionized water.
- xi. Air dry the membrane and store it in the dark.

5. Production of adsorbent (immobilized TB, TA and PDD) [93]

Step 1	Derivatization of the adsorbent	i. 500 mg Sepabeads® EC-EA ii. 0.5 mL 50% Glutaraldehyd solution (Glutaraldehyd=1,5-Pentandial) iii. 4.5 MI 20 mM MES (pH 6)
Step 2	Washing	i. 24 h incubation in an overhead shaker (F1 mode, 30 rpm) ii. Three times with 6.6 mL H ₂ O iii. 24 h incubation in an overhead shaker (F1 mode, 30 rpm)
Step 3	Simultaneous reduction with Na₂S₂O₄ and dyes immobilization	i. Add 6.6 mL 100 mM Na ₂ S ₂ O ₄ in 20 mM MES (pH6), 0.5 mL 2 mM aqueous TB, TA or PDD solutions ii. 12 h incubation in an overhead shaker (F1 mode, 30 rpm)
Step 4	Washing	i. Three times 6.6 mL H ₂ O ii. 24 h incubation in an overhead shaker (F1 mode, 30 rpm)
Step 5		iii. Three times with 6.6 mL 5 M NaCl in 20 mM MAB, pH1 iv. 24 h incubation in an overhead shaker (F1 mode, 30 rpm)
Step 6		v. Three times with 6.6 mL H ₂ O vi. 24 h incubation in an overhead shaker (F1 mode, 30 rpm)
Step 7	Drying	i. Dry at 50 °C until obtaining dried cyan or red-coloured beads

6. Application of particles for the purification of fucoidan from crude extract [93]

- Step 1 A stock solution of crude extract with 2.5 mg.mL⁻¹ fucoidan in 20 mM MAB (pH 1) or 20 mM MES (pH 6) was prepared
- Step 2
- Adsorption phase
 - To 50 or 75 mg derivatized beads (adsorbents) add 1.5 mL 2.5 mg mL⁻¹ crude extract
 - Incubation for 44 h room temperature for thiazine dyes or 16 h for perylene diimide derivatized beads (F1 mode, 30 rpm)
 - Centrifuge and remove the supernatant to be analyzed (calculation of adsorption rate and % of adsorbed fucoidan)
- Step 3
- Washing phase
 - Washing the adsorbents for 3 h with 1 mL H₂O at room temperature.
 - Centrifuge and take a sample from supernatant for analysis
- Step 4
- Washing with 1 mL of 0.1 M NaCl prepared in 20 mM MAB (pH 2) for 5 h at room temperature (F1 mode, 30 rpm)
 - Centrifuge and remove the supernatant.
- Step 5
- Elution phase
 - Incubation of 1.5 mL 3 M NaCl prepared in 30% (v/v) ethanol with loaded derivatized beads for 16 h in a thermoshaker (50°C, 800 rpm).
 - Centrifuge and collect the eluate
- Step 6
- Washing and storage
 - Washing adsorbents with 1 mL 20% ethanol in 20 Mm MES pH 6 for 8 h (room temperature, 30 rpm)
 - Storage of the adsorbents in 20% ethanol in 20 Mm MES pH 6
- Step 7
- Removal of ethanol and concentration of eluate
 - In a rotary evaporator (60 °C, 100 mbar) eluate was concentrated (1:0.3)
- Step 8
- Dialysis and removal of NaCl
 - In a Dialysis membrane of MWCO (3.5 kDa) concentrated eluate was dialyzed against completely deionized water
 - The process should be stopped when conductivity of replaced water (every 2-3 h) had stable and similar to fresh deionized water for at least 2 h.
- Step 9
- Lyophilization of dialyzed eluate
 - In a lyophilizer (- 20° C, 1.03 mbar), frozen eluate was transformed to fluffy powdered fucoidan.

Appendix E

Calibration curves, instruments' charts and analysis reports

1. Calibration curves

1.1. Total sugar content in crude fucoidan

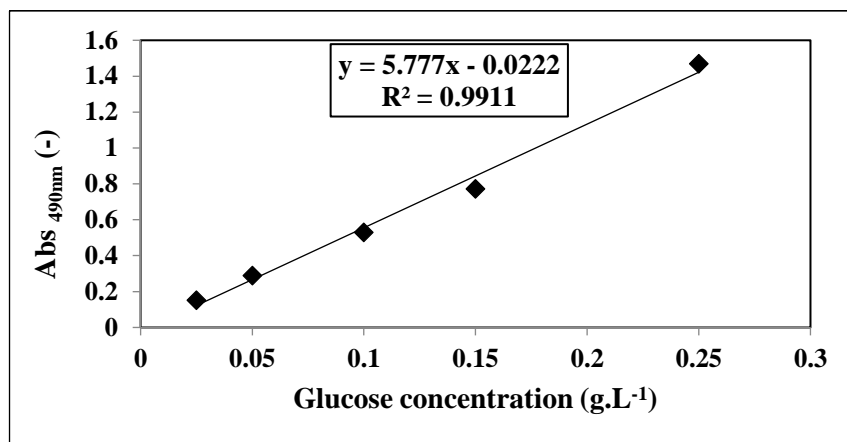


Fig. 75: Calibration curve of Dubois or phenol-sulphuric acid assay

Glucose was used as a standard and absorbance was measured at 490 nm.

1.2. Fucoidan content and purity of crude fucoidan

a. TB assay

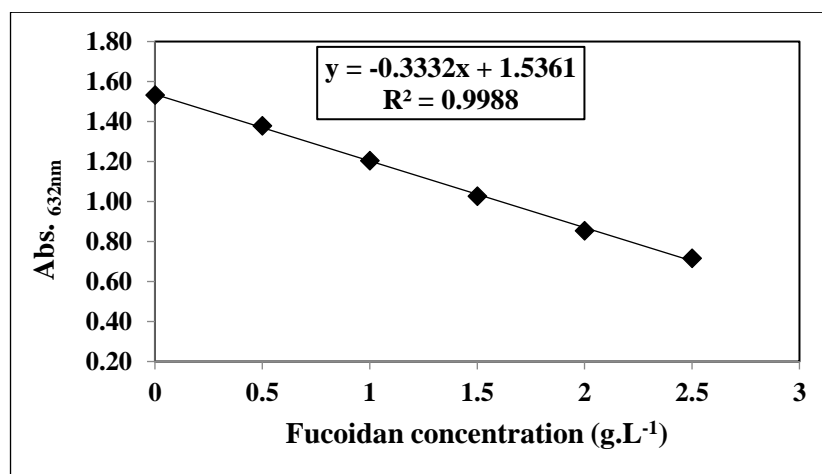


Fig. 76: Calibration curve of TB assay

Fucoidan (>95% pure, Sigma-Aldrich[®]) was used as a standard at different serial dilution and reacted with 0.06 mM TB and absorbance was measured at 632 nm.

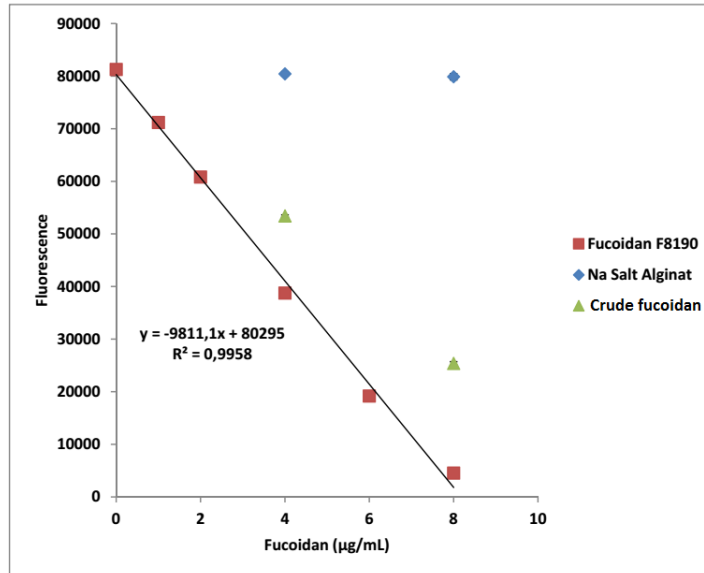
b. Heparin Red[®] assay

Fig. 77: Calibration curve of Heparin Red[®] Ultra assay

The figure shows replicates from crude fucoïdan (**Fucoïdan_A**) and alginate sodium salts to confirm that there selectivity of the assay to fucoïdan. Fucoïdan (F8190, >95% pure Sigma-Aldrich[®]) was used as a standard. Excitation λ at 570 nm and emission was recorded at 605 nm.

1.3. Fucose content in crude fucoïdan

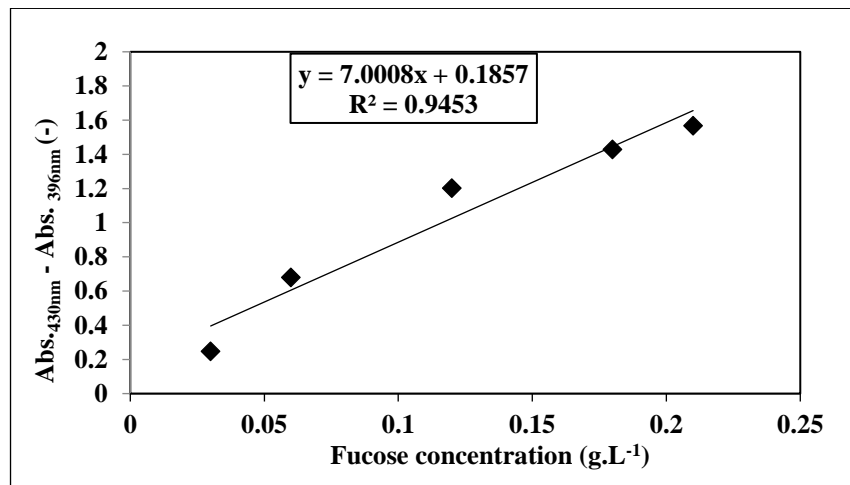


Fig. 78: Calibration curve of Dische assay

L-fucose was used as a standard. Absorbance was measured at two λ and the differences were plotted against fucose concentration.

1.4. Sulphate content in crude fucoidan

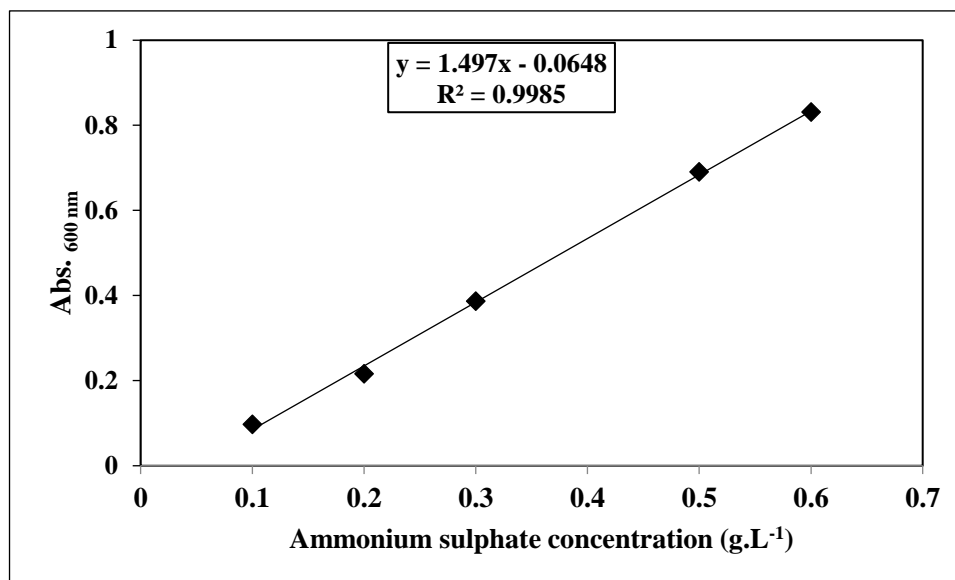


Fig. 79: Calibration curve of BaSO₄ test

Ammonium sulphate was used as a standard and absorbance was measured at 600 nm.

1.5. Phosphate standard calibration curve for FucTs activity assay

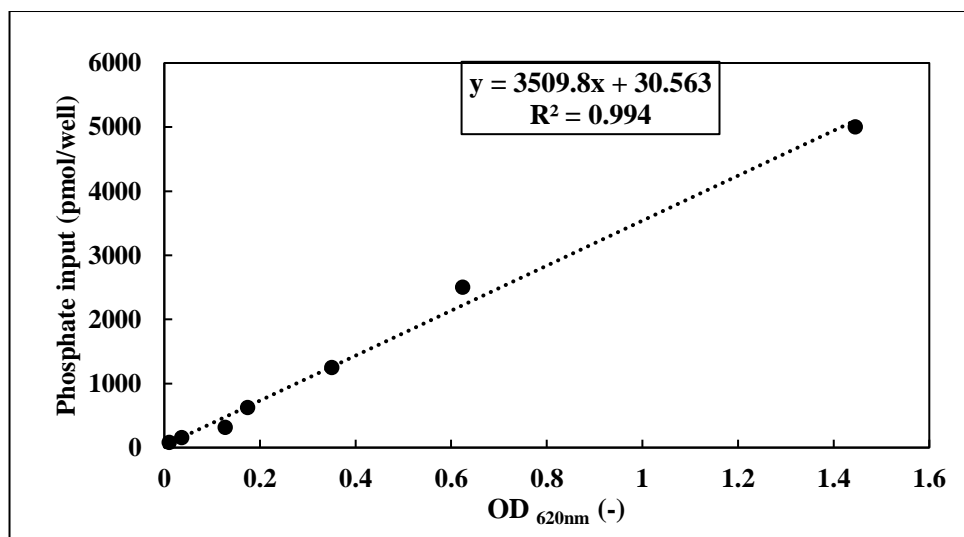


Fig. 80: Phosphate standard calibration curve for FucTs activity assay

Detection was performed by malachite green assay using KH₂PO₄ as a standard, following the provider's manual. The slope of the curve was used to determine the specific activity of FucTs₅₀ as stated in the Glycosylation activity kit's manual.

1.6. Phosphate standard calibration curve for STs activity assay

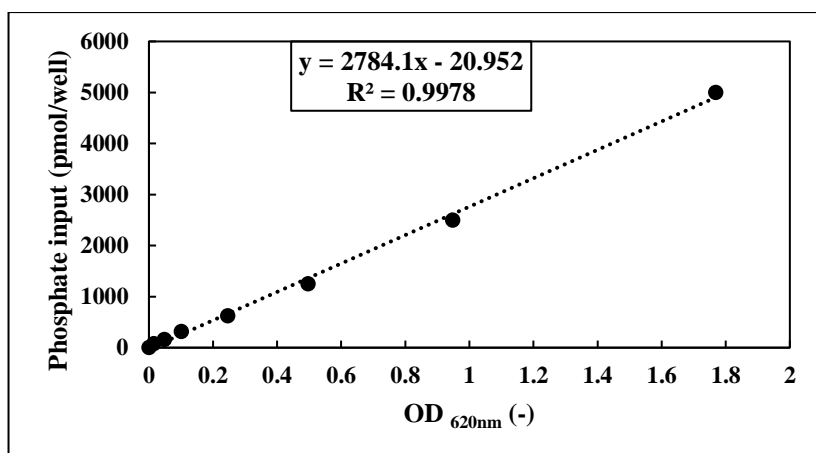


Fig. 81: Phosphate standard calibration curve for STs activity assay

Detection was performed by malachite green assay using KH_2PO_4 as a standard. The slope of the curve was used to determine the specific activity of FucTs_50 as stated in the Universal sulphotransferase activity kit's manual.

2. 3D structure of over-expressed algal FucTs and STs

3D structure of both enzymes were traced by the online free service Phyre² and PyMOL software, as shown in **Fig. 82** and **83** to show their building units and folding.

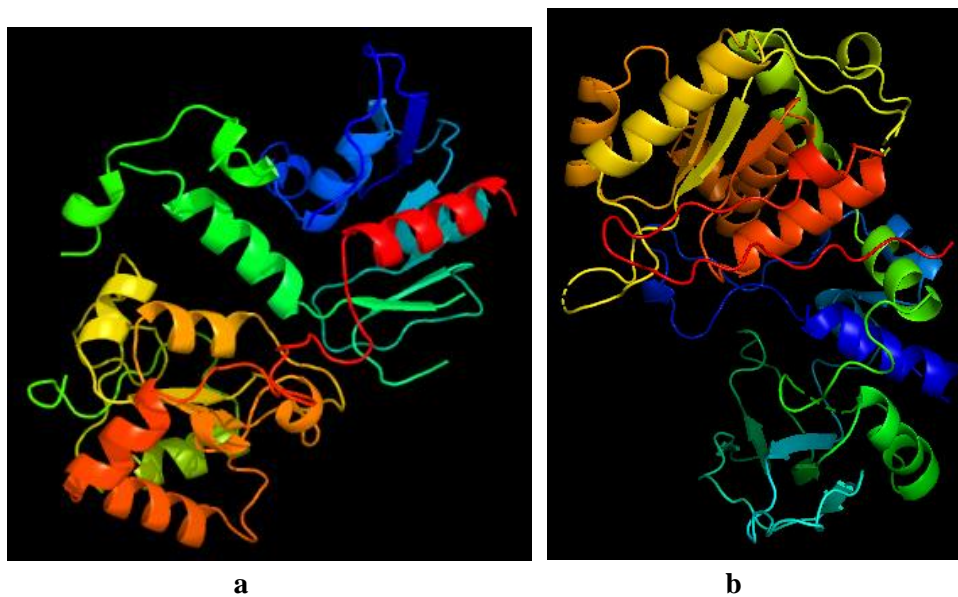


Fig. 82: 3D structures of FucTs_50 (a) and FucTs_21 (b) as traced by the free online Phyre² server and PyMOL software

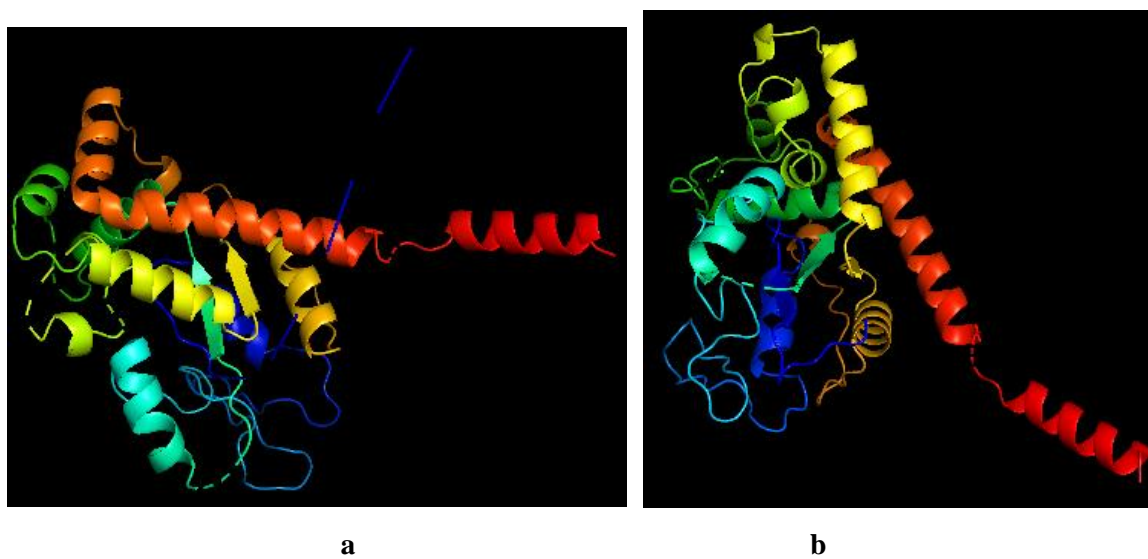
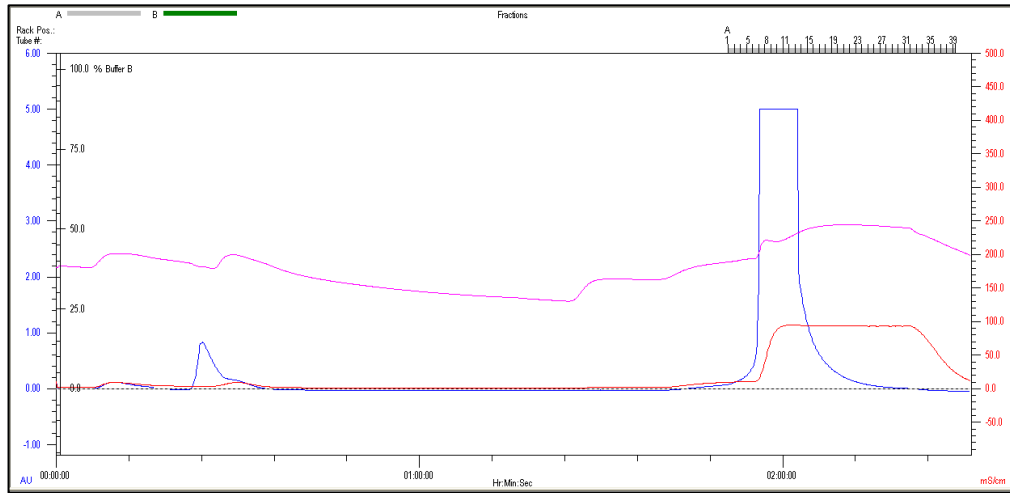


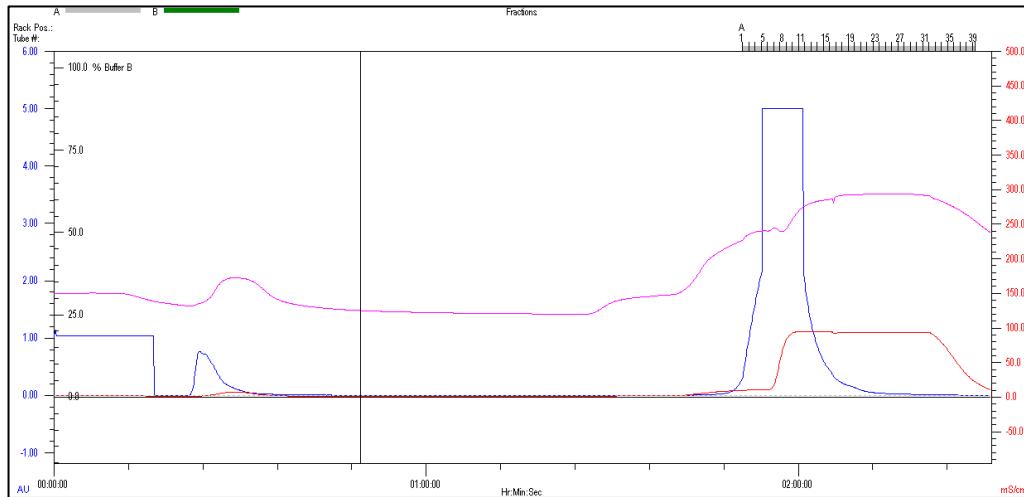
Fig. 83: 3D-structures of STs_32 (a) and STs_283 (b) as traced by the online service Phyre² and PyMOL software

3. Instruments' charts

3.1. Automated purification of fucoidan by immobilized PDD



a



b

Fig. 84: FPLC chromatograms for fucoidan purification by immobilized PDD

a: 1st cycle of purification; **b:** 2nd cycle of purification. Blue line= UV absorbance at 280 nm; Red line= conductivity, Pink line= pH

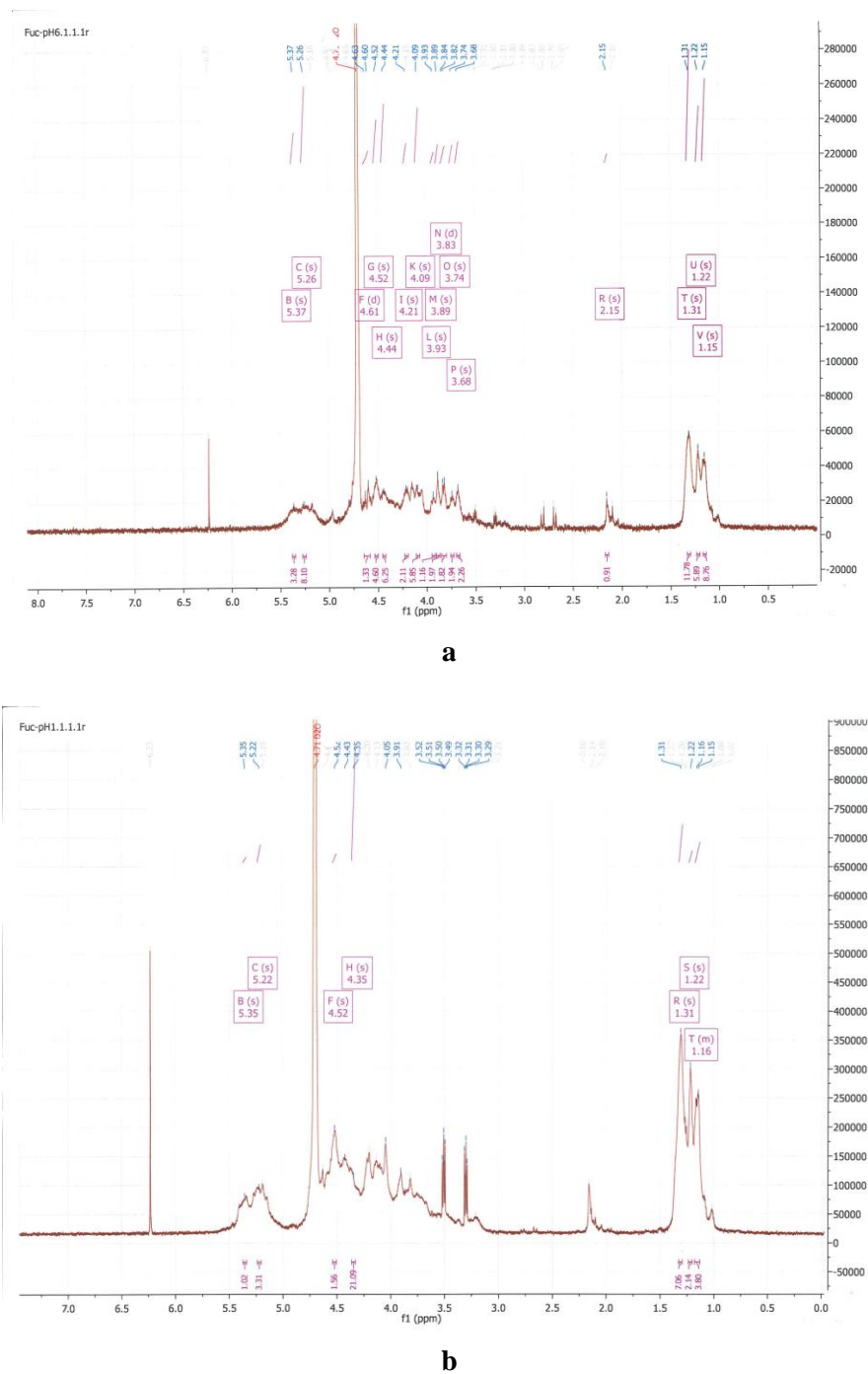
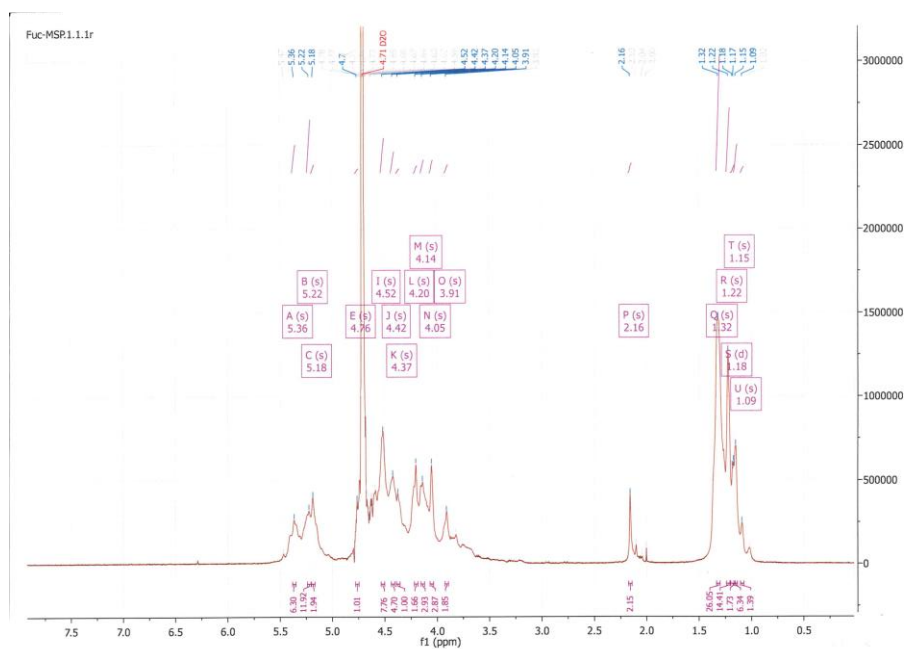
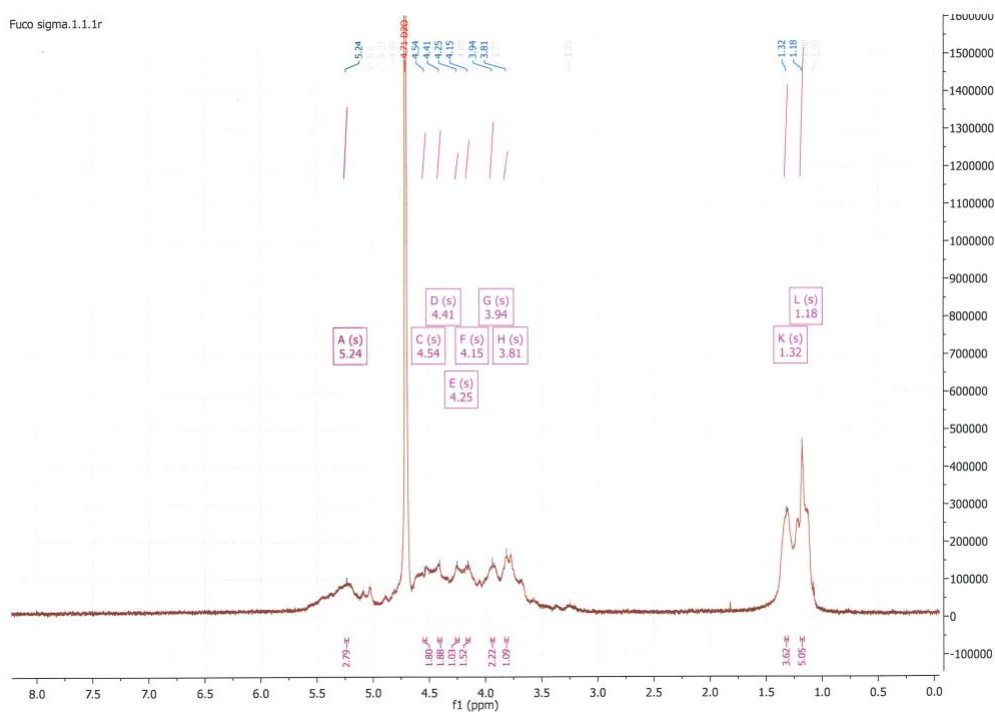
3.2. $^1\text{H-NMR}$ spectra of purified fucoidan

Fig. 85: $^1\text{H-NMR}$ spectra of fucoidan fractions in comparison with fucoidan purchased from Sigma-Aldrich[®]

Analysis resulted in poorly-translated spectra and revealed in complex nature of fucoidan. (400 MHz, in D_2O); **a:** Fucoidan_6; **b:** Fucoidan_1; **c:** Fucoidan_M; **d:** commercial fucoidan



c



d

Cont., Fig. 85: $^1\text{H-NMR}$ spectra of fucoidan fractions in comparison with fucoidan purchased from Sigma-Aldrich®.

Analysis resulted in poorly-translated spectra and revealed in complex nature of fucoidan. (400 MHz, in D_2O); a: Fucoidan_6; b: Fucoidan_1; c: Fucoidan_M; d: commercial fucoidan

4. Others

4.1. Anti-microbial activity of fucoïdan

4.1.1. Anti-fungal activity

Fig. 86 demonstrated the results of the studied anti-fungal activity of fucoïdan fractions and commercially-available product against *C. albicans* in comparison with Ampho B. For *C. troïcalis* and *glabrata*, fucoïdan fractions showed a similar pattern and confirmed its inactivity.

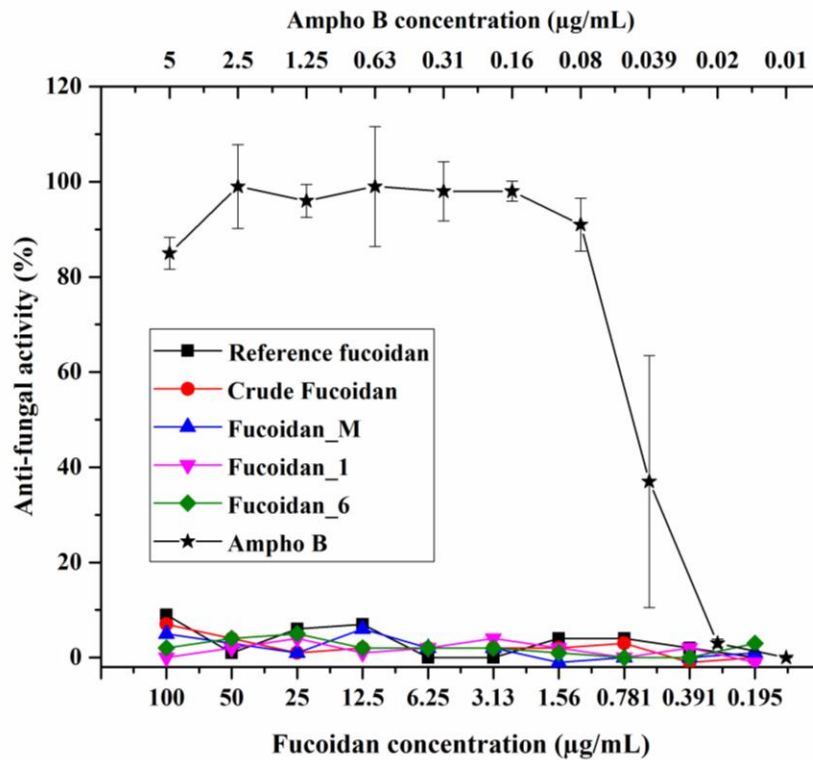
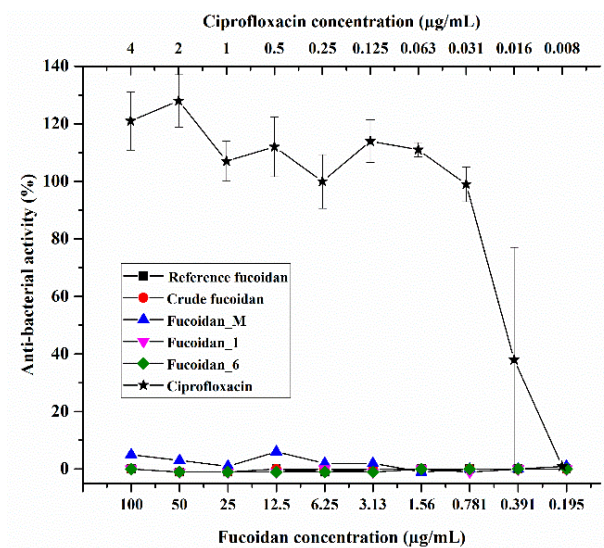


Fig. 86: Anti-fungal activity of different fucoïdan fractions against *C. albicans*, in comparison with the reference commercial product following the protocol of Kleymann and Werling [115]

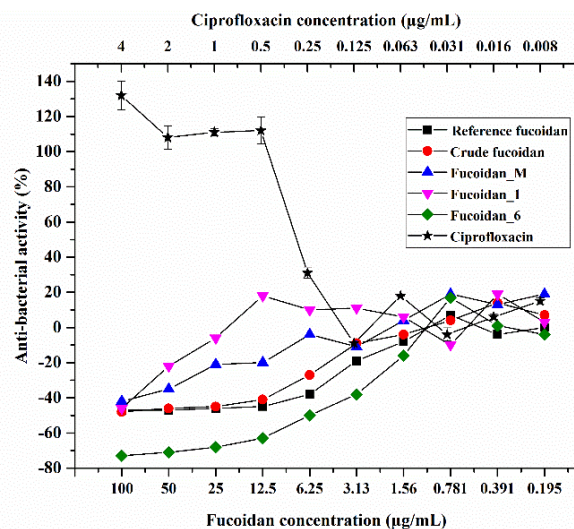
The anti-fungal drug Ampho B was used as a positive control. The figure confirmed inactivity of fucoïdan as anti-fungal agent.

4.1.2. Anti-bacterial activity

As shown in **Fig. 87**, there were no anti-bacterial activity of fucoidan fractions against Gram +ve and G-ve bacteria. Interestingly, in anti-Gram +ve activity assay, with high fucoidan concentration, the viability, however, was increasing and might prove the nourishment of fucoidan for bacteria.



a



b

Fig. 87: Anti-bacterial activity of different fucoidan fractions against *E. coli* (a) and *S. aureus* (b) in comparison with the reference commercial product and following the protocol of Kleymann and Werling [115]

The anti-bacterial ciprofloxacin was used as a positive control. The figure confirmed inactivity of fucoidan as an anti-bacterial agent.

4.2. CHNS analysis of fucoidan fractions



Birgit Dusch
FB Chemie / TU Kaiserslautern
Erwin-Schrödinger-Strasse 54
67663 Kaiserslautern



Analytik – Organische Chemie
Tel.: 0631-205-2477
FAX: 0631-205-3921
e-mail: dusch@chemie.uni-kl.de

Technische Universität Kaiserslautern
FB Maschinenbau und Verfahrenstechnik
Lehrgebiet Bioverfahrenstechnik
Prof. Dr. rer. nat. R. Ulber

z.Hd. Herrn M. Sc. Ahmed Zayed

67663 Kaiserslautern

Mittwoch, 19. November 2014

Analysebericht:

CHNS- Analyse

Probenbezeichnung: **Fuc. (Sigma), Fuc. 40%, Fuc. 70%_1, Fuc. 70%_2**

Eingangsdatum: 19.11.2014

Prüfverfahren: in Anlehnung an DIN EN 51732

Interne LA-Nr.: 141111

Probe	N [%]	C [%]	H [%]	S [%]
Fuc. (Sigma)	-	24,78	4,42	8,89
Fuc. 40%	-	18,38	3,89	12,26
Fuc. 70%_1	-	24,61	4,79	8,16
Fuc. 70%_2	0,55	23,42	4,22	6,78

Kaiserslautern, den 19.11.2014

(Birgit Dusch)



Birgit Dusch
FB Chemie / TU Kaiserslautern
Erwin-Schrödinger-Strasse 54
67663 Kaiserslautern



Analytik – Organische Chemie
Tel.: 0631-205-2477
FAX: 0631-205-3921
e-mail: dusch@chemie.uni-kl.de

Technische Universität Kaiserslautern
FB Maschinenbau und Verfahrenstechnik
Lehrgebiet Bioverfahrenstechnik
Prof. Dr. rer. nat. R. Ulber

z.Hd. Herrn M. Sc. Ahmed Zayed

67663 Kaiserslautern

Dienstag, 25. November 2014

Analysebericht:

CHNS- Analyse

Probenbezeichnung: **Fuc. (Sigma), Fuc. 40%, Fuc. 70%_1, Fuc. 70%_2**

Eingangsdatum: 19.11.2014

Prüfverfahren: in Anlehnung an DIN EN 51732

Interne LA-Nr.: 141113

Probe	N [%]	C [%]	H [%]	S [%]
Fuc. (pH1)	0,30	24,14	4,43	11,18
Fuc. (pH6)	0,34	26,12	4,63	9,83
Fuc. (MSP)	0,26	23,31	4,28	12,11

Kaiserslautern, den 19.11.2014

(Birgit Dusch)



Analytik-Organische Chemie
AG Prof. Dr.-Ing. J. Hartung
Erwin-Schrödinger-Str. 54
67663 Kaiserslautern

Chemie

Analytik-Organische Chemie
Birgit Dusch
E-Mail: dusch@chemie.uni-kl.de
Tel.: 0631-205-2477

TU Kaiserslautern
FB Maschinenbau und Verfahrenstechnik
Lehrgebiet Bioverfahrenstechnik
Prof. Dr. rer. nat. R. Ulber

z.Hd. Herrn Ahmed Zayed

6 7 6 6 3 Kaiserslautern

Dienstag, 20.06.2017

Analysebericht

Projekt: Elementaranalyse von 3 Proben
Probeneingang: 19.06.2017
Int. Auftragsnummer: 170608
Probenbezeichnung: Crude fucoïdan, DDP-1 fucoïdan, DDP-2 fucoïdan
Probenvorbereitung: nicht erforderlich
Prüfmethode: Verbrennungsanalyse nach DIN 51732 (CHN) bzw. DIN 15178 (S)
Prüfgerät: Vario Micro Cube, Firma Elementar
Ergebnisse (Mittelwerte):

Probe	N [%]	C [%]	H [%]	S [%]
Crude fucoïdan	0,59	22,89	4,54	6,88
DDP-1 fucoïdan	0,30	25,77	4,57	8,78
DDP-2 fucoïdan	0,29	25,95	4,54	8,78

Anmerkung: Von allen Proben wurden Doppel- bzw. Dreifachmessungen durchgeführt. Die angegebenen Werte sind Mittelwerte. Probe Crude fucoïdan sieht inhomogen aus, deshalb wurde eine Dreifachmessung durchgeführt. Die Werte zeigen aber gute Übereinstimmung. Einzelergebnisse siehe beigefügte Excel-Datei.

Kaiserslautern, den 20.06.2017

(Birgit Dusch)



Analytik-Organische Chemie
 AG Prof. Dr.-Ing. J. Hartung
 Erwin-Schrödinger-Str. 54
 67663 Kaiserslautern



Analytik-Organische Chemie
 Birgit Dusch
 E-Mail: dusch@chemie.uni-kl.de
 Tel.: 0631-205-2477

TU Kaiserslautern
 FB Maschinenbau und Verfahrenstechnik
 Lehrgebiet Bioverfahrenstechnik
 Prof. Dr. rer. nat. R. Ulber

z.Hd. Herrn Ahmed Zayed

6 7 6 6 3 Kaiserslautern

Montag, 06.03.2017

Analysebericht

Projekt: Elementaranalyse von 1 Probe
Probeneingang: 06.03.2017
Int. Auftragsnummer: 170302
Probenbezeichnung: Fucoidan-FDD6

Probenvorbereitung: nicht erforderlich

Prüfmethode: Verbrennungsanalyse nach DIN 51732 (CHN) bzw. DIN 15178 (S)

Prüfgerät: Vario Micro Cube, Firma Elementar

Ergebnisse:

Probe Fucoidan-FDD6	N [%]	C [%]	H [%]	S [%]
	< 0,5	25,35	4,51	8,45

Anmerkung: -

Kaiserslautern, den 06.03.2017

(Birgit Dusch)

4.3. Melting point analysis of fucoidan fractions



Ruth M. Bergsträßer
 FB Chemie / TU Kaiserslautern
 Erwin-Schrödinger-Strasse 54
 67663 Kaiserslautern



Analytik – Organische Chemie
 Tel.: 0631-205-2965
 FAX: 0631-205-3921
 e-mail: rbergstr@rhrk.uni-kl.de

Technische Universität Kaiserslautern
 FB Maschinenbau und Verfahrenstechnik
 Lehrgebiet Bioverfahrenstechnik
 Prof. Dr. rer. nat. R. Ulber

02.12.2014

z.Hd. Herrn M. Sc. Ahmed Zayed

6 7 6 6 3 Kaiserslautern

Internal order number: 141113-II

Report: Melting Point- Analysis

Sample name: **Fuc. (MSP), Fuc. (pH 1), Fuc. (pH 6)**
 Date of receipt: 19.11.2014, ordering: 25.11.2014
 Method: Melting Point Apparatus: DigiMelt-MPA160, SRS,
 Scientific Instruments GmbH; Ramp 2°/min;

Sense:

Sample	Description	Quantity [g]
Fuc. (pH1)	white, lighty flakes, fluffy, very easy to pour into the capillary	ca. 0,035g
Fuc. (pH6)	white flakes, like cotton, difficult to pour into the capillary	ca. 0,020g
Fuc. (MSP)	Cream white, foliated, easy to pour into the capillary	ca. 0,061g

Results:

Sample	Starting Temperatur [°C]	Beginning of yellowing [°C]	Decomposition point [°C]
Fuc. (pH1)	130	132-133	135
Fuc. (pH6)	140	153-156	161
Fuc. (MSP)	130	133-134	136

Remark: Many organic substances are melting under decomposition. This is often evidenced by decoloration from yellow up to brown and black, often reflected by gas development. This decomposition point is often diffuse and not exactly reproducibile. Some substances are carbonizing.

Ruth Maria Bergsträßer, (Dipl.Chem.)

4.4. Specific optical rotation of fucoidan fractions



Ruth M. Bergsträßer
 FB Chemie / TU Kaiserslautern
 Erwin-Schrödinger-Strasse 54
 67663 Kaiserslautern



Analytik – Organische Chemie
 Tel.: 0631-205-2965
 FAX: 0631-205-3921
 e-mail: rbergstr@rhrk.uni-kl.de

Technische Universität Kaiserslautern
 FB Maschinenbau und Verfahrenstechnik
 Lehrgebiet Bioverfahrenstechnik
 Prof. Dr. rer. nat. R. Ulber

15.12.2014

z.Hd. Herrn M. Sc. Ahmed Zayed

6 7 6 6 3 Kaiserslautern

Internal order number: 141113-III

Report: Specific Optical Rotation- Analysis

Sample name: **Standard Fucoidan** from Fucus vesiculosus $\geq 95\%$, Sigma Aldrich;
Fuc. (MSP); Fuc. (pH 1); Fuc. (pH 6)

Date of receipt: 19.11.2014, ordering: 03.12.2014

Method: P-2000 Digital Polarimeter, Fa. Jasco

Measurement details: sodium spectral lamp with $\lambda = 589\text{nm}$; path length = 100mm;
 temperature = 22°C; solvent = distilled water
 concentration of the solutions = 0,4 [weight/volume %];

Results:

Sample	Specific O.R. [α] ₅₈₉ ²² ; C=0.4; H ₂ O _{dest}
Standard Fucoidan	- 121
Fuc. (pH1)	- 128
Fuc. (pH6)	- 117
Fuc. (MSP)	- 130

Ruth Maria Bergsträßer, (Dipl.Chem.)

Appendix F

Lists of Figures, Tables, Schemes and devices

1. List of Figures

Fig. No.	Fig. Caption
1.	Seaweed production in the year 2014 by Aquaculture
2.	Global distribution of the major brown macroalgae species
3.	Overview of the different strategies dealt in the present work
4.	Cell wall model in a brown macroalgae showing various fucoidan physiological functions
5.	Published articles on fucoidan since 1900 till July 2017, according to ISI web of knowledge (Clarivate Analytics)
6.	a: Different chemical structures of fucoidan from some Fucales seaweeds b: Chemical structures of fucoidan from some Laminariales and Chordariales seaweeds
7.	Steps of immobilization protocol of TB on amino derivatized Sepabeads® EC-EA
8.	Habitat of <i>F. vesiculosus</i> or bladder wrack across the north Atlantic in more temperate zone
9.	Morphology and anatomical parts of <i>F. vesiculosus</i> thallus
10.	Growth of the brown macroalgae <i>F. vesiculosus</i> at the south beaches of Wilhelmshaven (North Sea, 53°31.236N, 8°13.849E, Germany)
11.	Extraction set of fucoidan from dried pretreated <i>F. vesiculosus</i>
12.	Overview of fucoidan extraction process from pre-treated <i>F. vesiculosus</i> biomass and obtained crude fucoidan
13.	Overview for isolated fractions of purified fucoidan
14.	Average composition of the dried biomass of <i>F. vesiculosus</i>
15.	Representation of polyanionic polysachharide reaction with fluorescent Heparin Red®
16.	Adsorption (%) of fucoidan by immobilized 2 mM TB, TA and mixed dyes at pH 1 and pH 6
17.	Comparison between adsorption (%) of fucoidan by immobilized 2, 4 and 6 mM TB at pH 1
18.	Adsorption (%) of fucoidan by 2 mM immobilized TB for 60 h of incubation at pH 1 and pH 6
19.	Adsorption (%) of fucoidan from Fucoidan_A by 75 mg of 2 mM immobilized TB at pH 1 and pH 6

Fig. No.	Fig. Caption
20.	Adsorbed fucoidan (%) by 75 mg of immobilized TB for two cycles at pH 1 and pH 6
21.	Effect of NaCl molarity in eluent on eluted fucoidan (%)
22.	Immobilized TB and TA on Sepabeads® EC-EA
23.	Molecular structure of a) perylene diimide derivative (<i>N,N'</i> -Bis-(1-amino-4,9-diaza dodecyl)-1,7-di bromo perylen-3,4:9,10-tetracarboxylic acid diimide, and b) Heparin Red®
24.	Immobilized PDD on Sepabeads® EC-EA
25.	Adsorption (%) of fucoidan from Fucoidan_A by immobilized PDD
26.	Multiple use of PDD-derivatized beads for three cycles
27.	Fucoidan elution pattern from FPLC column in two successive cycles
28.	FT-IR spectra of fucoidan before (Fucoidan_crude) and after (Fucoidan_PDD) in comparison with the commercially-available reference fucoidan purchased from Sigma-Aldrich® (>95% pure)
29.	Representation of an α -(1-3)-linked L-fucopyranoside repeating unit of fucoidan, as previously described by Cumashi, <i>et al.</i>
30.	a: Effect of different fucoidan fractions on aPPT at a concentration of 0.01 mg mL ⁻¹ b: A dose-dependent effect of Fucoidan_PDD on aPTT
31.	Effect of different types of fucoidan on PT at a concentration of 0.01 mg mL ⁻¹
32.	a: Effect of different fucoidan fractions on TT at a concentration of 0.01 mg mL ⁻¹ b: A dose-dependent anti-thrombin effect of Fucoidan_PDD
33.	Comparison between the anti-viral activities of fucoidan fractions against HSV-1
34.	Antioxidant activity of different fucoidan fractions in comparison with ascorbic acid
35.	Downstream process for fucoidan extraction and purification by either TB- or PDD-derivatized beads at pH 6
36.	Determination of Fucoidan_PDD purity using Heparin Red® Ultra assay, in comparison with the commercial standard product (>95% pure) purchased from Sigma-Aldrich®
37.	Callus and plantlet regeneration from an intact marine macroalgae thallus of <i>Agardhiella subulata</i>
38.	Summary of previously-applied growth conditions and variables to develop marine macroalgal cultures
39.	Applied growth conditions and variables to induce callus-like and protoplast cultures
40.	Different explants of <i>F. vesiculosus</i> incubated on MB50 (a, b, c, d and e) and LB (f) media at 17 °C and 26 °C, respectively, after different steps of Protocol 6

Fig. No.	Fig. Caption
41.	Enzymatic reduction of tetrazolium chloride (TTC) (Tetrazolium cation, colorless) to triphenylformazan (TPF) (Formazan, red color)
42.	Protoplasts after 72 h heterotroph cultivation in the protoplast medium showing start of cell multiplication and aggregation
43.	Development of a phototrophic callus-like growth from <i>F. vesiculosus</i> explant in ASP-12-NTA medium
44.	(a) Cultivation of <i>F. vesiculosus</i> explants in a wave bag bioreactor, (b) Filamentous callus-like growth from <i>F. vesiculosus</i> explant developed after four weeks of phototrophic cultivation in PES medium
45.	Development of crown gall or hairy-root in <i>F. vesiculosus</i> explants after transfection with <i>R. radiobacter</i> or <i>A. tumefaciens</i> DSM 30147
46.	The two different possible pathways for fucoidan biosynthesis in the brown algae <i>Ectocarpus siliculosus</i> (a) <i>De novo</i> pathway and b) salvage pathway
47.	Detailed <i>de novo</i> (a) and salvage pathway (b) for GDP-L-fucose biosynthesis either from GDP-mannose or cytosolic L-fucose, respectively
48.	Synthetic and cloned Esi0050_0098 and Esi0021_0026 in pMA-T and pMK plasmid vectors, respectively
49.	Features of pASK-IBA 45(+) plasmid vector as described by IBA GmbH
50.	Homology and phylogenetic relationships of algal FucTs_21 and FucTs_50 with other bacterial and human FucTs
51.	Gibson Assembly work flow; an example
52.	Agarose gel electrophoresis of amplified PCR products of Esi0021_0026 and Esi0050_0098
53.	Design of pASK-IBA 45(+)_Esi0021_0026 DNA construct showing some possible restriction sites and gel electrophoresis results after its digestion with <i>StuI</i> and <i>XbaI</i>
54.	Design of pASK-IBA 45(+)_Esi0050_0098 DNA construct showing some possible restriction enzymes and gel electrophoresis results after digestion <i>XbaI</i>
55.	Alignment of DNA templates (pASK_Esi0021 and pASK_0050) with the forward (fwd) sequence of the sequencing results
56.	SDS-PAGE (a) and Western blot (b) of overexpressed recombinant proteins from pASK_IBA 45(+)_Esi0021_0026 and pASK_IBA 45(+)_Esi0050_0098 DNA constructs, in comparison with an empty vector plasmid in a 2 L of LB medium of <i>E. coli</i> BL21(DE3)
57.	Western blot of expressed recombinant FucTs_50 from the pASK-IBA 45(+)_Esi0050_0098 construct in comparison with empty vector plasmid during purification cascade
58.	Glycosyltransferase activity kit principle, as described by the supplier (Bio-Techne®)

Fig. No.	Fig. Caption
59.	Measurement of catalytic activity of FucTs_50 on the donor substrate GDP-L-fucose by Glycosyltransferase activity kit
60.	FucTs_50 hydrolytic activity toward GDP-L-fucose as determined by MC-CE
61.	Catalysis of sulphonate group (SO ₃ ⁻) transfer to a hydroxyl group-containing compound by Sulphotransferases (STs) using PAPS as a donor substrate
62.	Cloned <i>E. coli</i> _opt. Esi0032_0064 and Esi0283_0018 in pMA-T plasmid vector
63.	A homology study between algal STs_283, STs_32 and the human Galactose-3- <i>O</i> -sulfotransferase 2 (G3ST2)
64.	Agarose gel electrophoresis of (a) amplified Esi0032_0064 (1386 bp) and (b) Esi0283_0018 (1032 bp) with their overlapping ends from EcoRI/SacI restriction sites of the vector pASK-IBA 45(+)
65.	Designed pASK-IBA 45(+)_Esi0032_0064 (a) and pASK-IBA 45(+)_Esi0283_0018 (b) templates by pDRAW32 DNA analysis software
66.	Agarose gel electrophoresis of extracted DNA constructs; pASK-IBA 45(+)_Esi0032_0064_Opt. and pASK-IBA 45(+)_Esi0283_0018_Opt. after digestion with <i>Xba</i> I
67.	Alignment of sequencing results of fwd DNA constructs; pASK-IBA 45(+)_Esi0032_0064_Opt. (a) and pASK-IBA 45(+)_Esi0283_0018_Opt. (b) with the designed templates
68.	Western blot of purified heterologously expressed STs_32 by <i>E. coli</i> BL21 (DE3)
69.	Western blot of purified heterologously expressed STs_283 by <i>E. coli</i> BL21 (DE3)
70.	Principle of the Universal Sulphotransferase activity kit as described by the supplier (Bio-Techne [®])
71.	a: Relationship between purified STs_32 at different concentrations and liberated free phosphate from PAPS detected by malachite green and measured at 620 nm b: Relationship between purified STs_283 at different concentrations and from PAPS detected by malachite green and measured at 620 nm
72.	Simulated fucosylation reaction of GlucNAc catalyzed by heterologously expressed FucTs_50
73.	Chemical structures of some selected marine-derived compounds previously-mentioned in Table 1
74.	SDS-PAGE plate showing its building components
75.	Calibration curve of Dubois or phenol-sulphuric acid assay
76.	Calibration curve of TB assay
77.	Calibration curve of Heparin Red [®] Ultra assay

Fig. No.	Fig. Caption
78.	Calibration curve of Dische assay
79.	Calibration curve of BaSO ₄ assay
80.	Phosphate standard calibration curve for FucTs activity assay
81.	Phosphate standard calibration curve for STs activity assay
82.	3D structures of FucTs_50 (a) and FucTs_21 (b) as traced by the free online Phyre ² server and PyMOL software
83.	3D-structures of STs_32 (a) and STs_283 (b) as traced by traced by the online service Phyre ² and PyMOL software
84.	FPLC chromatograms for fucoidan purification by immobilized PDD
85.	¹ H-NMR spectra of fucoidan fractions in comparison with fucoidan purchased from Sigma-Aldrich [®]
86.	Anti-fungal activity of different fucoidan fractions against <i>C. albicans</i> , in comparison with the reference commercial product following the protocol of Kleymann and Werling
87.	Anti-bacterial activity of different fucoidan fractions against <i>E. coli</i> (a) and <i>S. aureus</i> (b) in comparison with the reference commercial product and following the protocol of Kleymann and Werling

2. List of Tables

Table. No.	Table title
1.	Selected categories and examples of marine-derived products.
2.	Taxonomy of <i>F. vesiculosus</i>
3.	Description of an automated fucoidan purification process by immobilized PDD using FPLC
4.	Sugar, fucoidan, fucose and sulphate contents in different crude extracted fucoidan fractions from <i>F. vesiculosus</i> by Procedure_A and C
5.	Elemental analysis (CHNS) and degree of sulphation results of different fucoidan fractions
6.	a: Molecular weight parameters and polydispersity index (PDI) of different purified fucoidan fractions. b: Molecular weight parameters of fractions obtained by different NaCl molarity
7.	Comparison among the different fucoidan fractions purified by immobilized TB, regarding start, colour change and decomposition temperature points
8.	Comparison among the different fractions of fucoidan regarding specific optical rotation
9.	Monomeric composition (%) of different purified fucoidan fractions
10.	IC ₅₀ (µg.mL ⁻¹) of different fucoidan fractions isolated and purified from <i>F. vesiculosus</i> against HSV-1 in comparison with aciclovir
11.	Some selected trials with callus cultures and plant regeneration in marine macroalgae organisms
12.	Antibiotic stock solution (30x) composition
13.	Summary of processes performed in all surface sterilization protocols
14.	Examples of previous trials with heterologous expression to overexpress similar enzymes from different resources to that involved in fucoidan biosynthesis
15.	Designed primers for cloning of Esi0050_0098 and Esi0021_0026 in pASK-IBA 45(+), according to NEBuilder® Assembly Tool
16.	Overview of different algal STs, regarding their names, sizes of encoded genes, number of amino acids and putative functions
17.	Designed primers for cloning of <i>E. coli</i> -adapted Esi0032_0064 and Esi0283_0018 in pASK-IBA 45(+), according to NEBuilder® Assembly Tool
18.	PCR steps used in amplification of synthetic Esi0021_0026, Esi0050_0098, Esi0283_0018 and Esi0032_0064

3. **List of schemes**

Scheme No.	Scheme caption
1.	Overview of pre-treatment steps of the dried algae biomass before fucoidan extraction
2.	Graphical summary for fucoidan purification process from <i>F. vesiculosus</i>

4. List of used devices and instruments

Name of the device	Company	Country
- A Glass column (XK 16/20)	GE Healthcare Europe GmbH	Germany
- Analytical balance (KERN ABS)	KERN & SOHN GmbH	Germany
- Autoclave (Systec V-150)	SYSTEC GmbH Labor- Systemtechnik	Germany
- Bench centrifuge for eppis (Centrifuge 5415 D)	Eppendorf	Germany
- Blood coagulation system (BCS [®] System)	Siemens Healthcare Diagnostics Products GmbH,	Germany
- Capillary electrophoresis (cePRO 9600 TM)system	Advanced Analytical Technologies	USA
- Conductivity meter set (Qcond 2200)	VWR International GmbH	Germany
- Cryopreservation refrigerator (Ultra low temperature freezer AV039P)	Labortect	Germany
- Digital polarimeter (P-2000)	JASCO Deutschland GmbH	Germany
- Drying oven	Binder GmbH	Germany
- Electrotansfer cell (Trans-Blot [®] SD Semi-Dry Transfer Cell)	Bio-Rad	USA
- Elemental Vario Micro cube apparatus (WLD Board, V 2.0.11)	Elementar Analysensysteme GmbH	Germany
- FPLC (BioLogic Duo-Flow TM) supplied	Bio-Rad	USA
- Freeze dryer (Christ [®] LDC-1m, Alpha 2-4)	Martin Christ Gefriertrocknungsanlagen GmbH	Germany
- FT-IR (Spectrum 100)	Perkin Elmer	USA

Name of the device	Company	Country
- GEL iX20 Imager (windows version)	Intas Science Imaging Instruments GmbH	Germany
- HPLC-GPC system is composed of:	- Merck-Hitachi	- Germany
i. pump (L 7100),		
ii. auto sampler (AS-2000 A),	- PSS	- Japan
iii. GPC_MCX column (8x30 mm),	- Shimadzu Corporation	- Czech Republic
iv. Detector (Shodex® RI-10), and	- Clarity	
v. Clarity GPC Extension software for data analysis		
- HPLC-UV-ESI-MS system (Ultimate 3000RS) is composed of:	Dionex, Thermo Fisher Scientific	Germany
i. degasser (SRD 3400),		
ii. a pump module (HPG 3400RS),		
iii. an autosampler (WPS 3000TRS),		
iv. column compartment (TCC 3000RS),		
v. column (Gravity C18, 100x2 mm, 1.8 µm particle size; Macherey-Nagel)		
vi. diode array detector (DAD 3000RS),		
vii. an ESI-ion-trap unit (HCT; Bruker),		
viii. Accurate-Post-Column-Splitter, and		
ix. Bruker Hystar, QuantAnalysis and Dionex Chromelion software for data collection and analysis.		

Name of the device	Company	Country
- Magnetic stirrer with heating (MR Hei-Standard)	Heidolph Instruments GmbH & Co. KG	Germany
- Melting point apparatus (DigiMelt-MPA 160)	SRS Scientific Instruments GmbH	Germany
- Microfluidizer (Microfluidics)	Quadro Engineering Corp.,	Canada
- Microplate reader (EL808) provided with Microplate Data Collection & Analysis Software	BioTek Instrument	USA
- Microscope (ECLIPSE Ni-U) with NIS-Element software	Nikon	Japan
- Nanodrop spectrophotometer, with NanoDrop 2000/2000c Software	Thermo Scientific	USA
- NMR Spectrometer (400 MHz, Bruker® 600 Ultrashield)	Bruker	Germany
- Orbital shaker (unimax 1010)	Heidolph	Germany
- Overhead shaker (Multi Bio RS-24)	Biosan	Latvia
- PCR thermocycler (T-Gradient thermoblock)	Analytik Jena AG	Germany
- pH meter (pH211)	Hanna® Instrument	USA
- Photoincubator (AlgaTron AG230 ECO)	PSI	Czech Republic
- Rotary evaporator (Laborota 4003)	Heidolph Instruments GmbH & Co.KG	Germany
- Shaker incubator (Infors HT Ecotron)	Infors AG	Switzerland
- Shaker incubator (Innova® 44 incubator shaker series)	New Brunswick Scientific/Eppendorf AG	Germany
- Spectrofluorometer (FP-8300)	JASCO Deutschland GmbH	Germany

Name of the device	Company	Country
- Superspeed Centrifuge (SORVALL LYNX [®] 6000)	ThermoFischer Scientific	USA
- Thermoshaker (TS-100)	Biosan	Latvia
- Tissuelyzer (MM 200)	Retsch	Germany
- Top shaker (Rocker 3D basic)	IKA [®] -Werke GmbH & Co. KG	Germany
- Ultrasonic bath (Sonorex [®] Digital 10 P)	Bandelin	Germany
- UV/Vis-spectrometer (Cary 60 Uv-Vis)	Agilent Technologies	USA
- Vertical electrophoresis cell for SDS-PAGE (Mini-PROTEAN [®] Tetra cell) with PowerPac [™] Basic Power Supply	Bio-Rad	USA
- Visible spectrophotometer (Amersham Biosciences Einstrahl-Spektralfotometer Novaspec III)	Klüver & Schulz GmbH	Germany
- Water ultra-purification system (Ultra Clear TWF/ EI-ION UV plus [™])	Siemens/Evoqua water technologies	Germany
- Wave bag bioreactor (BIOSTAT [®] RM)	Sartorius Stedim Biotech GmbH	Germany

Publications in peer-reviewed journals and conferences

Partial results from this work have been pre-published in the following papers.

Journals:

1. A. Zayed, C. Dienemann, C. Giese, R. Krämer, R. Ulber, “An immobilized perylene diimide derivative for fucoidan purification from a crude brown algae extract,” *Process Biochem.*, **2018**. 65, 233 – 238. DOI: 10.1016/j.procbio.2017.10.012
2. A. Zayed, R. Ulber, “Heterologous Expression of Heteropolysaccharides,” *Chem. Ing. Tech.* **2016**. 88(9), 1399. DOI: 10.1002/cite.201650230
3. A. Zayed, R. Ulber, “Downstream Processing of Bioactive Heteropolysaccharides,” *Chem. Ing. Tech.* **2016**. 88(9), 1398. DOI: 10.1002/cite.201650238
4. A. Zayed, K. Muffler, T. Hahn, S. Rupp, D. Finkelmeier, A. Burger-Kentischer, and R. Ulber, “Physicochemical and Biological Characterization of Fucoidan from *Fucus vesiculosus* Purified by Dye Affinity Chromatography,” *Mar. Drugs* **2016**. 14(4), 79. DOI: 10.3390/md14040079.
5. T. Hahn, M. Schulz, R. Stadtmüller, A. Zayed, K. Muffler, S. Lang, and R. Ulber, “A Cationic Dye for the Specific Determination of Sulfated Polysaccharides”. *Anal. Lett.*, **2016**. 2719, 1948-1962. DOI: 10.1080/00032719.2015.1126839.
6. T. Hahn, A. Zayed, M. Kovacheva, R. Stadtmüller, S. Lang, K. Muffler, and R. Ulber, “Dye affinity chromatography for fast and simple purification of fucoidan from marine brown algae,” *Eng. Life Sci.*, **2016**. 16(1), 78–87. DOI: 10.1002/elsc.201500044.

Talk in Conferences:

1. A. Zayed, T. Hahn, S. Rupp, R. Krämer, R. Ulber, “Fucoidan as a Natural Anticoagulant, Antiviral and Anti-cancer Drug”, 3rd German Pharm-Tox Summit **2018** (26 February- 1 March 2018, Göttingen, Germany).
2. A. Zayed, R. Ulber. “Downstream processing of bioactive heteropolysaccharides”. ProcessNet-Jahrestagung und 32. DECHEMA-Jahrestagung der Biotechnologen **2016**. (12.- 15. September 2016, Aachen, Germany).
3. A. Zayed, K. Muffler, R. Ulber. “Novel and rapid extraction and purification procedure for fucoidan from *F. vesiculosus*”. Jahrestreffen der Fachgruppe Phytoextrakte (23rd February **2015**, Bonn, Germany).

Poster:

1. A. Zayed, C. Dienemann, C. Giese, R. Krämer, R. Ulber. “Fucoidan Purification: A Scale-Up Approach”. Himmelfahrtstagung **2018**: Heterogeneities - A key for understanding and upscaling of bioprocesses in up- and downstream (7 – 9th May 2018 Herrenkrug Parkhotel, Magdeburg, Germany).
2. A. Zayed, C. Dienemann, R. Krämer, R. Ulber. “A Perylene Diimide Derivative for Sulphated Heteropolysaccharides Purification (e.g., Fucoidan from Crude Brown Algae Extract)”. French Chemical and Process Engineering Society (SFGP), (July 11-13th **2017**, Nancy, France - German-French day - July 12th, 2017).
3. A. Zayed, C. Dienemann, R. Krämer, R. Ulber. “A simple and Time-saving Purification of Fucoidan from Crude Brown Algae Extracts. Himmelfahrtstagung **2017**: Models for Developing and Optimising Biotech Production, (May 22. - 24. 2017, Neu-Ulm, Germany).
4. A. Zayed, B. Ledermann, N. Frankenberg-Dinkel, R. Ulber. “Evaluation of Heterologously Expressed Algal Fucosyltransferases and Sulfotransferases in *E. coli*”. Himmelfahrtstagung **2017**: Models for Developing and Optimising Biotech Production, (22. - 24. May 2017, Neu-Ulm, Germany).

5. A. Zayed, B. Ledermann, N. Frankenberg-Dinkel, R. Ulber. "Heterologous expression of heteropolysaccharides". ProcessNet-Jahrestagung und 32. DECHEMA-Jahrestagung der Biotechnologen **2016**, (12. - 15. September 2016, Aachen, Germany).
6. A. Zayed, K. Muffler, T. Hahn, R. Ulber. "Cultivation of macro algae in wave bag reactors for the production of sulfated heteropolysaccharides". Himmelfahrtstagung **2016**: New Frontiers for Biotech-Processes (2. - 4. May 2016, Koblenz, Germany)

Curriculum Vitae

Personal information

Name: Ahmed Elsayed Ahmed Farag Zayed

Birth place: Tanta/Gharbeya, Egypt

Education

1987 - 1991 Ground school in Tanta/Gharbeya, Egypt

1992 - 1995 Preparatory school Mehalla Elkobra/Gharbeya, Egypt

1996 - 1998 Secondary school in Mehalla Elkobra/Gharbeya, Egypt

1998 - 2003 Faculty of Pharmacy, Tanta University, Egypt

Final degree: B. Sc. in Pharmaceutical sciences (Excellent with honor,
Rank: 4th)

2003 - 2012 Instructor

Pharmacognosy Department,

Faculty of Pharmacy, Tanta University, Egypt

2004 – 2006 Pre-master student

Pharmacognosy Department,

Faculty of Pharmacy,

Tanta University, Egypt

2006 - 2012 M. Sc. Student

Pharmacognosy Department,

Faculty of Pharmacy,

Tanta University, Egypt

Final Degree: Passed. M. Sc. in Pharmaceutical sciences (Pharmacognosy)

Since 2012

Assistant lecturer

Pharmacognosy Department,

Faculty of Pharmacy,

Tanta University, Egypt

4/2014-3/2018

Doctoral student as a DAAD scholarship holder (GERLS program)

Bioprocess Engineering Institute,

Prof. Dr. rer. nat. Roland Ulber

TU Kaiserslautern, Germany

Since 4/2018

Doctoral student as an insitutional scholarship holder

Bioprocess Engineering Institute,

Prof. Dr. rer. nat. Roland Ulber

TU Kaiserslautern, Germany